



University
of Glasgow

Bain, Calum Cunningham (2012) *Resident and inflammatory macrophages in the intestine.*

PhD thesis

<http://theses.gla.ac.uk/3441/>

Copyright and moral rights for this thesis are retained by the author

A copy can be downloaded for personal non-commercial research or study, without prior permission or charge

This thesis cannot be reproduced or quoted extensively from without first obtaining permission in writing from the Author

The content must not be changed in any way or sold commercially in any format or medium without the formal permission of the Author

When referring to this work, full bibliographic details including the author, title, awarding institution and date of the thesis must be given

Resident and Inflammatory Macrophages in the Intestine

Calum Cunningham Bain

A thesis submitted to the College of Medicine, Veterinary and Life Sciences,
University of Glasgow in fulfilment of the requirements for the degree of Doctor of
Philosophy

February 2012

Institute of Infection, Immunity and Inflammation
University of Glasgow
120 University Place Glasgow
G12 8TA

Acknowledgements

Firstly, I would like to thank my supervisor, Allan Mowat, who has given me a great deal of support and encouragement throughout my PhD. I am especially appreciative of the time he has devoted to reading and correcting this thesis, and the time he has spent on re-drafting many different versions of manuscripts.

I would also like to thank the past and present members of 'Team Mowat'. First of all to Andy, who started this project during his PhD and who has given me invaluable advice throughout my project. Also Dr. Vonny for showing me the ropes during my first year, but also for her song writing ability. I doubt I will ever work again with someone who can incorporate 'Bainer' into so many songs. Also thanks to Elinor for her help in the lab, advice in the office and craic in the pub! To Aude, Charlie and Alberto, who have helped with numerous experiments, read drafts of this thesis and made working in the lab great fun. A special thanks to Charlie who has devoted a huge amount of time and energy to carry out PCR experiments to complete our paper.

A big thank you to all the Millings, you make the office a very quiet and studious environment to work in!! A special thanks to Vuk for taking time to read through the Discussion of this thesis and for providing constructive criticism throughout my PhD!

Also thanks to former members of the Harnett group - Angela, Theresa and Mairi - who all made me very welcome when I first joined the department. Many thanks to Helen Arthur for providing the answers to all the random day-to-day queries, and also to all the staff at the CRF, especially Craig, who helped me with my the adoptive transfer experiments. I would also like to thank all those who provided mice during my studies, including Bill Agace, Rob Nibbs, Paul Garside, Kevin Couper, Tracey Hussell and Andrew Dick.

I must also thank the former Faculty of Medicine for providing funding for my PhD, but also the British Society for Immunology for the generous travel awards I received during my PhD.

I would also like to thank family and friends for their encouragement throughout my studies. In particular, thanks to the Bains and the Sinclairs for the support, both emotional and financial, during my time at university. I appreciate that some believed seven years of study was rather excessive, but I hope they'll agree it has been worth it!

And finally, I must thank Michelle for being amazingly patient and supportive during my PhD, especially over the last few months while writing up, when at times, I have been slightly difficult to live with!

Table of Contents

Acknowledgements	2
List of Figures and Tables	7
Author's Declaration	10
List of Publications	11
List of Abbreviations	12
Summary	15
Chapter 1. General Introduction	20
1.1 Introduction.....	21
1.2 Macrophages and the Mononuclear Phagocyte System.....	21
1.2.1 How to Identify a Macrophage	22
1.2.2 Macrophage Development.....	24
1.2.3 Growth Factors in Macrophage Development	27
1.2.4 Self-Renewal of Tissue Resident Macrophages	28
1.3 Macrophage 'Activation'	30
1.3.1 Classical Macrophage Activation	30
1.3.2 Alternative Macrophage Activation	31
1.3.3 Regulatory Macrophages.....	32
1.3.4 Regulation of Macrophage Activation	33
1.4 The Gastrointestinal Tract	39
1.4.1 Protective Immunity versus Tolerance in the Intestine	40
1.4.2 The Commensal Microbiota	42
1.4.3 Inflammatory Bowel Disease	43
1.5 Intestinal Macrophages	46
1.5.1 CX3CL1 and Its Receptor	49
1.5.2 Mechanisms Governing Macrophage Unresponsiveness.....	50
1.5.3 Intestinal Macrophages During Inflammation.....	52
1.6 Thesis Aims	53
Chapter 2. Materials and Methods	55
2.1 Mice	56
2.2 Isolation of Peritoneal Macrophages	57
2.3 Isolation of Colonic Lamina Propria cells	57
2.4 Generation of Bone Marrow Derived Macrophages	58
2.5 Isolation of Alveolar and Lung Macrophages	58
2.6 Processing of Whole Blood	58
2.7 <i>In vitro</i> Stimulation of BMM and Purified Monocytes	58
2.8 Flow Cytometry and Antibodies.....	59
2.8.1 Surface Staining.....	59
2.8.2 Detection of Intracellular Cytokines by Flow Cytometry.....	59
2.8.3 Detection of CCR2 Chemokine Receptor by Flow Cytometry	60
2.9 Purification of Tissue Macrophages by FACS	60
2.10 Assessment of Phagocytosis	61
2.11 Induction of DSS Colitis.....	61
2.12 Measure of Cell Turnover by BrdU Incorporation.....	63
2.13 Adoptive Transfer of Purified Monocytes	63
2.14 Competitive Adoptive Transfer of BM cells	64
2.15 Transfer of Monocytes into Mice Depleted of CD11c ⁺ cells	64
2.16 Generation of BM Chimeric Mice	64
2.17 Administration of Growth Factors <i>In Vivo</i>	64
2.18 Cytospins.....	65
2.19 RNA Extraction	65
2.20 cDNA Synthesis from RNA.....	65
2.21 Quantitative/Real Time PCR	66
2.22 Statistical Analysis.....	66

Chapter 3. Phenotypic Characterisation of Lamina Propria Macrophages During Homeostasis and Inflammation	68
3.1 Introduction.....	69
3.2 Preliminary Identification of Macrophages in Steady State Colon.....	70
3.3 CX3CR1 Expression Defines 3 Populations of CD11b ⁺ Cells.....	71
3.3.1 CX3CR1 ^{neg} Cells.....	71
3.3.2 CX3CR1 ^{high} Cells	73
3.3.3 CX3CR1 ^{int} Cells	73
3.4 Lamina Propria Myeloid Cells During Inflammation	74
3.4.1 Induction of Intestinal Inflammation	75
3.4.2 Effects of Inflammation on the Mucosal Myeloid Compartment.....	75
3.5 Summary	77
Chapter 4. The Origin of Lamina Propria Macrophages During Intestinal Homeostasis.....	97
4.1 Introduction.....	98
4.2 Recruitment of Monocytes to the Resting Intestine.....	98
4.3 Monocyte Recruitment to the Colon Following Diphtheria Toxin-Mediated Mononuclear Phagocyte Depletion	99
4.4 Analysis of Monocyte Recruitment in CCR2-deficient Mice	101
4.5 Population Dynamics of Intestinal Macrophages <i>In Situ</i>	104
4.6 Effects of CSF-1 on Colonic Macrophage Development <i>In Vivo</i>	106
4.7 Differentiation of Monocytes <i>In Vitro</i>	106
4.8 Examining for the Presence of Radio-resistant Intestinal Macrophages.....	107
4.9 Summary	107
Chapter 5. Functional Analysis of Colonic Macrophage Populations in Homeostasis and Inflammation.....	133
5.1 Introduction.....	134
5.2 Baseline Cytokine Production by LP Myeloid Subsets.....	134
5.3 TLR Responsiveness of Intestinal CX3CR1 ⁺ Subsets	136
5.4 Phagocytic Activity of CX3CR1 ⁺ LP Myeloid Cells	137
5.5 Costimulatory Molecule Expression	138
5.6 Are Intestinal Macrophages 'Alternatively Activated'?	138
5.7 Cytokine Production During Inflammation	139
5.8 Summary	141
Chapter 6. The Contribution of Ly6C^{high} Monocytes to Colonic Inflammation.....	155
6.1 Introduction.....	156
6.2 Monocyte Differentiation During Inflammation	156
6.3 The Role of Ly6C ^{high} Monocytes during Inflammation	157
6.4 Pathogenic Role of Ly6C ^{high} Monocytes in Inflamed Colon.....	159
6.5 Monocytes and Macrophages in the Resolution of Colonic Inflammation.....	160
6.6 Summary	162
Chapter 7. The Role of CD200R1 in the Regulation of Intestinal Macrophage Activity.....	174
7.1 Introduction.....	175
7.2 Expression of CD200R1 by Colonic Macrophages	175
7.3 CD200 Expression in Steady State Colon.....	176
7.4 Characterisation of Colonic Macrophages from CD200R1 KO Mice.....	177
7.5 TLR Responsiveness of CD200R1 KO Macrophages	177
7.6 Characterisation of Aged CD200R1 KO Mice	178
7.7 Experimental Colitis in CD200R1 KO Mice	180
7.8 Characterisation of CD200 KO Mice	181
7.9 Experimental Colitis in CD200 KO Mice.....	181
7.10 Effects of CD200-Fc Fusion Protein on Macrophage Responsiveness	182
7.11 Summary	182

Chapter 8. General Discussion	203
8.1 Introduction.....	204
8.2 Macrophages in Steady State Colon.....	205
8.2.1 The Phenotype of Macrophages in the Steady State Mucosa.....	205
8.2.2 Ontogeny of Steady State Colonic Macrophages.....	211
8.2.3 Functional Attributes of CX3CR1 ^{high} Macrophages and their CX3CR1 ^{int} Precursors.....	216
8.3 Effects of Inflammation on Colonic Macrophages.....	221
8.4 Factors Influencing Colonic Macrophage Behaviour.....	228
8.4.1 The Role of Cytokines and Chemokines.....	228
8.4.2 Control of Macrophage Function by Inhibitory Receptors.....	233
8.5 Concluding Remarks.....	236
References	241

List of Figures and Tables

Figure 1.1: The Accepted View of the Mononuclear Phagocyte System	29
Figure 1.2: Pattern Recognition Receptors expressed by Macrophages.....	32
Figure 1.3: Macrophage Activation	34
Figure 1.4: Expression Pattern of CD200R1 and its ligand CD200	37
Figure 3.1: Original Gating Strategy for Identification of Colonic Macrophage Subsets	80
Figure 3.2: Refined Gating Strategy for the Analysis of Colonic Myeloid Cells	81
Figure 3.3: Colonic Myeloid Cell Populations Defined by CX3CR1 Expression	82
Figure 3.4: Phenotypic Characterisation of Colonic Myeloid Cells Identified by Levels of CX3CR1 Expression	83
Figure 3.5: CD11b ⁺ CX3CR1 ^{neg} SSC ^{high} Cells in the Colonic Mucosa are Eosinophils and Neutrophils	84
Figure 3.6: SiglecF ⁺ Cells in the Colonic Mucosa are Eosinophils	85
Figure 3.7: Heterogeneity within the CX3CR1 ⁺ Populations of Colonic Myeloid Cells	86
Figure 3.8: Post-sort Purity of FACS-purified CX3CR1 ⁺ Populations of Colonic Myeloid Cells.....	87
Figure 3.9: CX3CR1 Expression by Different Myeloid Cell Populations	88
Figure 3.10: Effects of <i>In Vivo</i> Administration of flt3L on Colonic CX3CR1 ⁺ Subsets.....	89
Figure 3.11: Development of Acute Experimental Colitis is Comparable in CX3CR1 ^{+/gfp} and WT Mice	90
Figure 3.12: Accumulation of Myeloid Cells During Acute Experimental Colitis	91
Figure 3.13: Changes in Colonic LP CX3CR1-defined Populations During DSS Colitis	92
Figure 3.14: Expansion of Mucosal CX3CR1 ^{neg} Myeloid Cell Numbers During Colitis.....	93
Figure 3.15: Expansion of Mucosal CX3CR1 ^{int} Myeloid Cell Numbers During Colitis	94
Figure 3.16: Expansion of Mucosal CX3CR1 ^{int} Myeloid Cell Numbers During Colitis	95
Figure 3.17: Effects of Acute Colitis on Colonic CX3CR1 ^{high} Cells	96
Figure 4.1: Purification of Bone Marrow Monocytes	109
Figure 4.2: Adoptive Transfer of Bone Marrow Monocytes into Resting Mice	110
Figure 4.3: Adoptively Transferred BM Monocytes in Bloodstream of Resting Mice	111
Figure 4.4: Alternative Gating Strategy for Identifying Colonic MP Subsets in Non-CX3CR1-GFP Mice	112
Figure 4.5: Ablation of Colonic Mononuclear Phagocytes in CD11c-DTR Mice	113
Figure 4.6: Accumulation of Transferred BM Monocytes in Colon of Depleted CD11c-DTR Mice	114
Figure 4.7: Presence of Transferred BM Monocytes in Blood of Depleted CD11c-DTR Mice.....	115
Figure 4.8: Circulating Ly6C ^{high} Monocytes in CCR2 KO Mice	116
Figure 4.9: CD11b ⁺ Myeloid Cell Compartment in Colon of CCR2 KO Mice	117
Figure 4.10: Eosinophils and Neutrophils in the Colon of CCR2 KO Mice	118
Figure 4.11: Intestinal Myeloid Compartment in CCR2 KO Mice.....	119
Figure 4.12: Intestinal Myeloid Compartment in CCR2 KO Mice.....	120
Figure 4.13: Accumulation of Transferred BM Monocytes in Colon of CCR2 KO Mice	121

Figure 4.14: Ly6C ^{high} Monocytes Give Rise to Long-lived CX3CR1 ^{high} Macrophages in CCR2 KO Colon.....	122
Figure 4.15: Presence of Adoptively Transferred Ly6C ^{high} Monocytes in Blood of CCR2 KO mice	123
Figure 4.16: Comparison of Fate of Donor Derived Monocytes in Different Tissues of CCR2 KO Mice	124
Figure 4.17: Adoptive Transfer of Ly6C ^{low} Monocytes into Resting CCR2 KO Mice	125
Figure 4.18: Short Term BrdU Incorporation by Bone Marrow and Blood Monocytes	126
Figure 4.19: Short Term BrdU Incorporation by Colonic Macrophage Subsets	127
Figure 4.20: Long Term BrdU Incorporation by Colonic Macrophage Subsets	128
Figure 4.21: Effects of CSF-1 Administration on Colonic Macrophage Subsets.....	129
Figure 4.22: Effects of Culture of Colonic and BM Monocytes <i>In Vitro</i>	130
Figure 4.23: Radio-resistant Macrophages in the Colonic Mucosa	131
Figure 4.24: Radio-resistant Macrophages in the Colonic Mucosa are Phenotypically Indistinguishable from BM-derived Resident Colonic Macrophages.....	132
Figure 5.1: Cytokine Production by Colonic Macrophage Subsets in Steady State Colon	142
Figure 5.2: Constitutive Production of IL10 by Intestinal Myeloid Subsets	143
Figure 5.3: Quantitative Analysis of Cytokine mRNA expression by CX3CR1 Defined Subsets of Colonic Macrophages	144
Figure 5.4: TLR expression by CX3CR1 Defined Subsets of Colonic Macrophages	145
Figure 5.5: TLR expression by Purified CX3CR1 Defined Subsets of Colonic Macrophages	146
Figure 5.6: Cytokine Production by Colonic Macrophage Subsets in Response to TLR4 Stimulation	147
Figure 5.7: Cytokine Production by Colonic Macrophage Subsets in Response to TLR2 Stimulation	148
Figure 5.8: Phagocytic Activity of CX3CR1 Defined Subsets of Colonic Macrophages	149
Figure 5.9: Expression of Costimulatory Molecules by CX3CR1 Defined Subsets of Colonic Macrophages	150
Figure 5.10: Expression of Alternatively Activated Macrophage Markers by CX3CR1 Defined Subsets of Colonic Macrophages	151
Figure 5.11: Cytokine Production by Colonic Macrophage Subsets During Inflammation.....	152
Figure 5.12: Cytokine Production by Colonic Macrophage Subsets in Response to TLR4 Stimulation During Inflammation	153
Figure 5.13: Cytokine Production by Colonic Macrophage Subsets in Response to TLR2 Stimulation During Inflammation	154
Figure 6.1: Fate of Adoptively Transferred Ly6C ^{high} Monocytes in the Inflamed Mucosa	163
Figure 6.2: Fate of Adoptively Transferred Ly6C ^{high} Monocytes in the Bloodstream of Colitic Mice	164
Figure 6.3: Progress of DSS Colitis in CCR2-deficient Mice	165
Figure 6.4: Enumeration of CD11b ⁺ Myeloid Cells in Colon of CCR2 KO Mice with DSS Colitis ..	166
Figure 6.5: Presence of Neutrophils in the Mucosa of CCR2 KO Mice with DSS Colitis.....	167
Figure 6.6: Presence of Eosinophils in the Mucosa of CCR2 KO Mice with DSS Colitis.....	168
Figure 6.7: Monocyte/Macrophage Subsets in the Mucosa of CCR2 KO Mice with DSS Colitis...	169

Figure 6.8: Class II MHC ⁺ Resident Macrophages and DC in the Mucosa of CCR2 KO Mice with DSS Colitis.....	170
Figure 6.9: Competitive Adoptive Transfer of WT and CCR2KO BM Cells into Colitic Mice	171
Figure 6.10: Effects of Adoptively Transferring WT Ly6C ^{high} Monocytes on the Outcome of DSS Colitis in CCR2 KO Mice.....	172
Figure 6.11: Myeloid Cells in Colon during Recovery from DSS Colitis.....	173
Figure 7.1: CD200R1 Expression by Myeloid Cells from Different Tissues.....	184
Figure 7.2: CD200 Expression in the Colon.....	185
Figure 7.3: Characterisation of Colonic Macrophages in CD200R1 KO Mice	186
Figure 7.4: Activation Status of Colonic Macrophages from CD200R1 KO Mice	187
Figure 7.5: Responsiveness of CD200R1 KO Bone Marrow Derived Macrophages to Pro-inflammatory Stimuli.....	188
Figure 7.6: TNF α Production by Colonic Macrophages from CD200R1 KO Mice following TLR Stimulation	189
Figure 7.7: Absence of Spontaneous Intestinal Inflammation in Aged CD200R1 KO Mice.....	190
Figure 7.8: T- and B-lymphocytes in the Colonic Mucosa of Aged CD200R1 KO Mice	191
Figure 7.9: Presence of Neutrophils in the Colon of Aged CD200R1 KO Mice	192
Figure 7.10: Characterisation of Colonic Macrophages from Aged CD200R1 KO Mice.....	193
Figure 7.11: Characterisation of Colonic Macrophages from Aged CD200R1 KO Mice.....	194
Figure 7.12: TLR Responsiveness of BM Macrophages from Aged CD200R1 KO Mice	195
Figure 7.13: Progress of Experimental Colitis in CD200R1 KO Mice	196
Figure 7.14: Characterisation of Myeloid Cells in Colon of CD200R1 KO Mice with DSS-induced Colitis	197
Figure 7.15: Characterisation of the Intestinal Myeloid Compartment of Resting CD200 KO Mice	198
Figure 7.16: Absence of Spontaneous Intestinal Inflammation in CD200 KO Mice.....	199
Figure 7.17: DSS Colitis in CD200 KO Mice.....	200
Figure 7.18: Effects of CD200-Fc Fusion Protein on Responsiveness of BMM to TLR Ligation ...	201
Figure 7.19: Effects of CD200-Fc Fusion Protein on Responsiveness of BMM to TLR Ligation ...	202
Figure 8.1: The Phenotype, Function and Origin of Intestinal Macrophages in the Normal and Inflamed Intestine.....	240
Table 1.1: Tissue Macrophage Populations during Homeostasis.....	23
Table 1.2: Cell Surface Markers of Tissue Macrophages	23
Table 2.1: Details of Mouse Strains	56
Table 2.2: List of Monoclonal Antibodies and Streptavidin Conjugates used for Flow Cytometry. ...	62
Table 2.3: Clinical Disease Score criteria used during DSS-induced colitis studies.....	63
Table 2.4: Primers used in qRT-PCR	67
Table 3.1: Summary of CX3CR1 ⁺ Mononuclear Phagocytes in Steady State LP.....	79
Table 3.2: Changes in CX3CR1 ⁺ Populations During Inflammation	79

Author's Declaration

I declare that all the experimental data contained in this thesis is the result of my own work, with the exception of the RT-PCR experiments, which were performed by Charlotte Scott and the competitive adoptive transfer experiments which were carried out in collaboration with Dr. Yvonne Bordon. No part of this thesis has been previously submitted for any other degree at the University of Glasgow or any other institution.

Signature.....

Printed Name.....

List of Publications

Platt, A. M., **C. C. Bain**, Y. Bordon, D. P. Sester, and A. M. Mowat. 2010. An independent subset of TLR expressing CCR2-dependent macrophages promotes colonic inflammation. *J Immunol* 184:6843-6854.

Mowat, A.Mcl., and **C. C. Bain**. 2010. News and Highlights: The curious case of the intestinal eosinophil. *Mucosal Immunol.* 3:420-421.

Bain, C. C., and A. Mcl. Mowat. 2011. Intestinal macrophages - specialised adaptation to a unique environment. *Eur. J. Immunol.* 41:2494-2498.

Mowat, A. Mcl., and **C. C. Bain**. 2011. Mucosal macrophages in intestinal homeostasis and inflammation. *J. Innate Immun.* 3:550-564.

Bain, C. C., and A. Mcl. Mowat. 2011. CD200 receptor and macrophage function in the intestine. *Immunobiology.*

Bain, C. C., C. L. Scott, H. Uronen-Hansson, S. Gudjonssen, O. Jansson, O. Grip, W. W. Agace and A. Mcl. Mowat. 2011. Resident and pro-inflammatory macrophages in the colon represent alternative context dependent fates of the same Ly6C^{hi} monocyte precursors. *Manuscript submitted*

List of Abbreviations

7-AAD	7-amino-actinomycin D
-APC	allophycocyanin
APC	antigen presenting cell
BLP	bacterial lipoprotein
BM	bone marrow
BMM	bone marrow derived m ϕ
BrdU	bromodeoxyuridine
CD	cluster of differentiation
cDC	conventional dendritic cell
CLR	C-type lectin receptor
CMP	common myeloid progenitor
CMF-HBSS	calcium/magnesium free Hank's buffered salt solution
CNS	central nervous system
CSF	colony stimulating factor
DC	dendritic cell
DT	diphtheria toxin
DSS	dextran sulphate sodium
EAE	experimental autoimmune encephalitis
EAU	experimental autoimmune uveoretinitis
EDTA	ethylenediaminetetraacetic acid
FACS	fluorescence activated cell sorting
FCS	foetal calf serum
FITC	fluorescein isothiocyanate
FSC	forward scatter
flt3L	<i>flms</i> -like tyrosine kinase 3 ligand
GALT	gastrointestinal associated lymphoid tissue
GFP	green fluorescent protein
GM-CSF	granulocyte macrophage colony-stimulating factor
GMP	granulocyte/macrophage precursor
HBSS	Hank's buffered salt solution
HSC	haematopoietic stem cell
IBD	inflammatory bowel disease
IDO	indoleamine-2,3-deoxygenase
IEL	intra-epithelial lymphocyte
IFN	interferon

Ig	immunoglobulin
IL	interleukin
ILF	isolated lymphoid follicle
i.p.	intraperitoneal
IRAK	IL1 receptor-associated kinase
IRF	interferon regulatory factor
i.v.	intravenous
KGF	keratinocyte growth factor
KO	knock out
LP	lamina propria
LPS	lipopolysaccharide
LT	lymphotoxin
M1	classically activated macrophage
M2	alternatively activated macrophage
MaFIA	macrophage Fas-induced apoptosis
MAPK	mitogen-activated protein kinase
MDP	macrophage and dendritic cell precursor
M ϕ	macrophage
MFI	mean fluorescence intensity
MHC	major histocompatibility complex
MLN	mesenteric lymph node
MP	mononuclear phagocyte
MPS	mononuclear phagocyte system
MyD88	myeloid differentiation factor 88
NADPH	nicotinamide adenine dinucleotide phosphate-oxidase
NK	natural killer
NLR	Nod-like receptor
NO	nitric oxide
NOD	nucleotide-binding oligomerisation domain
PAMP	pathogen associated molecular pattern
PBS	phosphate buffered solution
PCR	polymerase chain reaction
pDC	plasmacytoid dendritic cell
PE	phycoerythrin
PG	prostaglandin
PFA	paraformaldehyde
PMA	phorbol 12-myristate 13-acetate

PP	Peyer's patches
PPAR	peroxisome proliferator-activated receptor
PRR	pattern recognition receptor
RA	retinoic acid
RPMI	Roswell Park Memorial Institute-1640 medium
RT-PCR	reverse transcriptase polymerase chain reaction
SA	streptavidin
SD	standard deviation
SIRP	signal regulatory protein
SFB	segmented filamentous bacteria
SPF	specific pathogen free
SSC	side scatter
STAT	signal transducer and activator of transcription
TAM	tumour-associated macrophage
TED	transepithelial dendrites
TGF	transforming growth factor
TRAF	TNF receptor activated factor
TREM	triggering receptor expressed by myeloid cells
T _H 1	T helper 1
T _H 2	T helper 2
T _H 17	T helper 17
TLR	Toll-like receptor
TNF	tumour necrosis factor
TSLP	thymic stromal lymphopoietin
Treg	regulatory T cell
VEGF	vascular endothelial growth factor
VIP	vasoactive intestinal peptide

Summary

The healthy intestinal mucosa is home to the largest population of m ϕ in body. Like all tissue m ϕ , intestinal m ϕ play vital roles in maintaining tissue homeostasis by removing apoptotic cells and any other cellular debris. In addition they maintain the integrity of the epithelial barrier and support the differentiation and maintenance of regulatory T cells in the mucosa. By virtue of their high phagocytic and bactericidal activity, these m ϕ are also vital members of the innate immune system and are strategically positioned adjacent to the epithelium so that they can capture and eliminate any invading organism(s). However unlike other tissue m ϕ , those found in the normal gut have several functional adaptations, such as hyporesponsiveness to toll-like receptor (TLR) ligands, which allow them to function without provoking overt inflammation. M ϕ are also abundant during intestinal inflammation, where they show increased TLR responsiveness, pro-inflammatory cytokine and chemokine production and enhanced phagocytic ability. Under these conditions, m ϕ perpetuate inflammation. It remains unclear whether these distinct roles in healthy and inflamed intestine roles are carried out by discrete populations of m ϕ , or if the resident m ϕ alter their behaviour and become pro-inflammatory.

One of the main obstacles to gaining a better understanding of the immunobiology of intestinal m ϕ during steady state and inflammatory conditions is discriminating them from other mononuclear phagocytes (MP) in the mucosa, such as dendritic cells (DC). At the time of starting my project, it was becoming clear that markers such as F4/80 and CD11c were insufficient for distinguishing between m ϕ and DC when used in isolation. Therefore, the aims of this thesis were to first establish reliable multi-parameter flow cytometry staining protocols to allow precise phenotypic and functional characterisation of m ϕ in the healthy and inflamed mouse colon, and secondly, to explore the origins of these m ϕ populations to assess whether they were derived from distinct precursors, or whether a relationship existed between them. Lastly, I examined the potential mechanisms underlying the characteristic TLR hyporesponsiveness that intestinal m ϕ exhibit, focusing on the role of the inhibitory CD200R1-CD200 axis.

In Chapter 3, I first set out to characterise phenotypically the m ϕ populations present in the steady state mouse colon using multi-parameter flow

cytometry. These studies revealed that expression of the chemokine receptor CX3CR1 could be used to identify two main populations of myeloid cells, the bigger of which was a homogeneous population of CX3CR1^{high}CD11b⁺F4/80⁺MHCII⁺Ly6C^{neg} mφ that dominated the resting mucosa. A smaller population of CD11b⁺ cells expressing intermediate levels of CX3CR1 (CX3CR1^{int}) was also present in the steady state mucosa, but this was remarkably heterogeneous, with at least 4 subsets distinguishable on the basis of Ly6C, class II MHC, F4/80 and CD11c expression. These included F4/80⁺Ly6C^{high}MHCII^{neg}CD11c^{neg} cells that were phenotypically indistinguishable from blood monocytes, F4/80⁺Ly6C⁺MHCII⁺CD11c^{+/-neg} cells and F4/80⁺Ly6C^{neg}MHCII⁺CD11c^{+/-int} cells that were phenotypically and morphologically similar to CX3CR1^{high} mφ except for their lower level of CX3CR1. Finally there was a minor subset of F4/80^{neg}Ly6C^{neg}MHCII⁺CD11c^{high} cells that expanded markedly in response to *in vivo* flt3L treatment and appeared to be genuine DC. CX3CR1^{neg} cells were also found within the CD11b⁺ population in the healthy mucosa, most of which were Siglec F⁺ eosinophils, together with a few neutrophils. In the second half of Chapter 3, I examined how these populations changed during acute colitis induced by feeding dextran sodium sulphate (DSS). These experiments demonstrated that the CX3CR1^{int} compartment expanded dramatically during acute inflammation, with preferential accumulation of the Ly6C^{high} subsets and relative loss of the CX3CR1^{high} population as colitis progressed. Together these studies suggested that CX3CR1^{high} and CX3CR1^{int} cells represent resident and pro-inflammatory mφ respectively.

I next set out to explore the *in vivo* origin of the CX3CR1^{int} and CX3CR1^{high} populations, to address whether they were derived from independent precursors as would be predicted by current theories of monocyte heterogeneity, or if a relationship existed between them. By using adoptive transfer of purified BM monocytes, the studies described in Chapter 4 show that 'inflammatory' Ly6C^{high}, but not Ly6C^{low} 'resident' monocytes replenished the CX3CR1^{high} resident mφ population in the steady state mucosa. This appeared to involve local differentiation of Ly6C^{high} monocytes through CX3CR1^{int} intermediary stages, which was accompanied by the acquisition of class II MHC, loss of Ly6C and upregulation of F4/80 and CX3CR1. *In vivo* BrdU incorporation studies supported the idea that the majority of CX3CR1^{int} cells in the resting intestine represented short-lived intermediaries on their way to becoming CX3CR1^{high} mφ. Together

these studies suggested that rather than representing independent m ϕ subsets, the CX3CR1^{int} and CX3CR1^{high} cells in the resting colonic mucosa comprise a differentiation continuum from Ly6C^{high} monocytes to mature CX3CR1^{high} m ϕ . Analysis of BM chimeric mice confirmed that BM-derived monocytes were the source of the vast majority of colonic LP m ϕ . These findings were supported by the fact that CCR2 KO mice, in whom Ly6C^{high} monocyte egress from the BM is blocked, lack Ly6C^{high} colonic monocytes and have markedly reduced numbers of mature colonic m ϕ . In Chapter 4, I also explored whether factors present in the normal mucosa, such as colony stimulating factor (CSF)-1, TGF β and the chemokine CX3CL1, could direct monocytes to acquire the phenotype of mucosal m ϕ . Although initial *in vitro* studies suggest that none of these were effective on their own, *in vivo* administration of recombinant CSF-1 appeared to promote *in situ* monocyte differentiation in the gut. Taken together, the results in this chapter highlight that the CX3CR1^{high} m ϕ population is maintained by Ly6C^{high} blood monocytes and that their differentiation is controlled by local factors in the mucosa.

In Chapter 5, I went on to investigate whether the phenotypically identifiable differentiation of mucosal m ϕ was accompanied by alterations in their functional capacity. Intracellular cytokine staining, qRT-PCR and reporter gene expression revealed that as Ly6C^{high} monocytes differentiate locally through the CX3CR1^{int} stages into CX3CR1^{high} m ϕ , they progressively acquired the ability to produce IL10 and have reduced production of pro-inflammatory mediators. In addition, the maturation of monocytes was accompanied by an increased ability to phagocytose and kill bacteria. Their response to exogenous stimulation by TLR ligands also altered as differentiation proceeded, with the Ly6C^{high} monocytes responding robustly to TLR2 and TLR4 ligation in a TNF α dominated manner, whereas the CX3CR1^{high} m ϕ responded less vigorously and their TNF α production was balanced by IL10. This pattern was retained during experimental colitis, where the CX3CR1^{int} cells showed enhanced spontaneous TNF α production, whereas IL10 remained the dominant product of CX3CR1^{high} m ϕ . Adoptive transfer experiments in Chapter 6 then showed that donor Ly6C^{high} monocytes were recruited to the mucosa of colitic mice, but unlike in resting mice, they failed to acquire the CX3CR1^{high} phenotype. These results supported the idea that in inflammation, local differentiation of monocytes is arrested at an early stage before anti-inflammatory m ϕ can develop and that this allows inflammation to be perpetuated.

In Chapter 6 I also examined the role of inflammatory monocytes in the pathogenesis of colitis, again taking advantage of CCR2 KO mice. These mice showed reduced susceptibility to acute DSS colitis and this was associated with a lack of monocytes and their immediate descendants in the colon of resting KO animals. In parallel, CCR2 KO monocytes were unable to migrate to inflamed colon and together these findings confirmed that Ly6C^{high} monocytes are essential for the development of the pathology. Further experiments in Chapter 6 examined how the colonic m ϕ populations changed during the resolution phase of colitis. Within two weeks of withdrawing DSS, there was partial restoration of the CX3CR1^{high} m ϕ population and this was paralleled by a loss of the CX3CR1^{int} cells that had accumulated during inflammation. However, *in vivo* BrdU-labelling studies revealed that the reappearance of CX3CR1^{high} m ϕ was probably not due to the subsequent differentiation of recruited CX3CR1^{int} cells. These results imply that many of the Ly6C^{high} monocytes recruited during inflammation give rise to short-lived effector cells and that restoration of the resident m ϕ population may involve *de novo* recruitment of blood monocytes.

Finally, in Chapter 7, I explored some of the mechanisms that might underlie the hyporesponsiveness that intestinal m ϕ exhibit. In particular, I examined the role of the CD200R1-CD200 regulatory axis, as this has been shown to control m ϕ activity in other tissues. First, I established that resident colonic m ϕ express CD200R1 and that its ligand is expressed in the resting colon by both haematopoietic and non-haematopoietic cells. I then went on to examine the impact of CD200R1-deficiency on the colonic m ϕ pool by taking advantage of CD200R1 KO mice. This revealed that although these mice had an additional population of F4/80⁺MHCII^{int} colonic m ϕ , these lacked Ly6C expression and so were unlikely to represent recently recruited pro-inflammatory m ϕ . Colonic m ϕ from CD200R1 KO mice also expressed comparable levels of costimulatory molecules and TLR to WT mice, and showed no signs of hyper-reactivity to exogenous stimuli. Furthermore, neither CD200R1-deficiency nor lack of CD200 resulted in the development of spontaneous intestinal inflammation, or increased susceptibility to DSS colitis. Final experiments in this chapter suggested that deliberate ligation of CD200R1 on CSF-1 generated BM-derived m ϕ had little or no effect on the responsiveness of these cells to innate stimuli. Taken together, the data in Chapter 7 suggested that unlike alveolar m ϕ and microglia, the CD200R1-CD200 axis plays little or no role in controlling colonic m ϕ activity.

Collectively, the results presented in this thesis make important steps forward in our understanding of the complex network of MP in the colon during homeostasis and inflammation. By using precise characterisation of mucosal myeloid cell subsets, I have been able to show that 'inflammatory' Ly6C^{high} monocytes constantly enter the steady state mucosa, where they differentiate locally through a series of CX3CR1^{int} intermediaries to replenish the majority CX3CR1^{high} m ϕ population. This maturation process is accompanied by alterations in function, so that resident CX3CR1^{high} m ϕ are relatively desensitised to exogenous stimuli, but retain high phagocytic activity and produce IL10 constitutively. The exact factors that influence monocyte maturation and control m ϕ activity in the normal gut are still unclear, although signalling through CD200R1 alone appears to play no role in this. My studies have also established that pro-inflammatory m ϕ in the colon arise from the same Ly6C^{high} monocyte precursor and accumulation of these cells during chemically induced colitis is partly due to the arrest in the local differentiation process. The recruitment of Ly6C^{high} monocytes and their derivatives in acute inflammation is dependent on CCR2 and is central for pathology, probably due to their readiness to produce pro-inflammatory mediators such as TNF α . To the best of my knowledge, these results demonstrate for the first time that 'resident' and 'pro-inflammatory' m ϕ in the colon are not independent cell types, but rather represent alternative, context-dependent differentiation outcomes of the same monocyte precursor. These findings have important implications, as targeting of inflammatory monocyte infiltration has been considered as a potential strategy for the treatment of inflammatory bowel disorder (IBD). However given my observations that these monocytes also replenish the resident m ϕ population, the depletion or blockade of these monocytes may have impact on 'resident' m ϕ populations and might impair their immunoregulatory roles.

Chapter 1

General Introduction

1.1 Introduction

The immune system has evolved to be able to successfully detect, isolate and eliminate infectious agents. The innate and adaptive arms of the immune system work in tandem to ensure that this process is highly efficient. The innate immune system provides a robust and rapid response to pathogenic challenge and tissue damage, but this response is not antigen-specific. In contrast, although the adaptive immune system's response is delayed, it is specific to individual antigens and long-lived immunological memory is generated to allow rapid responses upon re-exposure to the same antigenic stimulus. However the immune system must also tolerate exposure to other foreign antigens, such as dietary components, environmental antigens and commensal and mutualistic bacteria. Active immune responses targeted against these antigens would not only be wasteful, but also potentially dangerous to the host. As discussed in more detail below, this is particularly important in the intestine, which encounters more foreign antigen than any other part of the immune system.

1.2 Macrophages and the Mononuclear Phagocyte System

Since being first described by Elie Metchnikoff in the 19th century, it has been appreciated that macrophages ($m\phi$) are present in almost every tissue of the body (Table 1.1). $M\phi$ are large, tissue resident myeloid cells that display stellate morphology and are characterised by the presence of pseudopodia, non-specific esterases and phagocytic granules, which give $m\phi$ a 'foamy' appearance. Although most immunologists regard $m\phi$ as effector cells of the innate immune system, they play a much wider role in the body. As implied by their name, $m\phi$ are highly efficient phagocytes and they contribute to the maintenance of tissue homeostasis through the clearance of apoptotic, senescent and damaged cells generated by tissue wear and tear. Their ability to scavenge dying material means that $m\phi$ also play a vital role during organogenesis in embryonic development, where they are highly concentrated at sites of high cell death, such as developing limb buds (1). These tissue remodelling functions are maintained in the adult, where $m\phi$ are crucially involved in wound healing after infection, injury or insult. However $m\phi$ also perform tissue-specific functions. For example, $m\phi$ in the liver (Kupffer cells) aid the removal of toxins from the circulation, while $m\phi$ in the alveolar space of the lung are specialised at engulfing and eliminating inhaled

environmental antigens, and osteoclasts are essential for bone remodelling. Although scavenging cellular debris may be their primary role under normal conditions, $m\phi$ also secrete a raft of soluble mediators that contribute to maintenance of homeostasis, including enzymes, cytokines, chemokines, arachidonic acid derivatives and glycoproteins such as fibronectin (2).

As members of the innate immune system $m\phi$ function as sentinels in all tissues, where they are strategically located close to the body's epithelial surfaces. Using a plethora of germ-line encoded pattern recognition receptors (PRR), such as toll-like receptors (TLR), Nod-like receptors (NLR), C-type lectin receptors (CLR) and other scavenger receptors, $m\phi$ can detect conserved structural motifs, or so-called pathogen associated molecular patterns (PAMP), allowing them to rapidly capture and engulf any invading microorganisms. Ingested material is encapsulated in a phagosomal compartment which then fuses with highly degradative lysosomes ensuring that engulfed material is eliminated. Furthermore, by virtue of their ability to acquire antigen and their expression of class II MHC, as well as production of regulatory cytokines, $m\phi$ can also contribute to the adaptive arm of the immune system by influencing T cell behaviour. As a result, $m\phi$ play a critical role in protective immune responses. However aberrant $m\phi$ activity has been shown to be associated with many inflammatory conditions such as rheumatoid arthritis, atherosclerosis and inflammatory bowel disease (IBD), as well as malignant disease.

1.2.1 How to Identify a Macrophage

In mice, the best and most commonly used marker to identify $m\phi$ is F4/80 (Table 1.2). Although some $m\phi$ fail to express F4/80, such as splenic marginal zone $m\phi$ and osteoclasts, and others such as alveolar $m\phi$ express it only at low levels, it still proves to be the most reliable marker of murine $m\phi$ (3, 4). In addition to F4/80, most murine $m\phi$ populations also express the pan-myeloid marker CD11b and CD68 (macrosialin), as well as CD115, the receptor for CSF-1 (5), consistent with their derivation from monocytes. As discussed in detail below, some $m\phi$ in mice also express the DC marker CD11c. F4/80 is not a useful $m\phi$ marker in man, as it is expressed predominantly by eosinophils (6) and therefore expression of CD68 or CD33 is used to characterise human $m\phi$. Interestingly,

murine eosinophils have also been shown to express F4/80, albeit at lower levels than m ϕ (7).

Table 1.1: Tissue Macrophage Populations during Homeostasis

Tissue	Macrophage Population(s)	Phenotype
Central Nervous System	Microglia	CX3CR1 ^{high} F4/80 ⁺ CD11b ⁺ CD68 ⁺ MHCII ^{neg}
Lung	Alveolar macrophages	CX3CR1 ^{neg} F4/80 ^{low} CD11b ^{neg} CD11c ⁺ MHCII ^{neg}
Liver	Kupffer cells	CX3CR1 ^{neg} F4/80 ⁺ CD11b ^{low} CD68 ⁺ MHCII ⁺
Spleen	Metallophilic macrophages Marginal zone macrophages	CX3CR1 ^{neg} F4/80 ^{low/neg} CD11b ^{low/-} CD68 ⁺ MHCII ^{neg}
Bone Marrow	Bone marrow macrophages Osteoclasts	CX3CR1 ^{neg} F4/80 ⁺ CD11b ^{low} CD68 ⁺ MHCII ⁺ CD169 ⁺
Skin	Langerhans cells	CX3CR1 ⁺ F4/80 ^{neg} CD11b ⁺ MHCII ⁺ Langerin ⁺
Gastrointestinal Tract	Intestinal macrophages	CX3CR1 ^{high} F4/80 ⁺ CD11b ⁺ CD68 ⁺ MHCII ⁺
Uterus	Uterine macrophages Decidual macrophages	CX3CR1 ⁺ F4/80 ⁺ CD11b ⁺ MHCII ^{+/neg}
Peritoneum	Peritoneal macrophages	CX3CR1 ^{neg} F4/80 ^{high} CD11b ⁺ CD68 ⁺ MHCII ^{neg}

Table 1.2: Cell Surface Markers of Tissue Macrophages

Surface Marker	Gene	Expression/Comments	Proposed Function
F4/80	<i>Emr1</i>	Pan-m ϕ marker Variable levels of expression Unknown ligand	Adhesion Maintaining peripheral tolerance
CD11b	<i>Itgam</i>	Pan-myeloid integrin Expressed by numerous cells Component of complement receptor 3 (CR3)	Phagocytosis Adhesion to endothelium
CD11c	<i>Itgax</i>	Expressed by most, if not all tissue m ϕ Typically associated with DC Component of complement receptor 4 (CR4)	Phagocytosis Adhesion
CD68	<i>Cd68</i>	Expressed by all mouse and human m ϕ Expressed intracellularly - limited usefulness for functional analysis	Phagocytosis Potentially involved in regulating antigen processing
CD115	<i>Csf1r</i>	Receptor for CSF-1 Expressed on all cells of the m ϕ lineage	Receptor for CSF-1 Survival, proliferation and differentiation of m ϕ

1.2.2 Macrophage Development

M ϕ , along with monocytes and DC, are part of the mononuclear phagocyte system (MPS). The concept of the MPS was originally proposed by van Furth and colleagues (8) in the 1970's and was described as a family of cells that are derived from a common BM progenitor that differentiates into blood monocytes, which in turn give rise to tissue resident m ϕ and DC throughout the body. Although the basic concept of the MPS still remains, this linear model is rather simplistic and it is now appreciated that there is considerable heterogeneity within the MPS (9).

Monocytopoiesis in the BM involves the differentiation of monocytes from haematopoietic stem cells (HSC) through a number of morphologically distinct intermediate stages, from the common myeloid progenitor (CMP), to the granulocyte/m ϕ progenitor (GMP) and the m ϕ /dendritic cell progenitor (MDP) (Fig. 1.1). At each of these stages there is progressive lineage commitment and cells lose the potential to give rise to the other cell types. The MDP, which has lost granulopoietic potential, has been shown to give rise to monocytes and m ϕ , as well as both classical DC (cDC) and plasmacytoid DC (pDC) (10). The MDP is characterised by expression of CD115, CD117 (c-kit) and CD135 (flt3), together with the chemokine receptor CX3CR1 that is proposed to mark dedication to the myeloid lineage (10). Development of mature monocytes involves differentiation into monoblasts and pro-monocytes, both of which have a rapid turnover in the BM (11). Unlike their pro-monocyte precursors, newly differentiated monocytes are thought to exit cell cycle, thereby losing their proliferative potential (11, 12).

The development of cells of the MPS is reliant on a panel of transcription factors, which can be split into two groups. First, there are transcription factors that are essential for the direct control of myeloid cell differentiation in the BM, such as PU.1 and AML (13-15). This group also includes transcription factors that maintain survival of stem cells or pluripotent precursors in the BM, such as GATA-2, SCL and *c-Myb* (16-18). The second group of transcription factors activates or represses key m ϕ genes, but are not essential for m ϕ development and these include NF-M/C/EBP α , HOXB7 and *c-Myc* (19). Furthermore, specific transcription factors including C/EBP β , EGR-1, NF-Y, IFN-regulatory factor (IRF)-1, -4 and -5, as well as Jun/Fos and STAT proteins involved in cytokine signalling, have been shown to be involved in specific aspects of m ϕ differentiation/maturation (19).

PU.1 is the most vital of these transcription factors and it has been described as the 'master regulator' of m ϕ development, although it also plays a role in B cell development (13, 14). PU.1 belongs to the Ets transcription factor family and is in turn dependent on the activity of the Runt-related transcription factor (RUNX)-1 (20). Although not essential for initial commitment to the myeloid lineage, PU.1 is indispensable for the subsequent differentiation of myeloid progenitors into m ϕ . It not only activates specific genes such as CSF-1R, but also causes specific histone modifications in the enhancer regulatory elements of m ϕ -specific genes, thereby generating open DNA for other transcription factors such as NF- κ B to bind (21). Knockout of PU.1 is embryonic lethal, but whether this is due solely to a defect in m ϕ development is unclear, as PU.1 KO mice have defects in multiple haematopoietic lineages including m ϕ and granulocytes, as well as in B- and T-lymphocytes (14).

Once generated, monocytes leave the BM in a process that is highly dependent upon the chemokine receptor CCR2 and as a result CCR2-deficient mice have a significant defect in their circulating monocyte reservoir (22). Monocytes remain in the circulation for up to 2 days before migrating into tissues and differentiating into m ϕ (23). Although it is clear that monocytes have no proliferative potential in the bloodstream, it is poorly understood whether they can proliferate after arrival in tissues. Studies by Geissmann and colleagues have proposed that there may be at least two distinct monocyte subsets in mice (Figure 1.1) (12), an idea which has been long established in man (24). In mice, these subsets have been distinguished on the basis of differential expression of Ly6C (or Gr-1) and CX3CR1 (12). Monocytes that express high levels of Ly6C and intermediate levels of CX3CR1 (referred to hereafter as Ly6C^{high} monocytes), also express the chemokine receptor CCR2 and the adhesion molecule CD62L (L-selectin). These Ly6C^{high} monocytes are termed 'inflammatory' monocytes due to their propensity to migrate to sites of inflammation in multiple disease models and to produce pro-inflammatory cytokines during infection or tissue damage (12, 22, 25, 26). The second major monocyte subset in mice is defined by low expression of Ly6C, high levels of CX3CR1 and CD43, but low or no expression of CCR2 and CD62L (referred to here as Ly6C^{low}). These Ly6C^{low} monocytes have been denoted 'resident' monocytes as they were found in both resting and inflamed tissues following adoptive transfer (12). However little direct evidence currently exists to support the notion that Ly6C^{low} monocytes contribute significantly to

replenishment of tissue $m\phi$ in the steady state. More recently, Auffray *et al.* have used intra-vital microscopy to show that $Ly6C^{low}$ monocytes exhibit 'patrolling' behaviour in the vasculature, where they crawl along the blood vessel in a process that is independent of blood flow and dependent upon the $\beta 2$ integrin and CX3CR1 (27). It is postulated that this allows $Ly6C^{low}$ monocytes to scavenge dead cells, lipids and blood-borne pathogens present in the vascular system and that this may be their specialised function, rather than to replenish $m\phi$ populations in parenchymal tissues (27).

The exact relationship between $Ly6C^{high}$ and $Ly6C^{low}$ monocytes is complicated by studies suggesting the former may be the precursor of the latter. This concept is supported by the fact that $Ly6C^{high}$ monocytes appear to have a very short half-life *in vivo* and lose $Ly6C$ expression around 48hrs after adoptive transfer into congenic hosts (12, 28). Furthermore, studies employing clodronate liposome-mediated cell depletion strategies have demonstrated that reconstitution of the $Ly6C^{low}$ blood monocyte compartment is secondary to the establishment of the $Ly6C^{high}$ monocyte fraction (29). In addition, a third monocyte subset has been described with an intermediate phenotype ($Ly6C^{int}CX3CR1^+$), which may represent monocytes in transition from the $Ly6C^{high}$ to $Ly6C^{low}$ phenotype (30). However, other studies have suggested that $Ly6C^{high}$ monocytes can be depleted with little effect on $Ly6C^{low}$ monocytes (31) and thus conversion of blood monocytes remains a contentious issue.

Analogous monocytes subsets have been identified in humans, albeit using different cell surface markers. Differential expression of CD14, the LPS co-receptor, and CD16 ($Fc\gamma RIII$) allow segregation of at least two monocyte subsets, and gene expression profiling and cluster analysis have enabled parallels to be drawn between the human and mouse (32, 33). Monocytes expressing high levels of CD14 but lacking CD16 expression ($CD14^{high}CD16^{neg}$) comprise 80-90% of human blood monocytes (12). These monocytes also express high levels of CCR2 and are believed to be the equivalent to murine $Ly6C^{high}$ 'inflammatory' monocytes (12, 34). However the cytokine profiles of $CD14^{high}CD16^{neg}$ human monocytes and $Ly6C^{high}$ murine monocytes are distinct. Whereas murine $Ly6C^{high}$ monocytes produce a panel of pro-inflammatory cytokines (including $TNF\alpha$, IL1 and IL6) upon stimulation with LPS, $CD14^{high}CD16^{neg}$ human monocytes respond in an IL10

dominated manner to identical stimulation (35). Thus one must apply caution when drawing parallels between these monocyte populations in different species.

The smaller CD14⁺CD16^{high} subset of human monocytes expresses high levels of CX3CR1 and low levels of CCR2 and thus is similar to murine Ly6C^{low} 'resident' monocytes (12, 34). These cells also have poor phagocytic activity and do not produce pro-inflammatory cytokines in response to LPS stimulation, but their role in replenishment of tissue m ϕ remains elusive. As in mice, a third monocyte subset has been identified in human blood. This subset also displays an intermediate phenotype (CD14⁺CD16⁺) and again may represent monocytes in transition from the CD14^{high}CD16^{neg} to CD14^{dim}CD16^{high} phenotype. However, these CD14⁺CD16⁺ monocytes possess unique functional characteristics, such as robust pro-inflammatory cytokine production in response to LPS stimulation *in vitro* and they expand during inflammation, suggesting they may represent a distinct population of blood monocytes with inflammatory functions (36).

Although typically associated with m ϕ replenishment, monocytes have also been shown to give rise to classical DC. The differentiation of monocytes into DC was proposed to occur following transendothelial migration, whereas monocytes that remained in the subendothelial matrix differentiated into m ϕ (37). However it is now clear that there are DC-committed precursors which are independent of monocytes. The MDP has been shown to give rise to plasmacytoid DC (pDC) directly, and to the pre-cDC, which can differentiate into classical DC, but not pDC or m ϕ (10) (Fig. 1.1). Some believe that this occurs through a common dendritic cell precursor (CDP) intermediate (38, 39), although others have suggested that the MDP and the CDP are phenotypically and developmentally overlapping (40). Thus there are probably distinct precursors that replenish bona fide DC and tissue m ϕ during steady state and inflammatory conditions.

1.2.3 Growth Factors in Macrophage Development

Differentiation of HSC into monocytes via various intermediary progenitors is dependent on the presence of multiple growth factors, including colony stimulating factor (CSF)-1 (also known as m ϕ -colony stimulating factor; M-CSF), CSF-2 (granulocyte-macrophage stimulating factor; GM-CSF), IL3, stem cell factor (SCF; also known as c-kit-ligand) and IFN γ (41, 42). Of these, CSF-1 is

indispensable for m ϕ development *in vivo* and is the only cytokine able to drive m ϕ differentiation *in vitro* on its own. The requirement for CSF-1 is evidenced by the major m ϕ defects seen in CSF1^{op/op} mice, which have a naturally occurring frame-shift mutation in the gene encoding CSF-1 (41). These osteopetrotic mice have significant reductions in most tissue m ϕ populations, low body weight and skeletal abnormalities due to defective bone remodelling (41, 43). Mice with a targeted deletion of the CSF-1R display a more severe m ϕ phenotype than *op/op* mice (44), implying that CD34, the newly identified and only other CSF-1R ligand (45), may also play a crucial role in m ϕ development. In addition to a role in BM monocytopoiesis, it has been suggested that CSF-1 may play an equal, or even more important role in maintaining differentiated m ϕ populations in peripheral tissues. Indeed CSF-1^{op/op} mice have relatively preserved BM monocyte production, but vast reductions in most tissue m ϕ (46). Furthermore, tissue-restricted over-expression of CSF-1 leads to increases in local m ϕ numbers in mice (47, 48) and delivery of exogenous CSF-1 has been shown to expand some tissue m ϕ populations, as well as having an effect on blood monocyte numbers (46, 49). The exact mechanism by which CSF-1 increases tissue m ϕ numbers is unclear. Although a direct effect on m ϕ proliferation or survival is the most straightforward mechanism, CSF-1 has also been shown to induce resident m ϕ populations to produce chemokines that facilitate recruitment of blood monocytes to the uterus (50) and damaged kidney (51). Interestingly, m ϕ resident in lymph nodes and the thymus remain unaffected in CSF-1^{op/op} mice, implying that CSF-1 independent m ϕ may also exist (52). Alternatively, other growth factors such as CSF-2, fms-like tyrosine kinase 3 ligand (flt3L), vascular endothelial growth factor (VEGF)-A or lymphotoxin $\alpha_1\beta_2$ may compensate for the CSF-1 deficiency in CSF-1^{op/op} mice, a notion supported by the fact that the phenotype of osteopetrotic mice improves with age (53, 54).

1.2.4 Self-Renewal of Tissue Resident Macrophages

Although monocytes are likely to be the origin of most tissue m ϕ , there is evidence that tissue resident m ϕ may also be maintained through *in situ* self-renewal. Fate-mapping studies have demonstrated that m ϕ are already present in the yolk sac as early as d7.5 of embryonic development in the mouse (55). This is before the establishment of the circulatory system and thus these m ϕ are thought to arise independent of blood monocytes. M ϕ derived from these non-

haematopoietic precursors appear to persist into adult life through a process of self-renewal and examples include microglia of the central nervous system (CNS), Langerhans cells in the epidermis of the skin and alveolar m ϕ of the lung (56-58). Other studies employing parabiosis of congenic mice have confirmed that the homeostatic maintenance of these m ϕ populations under resting conditions has been shown to be largely independent of blood monocytes and CCR2 (57, 59-61). It remains unclear whether these m ϕ are present in all parenchymal tissues and what their functions are. However these cells could act as sentinels in the periphery as sensors of tissue damage or infection and release mediators that trigger other components of the immune response.

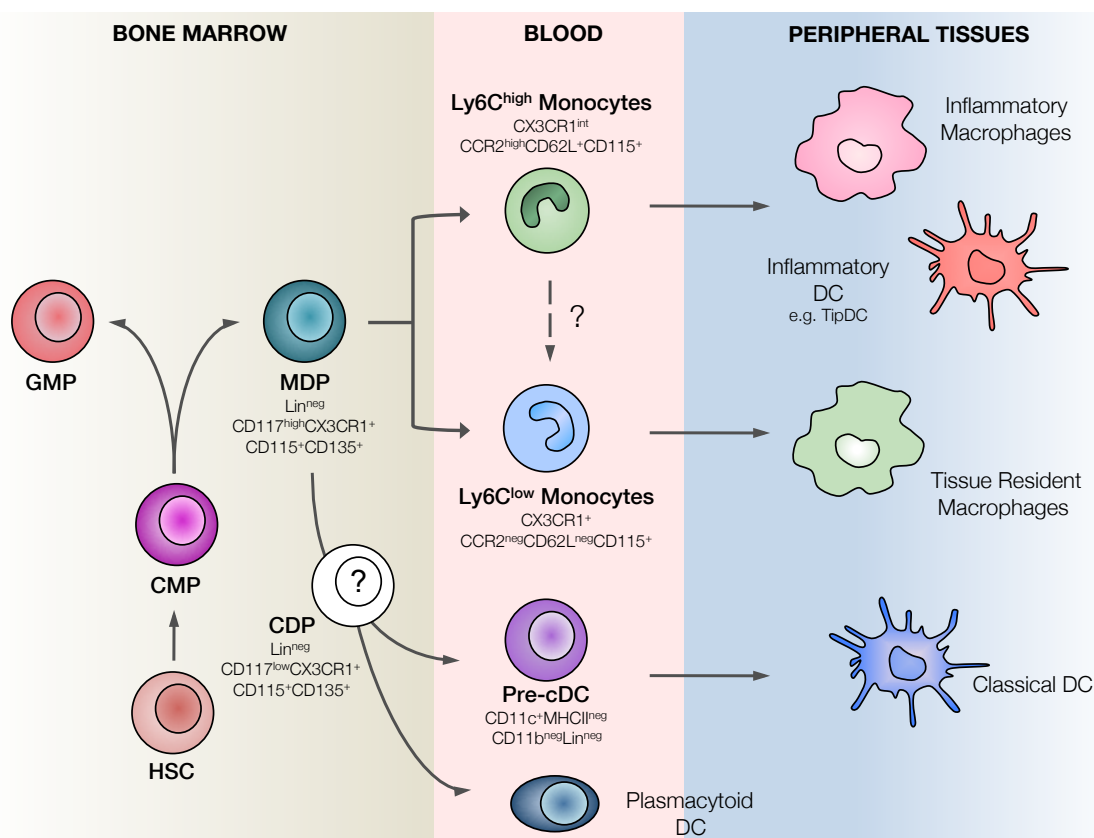


Figure 1.1: The Accepted View of the Mononuclear Phagocyte System

In the bone marrow (BM), haematopoietic stem cells (HSC) give rise to common myeloid progenitors (CMP), which in turn give rise to the macrophage and dendritic cell precursor (MDP). The MDP gives rise to monocytes, which have been shown to comprise of at least two subsets distinguished on the basis of Ly6C, CX3CR1 and CCR2 expression. Ly6C^{high}CX3CR1^{int}CCR2⁺ monocytes are classified as 'inflammatory' monocytes and give rise to inflammatory m ϕ and TNF α and iNOS-producing (Tip) DC in inflamed tissue. Ly6C^{low}CX3CR1⁺CCR2^{neg} monocytes are termed 'resident' and are reported to be involved in the homeostatic replenishment resident m ϕ populations, as well as patrolling the vasculature. MDP also gives rise to all DC subsets. Classical DC arise from DC-committed precursors (pre-cDC) that are downstream of the MDP, however it remains controversial whether this involves progression through a common DC progenitor (CDP) stage. Plasmacytoid DC (pDC) arise directly from the MDP/CDP without passing through a pre-DC stage.

1.3 Macrophage 'Activation'

As discussed above, m ϕ are highly plastic cells that play important roles in tissue homeostasis in every tissue of the body. However disruption of tissue homeostasis by infection, inflammation or trauma results in m ϕ activation, which is associated with phenotypic and functional alterations. Historically m ϕ activation was regarded as a uniform phenomenon that resulted in the increased capacity to destroy microbial pathogens and was followed by m ϕ 'deactivation'. However it is now appreciated that activated m ϕ can be 'polarised' into distinct phenotypes dependent upon the cues received from their tissue environment.

1.3.1 Classical Macrophage Activation

Classical m ϕ activation results from the recognition of PAMPs on the surface of Gram-positive and Gram-negative bacteria. M ϕ express a range of TLR and other PRR which are triggered during phagocytosis of pathogenic material (Fig. 1.2). As detailed below, this results in the production of pro-inflammatory cytokines including TNF α , IL1, IL6, IL12 and IL23 and chemokines such as CXCL9 (MIG) and CXCL10 (IP10) (62) (Fig. 1.3). Classical activation of m ϕ is dependent on the transcription factors STAT1 and IRF5 activity (63, 64). Pro-inflammatory mediators released by classically activated (or M1) m ϕ facilitate the recruitment of inflammatory leucocytes such as monocytes and neutrophils, as well as the polarisation of T lymphocytes to the T_H1 and/or T_H17 phenotype, cells which are known to perpetuate the inflammatory response. These m ϕ also express inducible nitric oxide synthase (iNOS or NOS2) allowing them to generate nitric oxide (NO) from L-arginine. NO causes DNA damage and is essential for the elimination of bacteria within m ϕ (65). M1 m ϕ also produce other cytotoxic mediators such as superoxide anions and other oxygen radicals through expression of the NADPH oxidase enzyme. Given that mice deficient in both iNOS and NADPH (phagocyte oxidase) develop large abscesses which are rich in enteric commensal bacteria (66), suggests that NO-mediated mechanisms are essential in the elimination of ingested bacteria by m ϕ . In addition, patients with chronic granulomatous disease (CGD) suffer from recurrent bacterial and fungal infections due to a defect in their NADPH oxidase gene. Together these effector functions demonstrate that classically activated m ϕ are highly specialised in destroying intracellular microorganisms. Furthermore, their ability to upregulate the

expression of class II MHC and costimulatory molecules, allows classically activated $m\phi$ to act as antigen presenting cells (APC) for T cells. However these potent pro-inflammatory properties also mean that classically activated $m\phi$ must be tightly controlled, as aberrant or excessive activity can lead to tissue damage. Indeed, $m\phi$ exhibiting M1 characteristics are commonly found in pathology associated with chronic inflammatory conditions such as atherosclerosis, rheumatoid arthritis and IBD (67-69).

1.3.2 Alternative Macrophage Activation

Although first associated with the ability to inhibit classical $m\phi$ activation, it is now clear that the T_H2 type cytokines IL4, IL13 and IL33 cause $m\phi$ to polarise to an 'alternative' activation state, a process controlled by the transcription factors IRF4, STAT6 and PPAR γ (70, 71). These alternatively activated (AAM or M2) $m\phi$ are commonly found during parasitic infection, allergy and in the healing phase after tissue damage (72). M2 $m\phi$ are characterised by their high phagocytic activity and expression of CD206 (mannose receptor), FIZZ1 (also known as Relm- α) and Ym-1 (also known as CHI3L3) (72). Unlike M1 $m\phi$, M2 $m\phi$ do not express iNOS and are poor producers of reactive oxygen and nitrogen species. Instead, these IL4/IL13/IL33 polarised $m\phi$ express arginase-1 (73), allowing them to convert L-arginine to L-ornithine, which is a precursor of polyamines and collagen, and facilitates tissue remodelling and encapsulation of helminths (72). The chitinase-like molecule Ym-1 has similar properties via its carbohydrate and matrix-binding activity (74). M2 $m\phi$ also have a unique cytokine and chemokine expression profile. Whereas M1 $m\phi$ produce high levels of pro-inflammatory cytokines such as TNF α and IL12, M2 $m\phi$ produce only low levels of these cytokines and instead produce high levels of the immunomodulatory cytokines IL10 and TGF β , as well as the pro-angiogenic cytokine VEGF (75). TGF β together with platelet-derived growth factor (PDGF) has been shown to stimulate fibroblast differentiation and proliferation thus adding to the tissue remodelling role of M2 $m\phi$ (76, 77). Consistent with their associations with T_H2 -mediated immune responses, M2 $m\phi$ also produce CCL17, CCL22 and CCL24 (78-80), all of which are ligands for CCR3 and CCR4, chemokine receptors expressed by T_H2 cells, eosinophils and basophils. This chemokine signature confirms their possible involvement in T_H2 -polarised immune responses such as parasitic clearance and in tissue repair, which is appropriate for large tissue dwelling organisms that disrupt the local

architecture. The maintenance of M1 versus M2 $m\phi$ also appears to involve distinct mechanisms. Whereas M1 $m\phi$ are thought to derive entirely from circulating blood monocytes, it has been shown recently that alternatively activated $m\phi$ that arise in the T_H2 setting may also be maintained through self-renewal, a process that is highly dependent on IL4 (81).

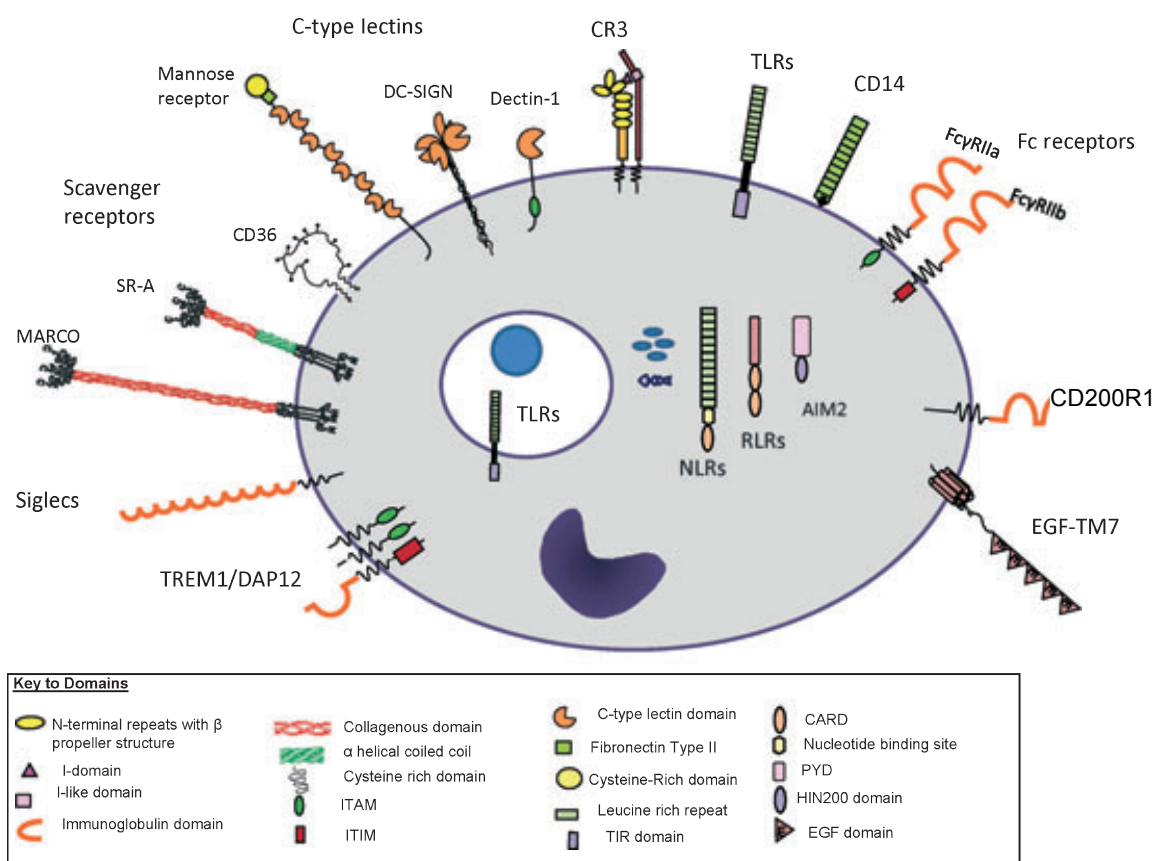


Figure 1.2: Pattern Recognition Receptors expressed by Macrophages

Tissue macrophages express a diverse range of pattern recognition receptors including Toll-like receptors (TLR), complement receptors and scavenger receptors. They also express inhibitory receptors such as CD200R1 which has been shown to negatively regulate macrophage activity. Taken from (82).

1.3.3 Regulatory Macrophages

There is growing appreciation that the idea of $m\phi$ polarisation into M1 or M2 states is probably over-simplistic and that these polarisation states likely represent two extreme ends of an activation spectrum, with many $m\phi$ phenotypes in between (62). One particular example of this is regulatory or 'M2-like' $m\phi$, which possess

some of the features of both M1 and M2 m ϕ . Regulatory m ϕ express CD206 and the scavenger receptor CD163 and like M2 m ϕ , they produce high levels of IL10 but low levels of TNF α and IL12 (83). Despite this inhibitory phenotype, regulatory m ϕ are avidly phagocytic and express class II MHC and costimulatory molecules, potentially allowing them to interact with T-lymphocytes (83). The exact conditions that lead to polarisation of m ϕ into this regulatory phenotype remain to be fully elucidated. However, glucocorticoids, IL10 and TGF β have been implicated (84, 85), as has phagocytosis of apoptotic cells, which may act by inducing TGF β (86). FcR-mediated signalling by immune complexes has also been proposed to cause induction of the regulatory phenotype in m ϕ , usually acting in concert with TLR ligands (87). Furthermore, CCL2 has been shown to induce M2-like phenotype in human monocytes (88). M ϕ exhibiting a regulatory/M2-like m ϕ phenotype have been shown to be present *in vivo* in the placenta and the uterus, and appear to be the major m ϕ type in tumours (50, 89, 90). Tumour associated m ϕ (TAM) promote tumour growth through the production of growth factors such as VEGF and by inducing/maintaining Treg via the production of IL10 and CCL22 (75, 91). Increased CSF-1 and CSF-1R expression correlates with poor prognosis in patients with certain cancers (92), and over expression of CSF-1 in mice leads to acceleration of tumour growth and metastasis (48), implying that m ϕ can support tumour development and growth.

Thus the plastic nature of tissue m ϕ allows them to adopt different phenotypic and functional/activation states in order to perform functions that are tailored to provide specific functions in distinct tissues and environments. Furthermore, it has been suggested that m ϕ can move between these activation states, as is likely to be necessary to fulfil the various requirements at different stages of infection or in distinct anatomical locations. As discussed more fully below, this is particularly true for intestinal m ϕ that require many adaptations to allow them to exist in harmony with their antigen and microbe rich environment.

1.3.4 Regulation of Macrophage Activation

As noted above, m ϕ possess a plethora of receptors that allow them to sense microbes and damaged tissue. These include TLR, NLR, retinoic acid inducible-I (RIG-I)-like receptors, as well as the mannose receptor (CD206) and scavenger receptors such as CD36, MARCO and scavenger receptor A (SR-A).

Furthermore, $m\phi$ express Fc receptors and complement receptors that allow them to recognise and engulf opsonised particles.

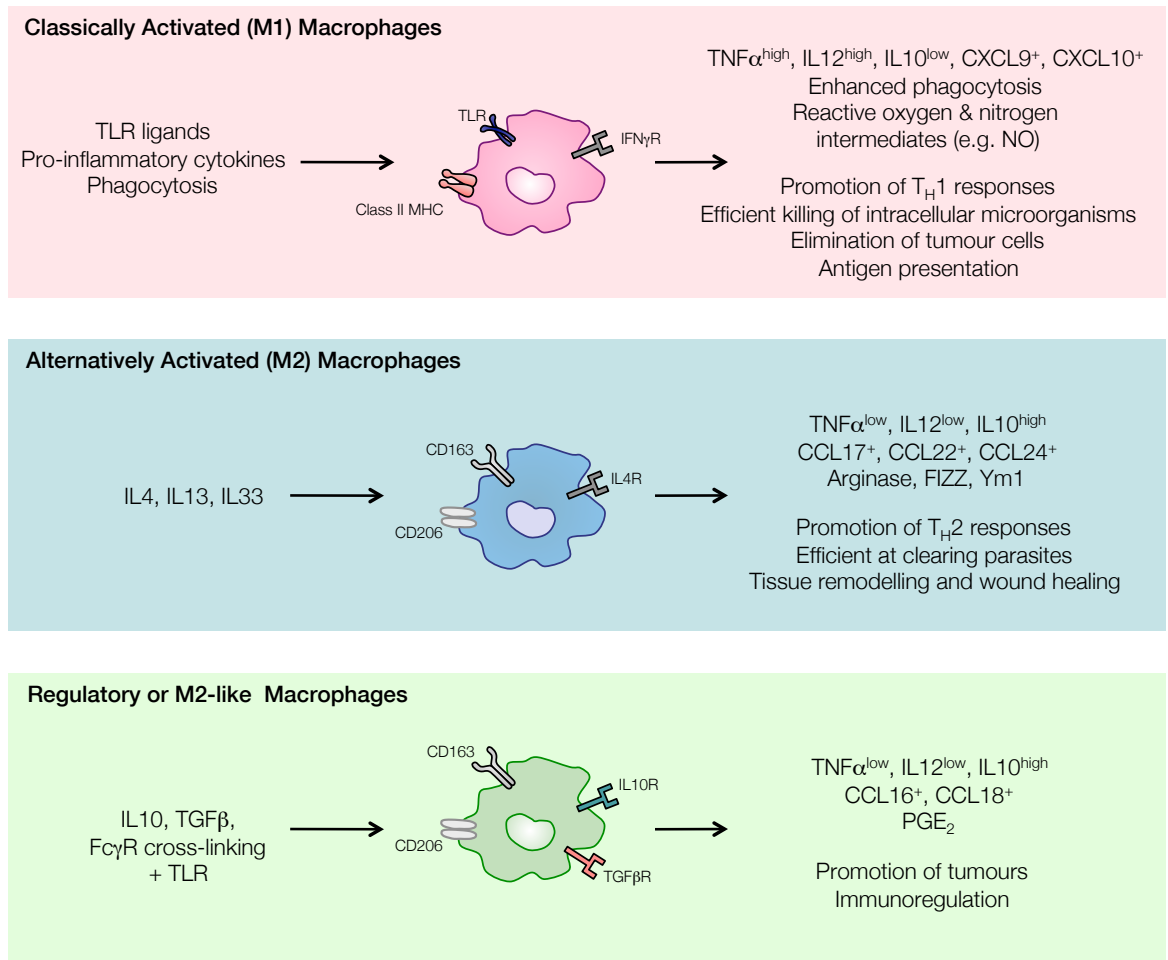


Figure 1.3: Macrophage Activation

The factors that induce and the characteristics that define classically activated, alternatively activated and regulatory macrophages.

The most studied family of receptors are the TLR. To date 10 TLR have been identified in humans and 13 in mice, and between them, they recognise many different PAMPs associated with bacteria, viruses, fungi and helminths, as well as endogenous ligands released by damaged cells (93). TLR have to dimerise to function and can be expressed on the cell surface or intracellularly. Surface TLR1 and TLR2 heterodimerise to recognise bacterial triacylated lipoproteins, while dimerisation of TLR2 with TLR6 allows recognition of bacterial diacylated lipoproteins. TLR4 and TLR5 form homodimers on the cell surface and recognise bacterial LPS and flagellin, respectively. TLR3, TLR7 and TLR9 are associated with endosomal compartments and recognise viral double stranded RNA, viral

single stranded RNA or unmethylated CpG-motifs in bacterial and viral DNA, respectively (93).

Recognition of ligands by TLR occurs through their extracellular leucine rich repeat (LRR) elements and causes a conformational change to occur, thereby bringing their intracellular Toll/IL1 receptor (TIR) domains together. For most TLR, the MyD88 adaptor molecule is recruited to the TIR domain, which in turn recruits IL1 receptor associated kinase (IRAK)4 (93). IRAK4 causes phosphorylation of IRAK1, which then binds TNF receptor activated factor (TRAF)6. The IRAK1-TRAF6 complex then dissociates from MyD88 and activates TGF β -activated kinase (TAK)1 and TAK1 binding protein (TAB)2. This leads to the phosphorylation of the inhibitory κ B (IKK) complex which in turn phosphorylates I κ B, causing the release of NF- κ B from inhibition and the activation of IFN regulatory factors (IRF). NF- κ B then translocates to the nucleus and allows the transcription of pro-inflammatory cytokines, chemokines and costimulatory molecules. TLR3 ligation does not employ the MyD88 pathway, but results in the recruitment of TIR-domain containing adaptor protein inducing IFN β (TRIF) that acts to induce the expression of the transcription factor IRF3, leading to the production of type I IFN. TLR4 signalling can signal via MyD88 or TRIF dependent routes, causing activation of the TRIF-related adaptor molecule (TRAM), which in turn leads to activation of IRF3 and NF- κ B. Together these pathways allow TLR ligation to generate robust pro-inflammatory responses.

Uncontrolled, prolonged or excessive m ϕ activation can be deleterious to the host due to the potential for m ϕ to cause pathology and therefore multiple mechanisms exist to ensure m ϕ activity is regulated. First, there are in-built negative feedback loops that terminate TLR signalling. For example LPS stimulation is known to cause the induction of MyD88s, a splice variant of the MyD88 protein that lacks the necessary domain to interact with IRAK4, thereby inhibiting positive TLR signalling (94). Similarly, IRAK-M is a TLR-inducible molecule that inhibits the dissociation of IRAK1-IRAK4 complexes from MyD88, thereby preventing further signalling (95), while TOLLIP prevents phosphorylation of IRAK (96). A20 is a molecule that terminates TLR signalling through the removal of ubiquitin from TRAF6, thereby interfering with the TLR signalling pathway (97). That A20 KO mice develop IBD, as well as spontaneous inflammation in other tissues, demonstrates that regulation of TLR by this

molecule is vital (98). Similarly, the single immunoglobulin IL1-receptor related molecule (SIGIRR; also known as Tir8) is a decoy for TRAF6 and IRAK1, and SIGIRR-deficient mice are more susceptible to intestinal inflammation (99). More recently it has been shown that microRNAs (miRNAs) can regulate TLR function. miRNAs are small non-coding RNAs that complex with the RNA-induced silencing complex, which causes posttranscriptional pro-inflammatory gene repression (100). The best documented of these is miR-146, which is induced in m ϕ by LPS (101) and targets IRAK1, IRAK2 and TRAF6 mRNA downstream of MyD88, thereby preventing activation and nuclear translocation of NF- κ B (101). The importance of miR-146 regulation of TLR stimulation is evidenced by heightened m ϕ responses to LPS and the development of a fatal spontaneous autoimmune disorder in miR-146 KO mice (102).

In addition to regulation of TLR, m ϕ express a multitude of inhibitory receptors that control their activation. Many of these inhibitory receptors are paired with structurally related receptors involved in activation, such as those belonging to the immunoglobulin domain superfamily and the C-type lectin family (103). Within the immunoglobulin superfamily, these include signal regulatory proteins (SIRP), triggering receptors expressed by myeloid cells (TREM) and the CD200 receptor (CD200R) family. SIRP α is an inhibitory receptor expressed by most myeloid cells that interacts with the ubiquitously expressed molecule CD47 (104). This interaction allows SIRP α to associate with the phosphatases SHP-1 and SHP-2 to downregulate pro-inflammatory features of myeloid cells. In contrast, SIRP β is associated with activation through its interaction with the adaptor molecule DAP-12, whereas very little is known about the third member of the family, SIRP γ (104). Similarly, whereas TREM-1 is a potent amplifier of pro-inflammatory responses in monocytes, m ϕ and some granulocytes (105), TREM-2 has been shown to attenuate m ϕ activation induced by TLR ligation and thus m ϕ from TREM2 KO mice showed enhanced pro-inflammatory cytokine release in response to TLR stimulation (106).

The CD200R family is more complex. There are currently five known members of the CD200R family (CD200R1-5 or CD200RLa-e), one of which has a well defined inhibitory role, namely CD200R1 (107). CD200R1 is expressed by m ϕ , DC, mast cells, as well as some peripheral T_H2 cells (108). There is currently only one identified ligand for the CD200R family, CD200 (formerly known as OX2),

which is expressed by a variety of non-haematopoietic cells including neurons of the central nervous system (CNS), keratinocytes, placental trophoblasts and endothelial cells, as well as B cells, activated T cells, follicular DC and thymocytes (Fig1.4) (109). Importantly, this pattern of expression is largely conserved between rodents and humans. The other CD200Rs have activating functions and it is controversial whether they bind CD200, or if they have distinct ligands (110, 111).

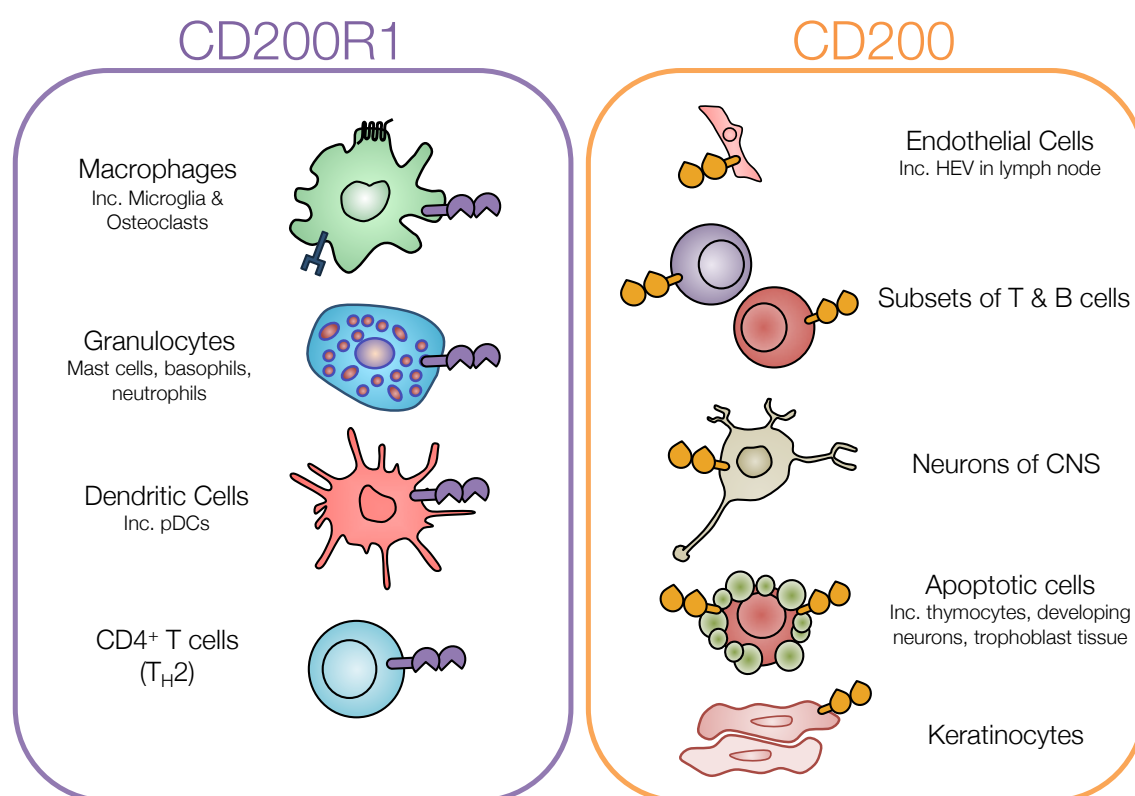


Figure 1.4: Expression Pattern of CD200R1 and its ligand CD200

Although originally thought to be a costimulatory molecule due to its structural homology with CD80 and CD86 (112), it is now believed that the primary role of CD200 is in the regulation of myeloid cell activity through CD200R1 (113, 114). The CD200-CD200R1 interaction delivers a unidirectional, negative signal to the CD200R1-bearing cell, whereas CD200 has a small cytoplasmic domain and so delivers no signal into the CD200⁺ cell (115). CD200-deficient mice have expanded populations of splenic and MLN m ϕ , as well as increased microglial activation under steady state conditions (113). Excessive m ϕ activation in CD200-deficient mice is associated with accelerated disease in experimental autoimmune encephalomyelitis (EAE) and increased susceptibility to collagen-induced arthritis

(CIA). CD200 KO mice show more intense infiltration of the retina by NO-producing m ϕ during experimental autoimmune uveoretinitis (EAU) (113, 116, 117). CD200-deficiency also renders mice resistant to UV-mediated induction of tolerance in the skin and lack of CD200 expression by keratinocytes leads to autoimmune destruction of hair follicles (118). More recently, CD200R1-mediated regulation of m ϕ has been reported in the lung, where alveolar m ϕ from CD200 KO mice showed uncontrolled activation characterised by excessive pro-inflammatory cytokine production. During experimental influenza infection this leads to extensive tissue pathology, although mice also show higher protection against the virus (119). Control of m ϕ activity in CD200 KO models can be restored using agonistic anti-CD200R1 antibodies or CD200-Fc fusion proteins, directly confirming the importance of the CD200-CD200R1 axis in controlling m ϕ behaviour (119, 120).

The cellular and molecular basis of the effects of the CD200-CD200R1 axis remain to be defined precisely. However, unlike most myeloid inhibitory receptors, CD200R1 does not possess an immunoreceptor tyrosine-based inhibitory motif (ITIM) that could bind inhibitory enzymes directly (103). In mast cells it has been shown that after binding CD200, CD200R1 is phosphorylated and recruits the adapter molecules Dok-1 and Dok-2 (121). This in turn recruits the inhibitory molecules SH2 domain containing inositol phosphatase (SHIP) and RasGAP, resulting in the inhibition of transcription factors of the Ras/MAPK pathway including ERK, JNK and P38 MAPK, and downregulation of pro-inflammatory signalling cascades (121). The role of Dok proteins in the inhibitory effects of CD200R1 is supported by the fact that Dok protein deficiency results in enhanced TNF α and NO production after LPS challenge of peritoneal m ϕ (122). Thus it appears that the CD200R1-CD200 axis represents a novel regulatory pathway independent of ITIMs.

CD200R1 has also been shown to be involved in the induction of indoleamine 2,3-dioxygenase (IDO) in plasmacytoid DC (pDC) in a type I IFN-dependent manner (123). Expression of IDO by DC can promote the induction of regulatory T cells, although this pathway has not been examined in CD200R1-bearing m ϕ . In addition, regulation by CD200R1 may be triggered by the uptake of apoptotic cells, as these cells have been shown to upregulate CD200 (124) and thus loss of CD200 could lead to m ϕ hyperactivity.

These findings have been backed up by a limited number of reports using CD200R1-deficient mice, in whom allograft rejection may be more rapid (125). In addition, splenocytes from these mice have heightened baseline pro-inflammatory cytokine production and respond more aggressively to LPS stimulation (125). CD200R1 KO alveolar m ϕ also have heightened pro-inflammatory cytokine release upon stimulation with IFN γ (119). However it has been suggested by others that CD200R1-mediated regulation of m ϕ is limited to activation via pro-inflammatory cytokines such as IFN γ and IL17, and that TLR ligands override CD200R1 signals, thereby allowing m ϕ to respond during infection (126).

Because of its ability to restrict m ϕ activation, CD200R1 has also become a target of pathogens trying to evade the immune system and many viruses such as herpesviruses and poxviruses express homologues of CD200. For example the human herpesvirus K14 protein binds the human CD200R1 with similar affinity to CD200, causing down regulation of pro-inflammatory cytokine release (127).

Thus there is substantial evidence that CD200R1-mediated down-modulation of m ϕ may be an important means of regulating m ϕ function *in vivo*. However, there are no studies evaluating the role of this regulatory axis in the control of intestinal m ϕ behaviour, although one poorly documented report has suggested that MP of the intestine express CD200R1 (119). Therefore examining the role of CD200R1 in the control of colonic m ϕ activity was one of the aims of this thesis.

1.4 The Gastrointestinal Tract

The gastrointestinal (GI) tract encompasses the stomach, small intestine, caecum, large intestine/colon and rectum. The primary role of the GI tract is to process foodstuffs and allow the efficient reabsorption of nutrients and water, processes which occur in the small and large intestines respectively. These physiologic functions demand that the barrier between the host and the external environment be accessible to dietary products. However such requirements create vulnerability to attack from pathogenic organisms, and considering most pathogens enter the body via mucosal surfaces and the surface of the GI tract is the largest mucosal surface in the body, this threat is very great indeed (128). In addition to food products and potentially pathogenic organisms, the GI tract also

houses a vast community of commensal bacteria, ten times more abundant than the number of cells in the human body (129). To deal with this massive antigenic load, the intestine is home to the largest compartment of the immune system in the body and it is the job of the intestinal immune system to discriminate between pathogenic microbes and harmless antigens and mount the appropriate immune response to each. As discussed below, breakdown in this discrimination results in the development of inflammatory bowel disease (IBD) and coeliac disease, where immune responses are targeted against innocuous antigens in commensals and food proteins respectively (128).

1.4.1 Protective Immunity versus Tolerance in the Intestine

That most humans do not suffer from chronic inflammatory conditions of the GI tract indicates that many mechanisms are present to ensure a balance between the physiological functions of the intestine, symbiosis with the microbiota and defence against pathogens. The immune system at the mucosal surface involves multiple layers of innate and adaptive immune mechanisms, as well as physical, biochemical and mechanical mechanisms that all maintain intestinal homeostasis. First, the anatomical make-up of the intestinal mucosa aids host protection. Despite being only one cell thick, the epithelial layer that exists along the entire length of the GI tract provides a robust physical barrier and disruption of its integrity is associated with the development of IBD in mice and humans (130). However the epithelium is more than an inert barrier and is able to initiate inflammatory responses by virtue of the expression of PRR such as TLR and NLR by enterocytes (131, 132). Most of the epithelial surface is also coated in a thick, viscous mucus layer that is maintained through mucin production by goblet cells, which are interspersed throughout the intestinal epithelium. Goblet cells also produce trefoil peptides which contribute to both barrier function and mucosal repair (133). The mucus layer, together with anti-microbial peptides such as α -defensins, cathelicidins and cryptidins from Paneth cells in the base of the crypts of Lieberkuhn collectively form the glycocalyx which traps and aids expulsion of invading microorganisms, a process aided by peristaltic movement. In addition, Paneth cells secrete degradative enzymes such as lysozyme and phospholipase A₂ that can break down the structure of microorganisms (134). Consistent with the increasing bacterial burden, the quantity of mucus increases along the GI tract. Given that the production of mucins such as MUC2 is altered in human IBD (135)

and MUC2 KO mice lack goblet cells and develop spontaneous colitis (136), mucus appears to be much more than a lubricant and essential for host protection.

Despite the presence of these physical, biochemical and mechanical barriers, some antigens will breach the epithelium and be exposed to cells of the immune system. The nature of the antigen determines the outcome of the immune response mounted. The intestine has a range of innate leucocytes present under steady state conditions, including mast cells, eosinophils, NK cells, innate lymphoid cells (ILC) and the largest population of $m\phi$ in the body. These various innate cells act as a first line of defence against pathogens, as well as producing immunoregulatory cytokines such as IL10, TGF β and IL22 that contribute to the maintenance of homeostasis (137). Initiation of specific immune responses requires the uptake of antigen by DC, which are located in organised lymphoid tissues such as Peyer's patches and isolated lymphoid follicles (ILF), as well as throughout the villous lamina propria (LP). These DC monitor the mucosa, capturing and constitutively transporting antigen to the draining mesenteric lymph nodes (MLN), where they present it to recirculating T cells. Recognition of cognate antigen on mucosal DC by T cells results in their expansion and differentiation and the acquisition of the gut homing molecules $\alpha 4\beta 7$ integrin and CCR9, which allow these T cells to return to the small intestine (138). Presentation of innocuous antigen such as dietary components or commensal bacteria does not result in protective immunity, but rather in the induction of a state of local and systemic immunological unresponsiveness known as oral tolerance. The exact mechanisms that underpin the maintenance of oral tolerance remain to be established with certainty, but clonal deletion or anergy of reactive T cells may be involved. In addition, FoxP3⁺ Tregs are induced, which migrate back to gut mucosa and prevent antigen-specific responses through cell-cell interactions and immunoregulatory cytokine production (139). Some of these Tregs can also regulate systemic immune responses, by mechanisms that are unclear. The intestinal immune system is also capable of generating potent effector responses when required and indeed the mucosa contains the majority of the body's lymphocytes, including CD4⁺, CD8⁺, $\gamma\delta$ T cells and IgA-producing plasma cells. Most of the T lymphocytes have an effector/memory phenotype and they are found in both the epithelial layer and the LP (128). The majority of intraepithelial lymphocytes (IEL) are CD8⁺ T cells, but $\gamma\delta$ T cells are also present. Although the exact role of IEL is unclear, they have been shown to be directly cytotoxic (140)

and play a protective role in *T. gondii* infection (141). However, IEL have also been shown to produce cytokines such as keratinocyte growth factor (KGF) (142) which may allow them to contribute to maintaining epithelial barrier integrity. In the LP, the majority of T cells are CD4⁺, however there is also a sizable CD8⁺ population. These LP lymphocytes produce high levels of a variety of cytokines, including IFN γ , IL17 and IL10 (143). Plasma cells secrete IgA which is transported from the mucosa to the luminal surface via the actions of the polymeric immunoglobulin receptor. IgA specific for bacteria associates with the glycocalyx and acts to sequester bacteria, limiting their contact with the epithelium in an attempt to prevent bacterial penetration (144). Given the presence of such a vast range of leucocytes under normal conditions, the intestine has been described as existing in a state of physiological inflammation (145), emphasising the delicate balance it needs to maintain to prevent tissue damage.

1.4.2 The Commensal Microbiota

Virtually all the functions of the intestinal immune system are dependent on the presence of the local commensal microbiota. The intestine of most mammals is colonised by trillions of bacteria consisting of over 1000 species (144). These bacteria are essential for life, as they provide vitamins and certain amino acids not produced by mammals, as well as fermenting otherwise non-digestible components of the diet. The fermentation of dietary fibre by the microflora releases short chain fatty acids which are essential for epithelial cell renewal, as well as having anti-inflammatory properties (146). The commensal bacteria also play a role in innate defence by occupying environmental niches that could otherwise be colonised by pathogens. Certain commensals, such as *Bacteriodes thetaiotaomicron*, stimulate anti-microbial peptide production by Paneth cells (132) and there is recent evidence suggesting that the ability of the immune system to produce effector cytokines such as IL17 is driven by specific components of the microbiota, including segmented filamentous bacteria (SFB) (147). It is no surprise therefore that broad-spectrum antibiotic treatment leads to increased susceptibility to enteric infection due to the ablation of commensal microorganisms. The intestinal microbiota also plays a fundamental role in influencing the development of the intestinal immune system, and germ free mice have poorly developed gut epithelium, lymphoid structures and virtually no intestinal leucocytes (144, 148). Mice that lack the cellular machinery to recognise bacteria and their derivatives,

such as MyD88 KO mice, have disrupted epithelial barrier function, resulting in enhanced susceptibility to chemically induced colitis (149). However the current understanding of the composition of the commensal microbiota is poor, primarily due to the fact that over 90% of commensals are unculturable using conventional techniques.

Under normal conditions, the microbiota exists in symbiosis with the host and commensal bacteria that penetrate the epithelial layer are rapidly engulfed and eliminated by $m\phi$ that are associated with the epithelium, and as discussed below, this happens without provoking inflammation. T cell responses are generated to commensal bacteria, but these are dominated by IL10- and TGF β -secreting Tregs. The involvement of Tregs in maintaining tolerance to commensal bacteria is supported by work with animal models of IBD, for example the development of colitis by transfer of colitogenic T cells which can be ameliorated by the co-transfer of Tregs (150). Similarly, IgA from plasma cells acts to prevent adhesion to and penetration of the epithelium by commensal bacteria. It is important to note however, unlike food antigens, tolerance to commensal bacteria appears to be local, with the immune system outside of the gut oblivious of their presence.

1.4.3 Inflammatory Bowel Disease

Crohn's disease and ulcerative colitis are chronic, relapsing and remitting inflammatory disorders that are increasingly common in developed countries, with prevalence rates of IBD reaching up to 396/100,000 inhabitants (151). Although many parallels can be drawn between Crohn's disease and ulcerative colitis, there are major differences in their clinical manifestations, immunological features and genetic basis. Crohn's disease can affect any area of the GI tract, although the terminal ileum is the most common site of pathology. The inflammation can be transmural and is non-continuous, characterised by the presence of granulomas with aggregates of activated $m\phi$ (130). Crohn's disease is also associated with a T_H1 or T_H17 skewed immune response, with high levels of the pro-inflammatory cytokines TNF α , IFN γ and IL17 (130, 152). In contrast, UC is associated with superficial and continuous inflammation that is restricted to the colon (130). Its pathology is characterised by a large infiltrate of neutrophils that cause micro-

abscesses in intestinal crypts and is usually considered to be a T_H2 skewed or antibody-mediated disease, associated with IL5, IL13 and TGFβ (153).

Although the aetiology of IBD is still unclear, work from animal models of IBD, along with human studies, has demonstrated that IBD involves multiple environmental factors in genetically predisposed individuals (130). Although there is strong heritability, there is limited concordance between monozygotic twins and the incidence of IBD is increasing rapidly in countries adopting a 'Western' lifestyle, suggesting that factors such as diet, stress and hygiene could be involved (153). The so-called 'hygiene hypothesis' suggests that children raised in an extremely hygienic environment are more susceptible to IBD, autoimmune disorders and allergy, as exposure to environmental antigens and diverse microbial material appears essential for full development of the immune system (151). This hypothesis also proposes that the lack of helminths in the GI tract of the western man also contributes to the susceptibility to intestinal inflammation, as helminths are thought to help prevent excessive inflammatory responses (151). Indeed the incidence of IBD is significantly lower in developing countries where helminth infection is commonplace. Furthermore recent clinical studies have documented that treatment of IBD patients with helminths or their derivatives improves their clinical outcome (154).

However there is growing consensus that IBD is a result of inappropriate immune responses directed against the commensal microbiota. This is supported by the fact that most animal models of IBD are dependent on the presence of commensal microorganisms and so do not develop in mice reared in germ-free conditions and appear rapidly upon colonisation with normal commensal bacteria (155). Colitis can also be induced by the transfer of commensals present in the intestine of colitic mice (156) and antibiotic treatment is therapeutically beneficial in some IBD patients, while probiotic treatment has been shown to ameliorate intestinal inflammation (157). Why the immune system reacts against host commensals in this way is still unclear and there remains a school of thought that considers there maybe a role for specific 'colitogenic' bacteria. It is well recognised that the composition of the enteric flora changes in patients with IBD, with an unusual prevalence of entero-adherent *E. coli* and reduction in the numbers of Firmicutes and Bacteroidetes species, which dominate the bacterial landscape in healthy individuals (158). Also it has long been suggested that atypical

Mycobacteria, such as *Mycobacterium paratuberculosis* might be involved (159). However no single species has ever been confirmed and 16S rRNA sequencing has shown that dysbiosis only occurs in a subset of IBD patients (158). Furthermore, it is usually very difficult to determine whether the changes seen in bacterial populations are primary effects, or are simply secondary to the presence of inflammation.

IBD is a polygenic disorder and in recent years the use of genome wide association studies (GWAS) has allowed at least 30 risk-conferring loci to be identified, some of which are common to Crohn's disease and ulcerative colitis, but most of which are related to Crohn's disease. An important outcome of these studies is that they have confirmed the involvement of the immune system in IBD with linkage to genes such as IL10, IL23 and STAT3, all of which had been suggested as candidate genes in experimental animals. The most frequent association with Crohn's disease are polymorphisms in receptors involved in bacterial recognition, the most important being NOD2. 30% of patients with small intestinal Crohn's disease have a non-functional polymorphism in NOD2 (160). Why polymorphisms in NOD2 contribute to intestinal inflammation is unclear and this is made more complex by the fact that NOD2 KO mice do not develop spontaneous colitis (161). However, patients with Crohn's disease and NOD2 KO mice appear to produce less anti-microbial peptides such as α -defensins (162), supporting the idea that dysregulation of the usual immune response to commensal flora is central to the pathogenesis of IBD. Further candidate genes identified by GWAS include ATG16L1 and IRGM, which are involved in autophagy and strongly imply that defects in the innate immune system underlie susceptibility to IBD. Mice with KO of ATG16L1 in myeloid cells show increased susceptibility to DSS-induced colitis and $m\phi$ from these mice show enhanced LPS responsiveness (160). Similarly $m\phi$ from IRGM KO mice display reduced bacterial killing and as a result, these mice are more susceptible to a range of bacterial infections (163, 164).

Much of this work emphasises the involvement of innate immunity in susceptibility to Crohn's disease. $M\phi$ are known to be major components of inflammation and their products have shown to be successful targets for treatment, such as $TNF\alpha$ and IL6 (165, 166). Thus there is considerable interest in $m\phi$ present in the intestine during homeostasis and disease.

1.5 Intestinal Macrophages

Despite forming one of the largest reservoirs of m ϕ in the body (167), the immunobiology of intestinal m ϕ remains poorly understood, partly due to the difficulty in isolating these cells. M ϕ are most abundant in the lamina propria, in close association with the epithelial layer, however they can also be found in deeper layers of the gut such as the submucosa and the muscularis mucosae (168). The presence of m ϕ appears to be partly dependent on the presence of commensal bacteria, since germ-free mice have reduced numbers of intestinal m ϕ (169). In addition, the number of m ϕ increases progressively from the almost sterile jejunum, to the colon where the commensal burden is the greatest (167).

Most of the current understanding of the phenotype and function of intestinal m ϕ is derived from work on human biopsy tissue. These studies have shown that human small intestinal m ϕ express CD13 and high levels of class II MHC (170, 171), while those from colon were found to have uniform expression of CD33, but low levels of CD11b and class II MHC (172). Both human small bowel and colonic m ϕ lack the expression of CD14, the LPS co-receptor, and CD16 (Fc γ RIII), markers that are expressed by blood monocytes (12). Less has been published on mouse intestinal m ϕ and as discussed below, the characterisation of these cells is now known to be more complex than originally believed, as their distinction from other myeloid cells requires careful attention. Nevertheless by the time I started my project, several consistent features of these cells had been established using conventional markers. Although there are subtle differences between mouse and man, and between the small and large intestines, there was consensus that intestinal m ϕ are highly adapted to their antigen- and microbe-rich environment.

Human and mouse intestinal m ϕ have been shown to be highly phagocytic, possess secondary lysosomes and are able to capture and kill bacteria without prior 'activation' (170, 171, 173). However, unlike m ϕ found in other tissues and blood monocytes, intestinal m ϕ do not produce pro-inflammatory cytokines following phagocytosis of particles or after stimulation with a range of bacterial products including LPS, *Helicobacter pylori* urease and heat-killed *Staphylococcus aureus* (171). This unresponsiveness of intestinal m ϕ extends to other stimuli including the NOD2 ligand MDP, pro-inflammatory cytokines and even PMA (171,

174). In addition, human intestinal m ϕ show no respiratory burst activity after stimulation with PMA or opsonised zymosan (175) and lack iNOS expression (176). Rather than producing pro-inflammatory cytokines, intestinal m ϕ have been shown to produce immunomodulatory cytokines such as IL10 and TGF β both constitutively and in response to stimulation with whole bacteria antigens (177-179). Furthermore, despite expressing high levels of class II MHC, human small intestinal m ϕ express only low levels of costimulatory molecules, again suggesting these cells are not classically 'activated' despite their appearance (170, 171). For these reasons, it is believed that one of the crucial roles of resident intestinal m ϕ is to remove cellular debris and act as a non-inflammatory waste disposal unit for commensal bacteria that have breached the epithelial layer.

Resident intestinal m ϕ perform other crucial homeostatic functions, such as contributing to the maintenance of the epithelial barrier integrity by COX2-dependent production of prostaglandin (PG)E₂, which induces proliferation of epithelial progenitors in the pericryptal niche (180, 181). Depletion of m ϕ in MaFIA mice, in which the CSF-1R promoter drives expression of Fas in m ϕ , results in increased epithelial cell injury and enhanced susceptibility to DSS colitis (182). Very recently, intestinal m ϕ have been implicated in the maintenance of antigen-specific peripheral tolerance through their local interactions with Treg. Murine small intestinal m ϕ have been shown to cause Treg differentiation *in vitro* in the presence of exogenous TGF β (178) and *in vivo* studies now show that intestinal m ϕ contribute to the terminal differentiation and maintenance of regulatory T cells in the LP (139, 183). These effects are dependent on IL10 production by the m ϕ and are absent in CX3CR1 KO mice, in whom oral tolerance to protein antigens does not develop (139). F4/80 KO mice also fail to develop oral tolerance due to a defect in CD8⁺ regulatory T cell function (184). Thus intestinal m ϕ possess several functional adaptations that allow capture of any bacteria breaching the epithelial monolayer without provoking overt inflammation, but also promote the generation and expansion of Treg that control specific immune responses against such antigens.

As noted above, the exact phenotypic characteristics of resident intestinal m ϕ in mice have become controversial. Although it has been clear for many years that these cells express F4/80 and are highly phagocytic (185, 186), they also express high levels of CD11b and class II MHC (186, 187), which are features of

many classical DC. Most work in the gut had classified DC and $m\phi$ on the basis of CD11c expression and had not combined this with other markers such as F4/80 and CD103. Around the time I began my project, it was becoming increasingly clear that some, if not all, tissue $m\phi$ express CD11c to some degree (188). In addition, several studies had used CD11b alone to identify intestinal $m\phi$ (177), and as I will show, this is a marker expressed by a number of myeloid cells in the mucosa. Work at this time in the Pabst and Agace labs proposed a new nomenclature for the discrimination of individual intestinal MP populations, based on the mutually exclusive expression of CD103 (α e integrin) and CX3CR1, the chemokine receptor for CX3CL1 (also known as fractalkine or neurotactin) (189). Both CD103⁺ and CX3CR1⁺ MP express class II MHC and can express CD11c, but they possess phenotypic, functional and developmental differences. CD103⁺CD11c⁺MHCII⁺ MP migrate in intestinal afferent lymph in a CCR7 dependent manner to the draining LN, where they interact with and cause differentiation of naïve T cells (138, 189). These are the only cells that can present intestinally-derived antigen and are the endowed with the ability to induce gut homing receptors such as CCR9 and α 4 β 7 on T cells, which allows them to transit back to the intestinal mucosa (138, 190). This requires the conversion of dietary vitamin A into retinoic acid (RA) by the CD103⁺ MP and this also allows them to induce the differentiation of naïve T cells into antigen-specific FoxP3⁺ Treg, a process that is also dependent on TGF β (191, 192). In terms of phenotype and function, CD103⁺ MP appear to be a specialised population of *bona fide* DC.

CX3CR1⁺ MP first aroused attention when they were found to extend transepithelial dendrites (TED) into the intestinal lumen to sense and perhaps sample intestinal contents (193, 194). This property, together with the expression of CD11c and class II MHC, resulted in these being classified as DC. However, using a combination of approaches including intra-vital microscopy, Schulz *et al.* (189) demonstrated that the intestinal afferent lymph was essentially devoid of CX3CR1⁺ MP, suggesting that CX3CR1⁺ MP are non-migratory, tissue resident cells. Consistently, the vast majority of CX3CR1⁺ MP express high levels of $m\phi$ markers such as F4/80, CD11b and CD115 (189, 195), as well as CD68 (169). That CD103⁺ and CX3CR1⁺ LP MP are distinct populations is supported by their distinct developmental origins. Whilst CD103⁺ MP are derived from the DC-committed pre-cDC that requires flt3L and/or CSF-2 for development (189, 195), CX3CR1⁺ cells are dependent on CSF-1 and CSF-2 and are replenished by

monocytes (28, 189, 195, 196). Further evidence for the CX3CR1⁺ population belonging to the m ϕ lineage is that they are significantly reduced in CSF1R KO mice (195) and that administration of an anti-CD115 antibody resulted in depletion of intestinal m ϕ (197).

These emerging studies indicated that many of the previous reports on 'DC' and 'm ϕ ' in the mucosa needed to be reinterpreted using appropriate combinations of markers to allow precise assessment of function. This was particularly important for m ϕ , as these had often been misclassified as DC and had not been examined for m ϕ behaviour directly. Also it was unclear whether the CX3CR1⁺ fraction was a uniform population, or if it contained multiple cell types.

1.5.1 CX3CL1 and Its Receptor

CX3CR1 is a receptor that recognises the chemokine CX3CL1. Chemokines are small chemotactic cytokines that act through G-protein coupled seven transmembrane receptors and are best known for their ability to cause directed migration of leucocytes and other cells. They are grouped into four families (CXC, CC, XC, CX3C) based on their structure, in particular the positioning of a conserved tetra-cysteine motif (198). Chemokines are produced by a variety of cells including leucocytes, epithelial, endothelial and stromal cells, and the vast majority are secreted as soluble proteins, although they are often immobilised on extracellular matrix proteoglycans to form chemotactic gradients (198).

One exception to this is CX3CL1, which is produced as a transmembrane molecule, with the chemokine domain anchored to the membrane through a mucin-like stalk (199). However following proteolytic cleavage by disintegrin-like metalloproteinase (ADAM)-10 or 17, CX3CL1 can also exist in soluble form (200, 201). In the intestine, CX3CL1 has been shown to be produced by epithelial cells (202) and more recently by goblet cells (203). However, vascular endothelial cells, smooth muscle and neurons, as well as DC and m ϕ have been shown to produce CX3CL1 elsewhere (204-208). To date, CX3CR1 is the only identified receptor for CX3CL1 and it is expressed by multiple cell types. As noted above, CX3CR1 is expressed by early progenitors of the MPS and the level of CX3CR1 expression has been used in conjunction with Ly6C to define 'inflammatory' and 'resident'

monocytes (12). In addition to intestinal m ϕ , m ϕ in the CNS (microglia) and skin (Langerhan's cells) express CX3CR1 at high levels (55, 60). In contrast, peritoneal, splenic and liver-resident Kupffer cells do not express CX3CR1, suggesting that its expression may be tissue-specific. Some T cells, NK cells and plasmacytoid DC can also express CX3CR1, albeit at lower levels than monocytes and m ϕ (209-211).

The exact role of CX3CR1 in the MPS remains to be established with certainty and the relative roles of its membrane bound and soluble forms are unclear. Membrane tethered CX3CL1 has been shown to mediate integrin-independent cell adhesion through interactions with CX3CR1 (212) and interestingly, CX3CR1 has been suggested to be necessary for TED formation in the gut, although this is controversial (193, 203, 213). Recently it has been proposed that the CX3CR1-CX3CL1 axis may also be involved in cell survival. In particular, CX3CR1 appears to play a role in the survival of Ly6C^{low}CX3CR1⁺ monocytes, as these cells are reduced in CX3CR1-deficient (CX3CR1^{gfp/gfp}) mice (214). That this is due to reduced survival is supported by the fact that introduction of the apoptosis inhibitor Bcl2 rescued the phenotype (214). Similarly, exogenous CX3CL1 prevents Fas-induced cell death of *in vitro* cultured microglia (215) and CX3CL1 has been shown to promote survival of human intestinal epithelial cells *in vitro* (216). CX3CL1 has also been shown to modulate the function of mature m ϕ , although there is conflicting evidence on whether these effects are anti- or pro-inflammatory. For example, CX3CL1 has been shown to attenuate pro-inflammatory m ϕ responses *in vitro* (217), but disruption of the CX3CR1-CX3CL1 axis in CX3CR1^{gfp/gfp} mice may protect mice from the development of atherosclerosis and experimental colitis (169, 218, 219).

1.5.2 Mechanisms Governing Macrophage Unresponsiveness

How intestinal m ϕ can exist in a state of 'inflammatory anergy' when in such close proximity to vast quantities of immunostimulatory material is unclear. Several mechanisms have been proposed, with no clear answer being offered. Human resident small intestinal m ϕ lack receptors involved in m ϕ activation, including the LPS co-receptor CD14 (170), TREM-1 (220), complement receptors (CR) 3 and 4, as well as the Fc receptors for IgA and IgG (CD89 and CD64 respectively) (170). Although it was originally reported that they also failed to express TLR (221, 222),

evidence is emerging that human intestinal m ϕ may express a full range of TLR (179) and this needs to be explored more fully. However, it seems more likely that the TLR unresponsiveness in intestinal m ϕ may reflect one or more of the mechanisms that have been shown to inhibit the TLR signalling cascade, as described above. Indeed intestinal m ϕ have markedly downregulated expression of MyD88, TRAF6, TRIF, IRAK1 and IRAK4 adaptor molecules compared with blood monocytes, resulting in a failure to phosphorylate and translocate NF- κ Bp65 to the nucleus (179).

The control of intestinal m ϕ activity is likely to be a multi-factorial process involving many mechanisms, one of which is conditioning of m ϕ by local environmental factors. IL10 is an obvious candidate for this, as intestinal m ϕ from IL10-deficient mice have heightened responsiveness to a range of TLR ligands, producing pro-inflammatory cytokines such as TNF α , IL12 and IL23 which facilitate the generation of pathogenic T_H1 and T_H17 cells (177, 178, 223) (Platt, A. personal communication). Furthermore, blockade of the IL10R has been shown to result in a loss of unresponsiveness by intestinal MP (224) and IL10R2 KO mice develop spontaneous colitis (225). In addition, IL10 KO mice or mice with a myeloid cell-specific deletion of the IL10R signalling molecule STAT3, also develop colitis (226, 227) and polymorphisms in the IL10R predispose to IBD development (228). IL10 is a well-known inhibitor of NF- κ B activation in m ϕ and this may involve induction of factors such as I κ BNS and Bcl-3, which inhibit the binding of NF- κ B to DNA (223, 229, 230). These inhibitory factors have been identified in gut resident m ϕ , but it is not known whether m ϕ themselves are the source of IL10. Aside from IL10, the LP is also a rich source TGF β , one of the most potent anti-inflammatory cytokines which has a well established ability to cause downregulation of the pro-inflammatory actions of m ϕ (231). TGF β is produced by leucocytes such as Treg, as well as by epithelial and stromal cells (179), and has been shown to attract monocytes to the mucosa together with IL8 (232). Furthermore, human IBD is associated with upregulated expression of Smad7, leading to defective TGF β R signalling (233).

Other local soluble factors have been shown to have effects on mucosal 'DC' and it is possible that they may also have the potential to influence m ϕ behaviour. These include vasoactive intestinal peptide (VIP) (234), RA (235), and PGE2 (236), all of which are available in the resting mucosa. Also ligands for the

nuclear receptor PPAR γ are abundant in the resting mucosa and these have been shown to control pro-inflammatory cytokine production by myeloid cells (237). As a result, mice with a m ϕ -specific deletion of PPAR γ show heightened pro-inflammatory m ϕ activity and increased susceptibility to DSS-induced colitis (238). Thus many overlapping mechanisms may exist to ensure gut m ϕ are maintained in this TLR-hyporesponsive state.

1.5.3 Intestinal Macrophages During Inflammation

It is well established that during inflammation, the composition of the intestinal m ϕ compartment alters markedly. In humans, the CD14^{neg} resident m ϕ pool becomes outnumbered by CD14⁺ m ϕ (239-242), which are believed to derive from blood monocytes (243). These CD14⁺ m ϕ express higher levels of TLR2 and TLR4, costimulatory molecules and inflammatory chemokine receptors CCR1 and CCR2 (221, 242). Furthermore, they express TREM-1 which may potentiate activation (220, 244). In addition, whereas resident intestinal m ϕ have been shown to produce TGF β and IL10 (177, 179, 242), the inflammatory CD14⁺ cells produce high levels of IL12, IL23, TNF α , and IL6 following stimulation with the commensal bacterium *Enterococcus faecalis* (242) and show greater respiratory burst activity (175). As in humans, many models of colitis are associated with the accumulation of m ϕ in the inflamed mouse intestine (245-250). Similar inflammatory m ϕ are seen during intestinal infection with *T. gondii* (25). However, these cells were frequently interpreted as being 'inflammatory DC', because they expressed class II MHC and CD11c (250). Therefore the exact relationship between these pro-inflammatory m ϕ and those found in the healthy mucosa remain unclear. Gaining a better understanding of the relationship between these cells is an important practical issue, as it could provide insight into possible new therapies for inflammatory diseases such as IBD.

Work carried out in our lab immediately before I started suggested that resident and inflammatory m ϕ in mice could be distinguished on the basis of TLR and CCR2 expression (222). These studies suggested that in the normal colon, most F4/80⁺ m ϕ lacked expression of TLR2, CCR2 and class II MHC and were also unresponsive to TLR stimulation. During DSS colitis, there was infiltration by TLR2⁺CCR2⁺MHCII^{+/neg} TNF α -producing, TLR responsive m ϕ , a few of which were present in the steady state colon. These findings were interpreted in the light of the

current paradigm of monocyte heterogeneity, and it was proposed that the resident and inflammatory $m\phi$ represented unrelated progeny of distinct populations of blood monocytes (222). However this was not shown directly and as I discussed above, it has never actually been shown that the so-called 'resident' population of $Ly6C^{low}CX3CR1^+$ monocytes could migrate into the healthy intestine. Indeed the only studies of monocyte transfer have suggested that $Ly6C^{high}$ inflammatory monocytes can migrate to the resting gut (28, 196), although these studies used intense depletion regimes to provide empty niches in the host and the resulting progeny were interpreted as inflammatory DC. Thus at the point of starting my project, no work had used wide combinations of markers to compare the nature and origins of precisely defined resident and inflammatory $m\phi$ and therefore this was one of the aims of my project.

1.6 Thesis Aims

It is clear that intestinal $m\phi$ can play essential roles in both tissue homeostasis and inflammation. However, to date, the definition of intestinal $m\phi$ has been stifled by increasing confusion generated by the use of overlapping $m\phi$ and DC markers such as F4/80 and CD11c. As a result, the exact nature of intestinal $m\phi$ in healthy mouse colon has remained unclear. In particular, it was not known how $m\phi$ in the steady state and inflamed intestine might be related to each other and their origins had not been defined properly.

The main aims of this thesis therefore, were to establish protocols that allowed the comprehensive phenotypic characterisation of colonic $m\phi$ under steady state conditions using multi-parameter flow cytometry and recently described markers of MP. Having established the composition of the $m\phi$ compartment during steady state conditions, I aimed to define the changes that occurred during inflammation using the DSS-induced model of acute colitis. If distinct populations were identified under these conditions, I intended to characterise them functionally and examine their origin to address whether they represented independent populations, or if they were related to each other.

Chapter 3 of this thesis introduces the phenotypic heterogeneity of the colonic MP compartment under normal physiological conditions and describes how individual $m\phi$ subsets can be distinguished on the basis of CX3CR1. This chapter

then goes on to detail the dramatic changes in these populations during experimental colitis. Chapter 4 sets out to examine the origin of the different m ϕ and explores the relationship between these subsets under steady state conditions, using a combination of adoptive transfer experiments. Chapter 5 then examines the functional characteristics of the colonic m ϕ subsets in resting and inflamed colon. The aim of Chapter 6 was to explore the role of recruited/elicited m ϕ in the pathology of experimental colitis and finally, in Chapter 7, I investigated the potential mechanisms underlying the characteristic TLR unresponsiveness of resident colonic m ϕ , including an in depth study of the role of the CD200-CD200R1 axis.

Chapter 2

Materials and Methods

2.1 Mice

All mice were maintained under specific pathogen free (SPF) conditions at the Central Research Facility (CRF) or Veterinary Research Facility (VRF) at the University of Glasgow and were used between 6 and 12 weeks of age, unless specified otherwise. Table 2.1 details the mouse strains used throughout these studies. Unless stated otherwise, all strains were on the C57/BL6 background and were bred in house. All procedures were carried out in accordance with UK Home Office regulations.

Table 2.1: Details of Mouse Strains

Strain	Source
C57BL/6 (B6; CD45.2 ⁺)	Harlan Olac (Bicester, Oxfordshire)
C57BL/6.SJL (CD45.1 ⁺ ; Ly5.1 ⁺)	Kindly provided by Prof. William Agace (Lund University, Sweden).
C57BL/6 (CD45.1 ⁺ /CD45.2 ⁺)	Generated by crossing C57BL/6 mice with C57BL/6.SJL
CX3CR1 ^{gfp/gfp} (B6.129P-CX3CR1 ^{tm1Litt/J})	Kindly provided by Prof. William Agace (Lund University, Sweden) (209). CX3CR1 ^{gfp/gfp} mice do not exhibit any developmental defects. All GFP ⁺ cells in blood of CX3CR1 ^{+/gfp} mice are stained with a CX3CL1-Fc fusion protein and all CX3CL1-Fc ⁺ cells express GFP, confirming GFP expression accurately represents CX3CR1 expression. CX3CL1-Fc did not bind GFP ⁺ cells from CX3CR1 ^{gfp/gfp} mice, confirming that these mice lack CX3CR1 and that there is no alternative receptor for CX3CL1. However due to the extended half-life of eGFP protein (>24hrs), not all GFP ⁺ cells in CX3CR1 ^{+/gfp} mice would necessarily be expected to be CX3CR1 ⁺ .
CX3CR1 ^{+/gfp} (CD45.2 ⁺)	Generated by crossing CX3CR1 ^{gfp/gfp} with C57BL/6 mice.
CX3CR1 ^{+/gfp} (CD45.1 ⁺ /CD45.2 ⁺)	Generated by crossing CX3CR1 ^{gfp/gfp} with C57BL/6.SJL.
CCR2 null	Kindly provided by Dr Robert Nibbs (University of Glasgow). Obtained originally from Jackson Laboratories (Maine, USA)
CD200R1 null	Kindly provided by Prof. Tracy Hussell (Imperial College, London) (125). CD200R1 null mice do not exhibit any developmental defects. These mice lack exons 2, 3 and 4 of the CD200R1 gene, which encode the extracellular domain of CD200R1.
CD200 null	Kindly provided by Prof. Andrew Dick (University of Bristol) (113).
CD11c-DTR-GFP	Kindly provided by Prof. Paul Garside (University of Glasgow) (251).
Vert-X (C57BL/6 IL10eGFP)	Kindly provided by Dr Kevin Couper (London School of Hygiene and Tropical Medicine) (252).

2.2 Isolation of Peritoneal Macrophages

To obtain resting peritoneal m ϕ , CO₂-euthanased mice were injected intraperitoneally (i.p.) with 8-10ml of ice-cold PBS (Gibco, Life Technologies, Paisley, Scotland) containing 1mM EDTA (Sigma-Aldrich, Poole, UK) and the peritoneal cavity massaged. Peritoneal exudate cells (PEC) were then harvested by lavage.

2.3 Isolation of Colonic Lamina Propria cells

To obtain leucocytes from the colonic LP, I used an established laboratory protocol. The large intestines of mice were excised and soaked in PBS. After removing all excess fat and faeces, the intestines were opened longitudinally, washed in Hank's balanced salt solution (HBSS; Gibco) 2% FCS, and cut into 0.5cm sections. The tissue was then shaken vigorously in 10 ml HBSS 2% FCS, and the supernatant was discarded. To remove the epithelial layer, 10 ml fresh calcium and magnesium-free (CMF) HBSS containing 2mM EDTA was then added, the tube placed in a shaking water bath (or shaking incubator) for 15mins at 37°C, before being shaken vigorously and the supernatant discarded. The intestinal tissue was washed by adding 10ml fresh CMF HBSS, shaking the tube vigorously and discarding the supernatant. After a second incubation in CMF HBSS/2mM EDTA, the wash step was repeated and the remaining tissue was digested with pre-warmed complete RPMI 1640 (RPMI 1640, 2mM L-glutamine, 100 μ g/ml penicillin, 100 μ g/ml streptomycin, 1.25 μ g/ml Fungizone, and 10% foetal calf serum (FCS) (all Gibco) containing 1.25mg/ml collagenase D (Roche Diagnostics GmbH, Mannheim, Germany), 0.85mg/ml collagenase V (Sigma-Aldrich), 1mg/ml dispase (Gibco), and 30U/ml DNase (Roche) for 30-45 minutes in a shaking water bath (or shaking incubator) at 37°C. To aid successful digestion, the tube was shaken vigorously every 5-10 minutes until complete digestion of the tissue. The resulting cell suspension was passed through a 40 μ m cell strainer (BD Falcon) and then washed twice in complete RPMI to ensure complete removal of residual enzymes. Cells were counted and kept on ice until use.

2.4 Generation of Bone Marrow Derived Macrophages

BM was flushed out of the femurs and tibias of adult mice in RPMI 1640. The BM cells were passed through Nitex mesh (Cadisch and Sons, London, UK) and counted. To generate macrophages 1ml of cells were added into 90cm Petri dishes (Sterilin, UK) at 3×10^6 cells/ml with 8ml complete medium (20% FCS), containing 1mM sodium pyruvate (Gibco), and 20% supernatant from L929 fibroblasts as a source of CSF-1 at 37°C in 5% CO₂. After 3 days, the medium was supplemented with 5ml complete medium and 20% CSF-1. On day 6/7 of culture, non-adherent cells were removed by washing with RPMI 1640 and the adherent cells were then collected by adding ice cold PBS/1mM EDTA for 5 minutes and then displacing them with cell scrapers (Costar). The purity of the harvested bone marrow-derived m ϕ (BMM) was assessed by flow cytometry and was typically >90% F4/80 positive.

2.5 Isolation of Alveolar and Lung Macrophages

Resting alveolar m ϕ were obtained from terminally anaesthetised mice by bronchoalveolar lavage (BAL) with 0.8ml (x2) ice-cold PBS/1mM EDTA via an intra-tracheal cannula. For lung m ϕ , lungs were removed from CO₂-euthanased mice, washed in 2% FCS HBSS and cut into small pieces. Lung tissue was then incubated for 1hr with 0.5mg/ml collagenase IV (Sigma-Aldrich) in complete RPMI in a shaking incubator at 37°C. Residual tissue was mashed through a 40 μ m cell strainer and washed twice in complete RPMI to ensure removal of residual enzymes.

2.6 Processing of Whole Blood

Heparinised blood was incubated on ice with ammonium chloride solution (0.8% NH₄Cl/0.1mM EDTA; Stem Cell Technologies, Grenoble, France) for 10 minutes to lyse red blood cells (RBC). Cells were washed twice in PBS and kept on ice until use.

2.7 *In vitro* Stimulation of BMM and Purified Monocytes

BMM were plated out at 1×10^6 cells/ml and whole colonic lamina propria (CLP) digest cell suspensions were plated at 2×10^6 cells per well in 1ml, in ultra low adherence, 24-well tissue culture plates (Costar). Cells were incubated either

in medium alone, or with 1µg/ml lipopolysaccharide (LPS) from *Salmonella typhimurium* (Sigma-Aldrich), 1µg/ml bacterial lipoprotein (BLP; Pam₃CSK₄) (Invivogen), and/or 100U/ml recombinant mouse interferon (IFN)_γ (BioSource) at 37°C in 5% CO₂. In some experiments BMM were pre-incubated with 2.5µg/ml CD200-Fc fusion protein (R&D Systems) for 1hr before stimulation with LPS and/or IFN_γ. FACS-purified colonic or BM Ly6C^{high} monocytes were cultured with 50ng/ml recombinant CX3CL1 (R&D Systems), 10ng/ml recombinant human TGFβ (Peprotech) or 20% supernatant from L929 fibroblasts as a source of CSF-1, at 37°C in 5% CO₂.

2.8 Flow Cytometry and Antibodies

2.8.1 Surface Staining

2-3x10⁶ cells were added to 12x75mm polystyrene tubes (BD Falcon), washed in ice cold FACS buffer (PBS containing calcium and magnesium + 4% FCS) and then incubated at 4°C with anti-CD16/CD32 ('Fc Block') to reduce non-specific binding via Fc receptors. Cells were washed once with ice cold FACS buffer and then incubated with the relevant primary antibodies (as detailed in Table 2.2) for 20-30 minutes at 4°C protected from light. Cells were then washed three times in ice cold FACS buffer and if required, incubated for a further 10-15 minutes with fluorochrome-conjugated streptavidin (SAv). Cells were washed once more in ice cold FACS buffer and analysed using a FACSCalibur, FACS Aria I or LSRII flow cytometer (all BD Biosciences). Dead cells were excluded from analysis by adding 10µl 7-aminoactinomycin D (7-AAD; BD Biosciences) to each sample immediately before acquisition. Appropriate isotype controls were included in all experiments. As detailed in Table 2.2, isotype controls were purchased from the manufacturer of the appropriate antibodies. All data generated were analysed using FlowJo software (Tree Star Inc, OR, USA).

2.8.2 Detection of Intracellular Cytokines by Flow Cytometry

When staining for intracellular cytokines, the staining protocol was adapted slightly to be compatible with the fixable dead cell exclusion dyes used. 2x10⁶ cells were incubated with or without TLR ligands for 4.5hrs in the presence of 1µM monensin and 10µg/ml Brefeldin A (both Sigma-Aldrich) to prevent cytokine secretion in 5ml polystyrene tubes. Cells were washed in PBS and then incubated

with LIVE/DEAD[®] fixable violet or aqua dead cell stain kits (Molecular Probes; Life Technologies) as per the manufacturer's guidelines, for 20-30 minutes protected from light. Cells were then washed in ice cold PBS, incubated with purified anti-CD16/CD32 and stained with the appropriate antibodies for cell surface antigens as described above, before being washed three times in PBS. Cells were then fixed using 4% paraformaldehyde (PFA; Thermo Scientific) in PBS for 10 minutes at room temperature and then washed in ice cold PBS. Cells were permeabilised using 'PermWash' (PBS containing 0.1% saponin/0.1% sodium azide/0.1% BSA (all Sigma-Aldrich)/0.2% FCS) before a further incubation with anti-CD16/CD32 to block intracellular Fc receptors. Cells were then resuspended in 'PermStain' (PBS/0.1% saponin/0.1% sodium azide/0.1% BSA/1% FCS) together with the appropriate fluorochrome-conjugated cytokine-specific antibodies for 20 minutes protected from light. Cells were then washed with 'PermWash', resuspended in FACS buffer and analysed by flow cytometry.

2.8.3 Detection of CCR2 Chemokine Receptor by Flow Cytometry

To examine the presence of the chemokine receptor CCR2, a specific monoclonal antibody (MC-21) was used (a kind gift from Prof. M. Mack, Department for Internal Medicine, University of Regensburg, Germany). Cells were first incubated with PBS/2% FCS/10% mouse serum (Biosera) for 1 hour at 4°C to reduce non-specific binding, before being washed three times with ice cold FACS buffer. Cells were then stained with 5µg/ml MC-21 or purified rat IgG2b (as an isotype control) at 4°C for a further hour. Cells were washed three times in FACS buffer and stained with a biotinylated polyclonal anti-rat IgG (BD Biosciences) for 30 minutes at 4°C before being washed as before. Cells were then incubated with SAV-QDot 605 (Molecular Probes) for 15 minutes at 4°C protected from light and then washed again. Other surface markers were then stained for as described above, except that the incubation step with anti-CD16/CD32 was omitted. CCR2 KO cells were used as the negative control for all CCR2 staining.

2.9 Purification of Tissue Macrophages by FACS

To obtain purified macrophage populations, colonic lamina propria cells and PEC were prepared as for flow cytometry in sterile conditions, as described above. Cells were then sorted using a FACS Aria I and the purity of sorted cells was routinely between 91-98%. Colonic LP myeloid cell subsets were sorted on the

basis of CD11b, CX3CR1-GFP, Ly6C, class II MHC, F4/80 and CD11c expression by live-gated cells (see Figure 3.8). Peritoneal m ϕ were sorted as CD45⁺ 7-AAD^{neg} F4/80^{high} CD11b⁺ SiglecF^{neg}. Colonic and peritoneal eosinophils were sorted as CD45⁺ 7-AAD^{neg} F4/80^{low} MHCII^{neg} SiglecF⁺.

2.10 Assessment of Phagocytosis

To measure the phagocytic activity of colonic LP m ϕ , LP leucocytes were isolated from CX3CR1^{+gfp} mice and 3x10⁶ cells stained for flow cytometry as above and phagocytosis was assessed according to the manufacturer's guidelines. Briefly, cells were incubated with 20 μ l pHrodo *E. coli* bioparticles (Molecular Probes) for 15mins at 37°C or at 4°C as a control, washed in Buffer C and analysed by flow cytometry.

2.11 Induction of DSS Colitis

To induce acute colitis, I used a well established protocol whereby mice received 2% dextran sodium sulphate (DSS) salt (reagent grade; MW 36,000-50,000 kDa; MP Biomedicals, Ohio), *ad libitum* in sterile drinking water for up to 8 days. In some experiments mice were fed DSS for 4 days and then returned to normal drinking water in order to assess the 'recovery' phase of disease. Mice were monitored daily for weight change, rectal bleeding and diarrhoea and a clinical score generated (Table 2.3). Mice that lost >20% of their initial bodyweight were sacrificed immediately in accordance with Home Office regulations. Water intake was measured daily for each group and the volume of water consumed per mouse was estimated by dividing the total volume of water consumed per cage by the number of animals in the cage. At each time point, the colons were removed and measured to assess the extent of colon shortening. In some experiments, sections of colon were fixed in 10% formalin, processed and stained with H&E for histological analysis by the Veterinary Biosciences unit within the School of Veterinary Medicine (University of Glasgow).

Table 2.2: List of Monoclonal Antibodies and Streptavidin Conjugates used for Flow Cytometry.

Primary antibodies were conjugated to either FITC, PE, PerCP-Cy5.5, PE-Cy7, APC, APC-Cy7, AlexaFluor 700, BD Horizon V450, V500, or were biotinylated and detected using fluorochrome-conjugated streptavidin.

Antibody	Clone	Isotype	Source
CD3	17A2	Rat IgG2b	BD Biosciences
CD4	RM4-5	Rat IgG2a	BD Biosciences
CD8	53-6.7	Rat IgG2a	BD Biosciences
CD11b	M1/70	Rat IgG2b	BD Biosciences
CD11c	HL3	Hamster IgG1	BD Biosciences
CD14	Sa2-8	Rat IgG2a	eBioscience
CD16/32	2.4G2	Rat IgG2b	BD Biosciences
CD19	1D3	Rat IgG2a	BD Biosciences
CD31	MEC 13.3	Rat IgG2a	BD Biosciences
CD40	3/23	Rat IgG2a	BD Biosciences
CD45	30-F11	Rat IgG2b	BD Biosciences
CD45.1	A20	Mouse IgG2a	BD Biosciences
CD45.2	104	Mouse IgG2a	BD Biosciences
CD45R (B220)	RA3-6B2	Rat IgG2a	BD Biosciences
CD80	16-10A1	Hamster IgG1	BD Biosciences
CD86	GL1	Rat IgG2a	BD Biosciences
CD103	M290	Rat IgG2a	BD Biosciences
CD103	2E7	Hamster IgG	eBioscience
CD115	AFS98	Rat IgG2a	eBioscience
CD117	2B8	Rat IgG2b	BD Biosciences
CD135	A2F10.1	Rat IgG2a	BD Biosciences
CD172a	P84	Rat IgG1	BD Biosciences
CD193	83103	Rat IgG2a	BD Biosciences
CD200	OX-90	Rat IgG2a	AbD Serotec
CD200R	OX-110	Rat IgG2a	AbD Serotec
CD206	MR5D3	Rat IgG2a	Biolegend
BrdU			BD Biosciences
F4/80	BM8	Rat IgG2a	eBioscience
IL-10	JES5-16E3	Rat IgG2b	BD Biosciences
Ki-67	B56	Mouse IgG1	BD Biosciences
Ly6C	AL-21	Rat IgM	BD Biosciences
Ly6G	1A8	Rat IgG2a	BD Biosciences
MHC II (IA-IE)	M5/114.15.2	Rat IgG2b	eBioscience
SiglecF	E50-2440	Rat IgG2a	BD Biosciences
TLR2	6C2	Rat IgG2b	eBioscience
TLR4	MTS510	Rat IgG2a	eBioscience
TNF α	MP-6XT22	Rat IgG1	BD Biosciences
Streptavidin QDot 605			Molecular Probes

Table 2.3: Clinical Disease Score criteria used during DSS-induced colitis studies

Score	Weight Loss	Rectal Bleeding	Stool
0	0%	None	Well-formed pellet
1	5-9.9%	Blood around anus	Pasty soft pellets
2	10-14.9%	Bleeding	Faeces around anus
3	15-19.9%	Gross Bleeding	Diarrhoea
4	>20%	N/A	N/A

2.12 Measure of Cell Turnover by BrdU Incorporation

For short term studies, mice were injected i.p. with 1mg 5-bromo-2'-deoxyuridine (BrdU; BD Biosciences) and then sacrificed at different time points thereafter. The incorporation of BrdU by isolated cells was assessed using the BD BrdU Flow Kit (BD Biosciences). Cells were treated as for intracellular staining, except that after fixation with 4% PFA, the cells were treated as per the Flow Kit instructions.

For long term BrdU administration, mice were injected once i.p. with 1mg BrdU and then received 0.8mg/ml BrdU in their drinking water for a maximum of 8 days. The BrdU-supplemented water was protected from light and replenished daily.

2.13 Adoptive Transfer of Purified Monocytes

Bone marrow was flushed from the tibiae and femurs of CX3CR1^{+gfp} CD45.2⁺ or CX3CR1^{+gfp} CD45.1⁺/CD45.2⁺ mice and the cells were incubated with ammonium chloride solution for 10 minutes on ice to lyse red blood cells (RBC). The remaining cells were stained for CD11b, CD117 (c-kit), Ly6G and Ly6C to allow discrimination between Ly6C^{high} monocytes (CD11b⁺CD117^{neg}Ly6G^{neg}Ly6C^{high}CX3CR1^{int}) and Ly6C^{low} monocytes (CD11b⁺ CD117^{neg}Ly6G^{neg}Ly6C^{low} CX3CR1⁺) and the subsets were sorted using a FACSAria I cell sorter into complete RPMI 1640. The purity of these monocyte populations was routinely >97%. Sorted monocytes were washed twice in sterile PBS and then 2x10⁶ Ly6C^{high} or 0.5-1x10⁶ Ly6C^{low} monocytes were transferred intravenously, in a volume of 0.1ml into resting or colitic congenic recipient mice, the genotype of

which varied between experiments. Recipient mice were examined for the presence of donor cells at different time points after monocyte infusion.

2.14 Competitive Adoptive Transfer of BM cells

To study the relative ability of CCR2-deficient and WT BM monocytes to migrate to the intestine, a 1:1 mix of total BM cells from C57Bl/6.SJL (CD45.1⁺) and CCR2KO (CD45.2⁺) mice was labelled with 5 μ M CellTrace™ Far Red DDAO-SE (Molecular Probes) in HBSS at RT for 5 minutes. Following labelling, the cells were washed twice with PBS/5% FCS and 12 x 10⁶ labelled cells in 0.2ml of PBS were injected i.v. into C57BL/6 (CD45.2⁺) mice that had received 2% DSS in their drinking water for 5 days to induce colonic inflammation, or into control mice that had received normal drinking water. Following cell transfer, recipient mice continued to receive DSS or normal drinking water for a further 24hrs, after which cells were harvested from the spleens and colons of the recipient mice and analysed for the presence of donor (Far Red DDAO-SE⁺) cells. The ratio of WT (CD45.1⁺) versus CCR2KO (CD45.2⁺) cells was then assessed in each tissue.

2.15 Transfer of Monocytes into Mice Depleted of CD11c⁺ cells

To deplete CD11c-expressing cells, CD11c-DTR-GFP mice were injected with 4ng/g bodyweight diphtheria toxin (DT; Sigma-Aldrich) and 24hrs after treatment, mice received 2x10⁶ Ly6C^{high} purified BM monocytes from CX3CR1^{+gfp} CD45.1⁺/CD45.2⁺ mice and were assessed for the presence of donor cells 24hrs or 4 days after transfer.

2.16 Generation of BM Chimeric Mice

8 week old female C57Bl/6 (CD45.2⁺) mice were irradiated with a total dose of 11 Gy 2 hrs apart. Mice then received 1x10⁷ BM cells from CD45.1⁺/CD45.2⁺ C57Bl/6 mice and were left for 8 weeks to allow BM engraftment. BM chimeric mice were generated by Dr. K.M. Lee, University of Glasgow.

2.17 Administration of Growth Factors *In Vivo*

To assess DC expansion CX3CR1^{+gfp} mice were injected i.p. with 10 μ g human recombinant CHO-derived flt3L (a kind gift of Amgen Corp, Seattle, USA)

in 0.2ml sterile PBS for 8 consecutive days to achieve maximal cell expansion, as previously optimised in the Mowat lab. To assess the role for CSF-1, 20,000U of recombinant CSF-1 (a kind gift of Dr. David Sester, Roslin Institute, Edinburgh) was injected i.p. in 0.2ml sterile PBS for 4 consecutive days, as this has been shown previously to expand tissue macrophage numbers (49). The extent of cell expansion was assessed by comparing cell numbers with non-injected resting CX3CR1^{+gfp} mice.

2.18 Cytospins

Aliquots of FACS-purified cells ($0.5-1 \times 10^5$ cells) were spun onto PolysineTM glass microscope slides (VWR International) at 300 RPM for 6 minutes using a cyto-centrifuge (Shandon, Runcorn, UK). Cells were then fixed in acetone for 10 minutes, allowed to air dry and then stained using the Rapid-Romanowsky staining kit (Raymond A. Lamb, Eastbourne, UK). Slides were washed thoroughly in distilled water, allowed to air dry and then mounted in DPX mountant (BDH, UK) under glass. Stained cells were assessed for morphology using an Olympus BX41 microscope.

2.19 RNA Extraction

Single cell suspensions (FACS-sorted cells or BMM) were washed twice with PBS, spun down and the supernatant discarded. RNA was then isolated using the RNeasy Micro or Mini Kit (Qiagen) (depending on cell number) according to the manufacturer's guidelines. Contaminating genomic DNA was removed on-column during RNA isolation with the RNase-free DNase Set (Qiagen) according to the manufacturer's instructions. The RNA was quantified using a spectrophotometer (Amersham Biosciences) and then stored at -20°C until use.

2.20 cDNA Synthesis from RNA

cDNA was reverse transcribed from DNase-treated RNA using Superscript II Reverse Transcriptase (RT) (Invitrogen) according to the manufacturer's instructions. Briefly, 13ng of RNA, 1 μl Oligo(dT)₁₂₋₁₈ (500 $\mu\text{g}/\text{ml}$; Invitrogen), 1 μl dNTP mix (25mM each; Invitrogen), and nuclease-free water (Ambion) were added to a nuclease-free microcentrifuge tube (ABgene, Surrey, UK) in a total volume of 12 μl . The mixture was heated at 65°C for 5 minutes, and then quick-

chilled on ice. 4µl 5X First-Strand Buffer (Invitrogen), 2µl 0.1M DTT (Invitrogen), and 1µl RNaseOUT (40 units/ml; Invitrogen) were added and incubated at 42⁰C for 2 minutes. 1µl (200 units) Superscript II RT was then added and the RNA was reverse transcribed at 42⁰C for 50 minutes. Superscript II RT was then inactivated by heating at 70⁰C for 15 minutes. cDNA was diluted 1:10 and then stored at -20⁰C until use. Negative control samples were incubated in the absence of Superscript II, and cDNA was stored at -20⁰C until use.

2.21 Quantitative/Real Time PCR

Gene expression was assayed by quantitative reverse transcription PCR (qRT-PCR) using Brilliant III Ultra Fast SYBR qPCR master mix (Agilent Technologies) on the 7900HT Fast system (Applied Biosystems) using the primers as detailed in Table 2.4. cDNA samples were assayed in triplicate and gene expression levels were normalised to Cyclophilin A (CPA). The mean relative gene expression was calculated using the $2^{-\Delta C(t)}$ method. All qRT-PCR experiments were carried out by Charlotte Scott.

2.22 Statistical Analysis

Results are presented as means + 1 standard deviation and groups were compared using a Student's t test, Mann Whitney test or for multiple groups, a one-way ANOVA followed by a Bonferroni post test using Prism Software (GraphPad Software, Inc.). Values of less than $p < 0.05$ were considered to be statistically significant.

Table 2.4: Primers used in qRT-PCR

Gene	Sense	Anti-sense	Reference
<i>Cyclophilin A</i>	GTG GTC TTT GGG AAG GTG AA	TTA CAG GAC ATT GCG AGC AG	(317)
<i>Cx3cr1</i>	TGT CCA CCT CCT TCC CTG AA	TCG CCC AAA TAA CAG GCC	(30)
<i>Cd163</i>	CCT TGG AAA CAG AGA CAG GC	TCC ACA CGT CCA GAA CAG TC	(317)
<i>Cd206</i>	TGT GGT GAG CTG AAA GGT GA	CAG GTG TGG GCT CAG GTA GT	(317)
<i>Tgfbr2</i>	ACA TTA CTC TGG AGA CGG TTT GC	AGC GGC ATC TTC CAG AGT GA	n/a
<i>Arginase-1</i>	CAG AAG AAT GGA AGA GTC AG	CAG ATA TGC AGG GAG TCA CC	(318)
<i>Ccr2</i>	ATC CAC GGC ATA CTA TCA ACA TC	CAA GGC TCA CCA TCA TCG TAG	(317)
<i>Il6</i>	CCA GTT GCC TTC TTG GGA CT	GGT CTG TTG GGA GTG GTA TCC	(317)
<i>inos</i>	GCC ACC AAC AAT GGC AAC A	GCC ACC AAC AAT GGC AAC A	(222)
<i>Il10</i>	GCT CTT ACT GAC TGG CAT GAG	CGC AGC TCT AGG AGC ATG TG	(317)
<i>Tnfa</i>	ACC CTC AACTC AGA TCA TCT TC	TGG TGGTTT GCT ACG ACG T	(319)
<i>Vegf</i>	CCT TCG TCC TCT CCT TAC CC	AAG CCA CTC ACA CAC ACA GC	(317)
<i>Tlr1</i>	TGG ACA CCC CTA CAG AAA CGT	AAT TTG GTT TAG TCA TTG TTG TAT GGC C	(320)
<i>Tlr2</i>	CTG GAG CAT CCG AAT TGC A	CAT CCT CTG AGA TTT GAC GCT TT	(320)
<i>Tlr3</i>	CCA GAA GAA TCT AAT CAA ATT AGA TTT GTC	TTT TGC TAA GAG CAG TTC TTG GAG	(320)
<i>Tlr4</i>	GGC AAC TTG GAC CTG AGG AG	CAT GGG CTC TCG GTC CAT AG	(320)
<i>Tlr5</i>	CAC TCC CTC GGA GAA CCC A	GGC CTT GAA AAA CAT CCC AAC	(320)
<i>Tlr6</i>	AAA GTC CCT CTG GGA TAG CCT CT	TGC TTC CGA CTA TTA AGG CCA	(320)
<i>Tlr7</i>	ACA GAA ATC CCT GAG GGC ATT	CAG ATG GTT CAG CCT ACG GAA G	(320)
<i>Tlr9</i>	GGG CCC ATT GTG ATG AAC C	CTT GGT CTG CAC CTC CAA CA	(320)

Chapter 3
**Phenotypic Characterisation of Lamina
Propria Macrophages During Homeostasis
and Inflammation**

3.1 Introduction

As discussed in Chapter 1, the precise characterisation of individual MP populations in the intestine has been stifled by the realisation that markers such as F4/80 and CD11c, previously thought to be specific for m ϕ and DC respectively, are inadequate for the identification of discrete populations when used in isolation. The position has been made more complex by the use of different isolation techniques, for example the use or not of density gradients to purify mononuclear cells. As a result, when I began my project, it was becoming increasingly apparent that many myeloid cell populations in the intestine had been misclassified, meaning there was confusion over their exact roles in homeostasis, protective immunity and pathology.

Studies carried out by the Mowat laboratory prior to my arrival had been limited to 4 colour flow cytometry and had concluded that the colonic LP housed two discrete F4/80⁺ m ϕ populations based on the presence or absence of surface TLR2 expression (222). The F4/80⁺TLR2^{neg} subset was shown to form the majority population (~70% of F4/80⁺ cells) within the steady state colonic LP and was characterised by lack of class II MHC and CCR2 expression, as well as unresponsiveness to TLR stimulation. In contrast, the F4/80⁺TLR2⁺ subset which made up ~30% of F4/80⁺ cells in the normal mucosa expressed high levels of class II MHC, responded to TLR ligation and came to dominate during inflammation, being recruited in a CCR2-dependent manner. Because of these phenotypic differences and the changes in abundance of the respective populations during inflammation, it was concluded that the F4/80⁺TLR2^{neg} and F4/80⁺TLR2⁺ subsets represented 'resident' and 'pro-inflammatory' m ϕ populations respectively. The presence of these two m ϕ subsets with distinct functional properties was thought to help explain the fact that intestinal F4/80⁺ m ϕ are essential for the maintenance of mucosal homeostasis and yet can also drive intestinal inflammation.

However when multi-parameter flow cytometry became available to us soon after I began work, it became apparent that the mucosal populations were much more complex and thus these initial conclusions about m ϕ in the colon needed revisited. Thus in this first chapter I set out to re-examine the phenotype of the

myeloid cell compartment present in the steady state colon and investigated how these populations changed during experimental colitis.

3.2 Preliminary Identification of Macrophages in Steady State Colon

The previous studies in the laboratory identifying m ϕ subsets using 4-colour flow cytometry had had to be restricted to F4/80, TLR2, 7-AAD (to exclude dead cells) and one other marker of e.g. activation. My first experiments were also limited to 4-colours, but when I added the pan-leucocyte marker, CD45 to exclude non-haematopoietic cells, I made the surprising discovery that many of the F4/80⁺TLR2^{neg} cells were not CD45⁺ (Fig. 3.1A and B). Furthermore, most of the cells in the CD45⁺ fraction of this TLR2^{neg} population had a high SSC profile more like granulocytes than myeloid cells (Fig. 3.1B). There were also significant numbers of these cells which appeared to be cell debris or aggregates, as shown when I gated for doublets (Fig. 3.1C).

I therefore devised an improved gating strategy in which single cells were first identified within whole LP digests using forward (FSC) and side scatter (SSC) parameters (Fig. 3.2A), and then live leucocytes were identified by gating on CD45⁺ 7-AAD^{neg} cells. This gating strategy resulted in far superior separation of F4/80⁺ populations (Fig. 3.2B) and revealed that the frequency of F4/80⁺TLR2^{neg} versus F4/80⁺TLR2⁺ populations was altered considerably, with F4/80⁺TLR2⁺ cells now dominating over the F4/80⁺TLR2^{neg} subset even in healthy colon.

At this point two major developments occurred which allowed me to exploit this revised gating strategy more fully. First, I was able to make use of 10-colour flow cytometry and secondly, CX3CR1^{+gfp} mice became available. As I discussed previously, not long after I started my project it had been proposed that the mutually exclusive expression of CD103 and the chemokine receptor CX3CR1 could be used to identify DC and m ϕ respectively in the intestine (189). Therefore having access to CX3CR1^{+gfp} mice, in which one of the genes encoding CX3CR1 has been replaced with the green fluorescent protein (*gfp*) (209), allowed me to examine the TLR2^{neg} and TLR2⁺ populations of the F4/80⁺ cells from the colon in more detail. This analysis confirmed my earlier conclusions that most of the TLR2^{neg} subset were not m ϕ , as they had a high SSC profile and lacked CX3CR1 expression (Fig. 3.2C and D). In contrast, all F4/80⁺TLR2⁺ cells expressed

CX3CR1, although the levels varied, suggesting that this population might be heterogeneous (Fig. 3.2D).

Thus together these data reveal that most of the F4/80⁺ cells originally thought to be m ϕ are either non-haematopoietic cells or not m ϕ , and that TLR2 cannot be used to distinguish m ϕ subsets in the colon. In addition, they indicate that CX3CR1 expression is more informative for the identification of individual MP populations.

3.3 CX3CR1 Expression Defines 3 Populations of CD11b⁺ Cells

Having established some fundamental parameters that appeared to allow clearer definition of MP in the colonic mucosa, I went on to use these gating strategies and multi-colour flow cytometry to characterise these cells more fully in CX3CR1^{+gfp} mice. First I used CD11b expression to identify the entire myeloid compartment of the CD45⁺7-AAD^{neg} cells in the mucosa and analysed CX3CR1-GFP expression. This revealed three distinct populations of CD11b⁺ cells: CX3CR1^{neg}, CX3CR1^{int} and CX3CR1^{high} that constituted 5.04 \pm 1.02%, 6.1 \pm 1.6% and 15.7 \pm 1.7% of the CD45⁺ fraction of all viable cells in resting mice, respectively (Fig. 3.3A and B). To explore the composition of each of these populations in more detail, I first examined their FSC and SSC profiles (Fig. 3.3C). The CX3CR1^{neg} population was heterogeneous in terms of FSC and SSC, with the majority of cells displaying high SSC characteristics akin to that of granulocytes, whereas the remainder of cells had low FSC and SSC profiles. The CX3CR1^{int} and CX3CR1^{high} populations had profiles typical of myeloid cells, although the CX3CR1^{high} population had higher FSC, indicating they were larger. I next went onto assess the expression of F4/80, CD11c, class II MHC, CD103 and Ly6C on these cells, as markers of putative m ϕ , DC and monocytes.

3.3.1 CX3CR1^{neg} Cells

Initial analysis of this population showed that most CX3CR1^{neg} cells expressed F4/80, albeit at lower levels than those on the CX3CR1^{high} cells and more comparable to CX3CR1^{int} cells (Fig. 3.4A). The vast majority of CX3CR1^{neg} cells lacked expression of class II MHC, but expressed intermediate levels of CD11c and Ly6C (Fig. 3.4A). Further examination of these markers in combination revealed that two distinct populations could be defined by their SSC profile and

CD11c expression (Fig. 3.5A). $SSC^{high}CD11c^{low-int}$ cells lacked class II MHC expression, whereas the minor SSC^{low} population expressed high levels of CD11c and class II MHC. This suggests that these $CX3CR1^{neg}SSC^{low}$ cells may be $CD11b^{+}$ DC, an idea supported by the fact that 20-30% of them co-expressed CD103 (Fig. 3.5B). However the vast majority of $CD103^{+}$ DC in the colon failed to express CD11b or CX3CR1 (not shown).

Because of the high SSC profile of the $CD11c^{low-int}$ cells and because recent studies have identified $F4/80^{low}$ eosinophils in the normal small intestine (253), I examined the $SSC^{high}CD11c^{low}$ population for the expression of SiglecF, a sialic acid-binding immunoglobulin lectin reported to be expressed exclusively by eosinophils (254). This revealed that over 90% of the $SSC^{high}CD11c^{low-int}$ population expressed SiglecF (Fig. 3.5C). Surprisingly, colonic LP SiglecF⁺ eosinophils failed to express the CCL11 (eotaxin) receptor CCR3 to any significant level (Fig. 3.5D), in contrast to what has been reported for eosinophils in the BM, small intestine and lung (253). The remainder of the $SSC^{high}CD11c^{low-int}$ cells appeared to be neutrophils, as determined by intermediate levels of Ly6C and uniformly high expression of the neutrophil-specific marker Ly6G (Fig. 3.5E). These neutrophils were extremely rare in the steady state intestine, constituting less than 0.5% of the total $CD45^{+}$ live fraction of cells and indicating the colonic LP populations were not contaminated significantly by blood.

To confirm that intestinal SiglecF⁺ cells were eosinophils, I FACS-purified them to >90% purity and assessed their morphological appearance (Fig. 3.6A and B). Similar to the small population of $F4/80^{low}SiglecF^{+}$ eosinophils FACS-purified from the resting peritoneal cavity, intestinal SiglecF⁺ cells exhibited typical eosinophil characteristics such as ring-shaped nuclei and the presence of eosinophilic granules (Fig. 3.6B and C).

Together these phenotypic analyses demonstrated that the $CD11b^{+}CX3CR1^{neg}$ population comprises: (1) $F4/80^{low}SiglecF^{+}$ eosinophils, (2) a small population of $CD11c^{+}MHCII^{high}$ putative DC and (3) a small population of $Ly6C^{int}$ ($Ly6G^{+}$) neutrophils.

3.3.2 CX3CR1^{high} Cells

The CX3CR1^{high} compartment of CD11b⁺ cells was a homogeneous population that uniformly expressed F4/80 and class II MHC at high levels, but lacked expression of CD103 or Ly6C (Fig. 3.4C and 3.7). This would have made up most of the F4/80⁺TLR2⁺ subset found using the former gating strategy (Fig. 3.2). Significantly, this population expressed CX3CR1 at levels much higher than any other myeloid cells I examined, including resident peritoneal m ϕ , CSF-1 generated BM m ϕ or either population of Ly6C^{high}CX3CR1⁺ 'inflammatory' or Ly6C^{low}CX3CR1^{high} 'resident' blood monocytes (Fig. 3.9A and B). The majority of CX3CR1^{high} cells also expressed low to intermediate levels of CD11c, a property that led to them being misclassified as DC in previous studies (195, 196). However the level of CD11c expression I found was extremely variable between experiments, being dependent upon the clone of antibody used and even the fluorochrome to which it was conjugated. Analysis of FACS-purified CX3CR1^{high} cells (purity Fig. 3.8) showed that they possessed the morphological features of mature m ϕ , including a large 'foamy' appearance and the presence of cytoplasmic vacuoles (Fig. 3.7B). In future experiments, they will be referred to as Population 4 (Table 3.1 and see below).

3.3.3 CX3CR1^{int} Cells

In contrast to the CX3CR1^{high} population, the CX3CR1^{int} fraction of CD11b⁺ cells was heterogeneous in terms of F4/80, class II MHC, CD11c and Ly6C expression (Fig. 3.4B). By examining all these markers in combination, I found that the CX3CR1^{int} fraction contained at least four populations of cells (Fig. 3.7A). For simplicity when referring to the subsets in the remainder of this thesis, these are numbered according to the scheme outlined in Table 3.1.

First I divided the CX3CR1^{int} compartment on the basis of F4/80 and CD11c expression. Although the exact proportions of these subsets varied between experiments, approximately two thirds of them usually expressed F4/80 and low to intermediate levels of CD11c. The remaining third (named P5) expressed high levels of CD11c, but generally lacked F4/80 expression and also uniformly expressed high levels of class II MHC (Fig. 3.7A). In contrast, the F4/80⁺ fraction of CX3CR1^{int} cells could be further subdivided on the basis of Ly6C and class II MHC expression to give three populations: Ly6C^{high}MHCII^{neg} (P1), Ly6C⁺MHCII⁺

cells (P2) and Ly6C^{neg}MHCII⁺ (P3). Although P1, P2, P3 and P5 all expressed 'intermediate' levels of CX3CR1, the exact level of expression varied between these populations. P5 expressed the lowest level of CX3CR1, whereas P1-P3 expressed CX3CR1 at a level comparable to blood monocytes (Fig. 3.9B). FACS-purified P1 and P3 possessed distinct morphological features. Whereas P3 contained prominent cytoplasmic vacuoles similar to CX3CR1^{high} cells, P1 cells were much smaller and monocytic in appearance, which would be consistent with a surface phenotype that is identical to blood monocytes (CD11b⁺Ly6C^{high}MHCII^{neg}CX3CR1^{int}) (Fig. 3.7B). Due poor cell yield I was unable to assess the morphological characteristics of P2 and P5.

Due to their phenotypic appearance (F4/80^{neg}CD11c⁺), I next set out to assess whether the cells in P5 were a population of CX3CR1⁺ DC by assessing their responsiveness to the growth factor flt3L *in vivo*. As expected, administration of flt3L to mice for 8 consecutive days expanded the numbers of archetypal mucosal CD103⁺ DC (Fig. 3.10A-C). However it had little or no effect on cells in P1-P4. Although P1 and P2 were increased in number, the difference from untreated mice was not significant. In contrast, flt3L treatment resulted in a 5.9-fold increase in the number of P5 cells (CD11c⁺Ly6C^{neg}MHCII⁺CX3CR1^{neg}) similar to that seen with the CD103⁺ DC population (Fig. 3.10A-C). These results confirm that the F4/80⁺ and CD11c⁺ populations within the Ly6C^{neg}MHCII⁺ fraction of the CX3CR1^{int} compartment are distinct and that the latter population represent *bona fide* DC.

3.4 Lamina Propria Myeloid Cells During Inflammation

It is well established that the composition of the intestinal MP pool changes dramatically during inflammation in both mouse and man (222, 242). However, the use of inappropriate markers has meant that many of the populations have not been documented accurately. Therefore as a first step to exploring the biology of the CX3CR1⁺ subsets I had defined in the normal colon, I used my newly established gating strategies to examine how these cells changed in acute colitis induced by feeding dextran sodium sulphate (DSS).

3.4.1 Induction of Intestinal Inflammation

I first compared disease progression in CX3CR1^{+gfp} mice and wild type (WT) C57 Bl/6 mice, to ensure that lack of one CX3CR1 allele did not alter susceptibility to DSS-induced colitis. WT C57 Bl/6 mice began to lose weight after 5-6 days of administering 2% DSS in their drinking water and this continued to progress over the remainder of the study (Fig. 3.11A). This was accompanied by rectal bleeding and diarrhoea that worsened over time, leading to a progressive increase in the clinical disease score (detailed in Table 2.3 in the Materials and Methods). There were no differences in weight loss or in the clinical features of disease in CX3CR1^{+gfp} mice (Fig.3.11B). In addition, comparable colon shortening, a further index of pathology in this model, was seen in B6 and CX3CR1^{+gfp} mice (Fig. 3.11C). C57BL/6 mice and CX3CR1^{+gfp} consumed equivalent amounts of DSS-containing water over the 9 days (Figure 3.11D).

3.4.2 Effects of Inflammation on the Mucosal Myeloid Compartment

I next examined the changes in CD11b⁺ populations during experimental colitis in CX3CR1^{+gfp} mice. Initial examination revealed that there was a massive increase in the total CD11b⁺ compartment in colitic animals compared with resting mice (Fig. 3.12). Whereas the total CD11b⁺ population constituted 23.3±6.1% of the CD45⁺7-AAD^{neg} fraction of cells in resting mice, this increased significantly to 40.1±6.6% and 51.1±5.1% on d4 and d6 of colitis respectively (Fig. 3.12A and B). This increase in proportion was matched by a significant increase in the absolute number of CD11b⁺ cells from 2.75x10⁵ ± 0.4 per colon in steady state to 6.2x10⁵ ± 2.1 and 12.1x10⁵ ± 2.4 per colon on d4 and d6 of colitis respectively (Fig. 3.12C). Thus, there is at least a 4-fold increase in the total myeloid compartment in established colitis.

I next examined the composition of the CD11b⁺ fraction using CX3CR1 to define the populations I had found in steady state LP. The induction of colitis had very dramatic effects on the composition of these populations found in the colon, with large increases in the proportions and numbers of both CX3CR1^{neg} and CX3CR1^{int} cells (Fig. 3.13A-C). As discussed above, the steady state CX3CR1^{neg} population contains SiglecF⁺ eosinophils, as well as small populations of CD11c⁺MHCII⁺ DC and Ly6G⁺ neutrophils. Administration of DSS resulted in an

intense influx of both populations of granulocytes (Fig. 3.14A and B), with the absolute number of Ly6C^{int} (Ly6G⁺) neutrophils increasing from $0.18 \times 10^4 \pm 0.05$ per colon during resting conditions to $2.3 \times 10^4 \pm 2.5$ per colon on d4 of colitis and to $13.5 \times 10^4 \pm 6.6$ per colon on d6 (Fig. 3.14C). This equated to a 75-fold increase in the number of neutrophils between d0 (resting) and d6. The number of SiglecF⁺ eosinophils increased over 6-fold from $3.3 \times 10^4 \pm 0.7$ per colon during resting conditions to $20.2 \times 10^4 \pm 7.4$ per colon on d6 of colitis (Fig. 3.14D). In contrast, the absolute number of CX3CR1^{neg} CD11b⁺ DC did not change significantly during colitis, suggesting that this population is generally unaffected by the presence of inflammation (Fig. 3.14E).

The CX3CR1^{int} compartment showed even greater expansion than the CX3CR1^{neg} population. Whereas the various CX3CR1^{int} populations constituted $6.1 \pm 0.7\%$ of the CD45⁺7-AAD^{neg} fraction during resting conditions, this increased significantly to $22.1 \pm 7.6\%$ on d4 of colitis and further yet to $28.2 \pm 7.4\%$ on d6 of colitis (Fig. 3.13A-C). This proportional increase was due to true expansion of this compartment as the absolute number of CX3CR1^{int} cells increased 9.2-fold from $7.3 \times 10^4 \pm 1.8$ per colon under normal physiological conditions to $66.8 \times 10^4 \pm 23.5$ on d6 of colitis (Fig. 3.13C).

Next, I examined the individual populations within the CX3CR1^{int} (P1, P2, P3 and P5) at different stages of colitis. DSS administration led to a statistically significant expansion in Ly6C^{high} MHC^{neg} cells (P1), which increased from $14.5 \pm 2.9\%$ of the CX3CR1^{int} population from during resting conditions to $26.1 \pm 4.6\%$ and $32.4 \pm 5.4\%$ on d4 and d6 of colitis respectively (Fig. 3.15A and B). This translated to a 25-fold increase in absolute numbers of P1 cells between resting and d6 of colitis (Fig. 3.15C). The proportion of Ly6C⁺MHCII⁺ cells (P2) within the CX3CR1^{int} population also increased markedly between resting and colitic mice (Fig. 3.15D), with a 14-fold increase in their number from $1.4 \times 10^4 \pm 0.6$ per colon during steady state conditions to $20.01 \times 10^4 \pm 8.2$ at d6 of colitis (Fig. 3.15E).

Despite a significant decrease in the proportion of the CX3CR1^{int} compartment occupied by the Ly6C^{neg}MHCII⁺ populations (P3 and P5), these populations increased in terms of absolute numbers during colitis, although this increase was not as dramatic as that of P1 and P2 cells (Fig. 3.16A). The

F4/80⁺MHCII⁺Ly6C^{neg} cells in P3 increased only 5-fold between resting conditions and d6 of colitis from $2.1 \times 10^4 \pm 0.5$ to $10.04 \times 10^4 \pm 3.8$ per colon respectively (Fig. 3.16B). In addition, their expansion appeared to lag behind that of P1 and P2 which occurred earlier in disease. Although there was a statistically significant increase in the number of the DC-like CD11c⁺MHCII⁺Ly6C^{neg}F4/80^{neg} cells in P5 between resting conditions and d6 of colitis ($2.2 \times 10^4 \pm 0.9$ versus $6.1 \times 10^4 \pm 2.1$ per colon, respectively), this only represented a 2.9-fold increase and their proportions fell markedly in comparison to the other CX3CR1^{int} cells (Fig. 3.16C).

In contrast to the CX3CR1^{neg} and CX3CR1^{int} populations, the CX3CR1^{high} population did not increase in abundance during colitis (Fig. 3.13). Indeed their proportion amongst the total viable CD45⁺ population decreased progressively as colitis developed ($12.03 \pm 4.7\%$ versus $3.0 \pm 1.1\%$ in resting and d6 colitic respectively; Fig. 3.13A and B). Although these differences did not translate into a statistically significant decrease in absolute number, there was a 2-fold decrease in the number of CX3CR1^{high} cells retrieved from the resting versus the colitic LP by d6 ($13.3 \times 10^4 \pm 2.0$ versus $6.7 \times 10^4 \pm 1.9$, respectively; Fig. 3.13C). Despite the massive disruption in the intestinal architecture and the infiltration of many inflammatory cells, the phenotype of CX3CR1^{high} resident m ϕ did not change during colitis, and they all remained F4/80^{high} MHCII^{high} Ly6C^{neg} (Fig. 3.17A and B).

3.5 Summary

In this chapter I set out to optimise a protocol for the characterisation of myeloid cells in the mouse colon using multi-parameter flow cytometry, as my initial studies established that 4-colour flow cytometry using classical markers was inadequate for this. By using CX3CR1-GFP mice, I was able to define individual myeloid cell subsets very precisely and this revealed unsuspected heterogeneity within the intestinal CD11b⁺ compartment under steady state and inflammatory conditions. This population comprised CX3CR1^{neg}, CX3CR1^{int} and CX3CR1^{high} cells. The CX3CR1^{neg} compartment contained eosinophils, CD11b⁺ DC and a small population of neutrophils. The CX3CR1^{high} cells resembled tissue resident m ϕ phenotypically and morphologically and dominated the CD11b⁺ compartment of the resting colonic mucosa. A smaller but distinct population of CX3CR1^{int} cells was also present within the steady state mucosa and included multiple 'subsets' of myeloid cells, including Ly6C^{high}MHCII^{neg} cells (P1), Ly6C⁺MHCII⁺ cells (P2),

Ly6C^{neg}MHCII⁺ F4/80⁺ cells (P3) and Ly6C^{neg}MHCII⁺ F4/80^{neg}CD11c^{high} cells (P5). Both the CX3CR1^{int} and CX3CR1^{neg} populations expanded dramatically during experimental colitis, dwarfing the CX3CR1^{high} population. This was largely due to a massive increase in the number of Ly6C^{high}MHC^{neg} (P1) and Ly6C⁺MHC⁺ (P2) cells. Thus the colonic LP seems to house populations of 'resident' and 'pro-inflammatory' mφ identified by differential levels of CX3CR1 expression and this may go some way to explain how intestinal mφ can play such distinct roles in homeostasis and inflammation.

In the next chapter I next set out to assess whether these CX3CR1-defined compartments represented independent subsets or if a relationship existed between them by examining the precursor-subset relationship between distinct blood monocytes and CX3CR1^{int} and CX3CR1^{high} LP cells.

Table 3.1: Summary of CX3CR1⁺ Mononuclear Phagocytes in Steady State LP

Population	Surface Phenotype						Proposed Cell Type
	CX3CR1	F4/80	CD11c	Ly6C	MHC II	CD103	
1	++	+	-	++	-	-	Monocyte-like
2	++	++	+	+	+	-	?
3	+++	++	+	-	++	-	?
4	++++	+++	+	-	++	-	Resident M ϕ
5	+	-	++	-	++	-	DC

Expression of surface markers and putative lineage of P1-P5 subsets of CD11b⁺ cells found in resting colon based on CX3CR1 expression (see text for details).

Table 3.2: Changes in CX3CR1⁺ Populations During Inflammation

Population	Cell Number (x10 ⁴)		Fold Increase
	Steady state	d6 Colitis	
Total CD11b ⁺	27.4±4.0	121.0±24.0	4.4
P1 (Ly6C ^{high} MHCII ^{neg} CX3CR1 ^{int})	1.03±0.2	24.8±3.0	24.1
P2 (Ly6C ⁺ MHCII ⁺ CX3CR1 ^{int})	1.4±0.6	20.01±8.2	14.4
P3 (F4/80 ⁺ MHCII ⁺ CX3CR1 ^{int})	2.1±0.5	10.04±3.8	4.8
P4 (F4/80 ⁺ MHCII ⁺ CX3CR1 ^{high})	13.3±2.0	6.7±1.9	0.5
P5 (CD11c ⁺ MHCII ⁺ CX3CR1 ^{int})	2.2±0.9	6.1±2.1	2.9

Total colonic CD11b⁺ cells and CX3CR1-defined myeloid subsets were enumerated in steady state and in mice that had received DSS for 6 days. Results are the means + 1SD for 4 mice/group. The right-hand column indicates the fold-increase in each population during colitis over steady state conditions.

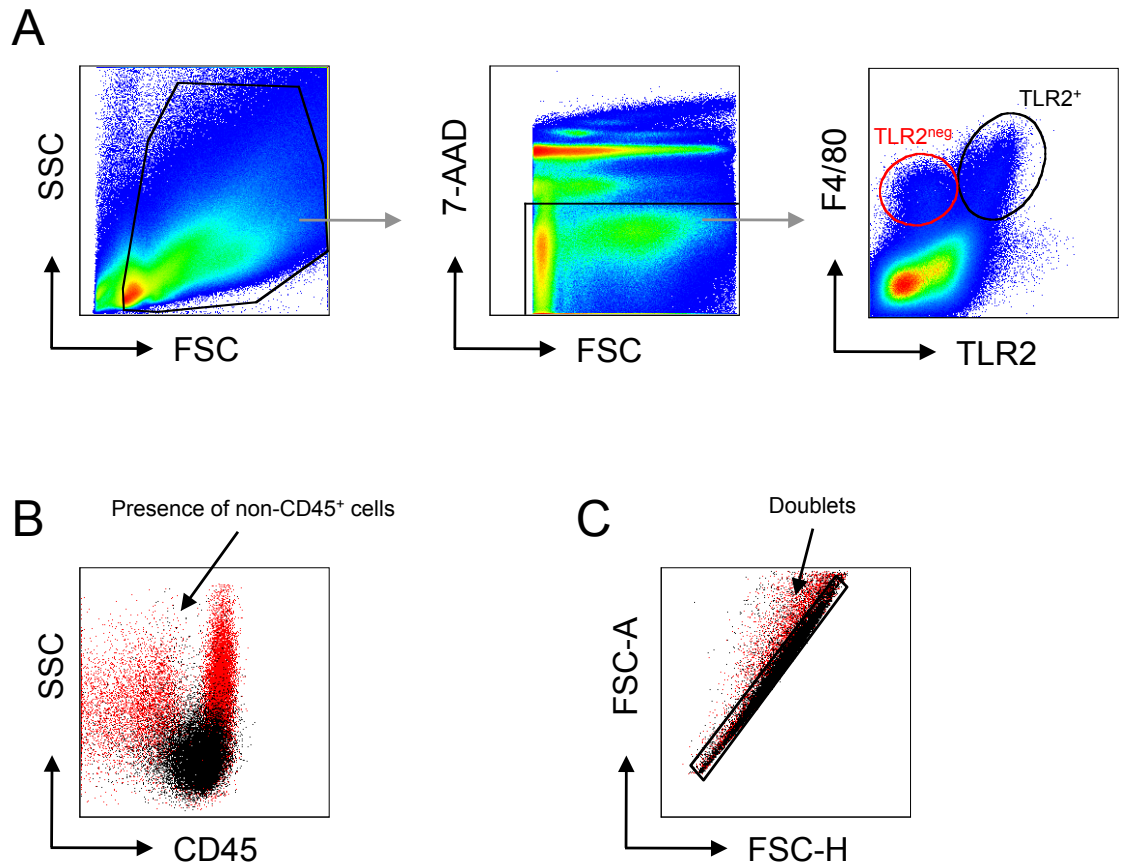


Figure 3.1: Original Gating Strategy for Identification of Colonic Macrophage Subsets

Colonic LP cells were isolated from WT mice and analysed for the expression of F4/80, TLR2 and CD45 by flow cytometry. **A.** Representative dot plots showing the original gating strategy using TLR2 to define subsets in which live (7-AAD^{neg}) cells were assayed for the expression of F4/80 and TLR2. **B.** Expression of CD45 and SSC profile of TLR2⁺ (black dots) and TLR2^{neg} (red dots) 'macrophage' subsets. **C.** FSC-Area (FSC-A) versus FSC-Height (FSC-H) of TLR2⁺ (black dots) and TLR2^{neg} (red dots) subsets. The gate shown identifies single cells and allows exclusion of doublets. Results are representative of at least 10 individual experiments.

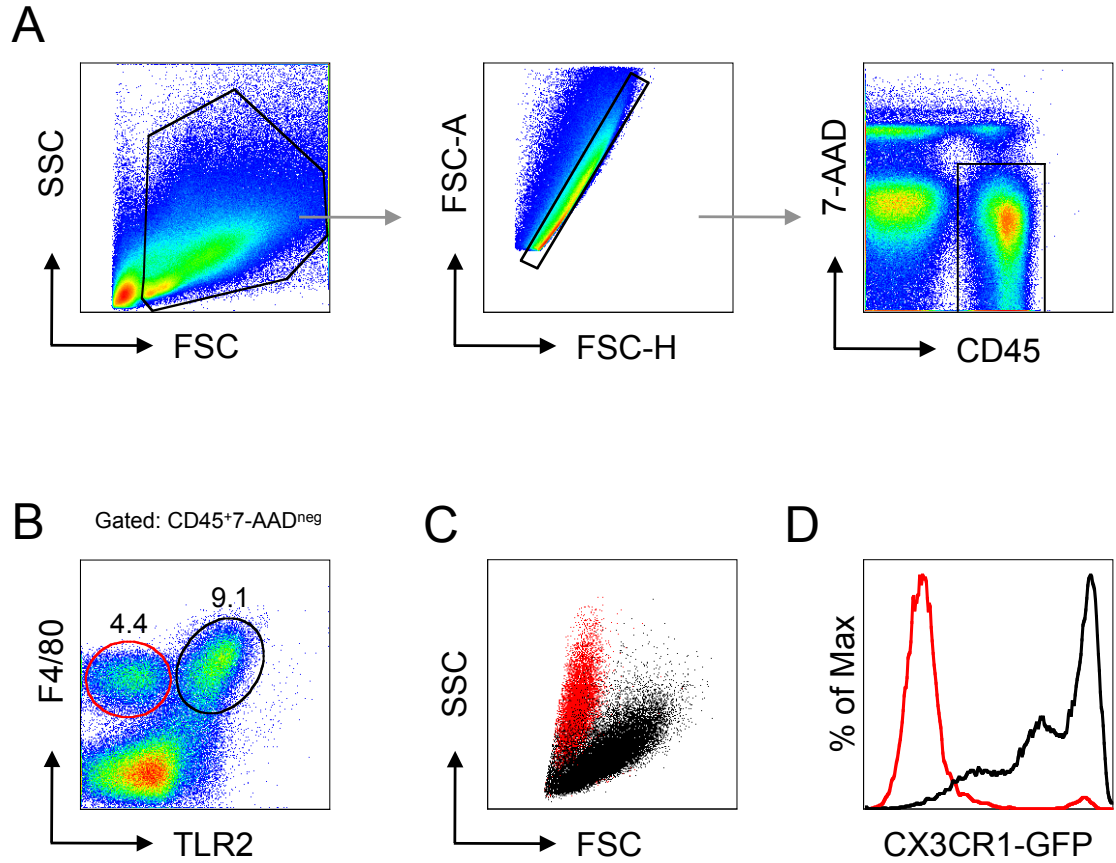


Figure 3.2: Refined Gating Strategy for Analysis of Colonic Myeloid Cells

Colonic LP cells were isolated from CX3CR1^{+gfp} mice and analysed for the expression of CD45, F4/80, TLR2 and CX3CR1-GFP by flow cytometry. **A.** Representative dot plots demonstrate the refined gating strategy that involves the exclusion of ‘doublets’ and the selection of CD45⁺ 7-AAD^{neg} (live haematopoietic cells). **B.** Expression of F4/80 and TLR2 on live leucocytes. **C.** FSC and SSC profiles of F4/80⁺TLR2^{neg} and F4/80⁺TLR2⁺ populations, highlighting the difference in size and granularity of these populations. **D.** Expression of CX3CR1 by F4/80⁺TLR2^{neg} and F4/80⁺TLR2⁺ populations. Results are representative of at least 10 individual experiments.

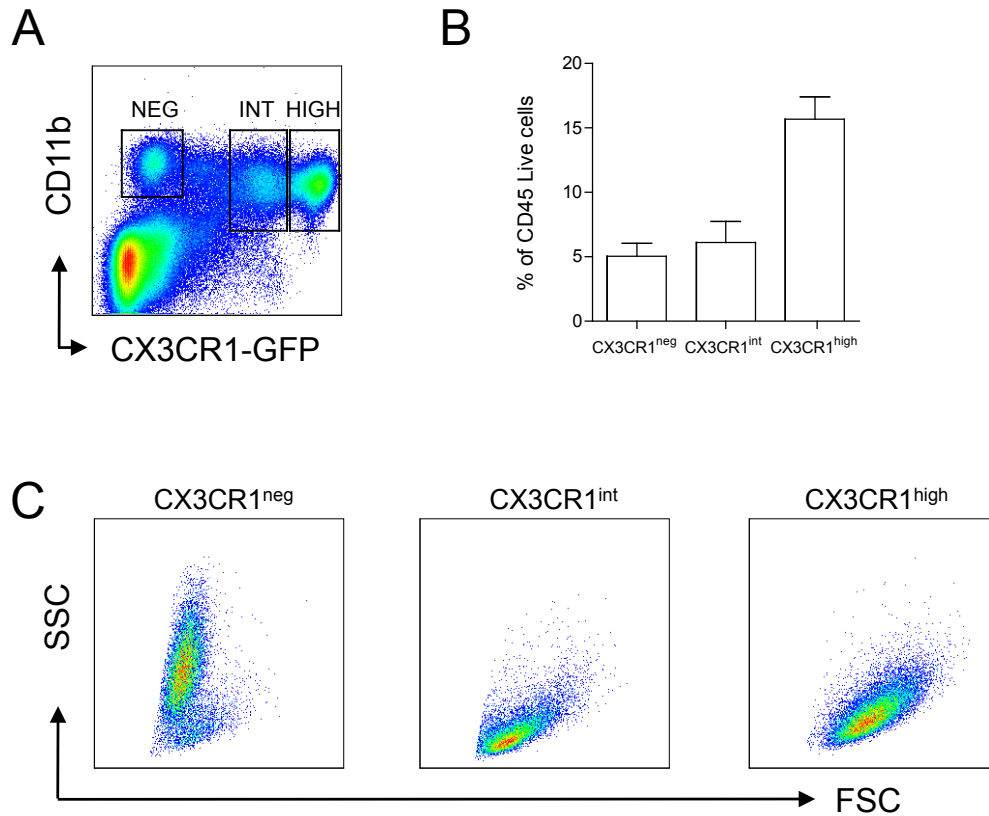


Figure 3.3: Colonic Myeloid Cell Populations Defined by CX3CR1 Expression

Colonic LP cells were isolated from resting CX3CR1^{+/-gfp} mice and CD11b⁺ populations identified on the basis of CX3CR1-GFP expression by flow cytometry. **A**. Representative dot plot of CD11b staining and CX3CR1-GFP expression by CD45⁺ live LP cells and **(B)** the relative frequencies of CX3CR1^{neg}, CX3CR1^{int} and CX3CR1^{high} CD11b⁺ cells as determined by flow cytometry. **C**. FSC and SSC profiles of each of the CX3CR1-defined populations. Results are representative of at least 10 individual experiments.

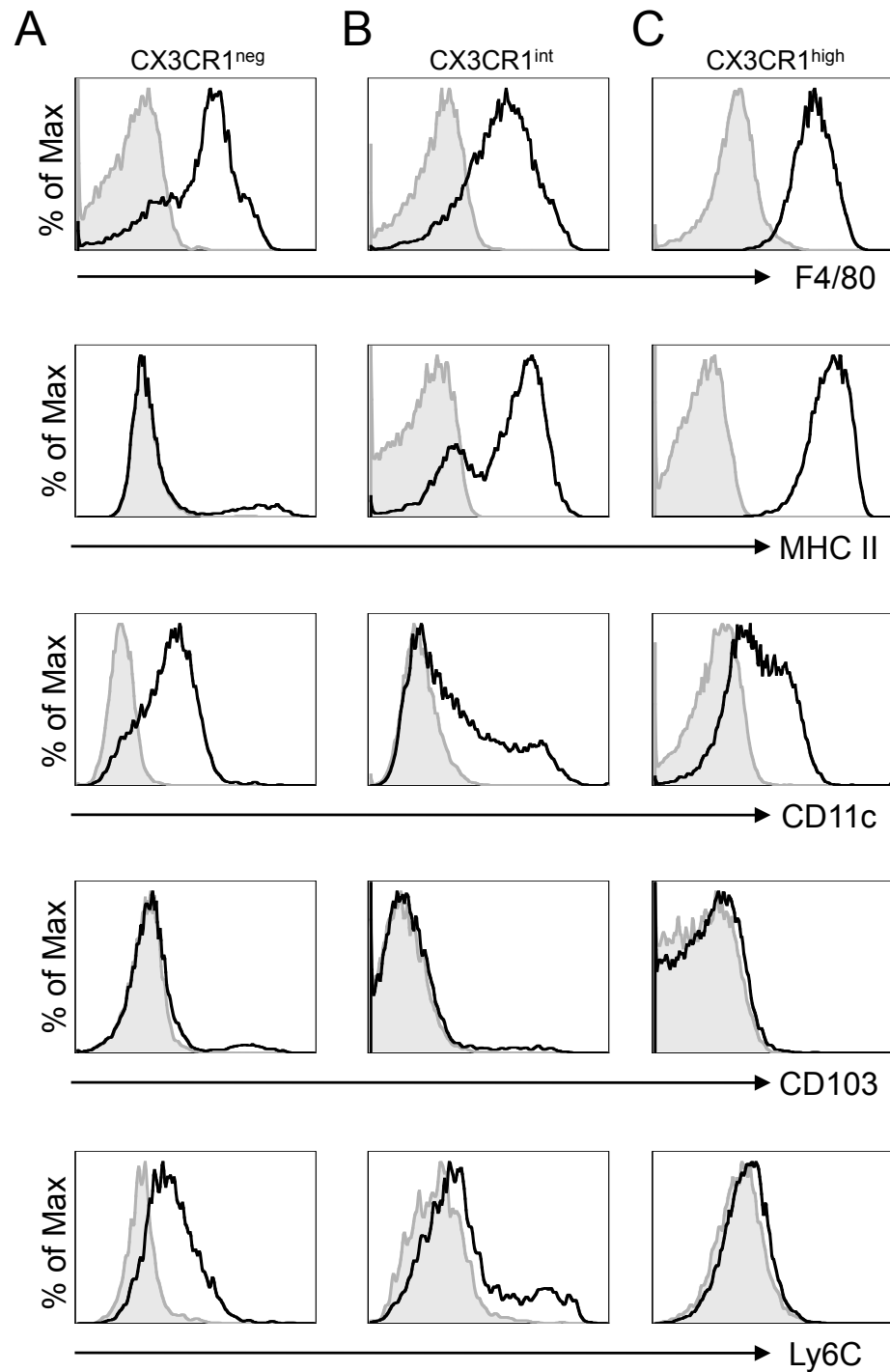


Figure 3.4: Phenotypic Characterisation of Colonic Myeloid Cells Identified by Levels of CX3CR1 Expression

Colonic LP cells were isolated from CX3CR1^{+/gfp} mice and subpopulations of CD11b⁺ cells identified on the basis of CX3CR1-GFP expression by flow cytometry. Expression of F4/80, class II MHC, CD11c, CD103 and Ly6C by CX3CR1^{neg} (**A**), CX3CR1^{int} (**B**) and CX3CR1^{high} CD11b⁺ (**C**) cells. Shaded histograms represent staining with the appropriate isotype control. Results are representative of 3 individual experiments.

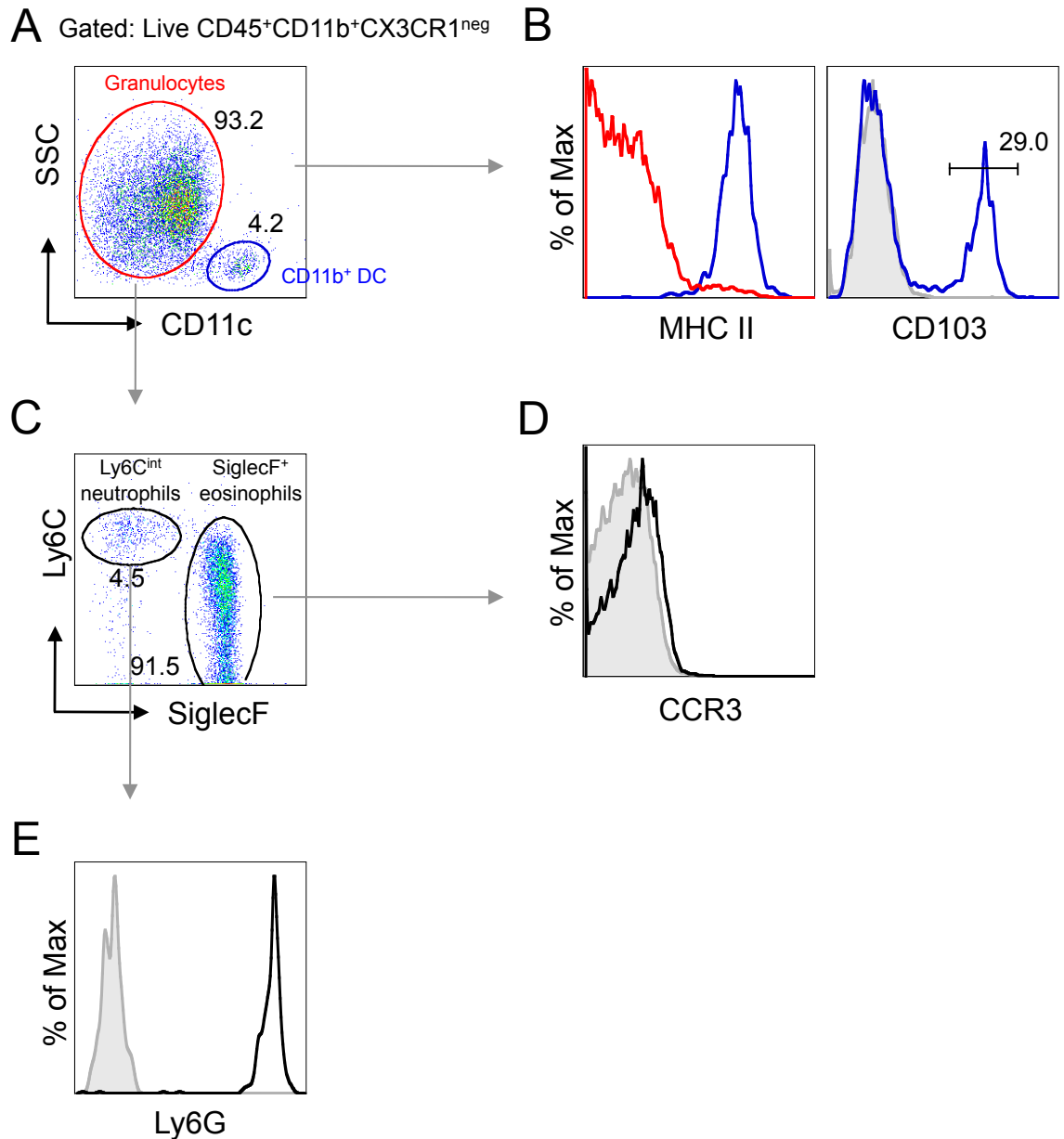


Figure 3.5: CD11b⁺ CX3CR1^{neg} SSC^{high} cells in the Colonic Mucosa are Eosinophils and Neutrophils

Colonic LP cells were isolated from CX3CR1^{+/gfp} mice and the CD11b⁺CX3CR1^{neg} fraction amongst live gated CD45⁺ cells was analysed for the expression of CD11c and SSC properties by flow cytometry. Representative dot plot of SSC versus CD11c expression (**A**) and the expression of class II MHC by SSC^{high}CD11c^{int} (granulocytes - red) and SSC^{low}CD11c^{high} cells (DC - blue) (**B**). **C**. Expression of Ly6C and SiglecF on SSC^{high}CD11c^{int} cells identifies SiglecF⁺ putative eosinophils and Ly6C^{int} cells. Expression of CCR3 by SiglecF⁺ eosinophils (**D**) and expression of Ly6G by Ly6C^{int} cells (**E**), confirming these as neutrophils. Shaded histograms represent staining with the appropriate isotype control. Results are representative of at least 3 individual experiments.

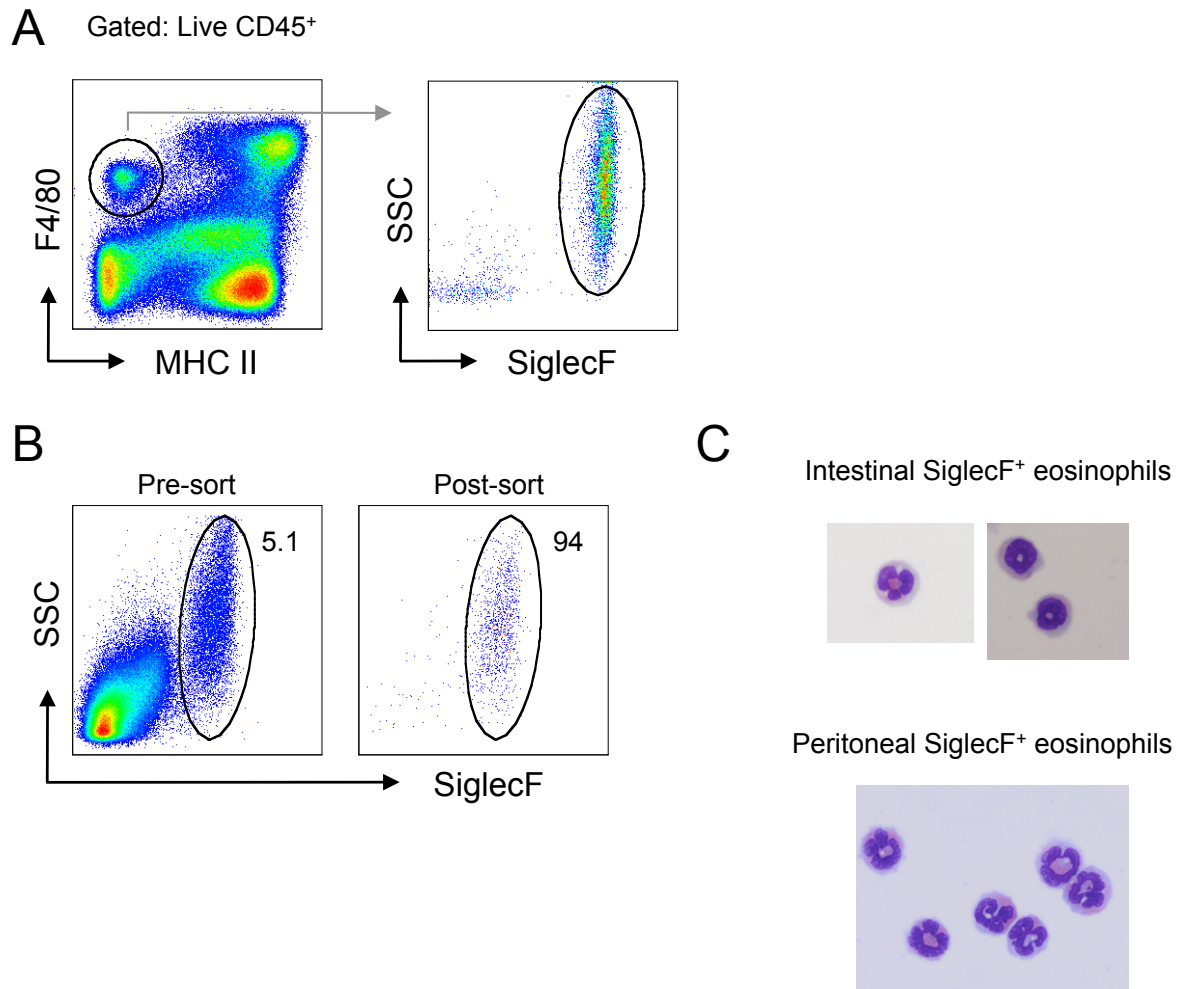


Figure 3.6: SiglecF⁺ Cells in the Colonic Mucosa Are Eosinophils

A. Colonic LP cells were isolated from WT mice and colonic eosinophils were identified amongst live-gated CD45⁺ F4/80^{low} MHCII^{neg} cells on the basis of SiglecF⁺ SSC^{high} and purified by FACS. **B.** Frequency of SiglecF⁺ eosinophils amongst live-gated CD45⁺ cells (*left panel*) and the post-sort purity of FACS-purified intestinal eosinophils (*right panel*). **C.** Cytospins of purified SiglecF⁺ intestinal cells were fixed and stained for morphological assessment and compared to FACS-purified F4/80^{low}SiglecF⁺ peritoneal cells (final magnification x400). Both had characteristic ring shaped nuclei and eosinophilic cytoplasmic staining. Results are representative of 2 individual experiments.

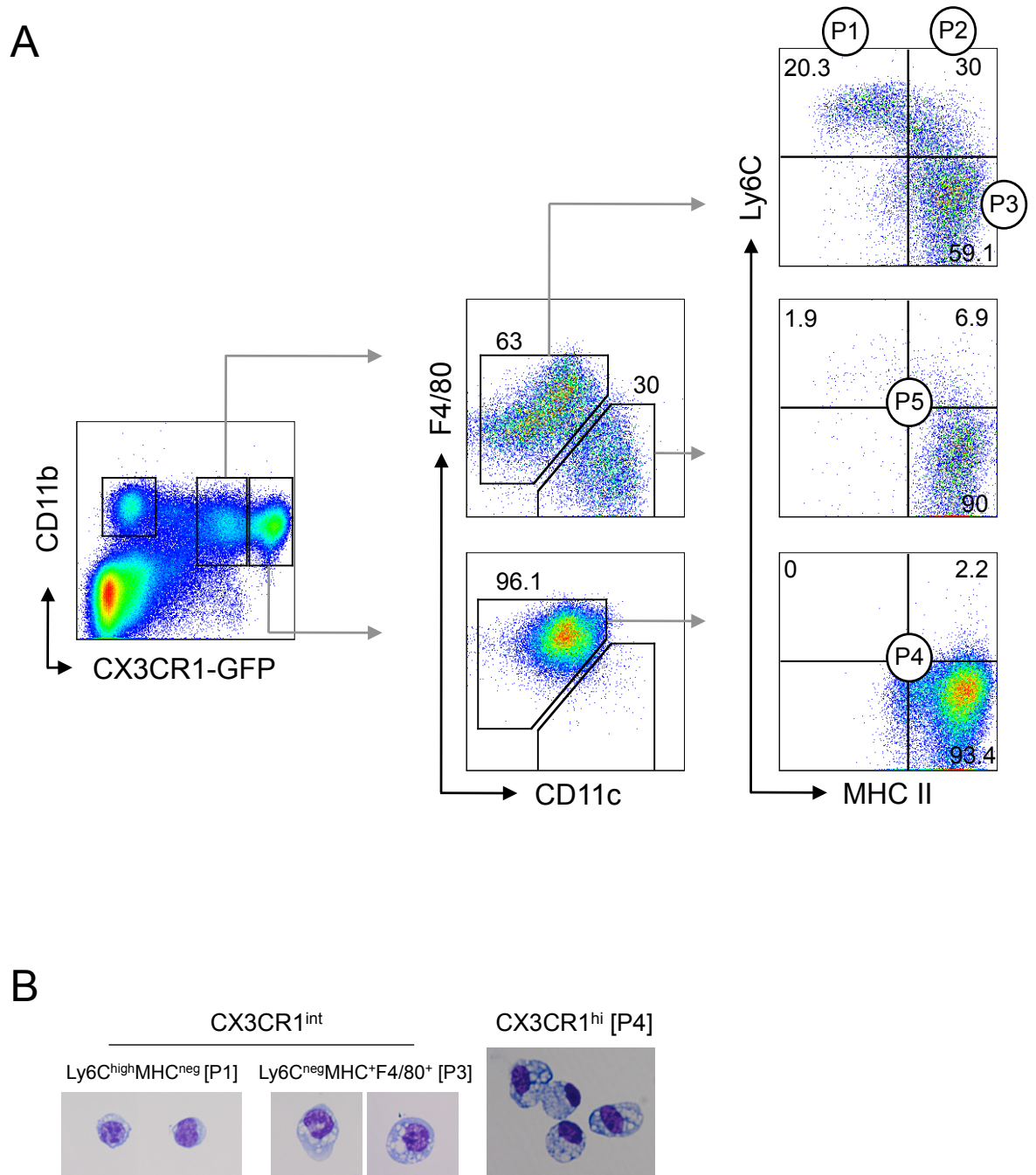


Figure 3.7: Heterogeneity within the CX3CR1⁺ Populations of Colonic Myeloid Cells

Colonic LP cells were isolated from resting CX3CR1^{+/gfp} mice and live-gated CD45⁺ CD11b⁺ populations characterised on the basis of CX3CR1-GFP expression by flow cytometry. **A.** Representative dot plots of F4/80, CD11c, Ly6C and MHC II expression by CX3CR1^{int} and CX3CR1^{high} CD11b⁺ cells, revealing a number of populations. As summarised in Table 3.1, these are CX3CR1^{int}Ly6C⁺MHC^{neg}F4/80^{low} (P1), CX3CR1^{int}Ly6C⁺MHC⁺F4/80⁺ (P2), CX3CR1^{int}Ly6C^{neg}MHC⁺F4/80⁺ (P3), CX3CR1^{high}Ly6C^{neg}MHC⁺F4/80^{high} (P4) and CX3CR1^{int}Ly6C^{neg}MHC⁺F4/80^{neg}CD11c⁺ (P5). Results are representative of at least 10 individual experiments. **B.** Morphological analysis of cytopins of FACS purified CX3CR1^{int}Ly6C^{high}MHC^{neg} (P1), CX3CR1^{int}Ly6C^{neg}MHC⁺ (P3) and CX3CR1^{high} cells (P4) (final magnification x400). Results are representative of a single experiment.

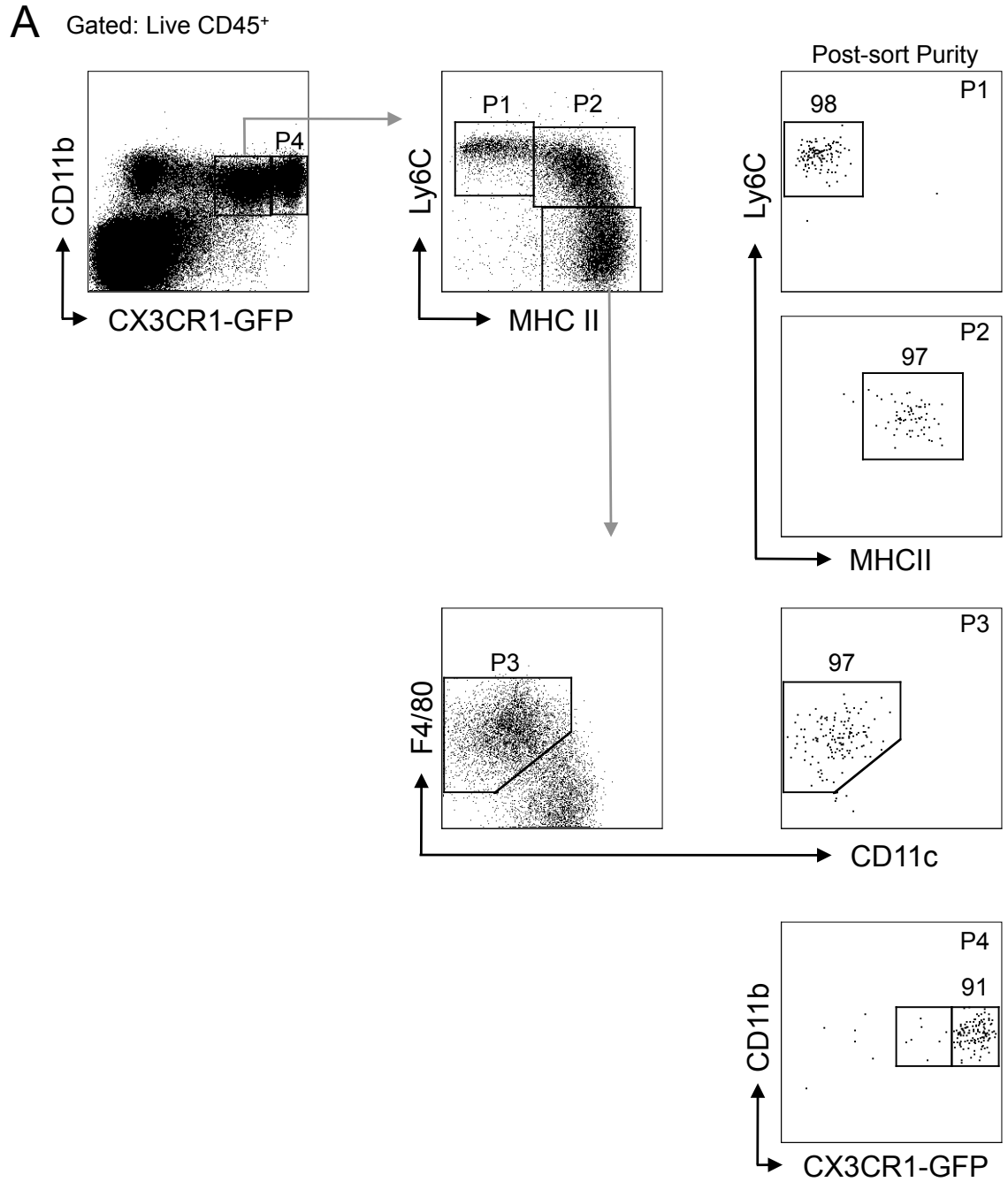


Figure 3.8: Post-sort Purity of FACS-purified CX3CR1⁺ Populations of Colonic Myeloid Cells

Colonic LP cells were isolated from resting CX3CR1^{+/gfp} mice and populations 1-4 were identified amongst live-gated CD45⁺ CD11b⁺ cells on the basis of CX3CR1-GFP, Ly6C, class II MHC, F4/80 and CD11c expression and purified by FACS. Representative plots of the post-sort purity of each population (1-4). Results are representative of at least 5 individual experiments.

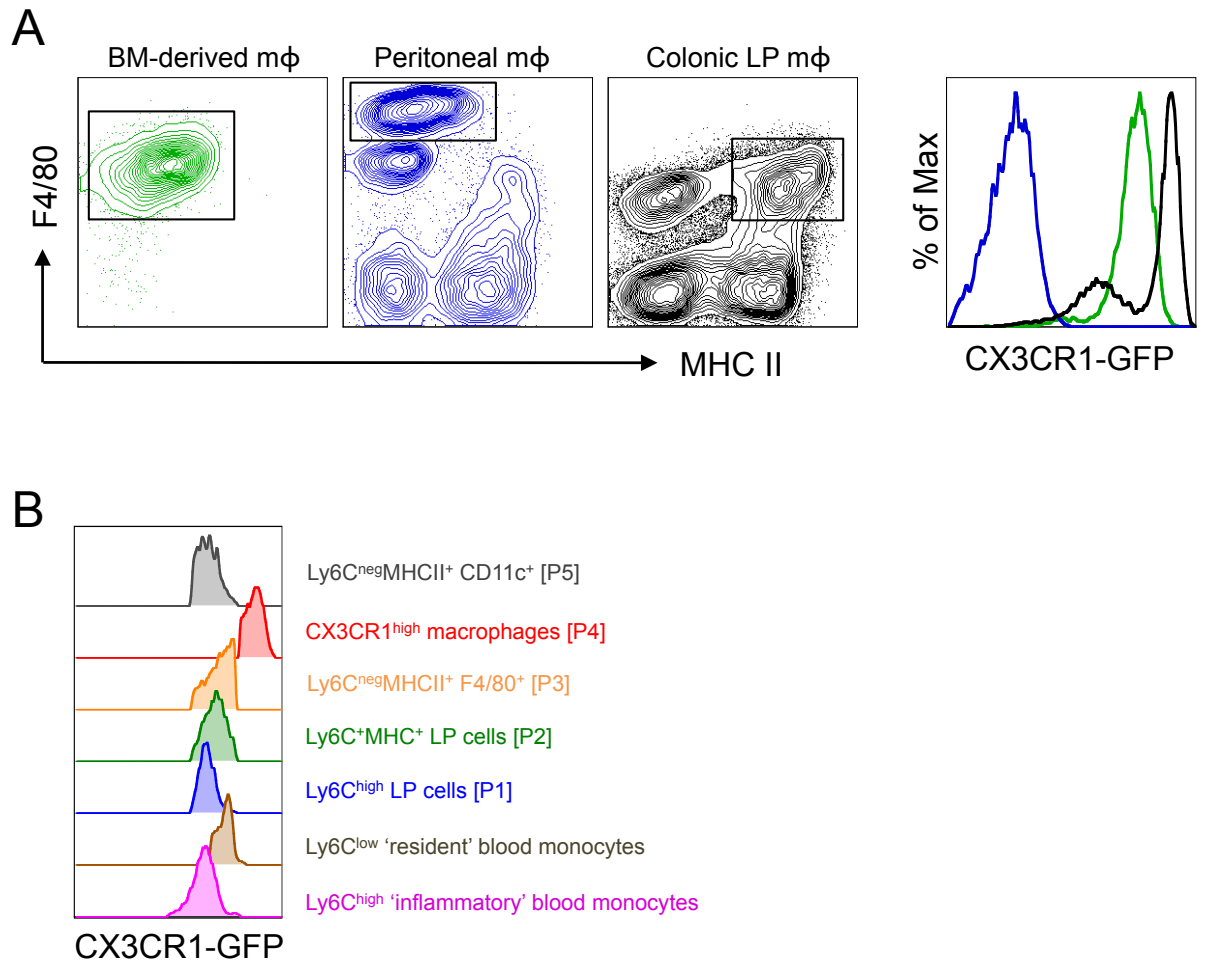


Figure 3.9: CX3CR1 Expression by Different Myeloid Cell Populations

A. Comparison of CX3CR1-GFP levels by CSF-1 generated BM mφ (F4/80⁺MHCII^{neg}), resident peritoneal mφ (F4/80^{high}MHCII^{neg}) and total colonic mφ (F4/80⁺MHCII^{high}) from resting CX3CR1^{+/gfp} mice. **B.** Histogram showing CX3CR1-GFP levels of colonic LP populations 1-5 versus 'resident' (CD11b⁺Ly6C^{low}CX3CR1⁺) and 'inflammatory' (CD11b⁺Ly6C^{high}CX3CR1^{int}) blood monocytes. Results are representative of 2 individual experiments.

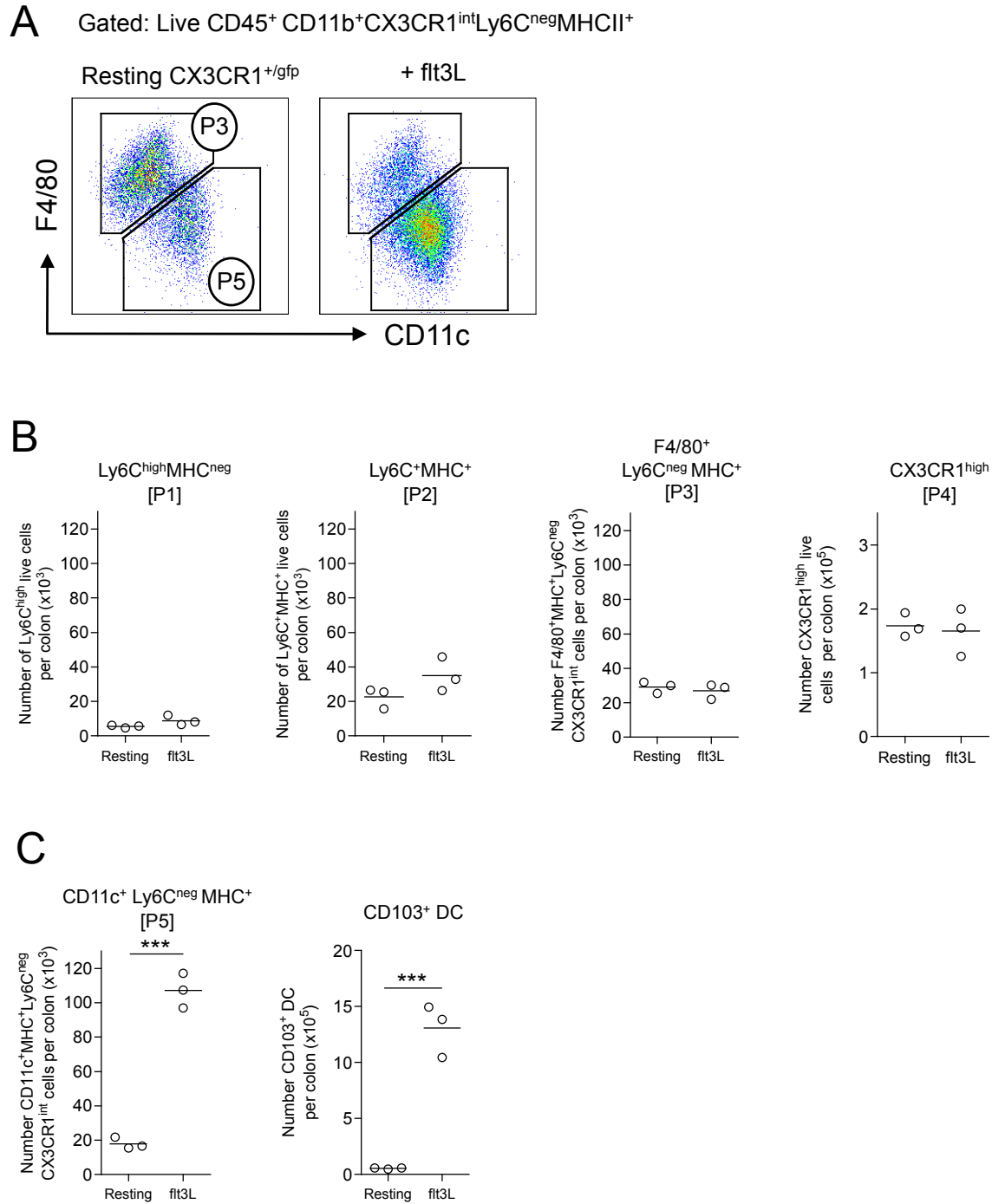


Figure 3.10: Effects of *In Vivo* Administration of Flt3L on Colonic CX3CR1⁺ Subsets

CX3CR1^{+/gfp} mice received flt3L for 8 consecutive days and the absolute numbers of cells in populations 1-5 of CX3CR1 expressing colonic LP leucocytes were enumerated and compared with those in untreated CX3CR1^{+/gfp} mice. **A**. Representative F4/80 and CD11c expression by live-gated CD45⁺CD11b⁺CX3CR1^{int}Ly6C^{neg}MHCII⁺ cells from untreated mice (*left panel*) or mice receiving flt3L (*right panel*) to identify P3 and P5. **B**. The absolute numbers of P1-P4 cells from untreated or flt3L treated mice. **C**. The absolute numbers of P5 cells and CD103⁺ DC (live gated CD11c⁺MHCII⁺CD103⁺) from untreated or flt3L treated mice. Data are representative of two individual experiments with 3 mice per group. (***) p<0.0001; Student's t test)

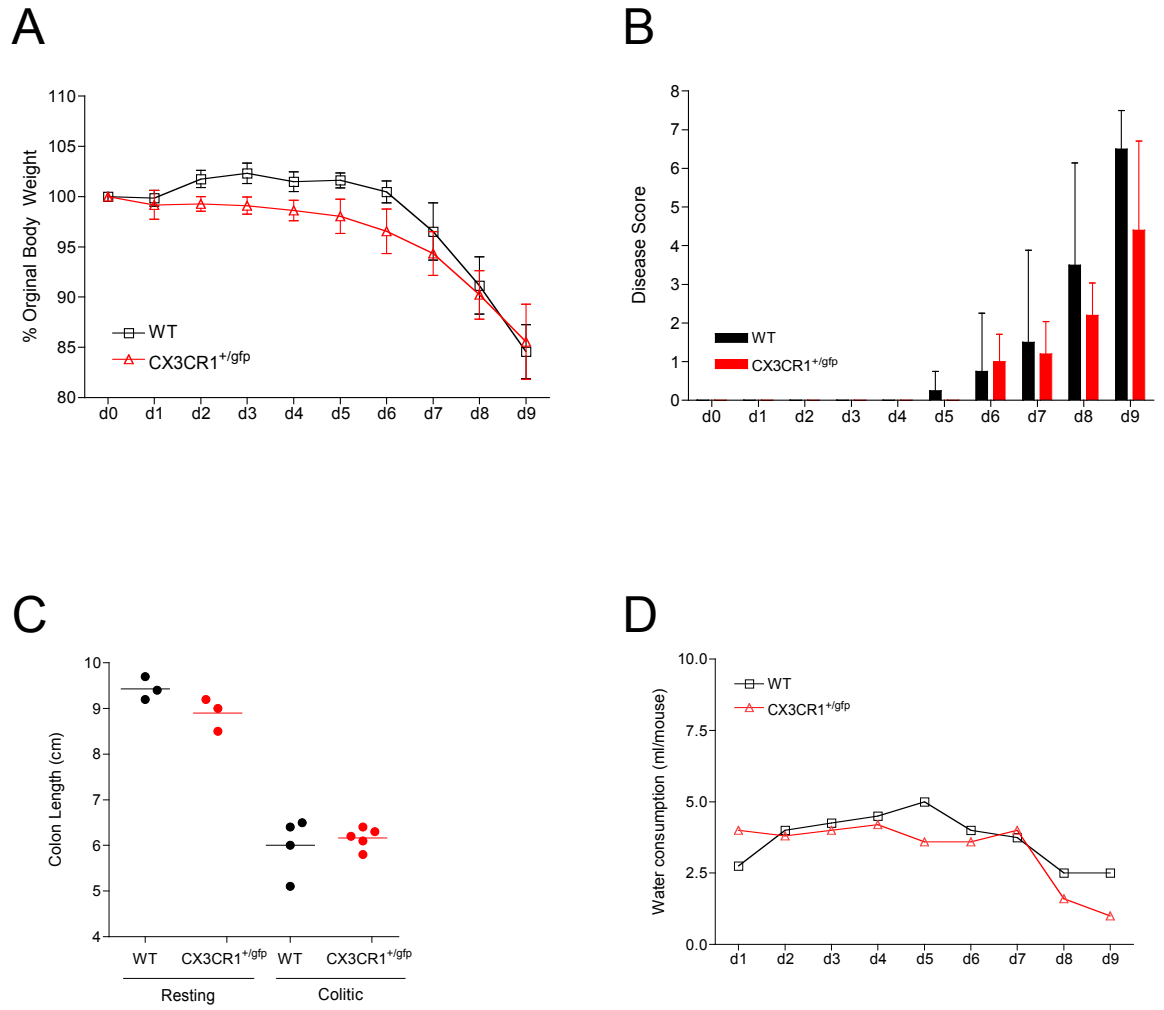


Figure 3.11: Development of Acute Experimental Colitis is Comparable in CX3CR1^{+/-gfp} and WT Mice

WT or CX3CR1^{+/-gfp} mice received 2% DSS-supplemented drinking water for 9 days and their bodyweights (**A**) and clinical disease scores (**B**) were recorded daily. Results are presented as the mean \pm 1 SD for 4 (WT) and 5 (CX3CR1^{+/-gfp}) mice for a single experiment. On day 9 mice were culled and their colons measured compared in comparison with resting mice (d0) (**C**). **D**. Water consumption (ml) per mouse on each day of colitis.

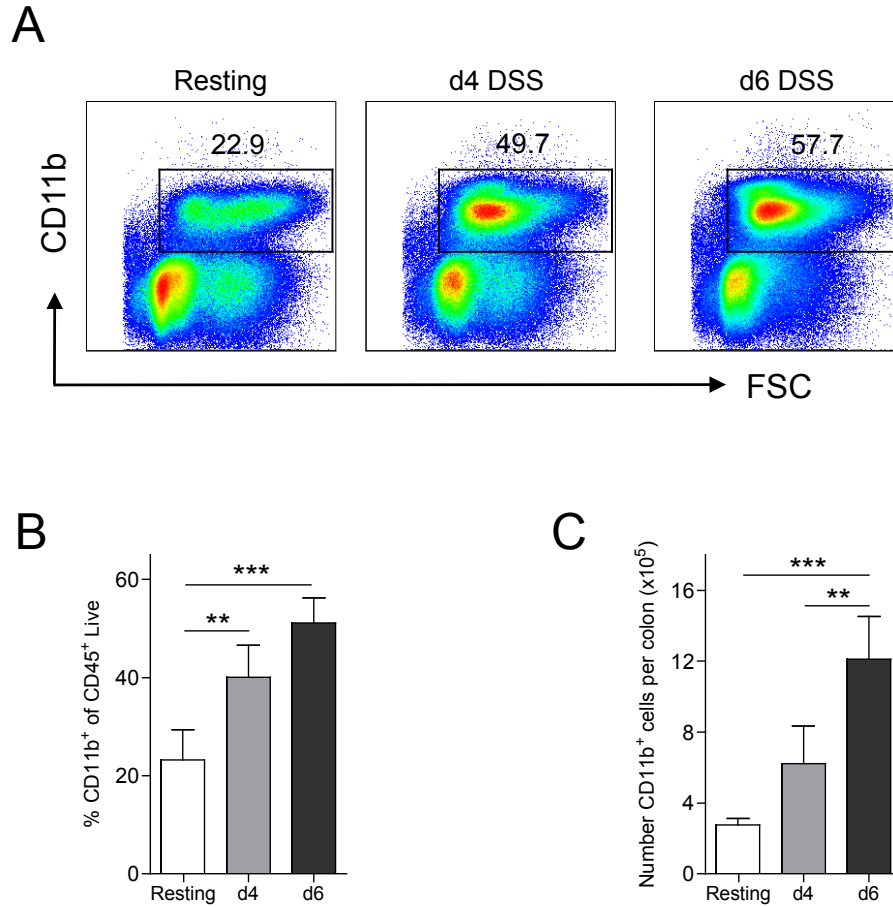


Figure 3.12: Accumulation of Myeloid Cells During Acute Experimental Colitis

CX3CR1^{+/gfp} mice received 2% DSS in their drinking water for 6 days and colonic LP CD11b⁺ cells were enumerated at different time points. **A**. Representative CD11b staining by live-gated (CD45⁺ 7-AAD^{neg}) colonic LP cells obtained from resting (*left panel*), d4 colitic (*middle panel*) and d6 colitic (*right panel*) mice. The proportions (**B**) and absolute numbers (**C**) of CD11b⁺ cells at d4 and d6 of colitis compared with steady state levels. Results are the mean + 1 SD for 4 mice at each time point and are representative of 3 individual experiments. (* p<0.05, ** p<0.01, *** p<0.001; One-way ANOVA with Bonferroni's post tests)

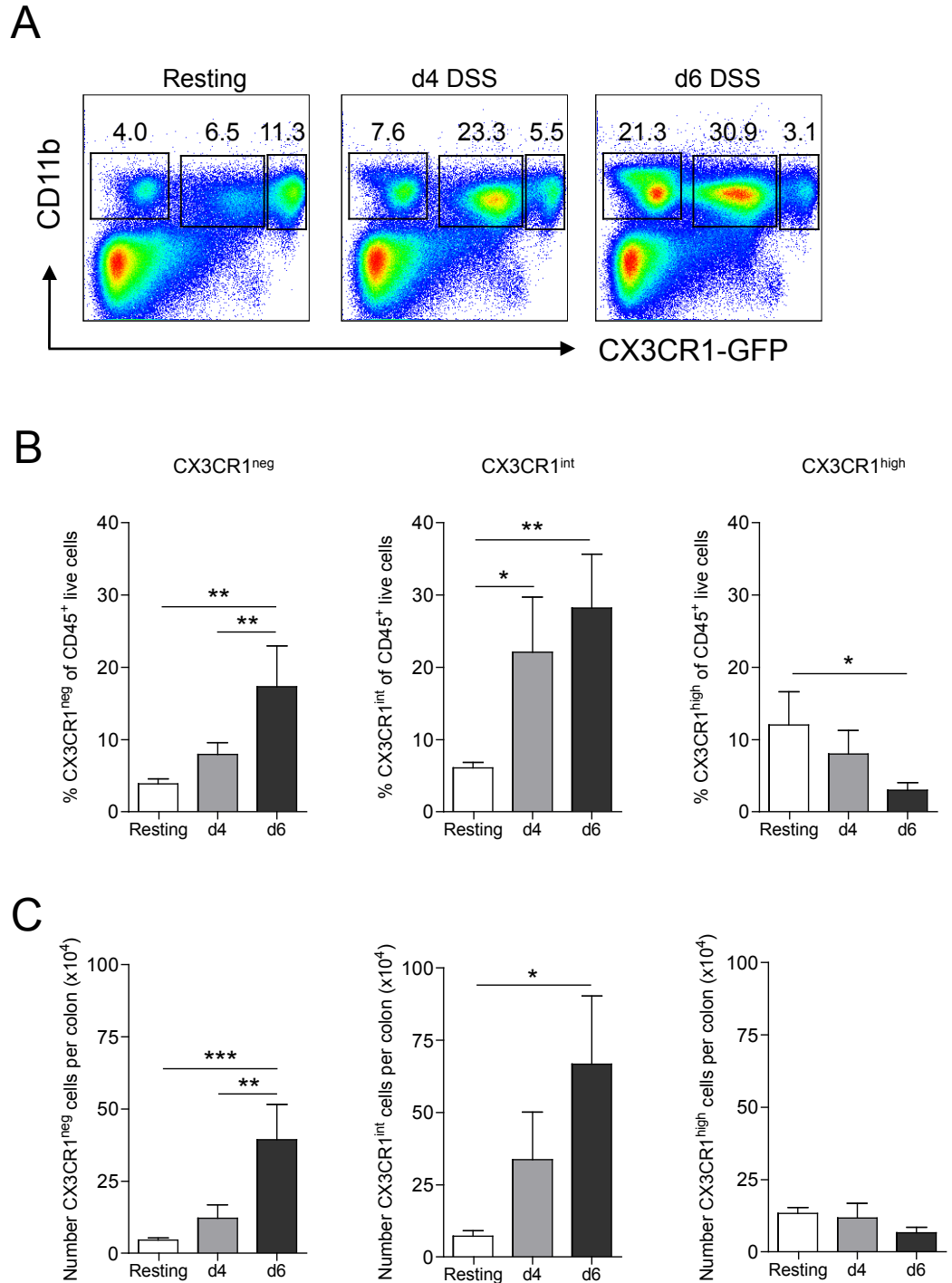


Figure 3.13: Changes in Colonic LP CX3CR1-defined Populations During DSS Colitis

CX3CR1^{+gfp} mice received 2% DSS in their drinking water for 6 days and the CX3CR1-defined populations were enumerated at d4 and d6 of colitis. **A**. Representative CD11b staining and CX3CR1-GFP expression by live-gated (CD45⁺7-AAD^{neg}) colonic LP cells obtained from resting (*left panel*), d4 colitic (*middle panel*) and d6 colitic (*right panel*) mice. The proportions (**B**) and absolute numbers (**C**) of CX3CR1^{neg}, CX3CR1^{int} and CX3CR1^{high} cells at d4 and d6 of colitis compared with steady state levels. Results are the mean + 1 SD for 4 mice at each time point and are representative of 3 individual experiments. (* p<0.05, ** p<0.01, *** p<0.001; One-way ANOVA with Bonferroni's post tests)

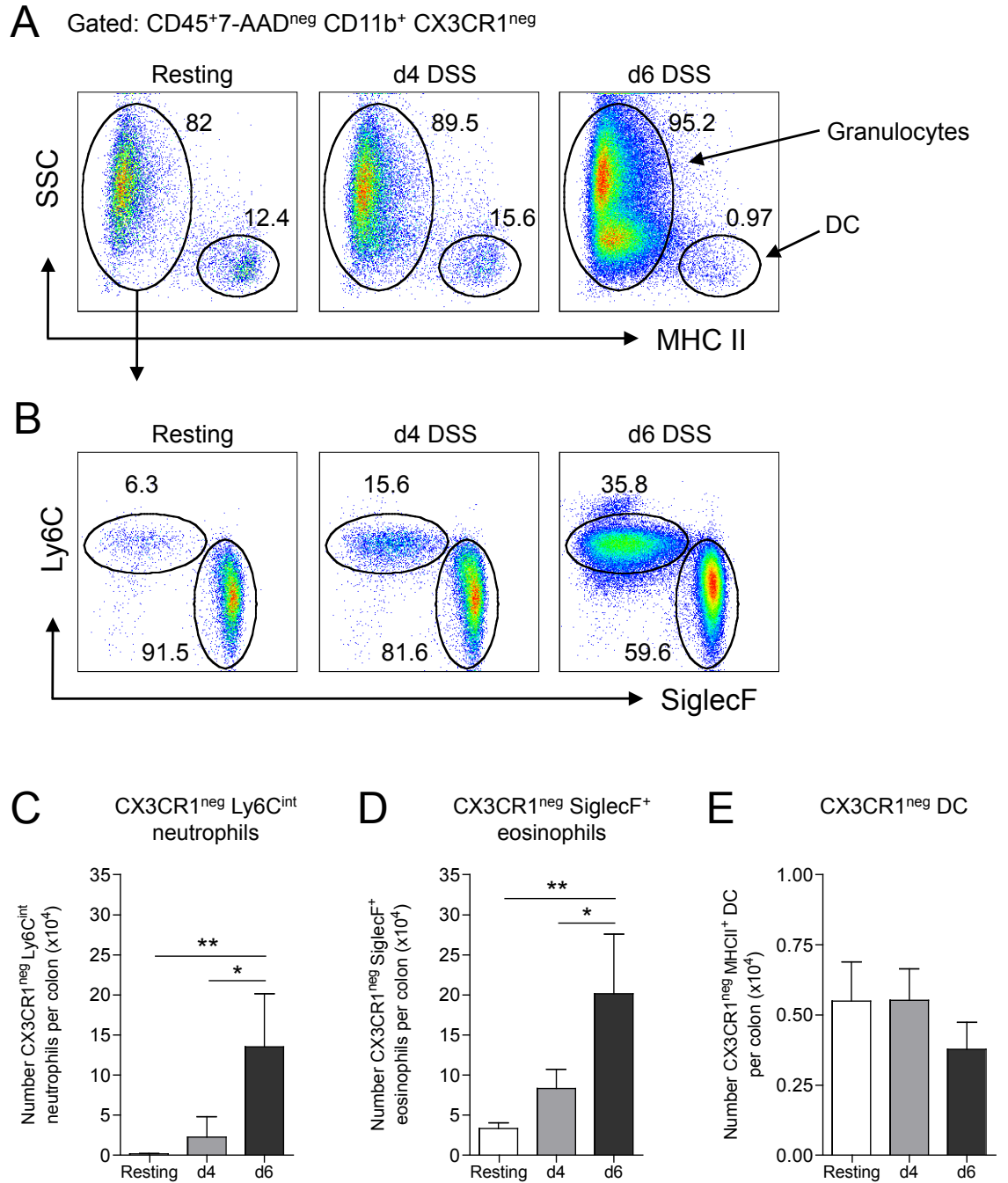


Figure 3.14: Expansion of Mucosal CX3CR1^{neg} Myeloid Cell Numbers During Colitis

CX3CR1^{+/gfp} mice received 2% DSS in their drinking water for 6 days and the composition of the colonic LP CD11b⁺ CX3CR1^{neg} compartment was examined at d4 and d6 of colitis. **A**. Representative MHC II expression by live-gated CD45⁺ CD11b⁺ CX3CR1^{neg} LP cells obtained from resting (*left panel*), d4 colitic (*middle panel*) and d6 colitic (*right panel*) mice. **B**. Representative Ly6C and SiglecF expression by SSC^{high} granulocytic cells at each time point. The absolute number of Ly6C^{int} neutrophils (**C**), SiglecF⁺ eosinophils (**D**) or CD11b⁺ DC (**E**) at d4 and d6 of colitis compared with resting mice. Results are the mean + 1 SD for 4 mice at each time point and are representative of 3 individual experiments. (* p<0.05, ** p<0.01, *** p<0.001; One-way ANOVA with Bonferroni's post tests)

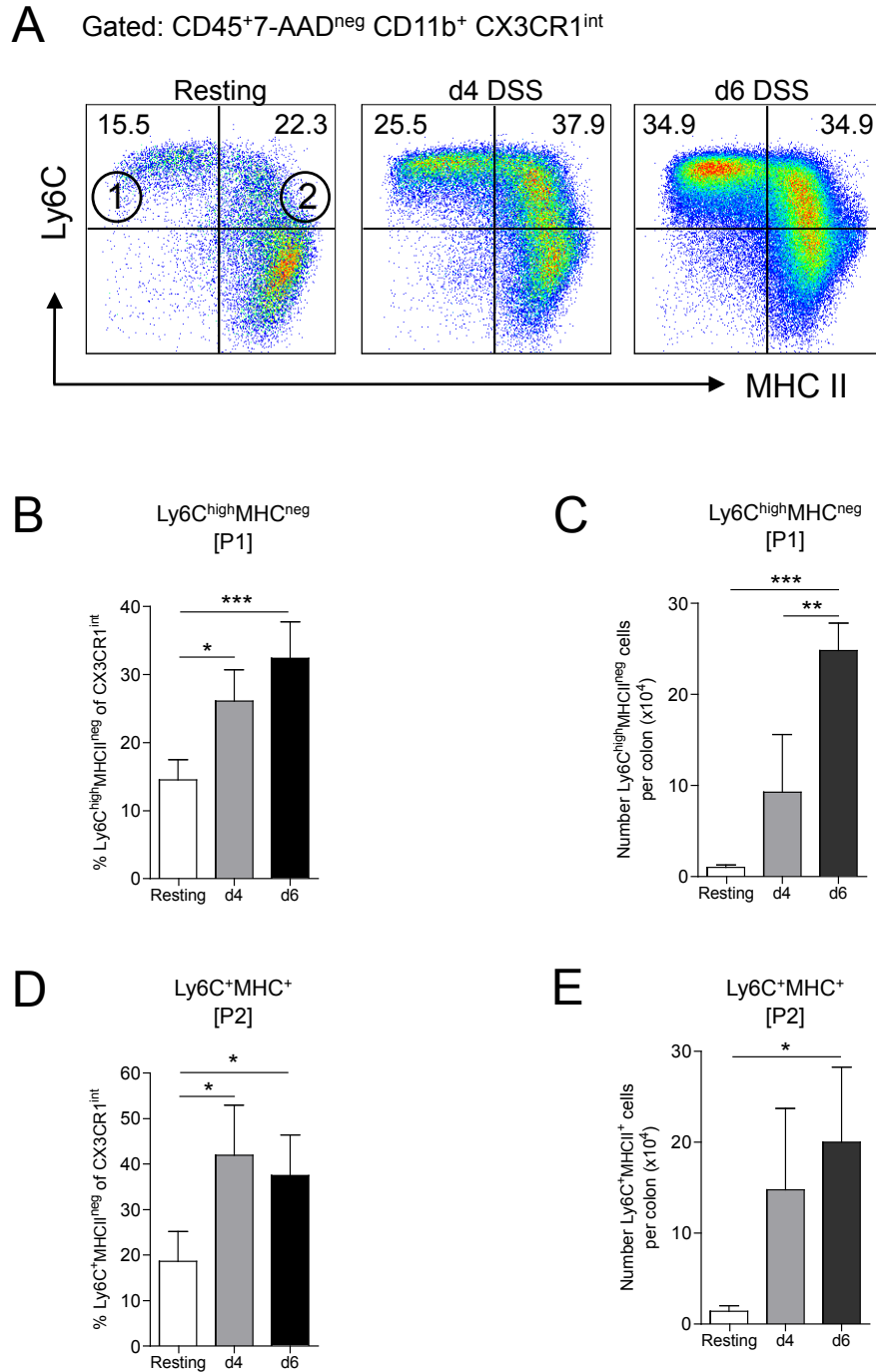


Figure 3.15: Expansion of Mucosal CX3CR1^{int} Myeloid Cell Numbers During Colitis

CX3CR1^{+/gfp} mice received 2% DSS in their drinking water for 6 days and the cellular composition of the colonic LP CX3CR1^{int} compartment was examined by flow cytometry at d4 and d6 of colitis. **A**. Representative Ly6C and class II MHC expression by live-gated CD45⁺ CD11b⁺ CX3CR1^{int} cells obtained from resting mice or d4 or d6 colitic mice. The proportion (**B**) and absolute numbers (**C**) of P1 (Ly6C^{high}MHCII^{neg}) cells per colon at each time point. The proportion (**D**) and absolute numbers (**E**) of P2 (Ly6C⁺MHCII⁺) cells per colon at each time point. Results are the mean + 1 SD for 4 mice at each time point and are representative of 3 individual experiments. (* p<0.05, ** p<0.01, *** p<0.001; One-way ANOVA with Bonferroni's post tests)

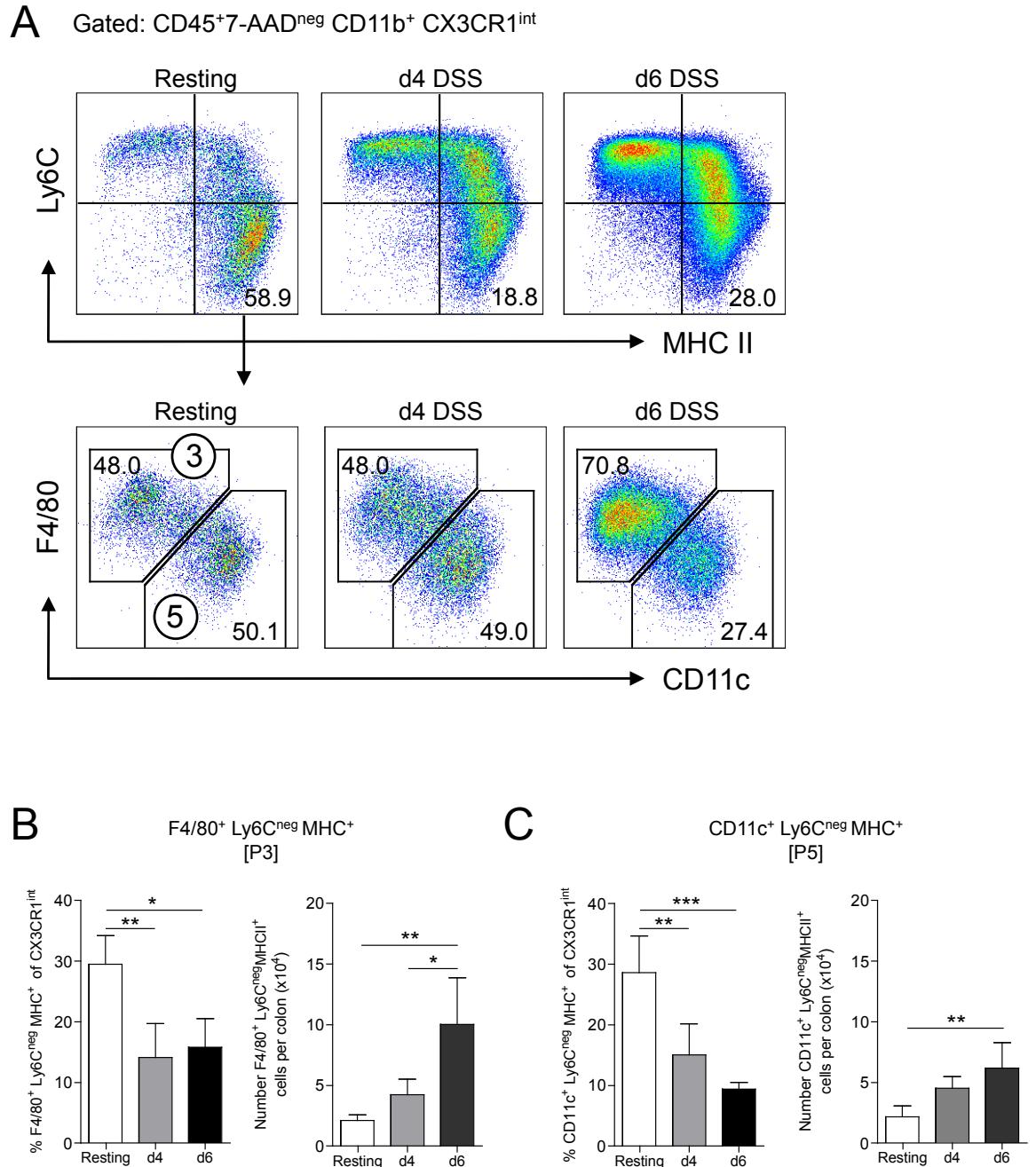


Figure 3.16: Expansion of Mucosal CX3CR1^{int} Myeloid Cell Numbers During Colitis

CX3CR1^{+/gfp} mice received 2% DSS in their drinking water for 6 days and the cellular composition of the colonic LP CX3CR1^{int} compartment was examined by flow cytometry at d4 and d6 of colitis. **A.** Representative Ly6C and class II MHC expression by live-gated CD45⁺ CD11b⁺ CX3CR1^{int} cells obtained from resting mice or d4 or d6 colitic mice. The proportions (of CX3CR1^{int} cells) and absolute numbers of P3 (F4/80⁺ Ly6C^{neg} MHCII⁺) (**B**) and P5 (CD11c⁺ Ly6C^{neg} MHCII⁺) (**C**) at each time point. Results are the mean + 1 SD for 4 mice at each time point and are representative of 3 individual experiments. (* p<0.05, ** p<0.01, *** p<0.001; One-way ANOVA with Bonferroni's post tests)

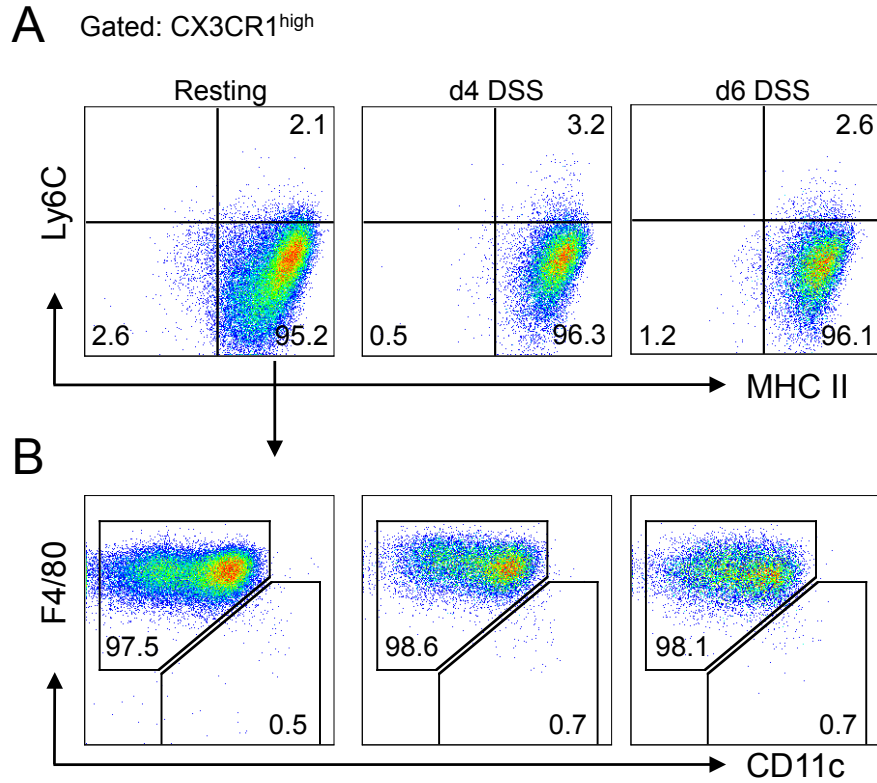


Figure 3.17: Effects of Acute Colitis on Colonic CX3CR1^{high} Cells

CX3CR1^{+gfp} mice received 2% DSS in their drinking water for 6 days and the cellular composition of the colonic LP CX3CR1^{high} compartment was examined by flow cytometry at d4 and d6 of colitis. Representative Ly6C and class II MHC expression (**A**) and F4/80 and CD11c expression (**B**) by live-gated CD45⁺ CX3CR1^{high} CD11b⁺ colonic LP leucocytes at d4 and d6 of colitis compared with CX3CR1^{high} CD11b⁺ LP leucocytes from resting mice. Results are representative of 3 individual experiments.

Chapter 4
The Origin of Lamina Propria Macrophages
During Intestinal Homeostasis

4.1 Introduction

In the previous chapter, I showed that the m ϕ populations of the colon were unexpectedly heterogeneous comprising two main groups that differed in the expression of CX3CR1. Those with high levels of CX3CR1 dominated the resting mucosa, whereas CX3CR1^{int} cells expanded during colitis. In this chapter, I set out to examine the relationship between these cells and their origins. It is generally accepted that monocytes are the precursors of most tissue m ϕ . However, this is complicated by the fact that the monocyte pool may itself be heterogeneous, with a paradigm having arisen that distinct blood monocyte populations replenish 'resident' and 'inflammatory' m ϕ in tissues (12). According to this idea, Ly6C^{low}CX3CR1⁺ monocytes are believed to migrate to peripheral tissues under normal physiological conditions and repopulate tissue resident m ϕ , whereas Ly6C^{high}CX3CR1^{int} monocytes give rise to pro-inflammatory m ϕ in many models of inflammation (12, 22, 25). A number of studies have shown that Ly6C^{high} monocytes can repopulate mouse intestine in the absence of overt inflammation and my initial studies identified for the first time a putative group of Ly6C^{high} monocyte-like cells in the resting colon. However this work is difficult to interpret because the primary focus was on populations of cells that were defined as 'DC' because they were CD11c⁺. As I showed in the previous chapter, most CD11c⁺ cells in the resting colon appear to be m ϕ and multiple markers are needed to distinguish individual MP subsets in the intestine (28, 196). In particular, none of the previous work used levels of CX3CR1 expression to define MP subsets. As a result, the origin of resident intestinal m ϕ is not clear and in this chapter, I set out to investigate directly whether monocytes could replenish CX3CR1^{int} and CX3CR1^{high} MP in the resting intestine and to obtain an idea of how these might be related. To do this I used a combination of adoptive transfer and BrdU labelling studies.

4.2 Recruitment of Monocytes to the Resting Intestine

I first examined whether Ly6C^{high} ('inflammatory') and Ly6C^{low} ('resident') monocytes could migrate to the intestine of unmanipulated CX3CR1^{+gfp} mice. Ly6C^{high} (CX3CR1^{int}) or Ly6C^{low} (CX3CR1⁺) monocytes were purified from the BM of CX3CR1^{+gfp} (CD45.2⁺) mice (Fig. 4.1) and transferred into resting CX3CR1^{+gfp} mice (CD45.1⁺/CD45.2⁺) (Fig. 4.2A) and the recipient LP assessed for the

presence of donor cells after 24hrs (Fig. 4.2B). At the time of transfer, donor Ly6C^{high} monocytes expressed high levels of Ly6C and CD115, but only low levels of F4/80 and lacked expression of CD11c or class II MHC (Fig. 4.1A-C). On the other hand, the transferred Ly6C^{low} donor monocytes expressed higher levels of CX3CR1 and F4/80 than Ly6C^{high} monocytes, as well as some class II MHC and CD11c, but lower levels of CD115 (Fig. 4.1C). 24 hrs after transfer of Ly6C^{high} monocytes into resting mice, very few donor cells could be found in the recipient colon, but these were detectable above the background of non-transferred mice and the majority had altered their phenotype from Ly6C^{high}MHCII^{neg}F4/80^{low} to Ly6C^{neg}MHCII⁺F4/80⁺ and had also upregulated their level of CX3CR1 expression (Fig. 4.2C and D). In contrast, I could not detect a clear population CD45.1⁺ CD45.2^{neg} donor cells above background in the colon of mice that had received Ly6C^{low} monocytes (Fig. 4.2C and D). Similarly, donor cells in the bloodstream were difficult to detect above background staining (Fig. 4.3).

4.3 Monocyte Recruitment to the Colon Following Diphtheria Toxin-Mediated Mononuclear Phagocyte Depletion

This preliminary evidence suggested that Ly6C^{high} monocytes might migrate to the resting mucosa and give rise to both CX3CR1^{int} and CX3CR1^{high} mφ. However this experiment was unsatisfactory in several ways. Not only were the numbers of donor cells obtained very low and so difficult to analyse, but the use of CX3CR1^{+gfp} mice as both monocyte donors and as recipients meant that donor cells could only be identified on the basis of lacking CD45.1 expression. This proved difficult due to background staining in the PBS control group.

Thus, I next took advantage of a strategy which allowed depletion of resident LP mφ in recipient mice in an attempt to enhance the visualisation of monocyte recruitment. The CD11c-DTR mouse has been used extensively for such studies, as they express the human diphtheria toxin receptor under control of the CD11c promoter and administration of diphtheria toxin (DT) results in depletion of CD11c⁺ MP in the intestine without causing significant inflammation (196, 251). First I characterised the effects of DT on the LP MP subsets I had defined in Chapter 3 by examining the LP CD11b⁺ compartment 24hrs after administering DT. Due to the lack of CX3CR1-GFP in these mice and the unavailability of a reliable anti-CX3CR1 antibody, I had to develop an alternative gating strategy which allowed me to define LP myeloid cell populations equivalent to those in

CX3CR1^{+gfp} mice (Figure 4.4). First, total CD11b⁺ cells were identified from within the CD45⁺ live fraction of cells and SSC^{high} cells were gated out to exclude eosinophils and any neutrophils. This approach revealed very similar populations to those described in Chapter 3, with Ly6C^{high}MHCII^{neg} cells (equivalent to P1) and Ly6C⁺MHCII⁺ cells (equivalent to P2) being readily identifiable. However the F4/80⁺MHCII⁺Ly6C^{neg}CD11c^{neg} contained both P3 and P4 subsets, since CX3CR1 expression is the only distinguishing feature between these subsets (Fig. 4.4A and B). In addition, the CD11c⁺MHCII⁺ Ly6C^{neg}F4/80^{neg} population is not identical to that defined previously as P5, as it will also include additional CD11b⁺ DC which would be CX3CR1^{neg} and thus usually excluded from the CX3CR1^{int} P5. Nevertheless, with these provisos, it seemed possible to define generally equivalent populations of MP. To confirm this, I applied the alternative gating strategy to CX3CR1^{+gfp} mice. This showed that all Ly6C^{high}MHCII^{neg} cells and Ly6C⁺MHCII⁺ cells expressed intermediate levels of CX3CR1, whereas the vast majority of the F4/80⁺MHCII^{high} cells were identified as CX3CR1^{high} (Fig. 4.4B). I therefore used this strategy in all subsequent analysis using non-CX3CR1^{+gfp} mice.

Administration of DT resulted in depletion of the majority (>85%) of F4/80⁺MHCII⁺ mφ (equivalent to P3+P4), but had little effect on P1 and P2 (Fig. 4.5A). Interestingly, DT treatment depleted all F4/80⁺ mφ regardless of their levels of CD11c expression and these appeared to be depleted to a greater extent than the CD11c⁺F4/80^{neg} cells assumed to be DC (Fig. 4.5B). Although somewhat surprising, this showed that the CD11c-DTR system could be used to deplete resident gut mφ and importantly, as P1 and P2 were relatively unchanged, it does not seem to affect monocyte recruitment. Therefore I went on to examine the fate of adoptively transferred Ly6C^{high} BM monocytes from CD45.1⁺/CD45.2⁺ CX3CR1^{+gfp} mice in CD11c-DTR mice (CD45.2⁺) that had received DT 24hrs previously (Fig. 4.6A).

Using this approach, donor cells were easily identifiable on the basis of both GFP and CD45.1 expression and were clearly distinct from endogenous CD11c⁺ cells in the CD11c-DTR recipient mice which expressed GFP under the CD11c promoter (Fig. 4.6B). 24hrs after transfer, essentially all donor cells were within the CX3CR1^{int} compartment and expressed variable levels of Ly6C and class II MHC, and low levels of F4/80 (Fig. 4.6B and C). However by 96hrs, the vast majority of

donor-derived cells were within the CX3CR1^{high} fraction and their phenotype had changed dramatically. They now lacked Ly6C expression, expressed high levels of class II MHC and F4/80 and had increased in size, as determined by an increase in their FSC profile (Fig. 4.6B and C). These changes were specific to the intestine, as donor cells that remained in the bloodstream did not display increased expression of F4/80 and upregulation of class II MHC was only moderate (Fig. 4.7A and B). In addition, although Ly6C expression was reduced on these circulating donor cells, this was not to the same extent as donor cells in the gut. This conversion from the Ly6C^{high} to Ly6C^{low} phenotype has been reported previously for blood monocytes (29). In parallel, the level of CX3CR1-GFP was moderately increased on circulating donor cells at 96hrs (Fig. 4.7A), but again this never reached the level expressed by donor m ϕ in the LP.

Taken together these results indicate that Ly6C^{high} 'inflammatory' monocytes can replenish CX3CR1^{high} tissue resident m ϕ following MP cell ablation and suggest that this process seems to involve the differentiation of Ly6C^{high} monocytes within the mucosa, arriving first as Ly6C^{high}MHCII^{neg}F4/80^{low}CX3CR1^{int} cells and subsequently maturing into F4/80^{high}CX3CR1^{high} cells. This is accompanied by a loss of Ly6C expression, upregulation of class II MHC and an increase in size.

4.4 Analysis of Monocyte Recruitment in CCR2-deficient Mice

Although the CD11c-DTR model is reported to cause no significant inflammation, the level of resident cell depletion was rather extensive, meaning that monocyte behaviour under these circumstances may not truly represent m ϕ replenishment during steady state conditions. Thus, to try to mimic steady state conditions more accurately I made use of CCR2-deficient mice which have a dramatic reduction in the frequency of circulating Ly6C^{high} monocytes (Fig. 4.8A and B) due to their high levels of CCR2 (Fig. 4.8C) and the indispensable role of CCR2 in BM egress (22).

Although CCR2-deficient and WT mice had similar proportions of CD11b⁺ cells amongst live leucocytes in the colon (Fig. 4.9A and B), the absolute number of CD11b⁺ cells per colon was significantly lower in CCR2-deficient mice ($1.3 \times 10^5 \pm 0.2$ versus $2.1 \times 10^5 \pm 0.4$ per colon for CCR2 KO and WT respectively; Fig.

4.9C). Within the CD11b⁺ fraction, SiglecF⁺ (SSC^{high}) eosinophils constituted a larger proportion of CD11b⁺ cells in CCR2 KO mice compared with their WT counterparts (32.9±1.0% versus 17.9±3.9%, respectively), although the absolute numbers of SiglecF⁺ eosinophils were comparable (Fig. 4.10A-C). Similarly, the proportions and absolute numbers of Ly6C^{int}Ly6G⁺ neutrophils were similar in the two strains (Fig. 4.10D and E).

Using the alternative gating strategy outlined above for non-CX3CR1^{gfp} mice, it was clear that the Ly6C^{high}MHCII^{neg} population of SiglecF^{neg}CD11b⁺ cells (P1) was essentially absent from the colon of CCR2 KO mice (Fig. 4.11A and B). There was a similar, but less dramatic reduction in the proportion and absolute number of Ly6C⁺MHC⁺ cells (P2) in CCR2-deficient mice compared with their WT counterparts (Fig. 4.11A, D and E). In contrast, the numbers of F4/80⁺ class II MHC⁺ mφ were only reduced by approximately 50% in CCR2 KO mice (3.4x10⁴ ±0.8 versus 7.0x10⁴ ±1.2 per colon, respectively; Fig. 4.12A and B). Interestingly, the CD11b⁺ DC population (which included the CX3CR1^{int} DC population as well as CD11b⁺CD103⁺CX3CR1^{neg} DC) was also significantly reduced in CCR2 KO mice compared with WT mice (Fig. 4.12D).

Antibody staining confirmed CCR2 expression on the Ly6C^{high} class II MHC^{neg} P1 cells that were absent in CCR2 KO mice. Unfortunately it proved impossible to determine whether the P2, P3+4 or the CD11b⁺ DC expressed CCR2 due to the high background staining of these populations in KO mice (Fig. 4.12).

Having established that CCR2 KO mice have partial depletion of mononuclear phagocytes in their colon, I next used them as recipients of adoptively transferred BM monocytes (Fig. 4.13A). Consistent with the results from the CD11c-DTR model, donor Ly6C^{high} monocytes could be found in the colon of unmanipulated CCR2 KO recipients within 24hrs of transfer, at which time all were CX3CR1^{int} and around 50% had acquired class II MHC (Fig. 4.13B and C). By 48hrs, almost 90% of donor cells had upregulated class II MHC and this was accompanied by the loss of Ly6C expression (Fig. 4.13B and C), as well as a moderate increase in CX3CR1 expression (Fig. 4.13D). As in CD11c-DTR recipients, by 96hrs after transfer virtually all donor cells had acquired class II MHC, upregulated F4/80 and now expressed high levels of CX3CR1 (Fig. 4.13D).

Again this phenotypic switch was accompanied by an increase in cell size (FSC) (Fig. 4.13D). In a separate experiment, Ly6C^{high} monocytes were transferred into CCR2 KO mice and the presence of donor cells was examined after 7 days. This showed that GFP⁺ CD45.1⁺/CD45.2⁺ cells were still present in the LP of recipient CCR2 KO mice after one week, implying that Ly6C^{high} monocytes can generate relatively long-lived CX3CR1^{high} tissue m ϕ (Fig. 4.14A). At this time point, the vast majority (>93%) of donor cells expressed F4/80 and did not seem to have entered the F4/80^{neg}CD11c⁺ compartment of putative DC (Fig. 4.14B). In addition, all donor cells had identical FSC profiles to endogenous CD11b⁺SSC^{low}MHC⁺ cells, indicating that they had matured fully (Fig. 4.14C).

Donor cells were also easily identifiable in the bloodstream of CCR2 KO recipient mice at all time points as donor monocytes constituted a much greater proportion of the total circulating monocyte pool compared with when CD11c-DTR mice were used as recipients (Fig. 4.15A). Analysis of donor cells showed that although donor Ly6C^{high}CX3CR1^{int} monocytes converted into Ly6C^{low}CX3CR1⁺ monocytes by 48hrs, these cells lacked class II MHC and did not adopt the CX3CR1^{high} phenotype seen in the LP (Fig. 4.15B and C). Therefore it is clear that donor cells within the LP preparations are not mere blood contaminants.

To examine whether differentiation of Ly6C^{high} 'inflammatory' monocytes into CX3CR1^{high} tissue m ϕ occurred in other mucosal tissues, I examined the lung parenchyma of CCR2 KO recipient mice for the presence of donor cells 96hrs after transfer. Although donor cells could be identified within the lung preparation, these cells were phenotypically indistinguishable from donor cells in the bloodstream and because the lungs were not perfused, these cells most likely reflected blood contaminants (Fig. 4.16A and B). Importantly, unlike in the colon, no CX3CR1^{high} CD45.1⁺ cells could be identified in the lung, again emphasising the gut specific nature of Ly6C^{high} monocyte maturation (Fig. 4.16C).

In all the adoptive transfer experiments detailed above, I noted that the phenotype of circulating donor cells changed with time from Ly6C^{high} (CX3CR1^{int}) to Ly6C^{low} (CX3CR1⁺) monocytes, a phenomenon that has been reported previously (29). Therefore it is possible that the Ly6C^{high} donor cells could first convert into Ly6C^{low} monocytes in the circulation or BM and provide a second wave of precursors of colonic m ϕ at later times. My attempt to transfer Ly6C^{low}

monocytes into resting WT mice had been complicated by the low numbers of donor cells I could find in the colon and by the fact that the 24hr time point I used in that experiment would not be sufficient to allow full conversion into resident m ϕ . Therefore I decided to repeat the transfer of Ly6C^{low} monocytes using CCR2-deficient mice as recipients. However as before, donor-derived Ly6C^{low} monocytes could not be found in the LP of recipient mice 96hrs after transfer, despite forming a clear population in the circulation at this time (Fig. 4.17A-C). Therefore, it seems unlikely that Ly6C^{low} monocytes derived from donor Ly6C^{high} monocytes repopulate the gut m ϕ pool.

Taken together these adoptive transfer experiments demonstrate that so-called 'inflammatory' monocytes appear to enter the intestinal mucosa and undergo a step-wise differentiation process into CX3CR1^{high} m ϕ through a CX3CR1^{int} intermediary stage. In contrast, Ly6C^{low} monocytes play little or no role in the homeostasis of the intestinal m ϕ compartment during steady state conditions.

4.5 Population Dynamics of Intestinal Macrophages *In Situ*

The adoptive transfer studies suggested that newly arrived Ly6C^{high} monocytes might be able to mature into CX3CR1^{high} resident m ϕ through a series of transitional stages. I next examined whether I could find evidence for a relationship between these subsets *in situ*. To do this, I first used BrdU incorporation *in vivo* to track the turnover and kinetics of the CX3CR1-defined populations I had defined phenotypically.

Mice were injected intraperitoneally with a single dose of BrdU and 3hrs later approximately 25% of the Ly6C^{high} monocytes in the BM were labelled (Fig. 4.18A and B), consistent with them being derived from actively dividing pro-monocytes (11). In contrast, no Ly6C^{high} blood monocytes were labelled at this time (Fig. 4.18C and D), consistent with their known non-cycling status (11, 12). Similarly, after 3hrs, no BrdU⁺ cells were present in any of the LP CX3CR1⁺ populations (Fig. 4.19A-D). 12hrs after the single pulse of BrdU, around 60% of Ly6C^{high} monocytes in the BM were BrdU⁺, as were 35% of Ly6C^{high} monocytes in blood, confirming exit from the BM within this period. There were still very few BrdU⁺ cells within the CX3CR1⁺ populations in the colon at this time, with P2, P3

and P4 cells showing no uptake over background staining. However, $4.7 \pm 1.6\%$ BrdU⁺ cells were detectable in P1 (Fig. 4.19A), suggesting that within the 12hr time frame, Ly6C^{high} monocytes had left the BM and migrated to the gut via the bloodstream.

These results support my earlier conclusions that the Ly6C^{high}MHCII^{neg} CX3CR1^{int} cells I identified in P1 are closely related to blood monocytes and are the earliest stage of colonic m ϕ development. To examine the kinetics of the intestinal m ϕ subsets in more detail, I used a long-term BrdU administration protocol, in which mice received a single intraperitoneal injection of BrdU followed by BrdU in their drinking water for 6 consecutive days, before being returned to normal drinking water.

After 4 days of continual BrdU administration, over 75% of the Ly6C^{high}MHCII^{neg}CX3CR1^{int} cells (P1) in the colon were BrdU⁺, as were Ly6C^{high} monocytes in blood, again supporting the close relationship between these cells (Fig. 4.20A). A similar frequency of BrdU⁺ cells was seen among Ly6C^{high} colonic monocytes after 6 days of BrdU administration, indicating these were maximal levels (Fig. 4.20B). When BrdU was withdrawn, the frequency of BrdU⁺ cells within P1 and amongst blood monocytes fell rapidly to baseline by 4 days (Fig. 4.20B). The colonic Ly6C⁺MHCII⁺CX3CR1^{int} cells in P2 also contained high levels of BrdU⁺ cells (~50% BrdU⁺) which were maximal after 4 days of administration, but in this case, the peak of BrdU uptake was maintained for 2 days after removal of BrdU, before decaying rapidly thereafter. The frequency of BrdU-labelled cells in the Ly6C^{neg}MHCII⁺CX3CR1^{int} population (P3) lagged behind that in P1 and P2, only reaching its peak 2 days after cessation of BrdU administration and then falling rapidly in parallel (Fig. 4.20B). In comparison, the proportion of BrdU⁺ CX3CR1^{high} m ϕ increased much more gradually during BrdU administration and unlike the other subsets, this level was maintained until at least 4 days after withdrawal of BrdU. Notably, although the proportion of BrdU⁺ cells in P4 at each time point was significantly lower than those in P1-3, the absolute number of BrdU⁺CX3CR1^{high} cells was significantly higher, suggesting that BrdU⁺ cells were accumulating in this compartment (Fig. 4.20C).

Together these data support the idea that the different populations of CX3CR1^{int} cells identified in resting colon are short-lived intermediaries that

represent progressive and *in situ* differentiation of a recently derived Ly6C^{high} monocyte, whose fate is to become a CX3CR1^{high} resident m ϕ .

4.6 Effects of CSF-1 on Colonic Macrophage Development *In Vivo*

To explore this further, I examined the effects of CSF-1 *in vivo*, as this cytokine is known to drive differentiation of mature m ϕ from monocytes (41). CX3CR1^{+gfp} mice were injected i.p. with rhCSF-1 for 4 consecutive days and the proportions and absolute numbers of the colonic CX3CR1⁺ populations were enumerated (Fig. 4.21). Treatment with CSF-1 did not cause as dramatic effects on the number of LP myeloid populations as flt3L did for DC which was carried out in parallel (Chapter 3). However there was a significant increase in the absolute numbers of CX3CR1^{high} m ϕ and this was paralleled, by a modest decrease in the numbers of cells in P1 and P2 (Fig. 4.21B-F). The relatively higher responsiveness of CX3CR1^{high} cells to CSF-1 correlated with them having the highest level of expression of the CSF-1R (CD115) amongst the colonic m ϕ subsets, as determined by qRT-PCR (Fig. 4.21G). While these results need to be confirmed, they would be consistent with the idea that CSF-1 responsive monocytes can differentiate into CX3CR1^{high} m ϕ in the colonic mucosa under the control of CSF-1.

4.7 Differentiation of Monocytes *In Vitro*

Next, I attempted to investigate whether Ly6C^{high} monocytes could be persuaded to differentiate into the equivalent of mucosal CX3CR1^{high} m ϕ *in vitro* as this would allow me to explore the factors that might be involved. To this end, LP Ly6C^{high}MHCII^{neg} cells in P1 were FACS-purified from resting CX3CR1^{+gfp} mice and I examined whether their phenotype changed after 24hrs culture *in vitro*. As shown in Figure 4.22A, these cells upregulated class II MHC after culture, but remained Ly6C⁺CX3CR1^{int} and so were similar to P2 cells. Due to the poor viability of the purified LP monocytes in culture, I was unable to study later time points to examine whether further differentiation might occur *in vitro*.

I then tried to overcome these difficulties by using Ly6C^{high} monocytes from BM. FACS-purified BM monocytes cultured alone did not upregulate class II MHC or CX3CR1, nor did they upregulate CX3CR1 when cultured with rTGF β , CSF-1 or CX3CL1 (FKN) (Fig. 4.22B), all factors abundant in the normal mucosa which

have been reported to influence m ϕ differentiation (179, 202, 255). Due to these negative results and the technical difficulties associated with culturing purified colonic cell *in vitro*, I decided not to pursue this approach further.

4.8 Examining for the Presence of Radio-resistant Intestinal Macrophages

Thus far, my experiments have concentrated on the idea that colonic m ϕ are derived from BM monocytes. However, there is growing evidence that all organs have a population of m ϕ derived directly from embryonic precursors that seed the tissues prior to the establishment of the circulatory system and are maintained through *in situ* proliferation rather than being replenished by monocytes (256). Such non-BM derived m ϕ include Langerhans cells in skin and microglia in the CNS (57, 60), and interestingly they appear to be relatively unaffected by CCR2-deficiency (257), unlike some resident colonic m ϕ .

An opportunity arose for me to address the possible presence of BM independent, radioresistant m ϕ using CD45.1/CD45.2 \rightarrow CD45.2 BM chimeric mice generated by another research group within the department. Consistent with them being derived from BM monocytes, colonic Ly6C^{high}MHCII^{neg} cells in these mice were entirely of donor origin (CD45.1⁺/CD45.2⁺), as were all the cells in P2 and the CD11b⁺ DC (Fig. 4.23). In contrast, 5-7% of the F4/80⁺MHCII^{high} population of m ϕ were of host origin in both mice 8 weeks after irradiation and these cells were phenotypically indistinguishable from the donor derived cells in this population (Fig. 4.23B and 4.24).

Whilst the results of this experiment need to be confirmed with larger experimental groups at different time points following irradiation and reconstitution, they would appear to indicate that although there is a population of truly resident m ϕ in the colonic mucosa, they form a much smaller population than that in other tissues such as the skin and brain. This underlines my earlier conclusions that the gut m ϕ pool is mostly replenished from blood monocytes.

4.9 Summary

In this chapter I explored the *in vivo* origins of CX3CR1^{int} and CX3CR1^{high} LP populations to assess whether they represent discrete populations of pro-

inflammatory and resident m ϕ . Using a combination of adoptive transfer experiments and BrdU incorporation studies, I was able to show that rather than representing independent subsets of m ϕ , the CX3CR1^{int} and CX3CR1^{high} compartments appear to represent cells at different stages of an *in situ* differentiation continuum of Ly6C^{high} monocytes into tissue m ϕ . BM chimera studies also confirmed the monocyte origin of the vast majority of colonic m ϕ . Together these studies indicate that the maintenance of the intestinal m ϕ compartment during steady state conditions is not compatible with the current monocyte paradigm which proposes that distinct blood monocytes repopulate independent m ϕ populations, since Ly6C^{low} 'resident' monocytes were unable to repopulate the mucosa. Instead these data show that under normal physiological conditions so-called 'inflammatory' Ly6C^{high} monocytes constitutively enter the colonic mucosa and subsequently undergo a differentiation/maturation programme to become resident CX3CR1^{high} m ϕ . Unfortunately I was unable to replicate this differentiation process *in vitro*, but in the next chapter, I went on to examine the functional implications of the transitional process I had uncovered.

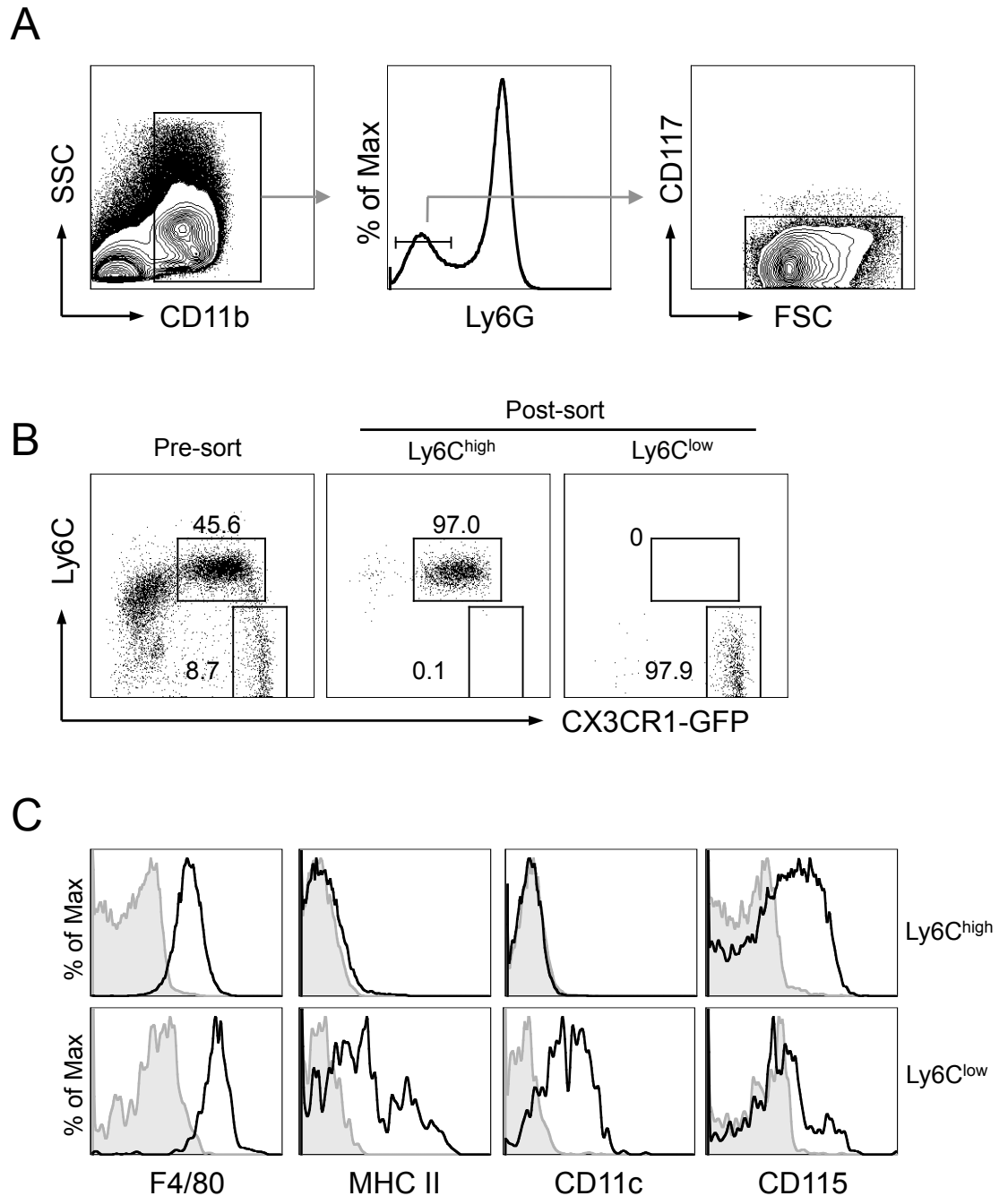


Figure 4.1: Purification of Bone Marrow Monocytes

BM cells were isolated from CX3CR1^{+/gfp} (CD45.1⁺/CD45.2⁺ or CD45.1^{neg}/CD45.2⁺) mice and single cells analysed for the expression of CD11b, Ly6G, CD117 (c-kit), Ly6C and CX3CR1-GFP by flow cytometry. **A.** CD11b⁺ cells were selected and Ly6G⁺ and CD117⁺ cells were gated out to exclude neutrophils and early haematopoietic progenitors, respectively. **B.** CD11b⁺Ly6G^{neg} CD117^{neg} cells were then examined for Ly6C and CX3CR1 expression to allow sorting of Ly6C^{high}CX3CR1^{int} 'inflammatory' and Ly6C^{low}CX3CR1⁺ 'resident' monocytes. **C.** Expression of F4/80, class II MHC, CD11c and CD115 on Ly6C^{high} (*upper panel*) and Ly6C^{low} (*lower panel*) monocytes. Representative of at more than 10 individual experiments.

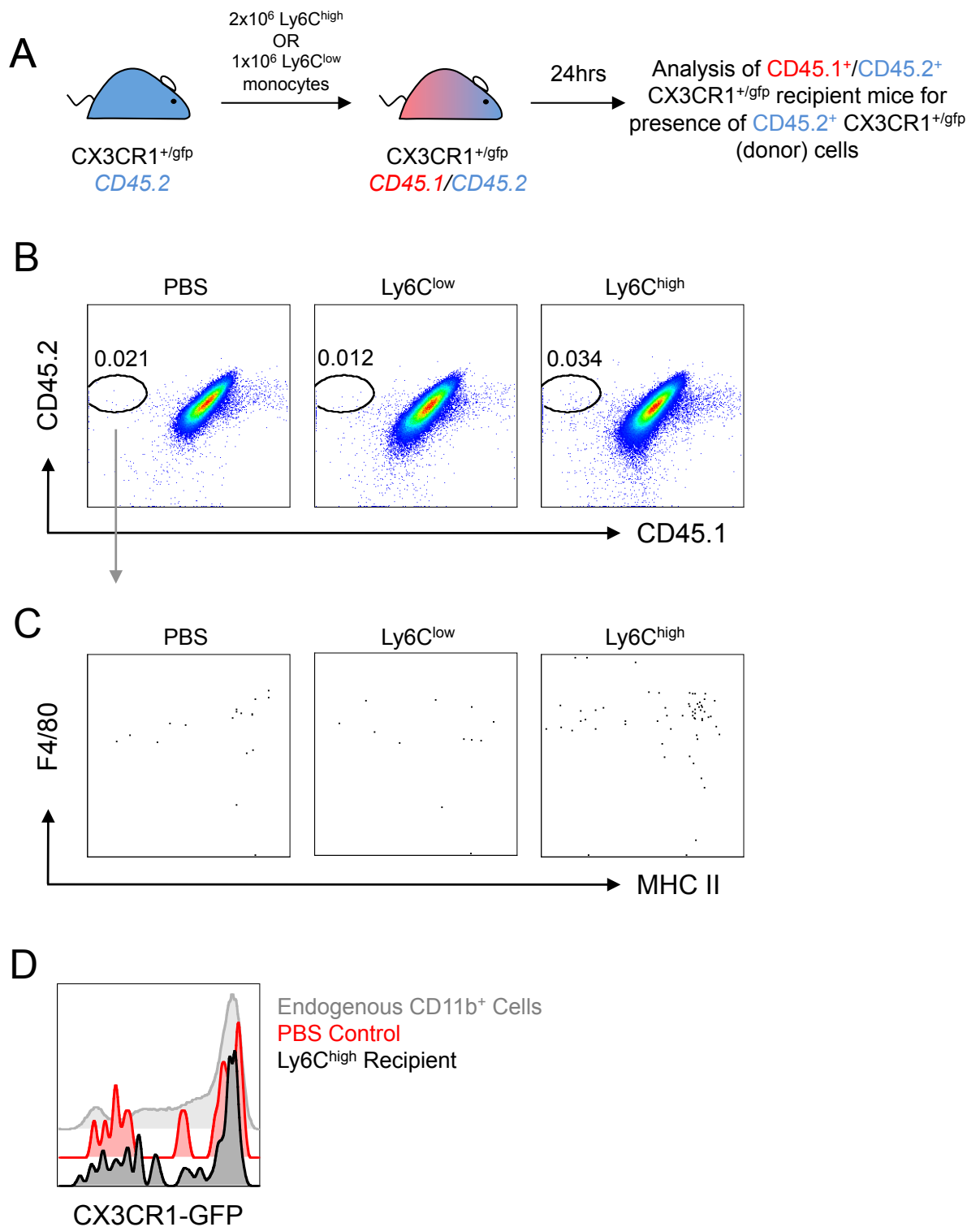


Figure 4.2: Adoptive Transfer of Bone Marrow Monocytes into Resting Mice

A. 2x10⁶ purified Ly6C^{high} BM monocytes or 1x10⁶ Ly6C^{low} BM monocytes from CX3CR1^{+/gfp} CD45.2⁺ mice were transferred into unmanipulated CD45.1⁺/CD45.2⁺ CX3CR1^{+/gfp} mice. **B.** Representative dot plots of CD45.1 and CD45.2 expression on live-gated CD45⁺ CD11b⁺ cells in the colon of recipients given PBS (*left panel*), Ly6C^{low} monocytes (*middle panel*) and Ly6C^{high} monocytes (*right panel*) 24hrs after transfer. Expression of F4/80 and class II MHC (**C**) and CX3CR1-GFP (**D**) by CD45.1^{neg}CD45.2⁺ cells from different recipients. 1 experiment with 2 recipient mice per group.

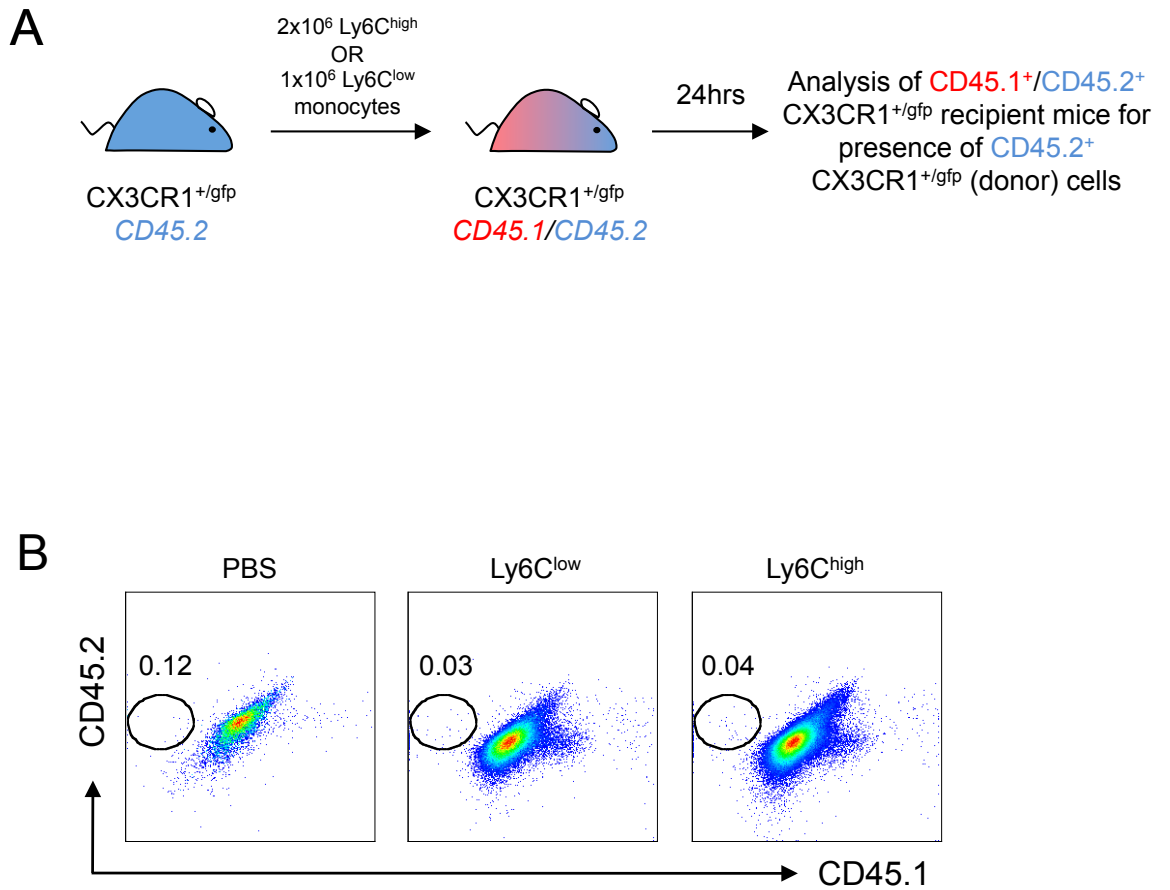


Figure 4.3: Adoptively Transferred BM Monocytes in Bloodstream of Resting Mice

A. 2x10⁶ purified Ly6C^{high} BM monocytes or 1x10⁶ Ly6C^{low} BM monocytes from CX3CR1^{+/gfp} CD45.2⁺ mice were transferred into unmanipulated CD45.1^{+/}CD45.2⁺ CX3CR1^{+/gfp} mice. **B.** Representative dot plots of CD45.1 and CD45.2 expression on live-gated CD45⁺ CD11b⁺ cells in the blood of recipients given PBS (*left* panel), Ly6C^{low} monocytes (*middle* panel) and Ly6C^{high} monocytes (*right* panel) 24hrs after transfer. 1 experiment with 2 recipient mice per group.

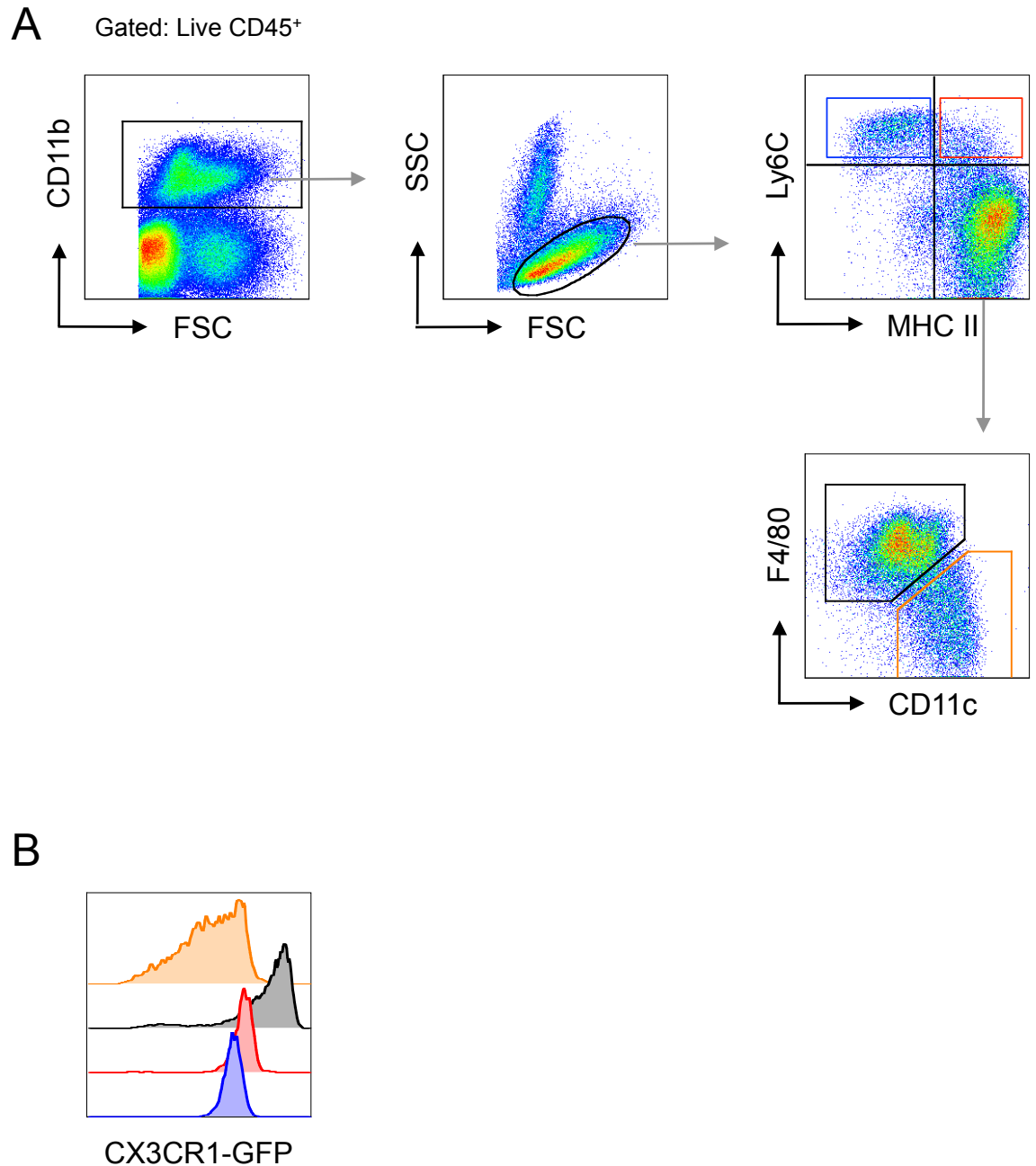


Figure 4.4: Alternative Gating Strategy for Identifying Colonic MP Subsets in Non-CX3CR1-GFP Mice

Colonic LP cells were isolated from C57Bl/6 mice and live-gated CD45⁺ cells analysed for the expression of CD11b, F4/80, Ly6C, MHC class II and CD11c by flow cytometry. **A.** SSC^{high} cells were gated out to exclude granulocytes (eosinophils and neutrophils) and the expression of Ly6C and class II MHC determined on SSC^{low} cells. Ly6C^{neg}MHCII⁺ cells were then assessed for the expression of F4/80 and CD11c. **B.** Expression of CX3CR1-GFP by the indicated populations obtained by applying the alternative gating strategy to CX3CR1^{+/-gfp} mice.

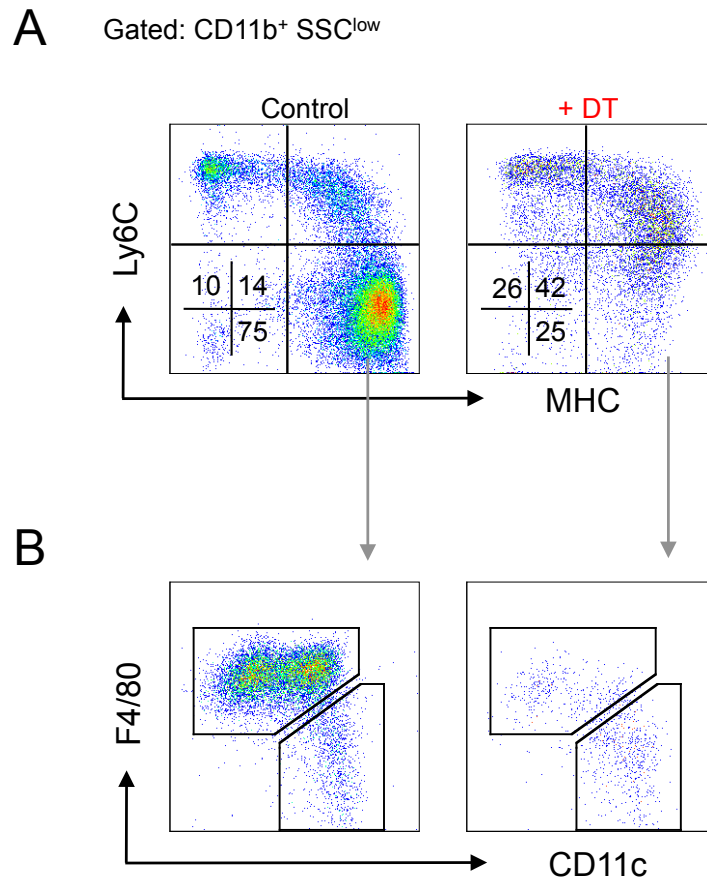


Figure 4.5: Ablation of Colonic MP Cells in CD11c-DTR Mice

CD11c-DTR mice were injected with DT (4ng/g bodyweight) or not and 24hr later colonic LP cells were isolated. **A.** Representative dot plots of Ly6C and class II MHC expression by live-gated CD45⁺ CD11b⁺ SSC^{low} cells. **B.** Representative dot plots of F4/80 and CD11c expression by Ly6C^{neg}MHCII⁺ cells, highlighting the depletion of both F4/80⁺ macrophages and CD11c⁺ DC. Representative of 2 individual experiments.

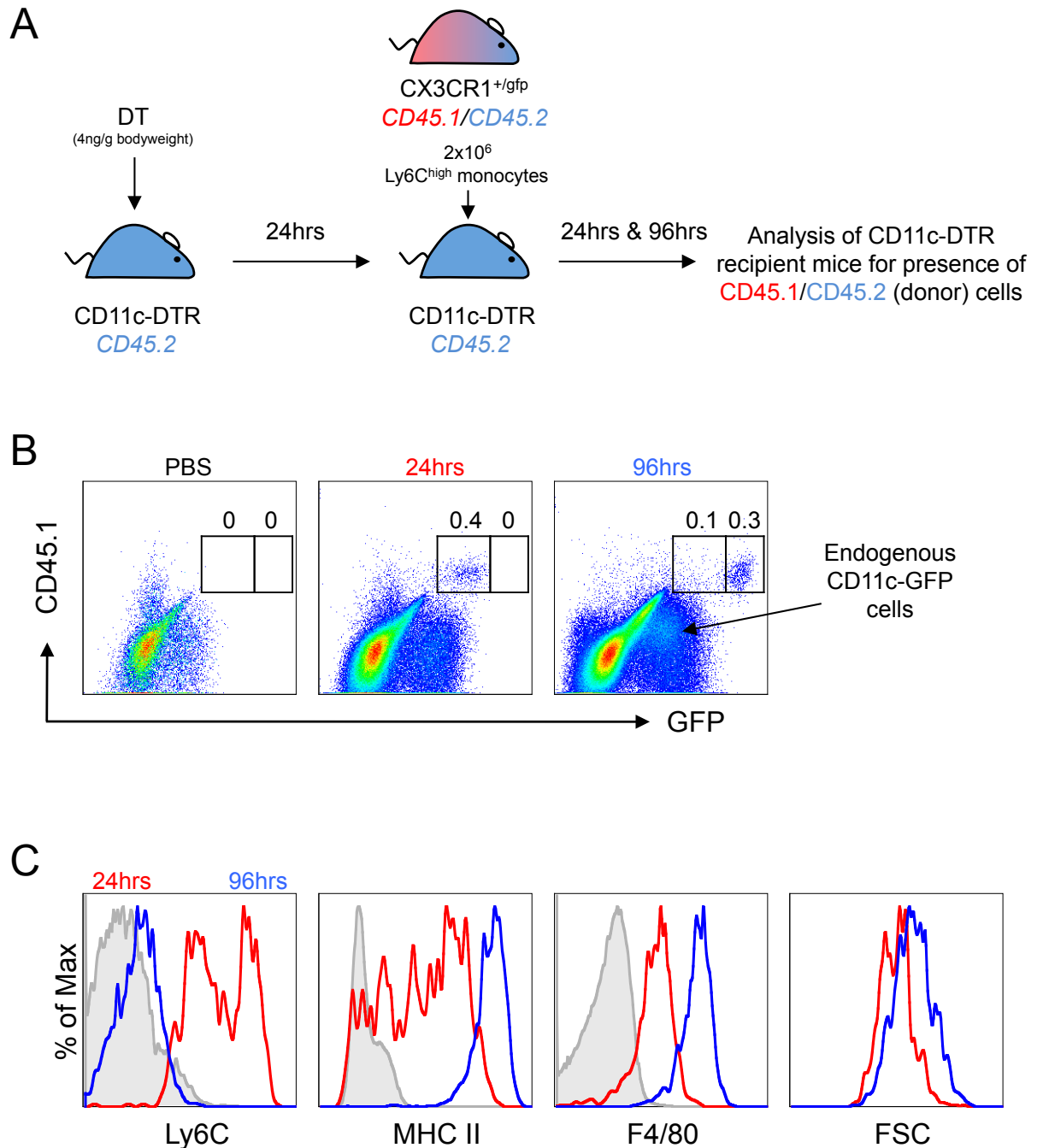


Figure 4.6: Accumulation of Transferred BM Monocytes in Colon of Depleted CD11c-DTR Mice

A. CD11c-DTR (CD45.2⁺) mice were injected with DT and 24hr later received 2x10⁶ purified Ly6C^{high} BM monocytes from CD45.1⁺/CD45.2⁺ CX3CR1^{+/gfp} mice. **B.** Representative dot plots of CD45.1 and GFP expression by live-gated CD45⁺ CD11b⁺ LP cells in the recipients given PBS (*left* panel), or receiving BM monocytes 24hr (*middle* panel) and 96hr before (*right* panel). **C.** Expression of Ly6C, class II MHC, F4/80 and FSC on donor-derived CD45.1⁺GFP⁺ cells at 24hrs (*red* line) and 96hr (*blue* lines). Shaded histograms represent staining with appropriate isotype controls. CD45.1^{neg}GFP⁺ cells in (B) represent endogenous CD11c⁺ cells from the CD11c-DTR-GFP mice. 1 experiment with 2 recipient mice per group.

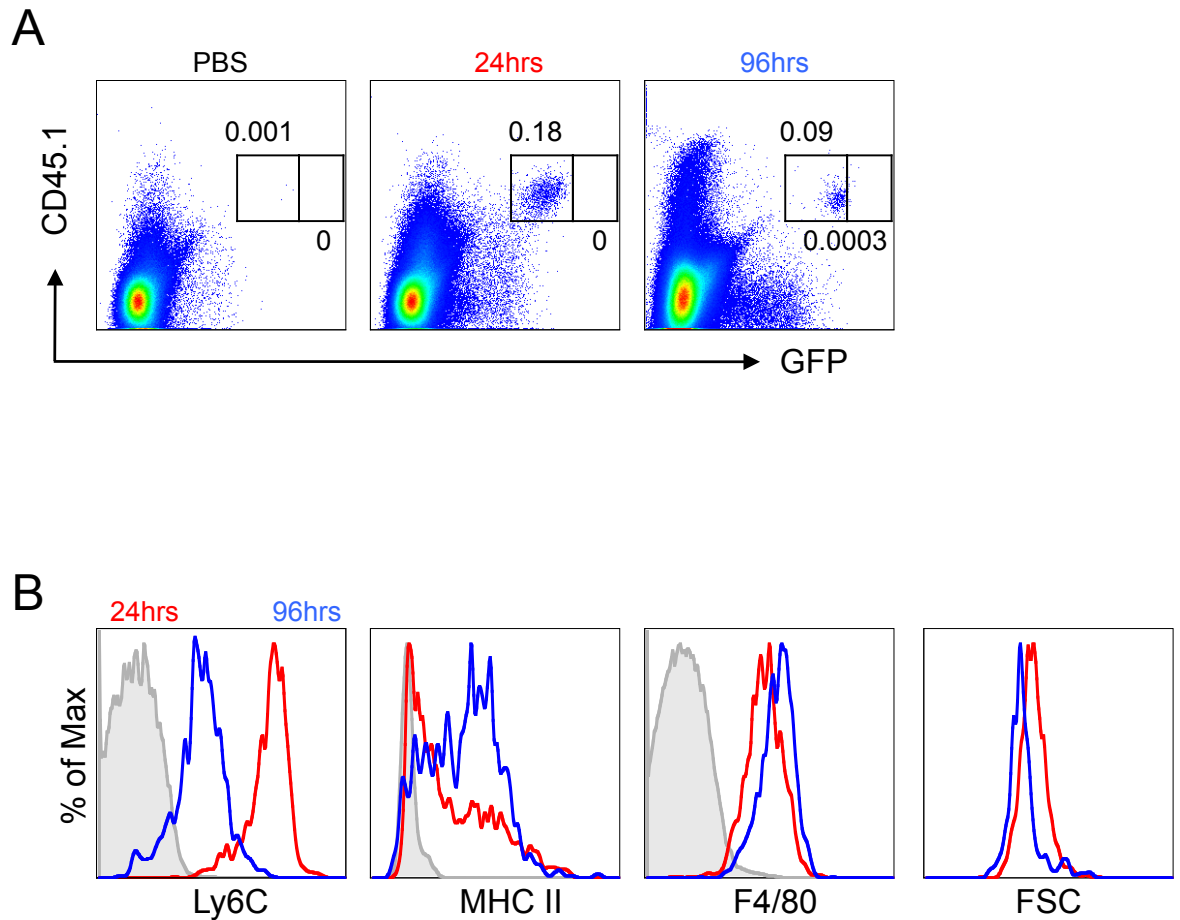


Figure 4.7: Presence of Transferred BM Monocytes in Blood of Depleted CD11c-DTR Mice

CD11c-DTR (CD45.2⁺) mice were injected with DT and 24hr later received 2×10^6 purified Ly6C^{high} BM monocytes from CD45.1⁺/CD45.2⁺ CX3CR1^{+/gfp} mice. **A.** Representative dot plots of CD45.1 and GFP expression by live-gated CD45⁺ CD11b⁺ blood leucocytes in the recipients given PBS (*left* panel), or receiving BM monocytes 24hr (*middle* panel) and 96hr before (*right* panel). **B.** Expression of Ly6C, class II MHC, F4/80 and FSC on donor-derived CD45.1⁺GFP⁺ cells at 24hrs (*red line*) and 96hr (*blue lines*). Shaded histograms represent staining with appropriate isotype controls. CD45.1^{neg}GFP⁺ cells in (B) represent endogenous CD11c⁺ cells from the CD11c-DTR-GFP mice. 1 experiment with 2 recipient mice per group.

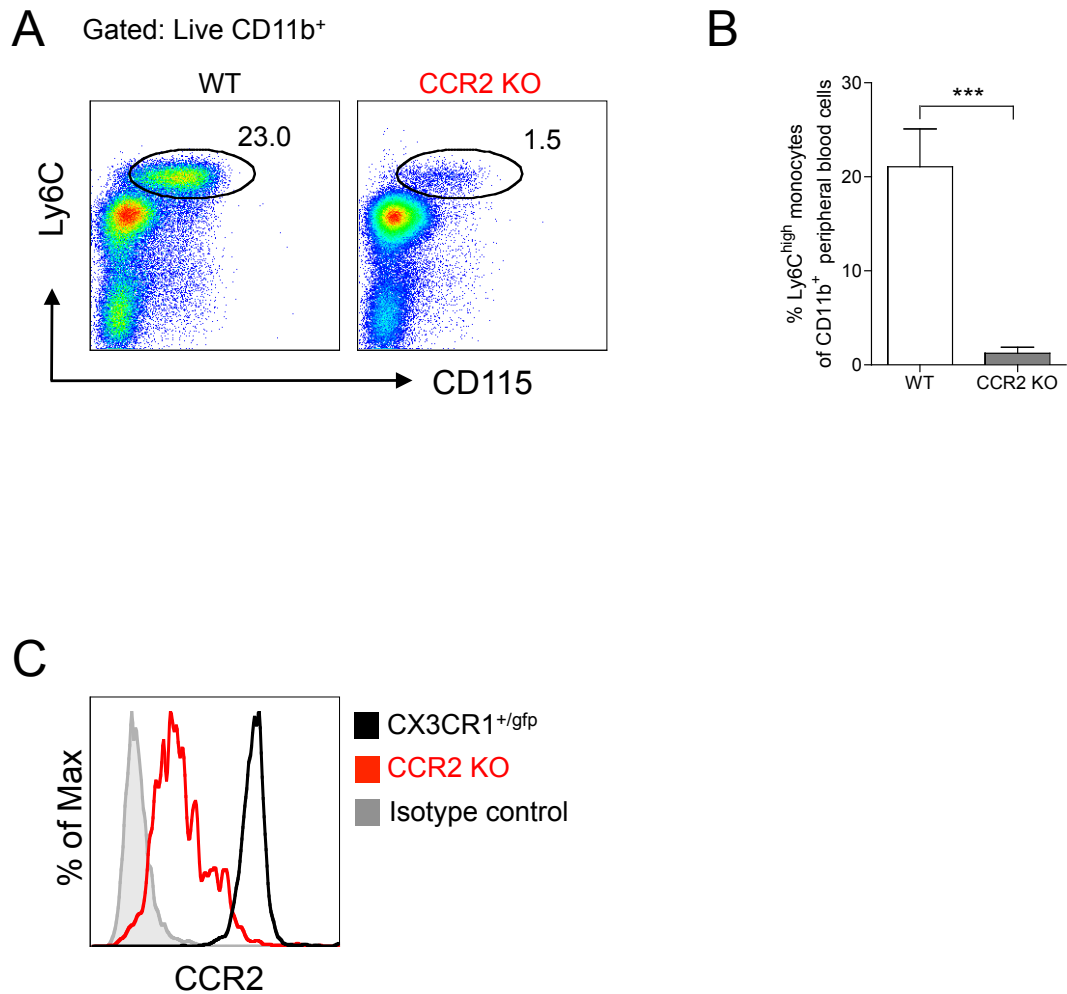


Figure 4.8: Circulating Ly6C^{high} Monocytes in CCR2 KO Mice

Whole blood was obtained from resting WT or CCR2 KO mice and red blood cells lysed. The remaining cells were analysed for the expression of CD11b, Ly6C and CD115 by flow cytometry. **A.** Representative dot plots of Ly6C and CD115 expression by WT and CCR2 KO live-gated CD45⁺ CD11b⁺ blood leucocytes and **(B)** the mean frequency of Ly6C^{high} blood monocytes within the CD11b⁺ cell fraction. **C.** Expression of CCR2 by Ly6C^{high} blood monocytes from WT and CCR2 KO mice as determined by flow cytometry. Results shown are the means + 1SD for 3-4 mice/group and are representative of 2 individual experiments. (***) $p < 0.001$ Student's t test)

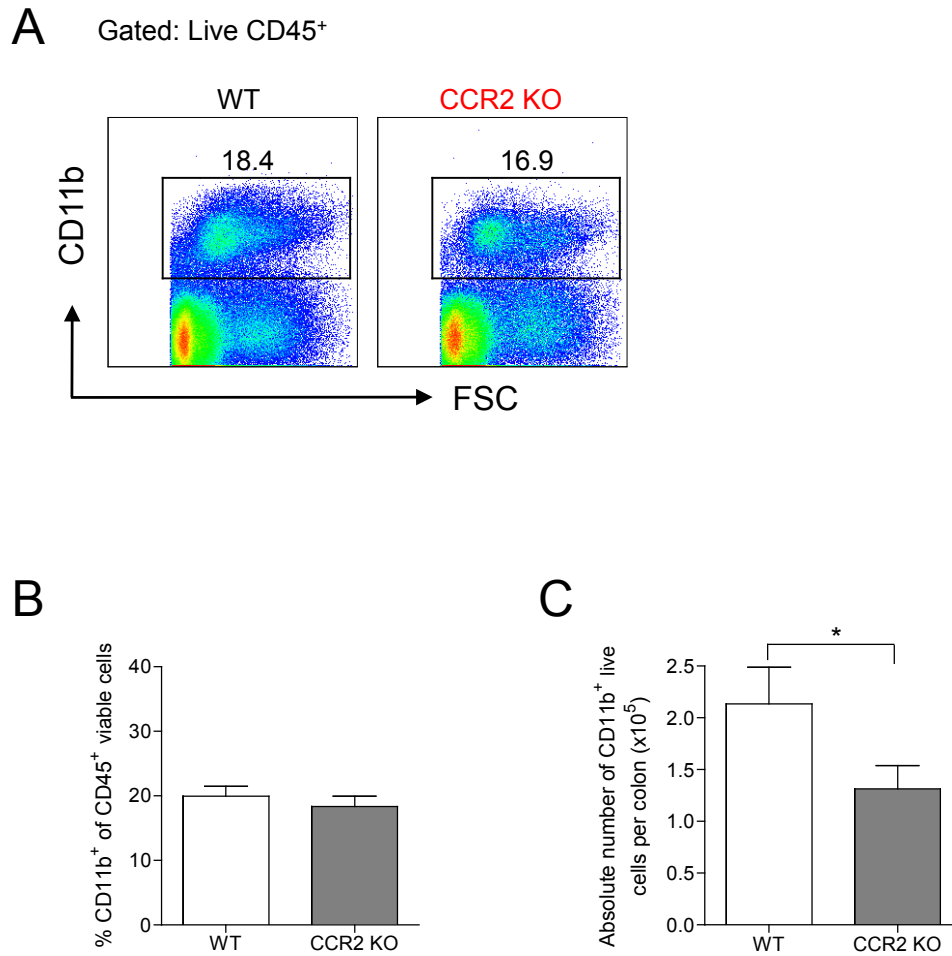


Figure 4.9: CD11b⁺ Myeloid Cell Compartment in Colon of CCR2 KO Mice

Colonic LP cells were isolated from resting WT or CCR2 KO mice and live-gated CD45⁺ cells were analysed for the expression of CD11b by flow cytometry. **A.** Representative dot plots of CD11b expression on WT and CCR2 KO LP cells. **B.** The mean proportion of CD11b⁺ cells amongst live CD45⁺ cells. **C.** The absolute number of CD11b⁺ live cells per colon. Results shown are the means + 1SD for 3-4 mice/group and are representative of 3 individual experiments. (* p<0.05 Student's t test)

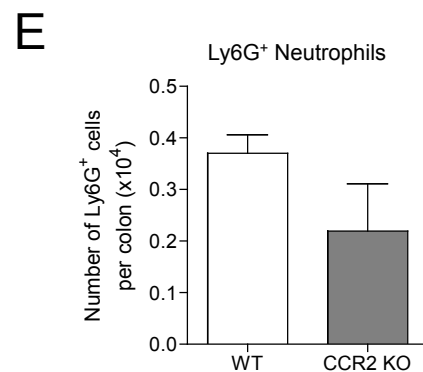
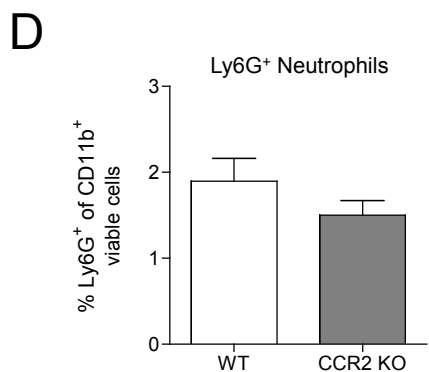
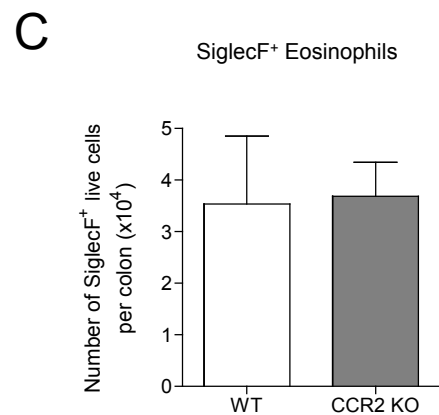
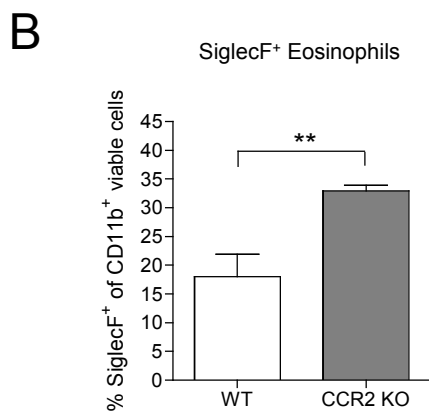
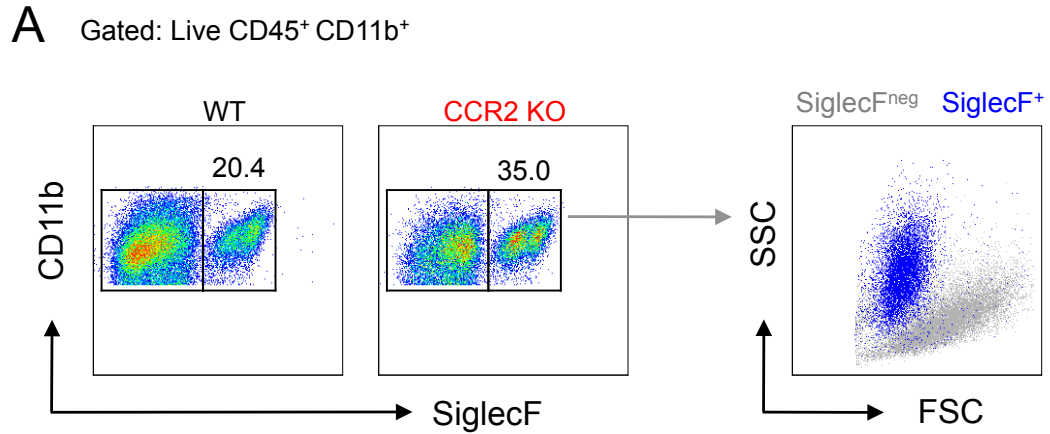


Figure 4.10: Eosinophils and Neutrophils in the Colon of CCR2 KO Mice

Colonic LP cells were isolated from resting WT or CCR2 KO mice and live-gated CD45⁺ CD11b⁺ cells analysed for the presence of SiglecF⁺ eosinophils and Ly6C^{int}(Ly6G⁺) neutrophils by flow cytometry. **A**. Representative dot plots of SiglecF expression on WT and CCR2 KO CD11b⁺ LP cells and FSC and SSC profile of SiglecF⁺ and SiglecF^{neg} cells. The percentage (**B**) and absolute numbers (**C**) of SiglecF⁺ eosinophils per colon. The percentage (**D**) and absolute numbers (**E**) of neutrophils per colon. Results shown are the means + 1SD for 3-4 mice/group and are representative of 3 individual experiments. (** p<0.01 Student's t test)

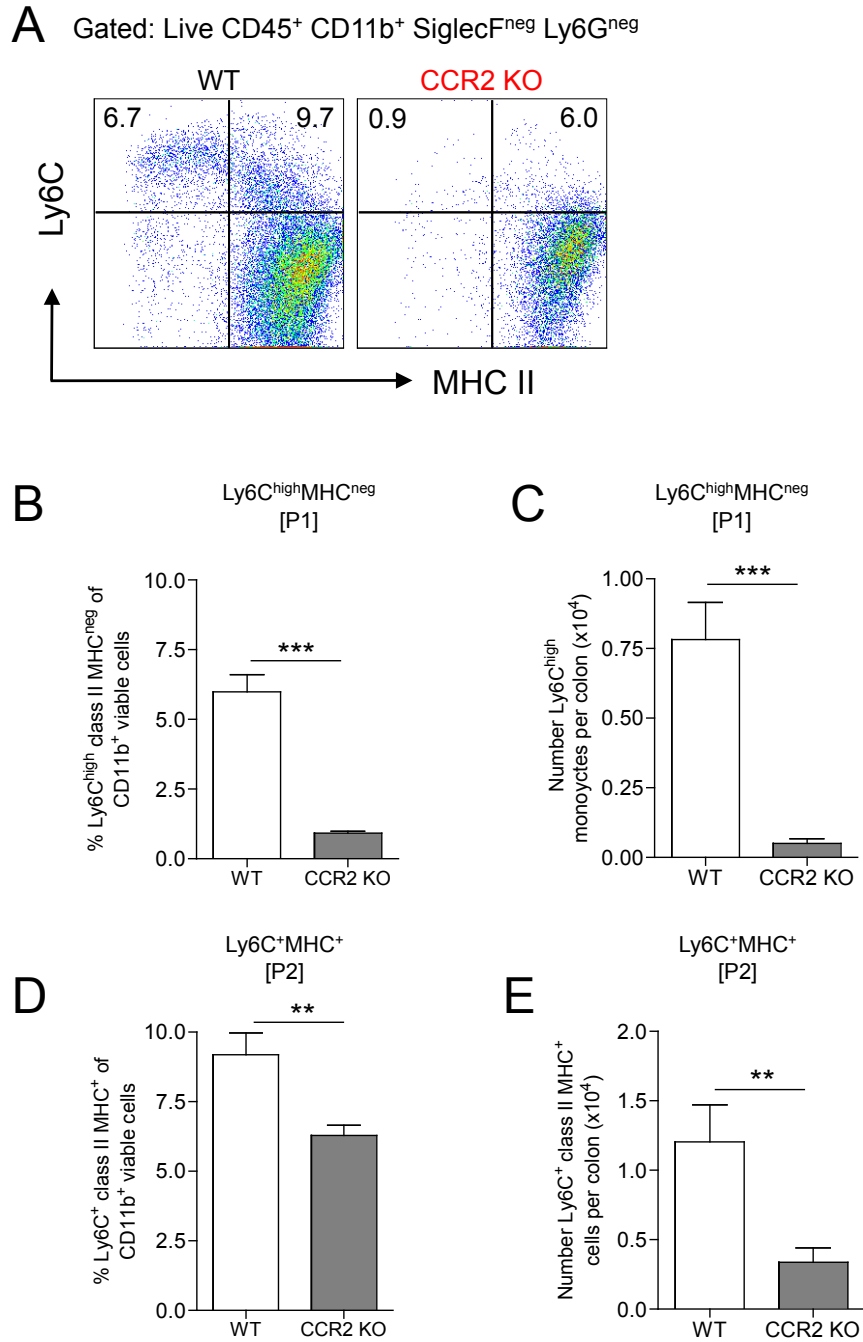


Figure 4.11: Intestinal Myeloid Compartment in CCR2 KO Mice

Colonic LP cells were isolated from resting WT or CCR2 KO mice and live-gated CD45⁺ CD11b⁺ SiglecF^{neg}Ly6G^{neg} cells were analysed for the expression of Ly6C and class II MHC by flow cytometry. **A**. Representative dot plots of Ly6C and class II MHC expression on WT and CCR2 KO CD11b⁺ LP cells. The percentage (**B**) and absolute number (**C**) of live Ly6C⁺MHC^{II}^{neg} cells (P1) and the percentage (**D**) and absolute number (**E**) of Ly6C⁺MHC^{II}⁺ cells per colon. Results shown are the means + 1SD for 3-4 mice/group and are representative of 3 individual experiments. (* p<0.05, ** p<0.01, *** p<0.001 Student's t test)

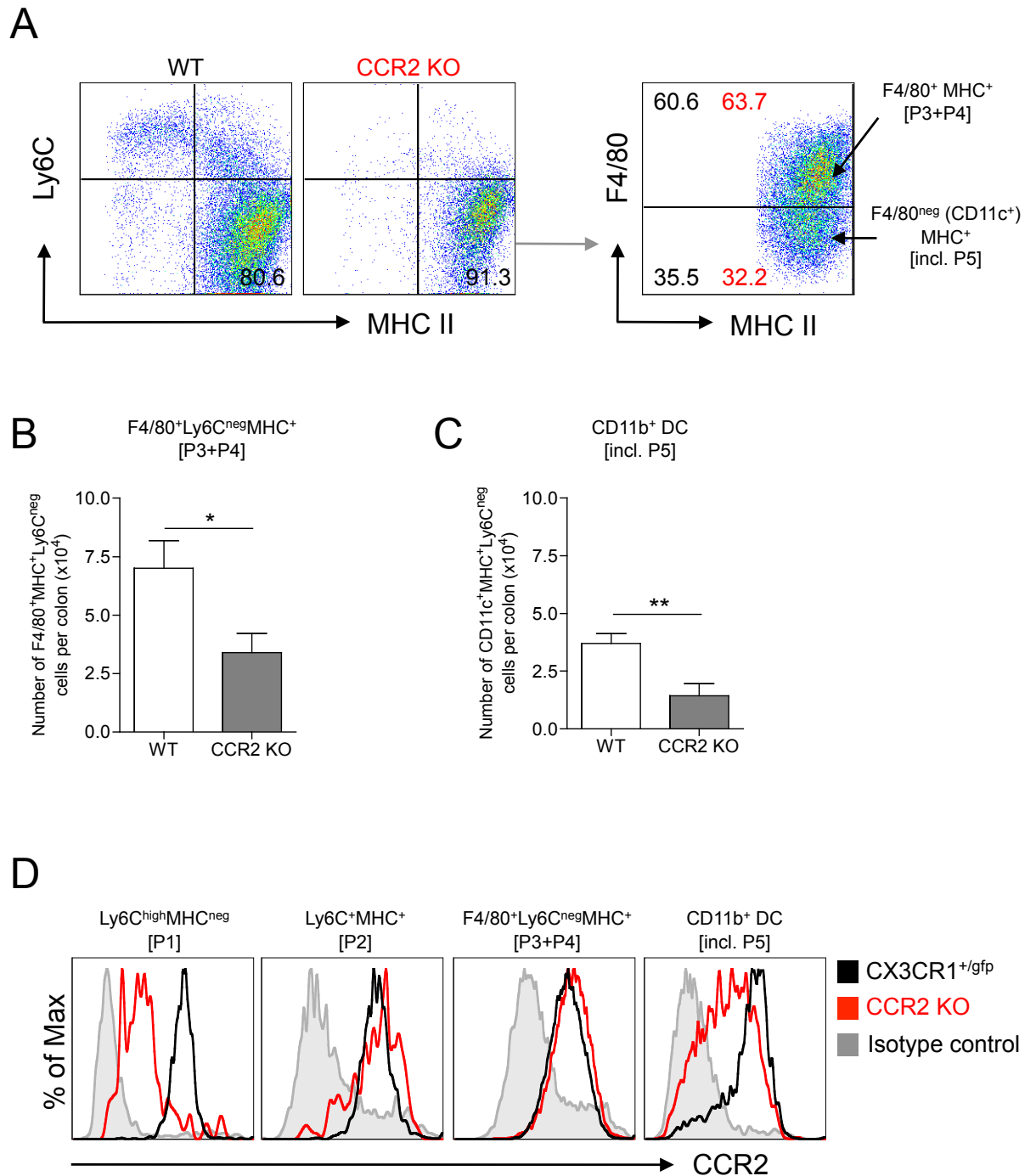


Figure 4.12: Intestinal Myeloid Compartment in CCR2 KO Mice

A. Colonic LP cells were isolated from resting WT or CCR2 KO mice and live-gated CD45⁺ CD11b⁺ SiglecF^{neg}Ly6G^{neg} cells were analysed for the expression of Ly6C and class II MHC and then Ly6C^{neg}MHCII⁺ cells analysed for the expression of F4/80. The absolute numbers of **(B)** F4/80⁺MHCII⁺ (P3+P4) cells and **(C)** F4/80^{neg}MHCII⁺ cells (CD11b⁺DC) per colon. **D.** Histograms show the expression of CCR2 by the indicated populations obtained from resting CX3CR1^{+/gfp} (black line) or CCR2 KO (red line) mice. Shaded histograms represent staining with the isotype control. Results shown are the means + 1SD for 3-4 mice/group and are representative of 3 individual experiments. (* p<0.05, ** p<0.01, *** p<0.001 Student's t test)

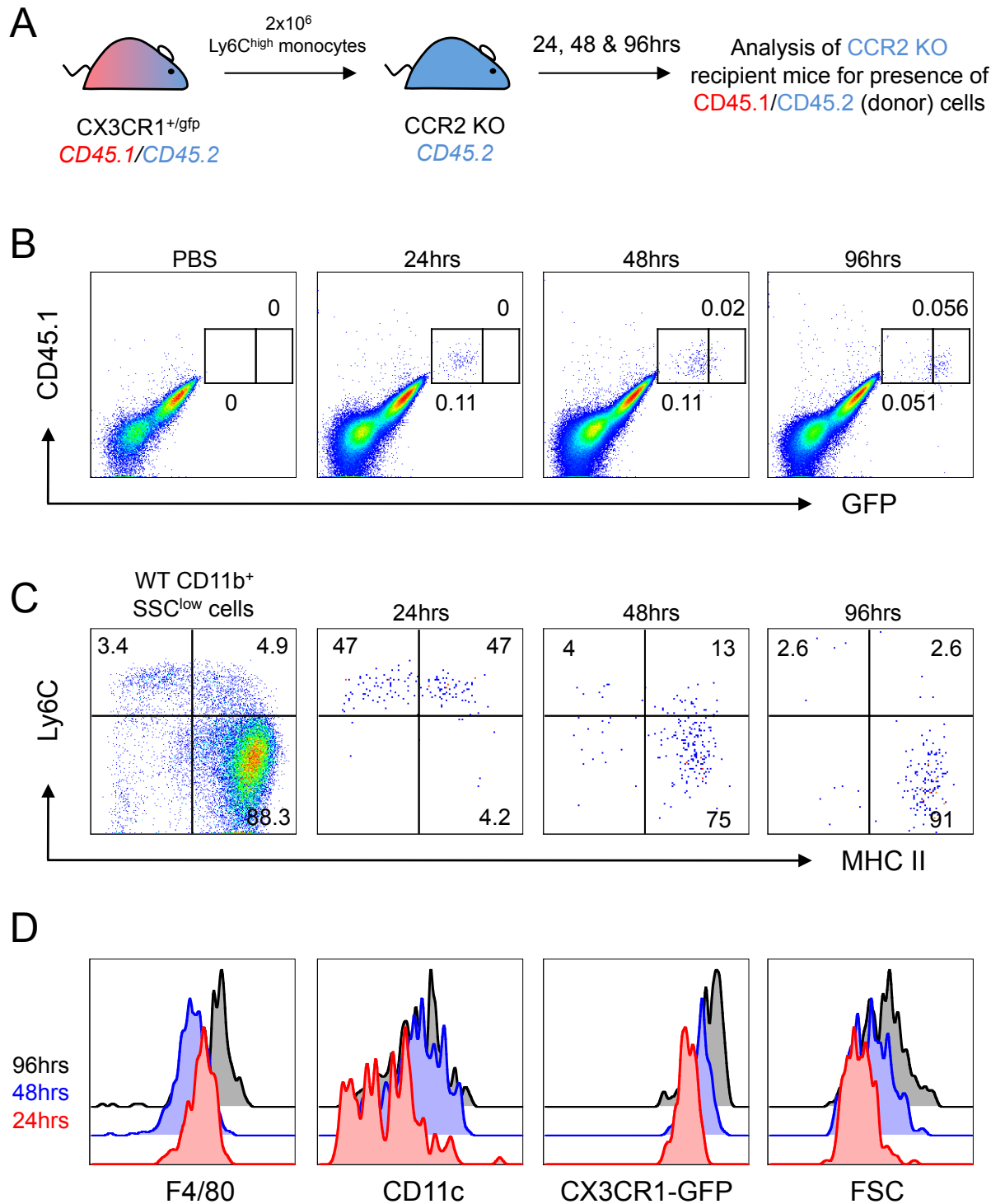


Figure 4.13: Accumulation of Transferred BM Monocytes in Colon of CCR2 KO Mice

A. CCR2 KO (CD45.2⁺) mice received 2x10⁶ purified Ly6C^{high} BM monocytes from CD45.1⁺/CD45.2⁺ CX3CR1^{+/gfp} mice. **B.** Representative dot plots of CD45.1 and GFP expression by live-gated CD45⁺ CD11b⁺ LP cells in the recipients given PBS, or receiving BM monocytes 24hrs, 48hrs and 96hrs before. **C.** Expression of Ly6C and class II MHC by live-gated CD45⁺CD11b⁺SSC^{low} cells from WT mice or by CD45.1⁺GFP⁺ donor cells at the indicated time points after transfer. **D.** Expression of F4/80, CD11c, CX3CR1-GFP and FSC on donor-derived CD45.1⁺GFP⁺ cells at 24hrs (red line), 48hrs (blue line) and 96hrs (black line). Representative of 2 experiments with 2 recipient mice per group.

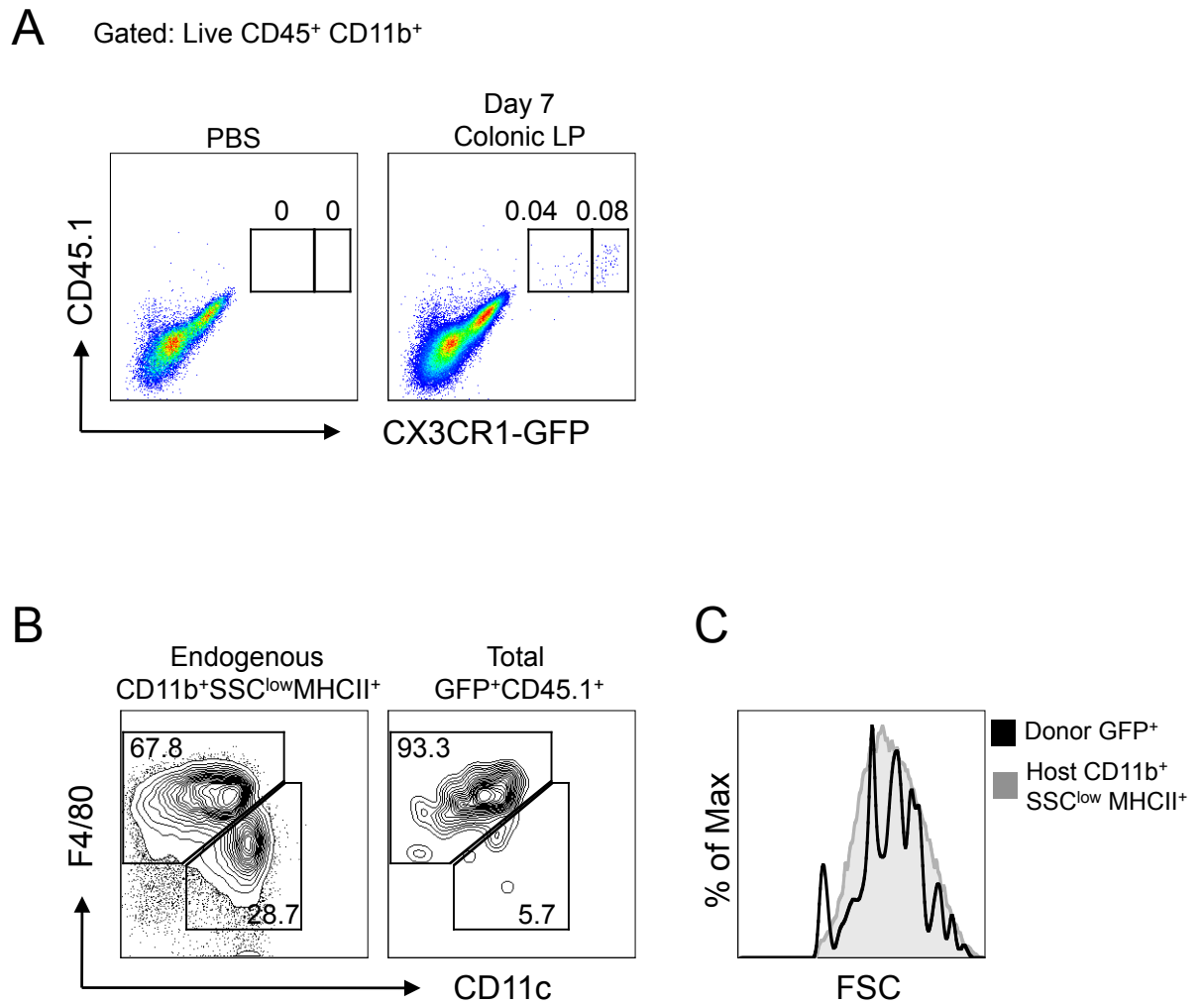


Figure 4.14: Ly6C^{high} Monocytes Give Rise to Long-lived CX3CR1^{high} Macrophages in CCR2 KO Colon

CCR2 KO (CD45.2⁺) mice received 2×10^6 purified Ly6C^{high} BM monocytes from CD45.1⁺/CD45.2⁺ CX3CR1^{+/gfp} mice and the presence of donor cells was analysed after 7 days. **A.** Representative dot plots of CD45.1 and GFP expression by live-gated CD45⁺ CD11b⁺ LP cells in the recipients receiving PBS or BM monocytes 7 days before. **B.** Expression of F4/80 and CD11c by CD11b⁺SSC^{low}MHCII⁺ recipient cells (*left panel*) compared with donor-derived CD45.1⁺GFP⁺ cells (*right panel*). **C.** FSC profile of CD11b⁺SSC^{low}MHCII⁺ recipient cells (grey) compared with donor-derived CD45.1⁺GFP⁺ cells (black). Representative of 2 experiments with 2 recipient mice per group.

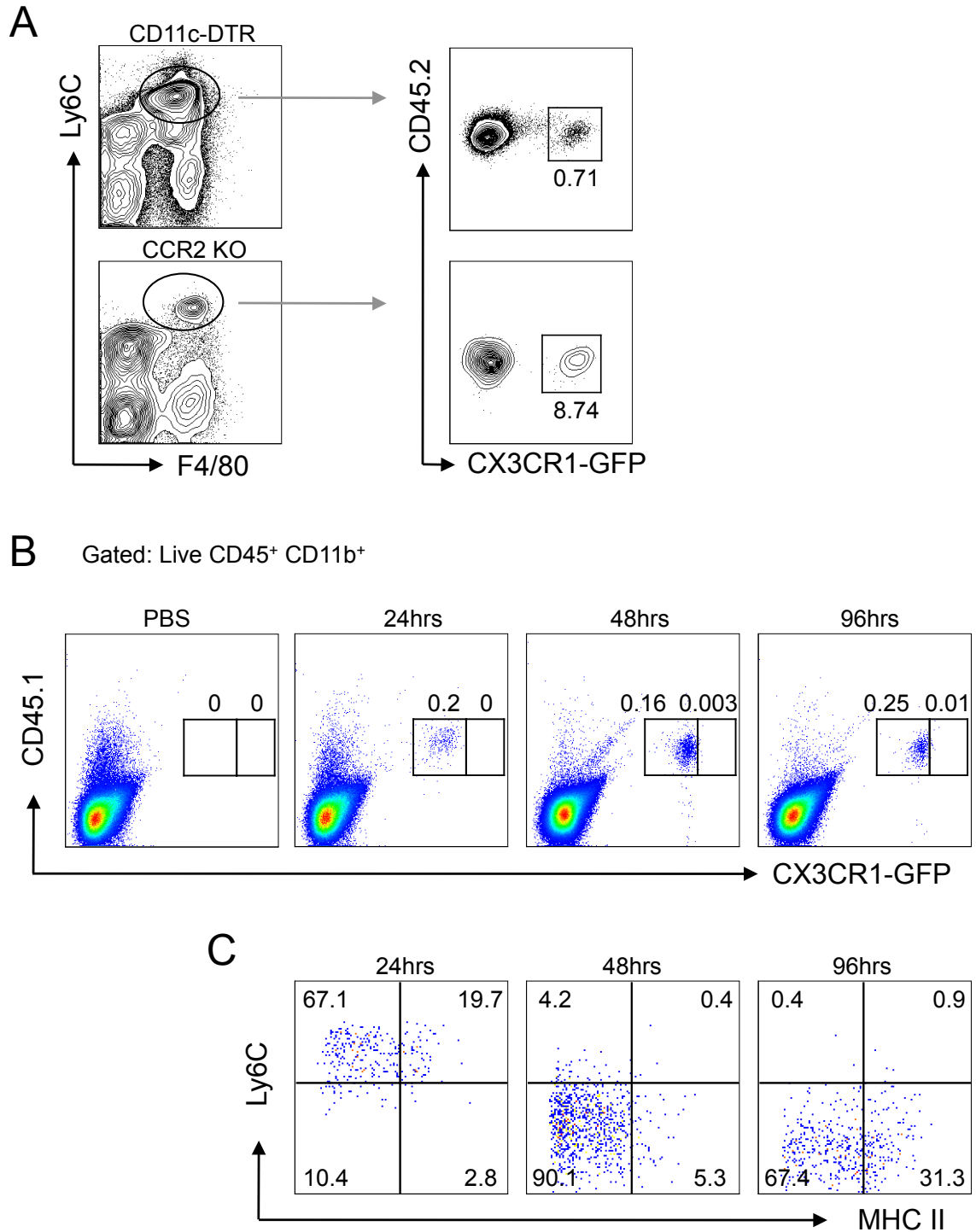


Figure 4.15: Presence of Adoptively Transferred Ly6C^{high} Monocytes in Blood of CCR2 KO mice

CCR2 KO (CD45.2⁺) mice received 2×10^6 purified Ly6C^{high} BM monocytes from CD45.1⁺/CD45.2⁺ CX3CR1^{+/gfp} mice and the presence of donor cells in the blood was analysed 24hrs, 48hrs and 96hrs later. **A.** The proportion of donor-derived cells (CX3CR1-GFP⁺) amongst Ly6C^{high} monocytes 24hrs after transfer into DT-treated CD11c-DTR mice or unmanipulated CCR2 KO mice. **B.** Representative dot plots of CD45.1 and GFP expression by live-gated CD45⁺ CD11b⁺ blood leucocytes in the CCR2 KO recipients receiving PBS or BM monocytes 24hrs, 48hrs and 96hrs before. **C.** Expression of Ly6C and class II MHC by CD45.1⁺GFP⁺ donor cells at the indicated time points after transfer. Representative of 2 experiments with 2 recipient mice per group.

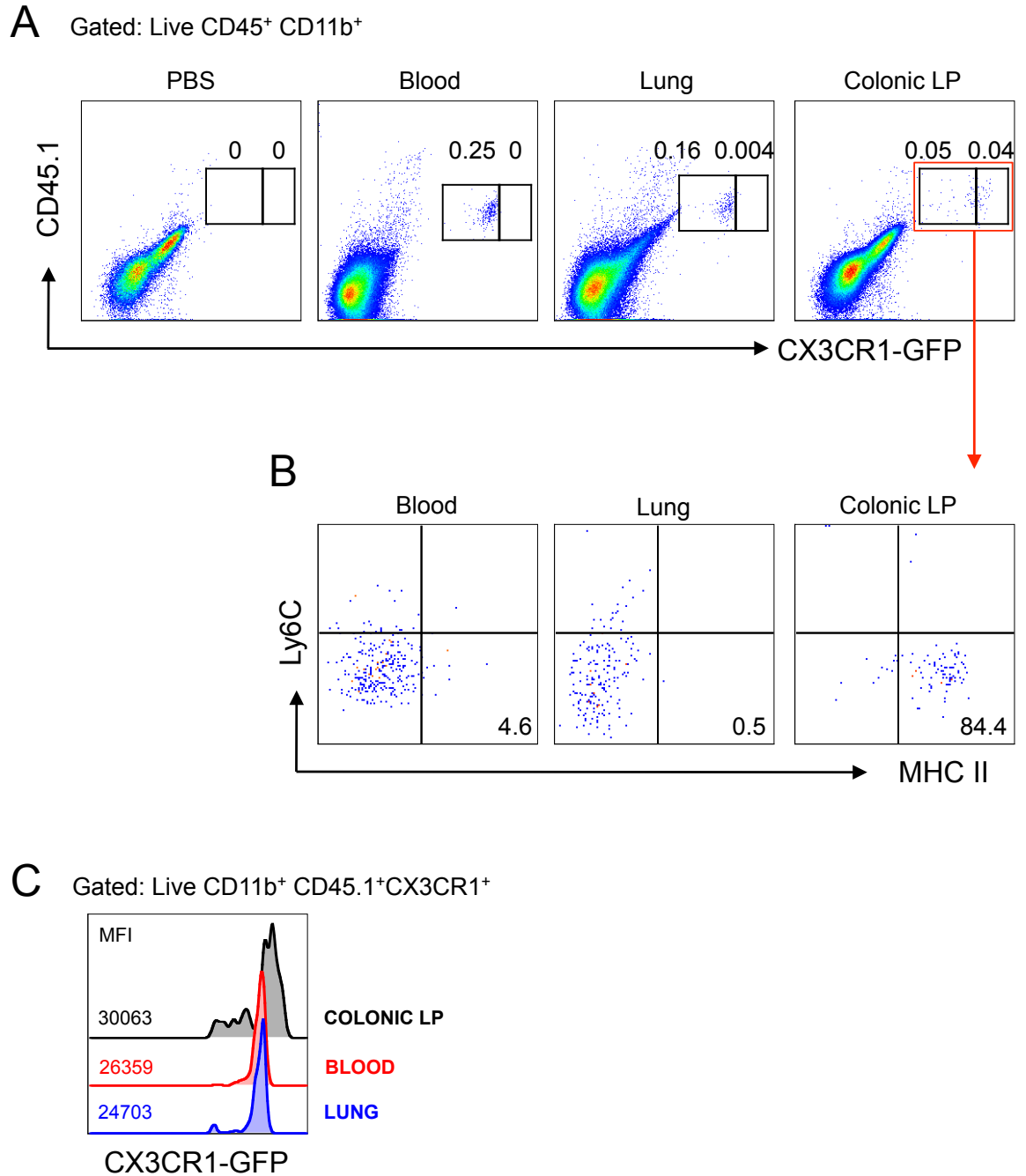


Figure 4.16: Comparison of Fate of Donor Derived Monocytes in Different Tissues of CCR2 KO Mice

CCR2 KO (CD45.2⁺) mice received 2×10^6 purified Ly6C^{high} BM monocytes from CD45.1⁺/CD45.2⁺ CX3CR1^{+/gfp} mice and the presence of donor cells in the blood, lung parenchyma and colonic LP was analysed 96hrs later. **A.** Representative dot plots of CD45.1 and CX3CR1-GFP expression by live-gated CD45⁺ CD11b⁺ cells from each tissue from recipients receiving PBS or BM monocytes 96hrs before. **B.** Expression of Ly6C and MHC II on donor-derived CD45.1⁺ CX3CR1⁺ cells. **C.** Comparison of CX3CR1-GFP levels of donor cells retrieved from each tissue. 1 experiment with 2 mice per group.

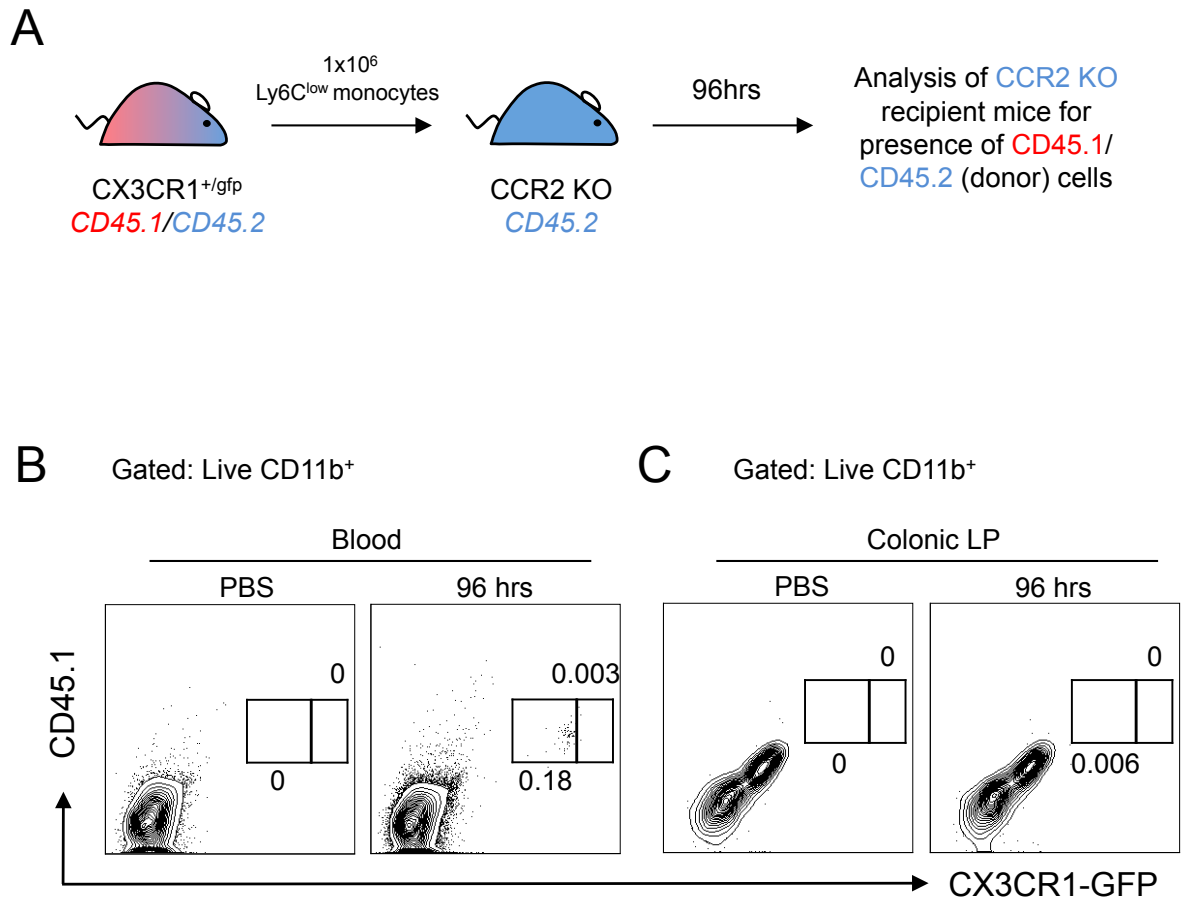


Figure 4.17: Adoptive Transfer of Ly6C^{low} Monocytes into Resting CCR2 KO Mice

A. CCR2 KO (CD45.2⁺) mice received 1x10⁶ purified Ly6C^{low} BM monocytes from CD45.1⁺/CD45.2⁺ CX3CR1^{+/gfp} mice and the presence of donor cells in the blood and colonic LP assessed 96hrs later. Representative dot plots of CD45.1 and CX3CR1-GFP expression by live-gated CD45⁺ CD11b⁺ (**B**) blood leucocytes and (**C**) colonic LP cells in the recipients receiving PBS or BM monocytes 96hrs before. 1 experiment with 1 mouse per group.

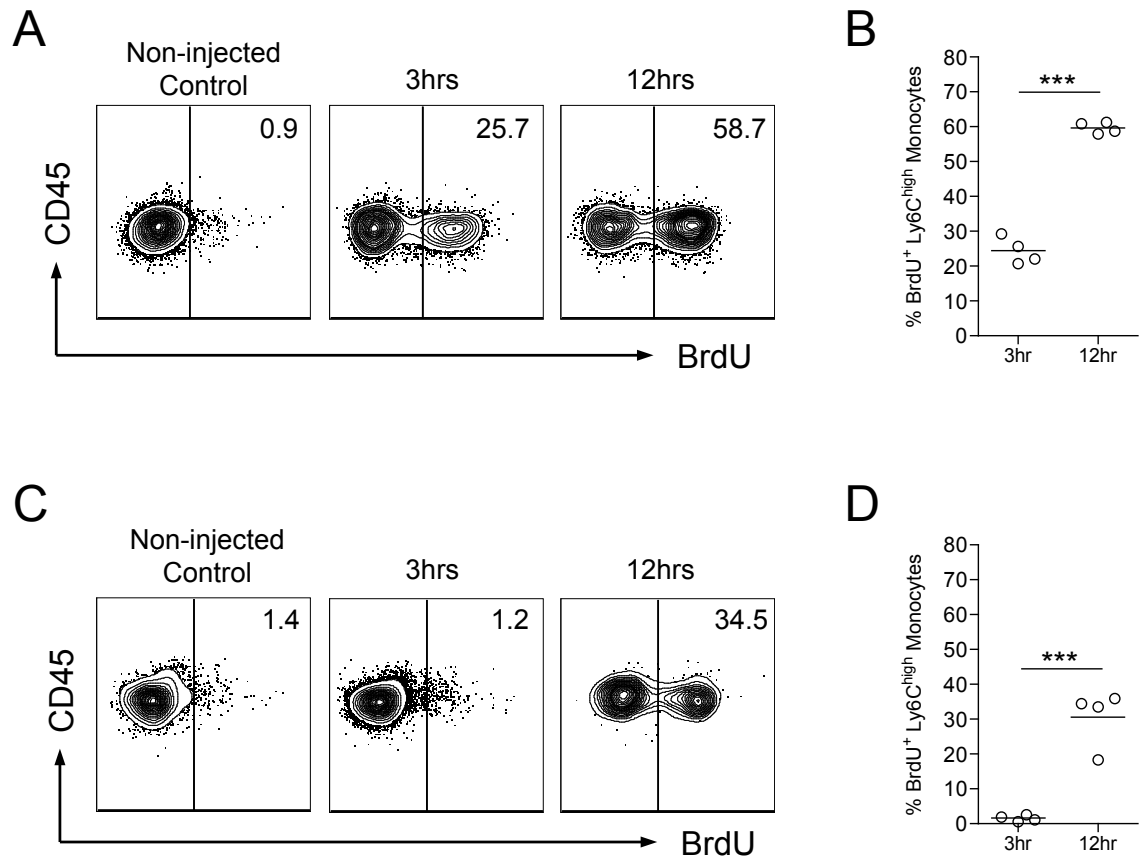


Figure 4.18: Short Term BrdU Incorporation by Bone Marrow and Blood Monocytes

CX3CR1^{+/gfp} mice received 1mg BrdU by i.p. injection and the incorporation of BrdU by BM and blood monocytes was examined after 3 and 12hrs by flow cytometry. **A.** Representative BrdU staining on live-gated CD45⁺CD11b⁺Ly6C^{high}CX3CR1^{int} BM monocytes at the indicated time points. **B.** The mean frequency of BrdU⁺ cells within the CD11b⁺Ly6C^{high}CX3CR1^{int} BM monocyte population at 3 and 12 hrs. **C.** Representative BrdU staining on live-gated CD45⁺CD11b⁺Ly6C^{high}CX3CR1^{int} blood monocytes at the indicated time points. **D.** The mean frequency of BrdU⁺ cells within the CD11b⁺Ly6C^{high}CX3CR1^{int} blood monocytes population at 3 and 12 hrs. Background staining was determined by comparison of the BrdU staining of non-injected control cells. Representative of 2 individual experiments with 4 mice/group. (* p<0.05, ** p<0.01, *** p<0.001 Student's t test)

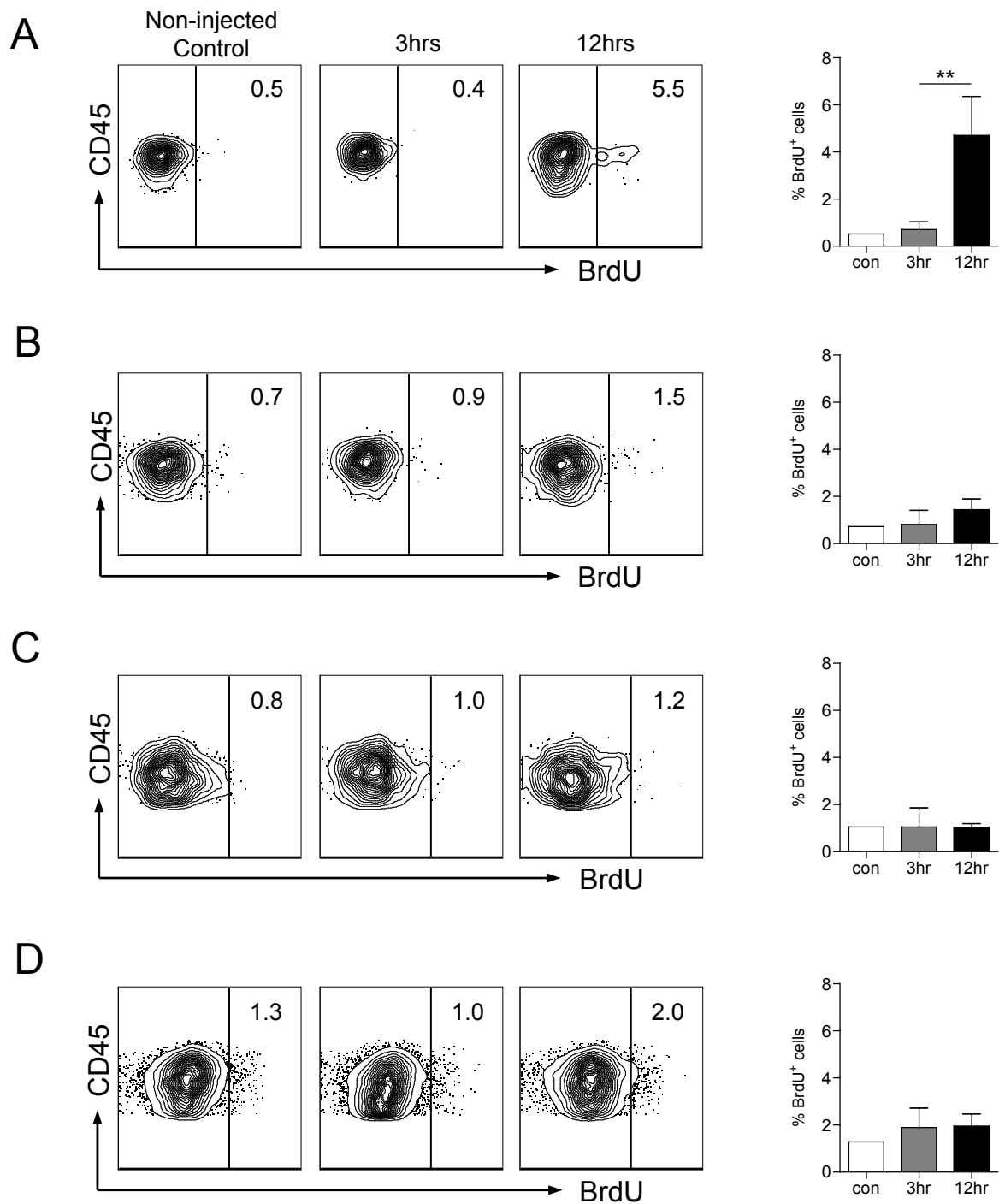


Figure 4.19: Short Term BrdU Incorporation by Colonic Macrophage Subsets

CX3CR1^{+/gfp} mice received 1mg BrdU by i.p. injection and the incorporation of BrdU by live-gated CD45⁺ colonic LP CX3CR1⁺ subsets (P1 to P4) was examined after 3 and 12hrs by flow cytometry. Representative BrdU staining and the mean frequency of BrdU⁺ cells within (A) P1, (B) P2, (C) P3 and (D) P4 at 3 and 12hrs compared with non-injected controls (con). Background staining was determined by the comparison of BrdU staining of non-injected control cells. Results are representative of 2 individual experiments and show the means + 1SD for 4 mice/group.

(** p<0.01 Student's t test)

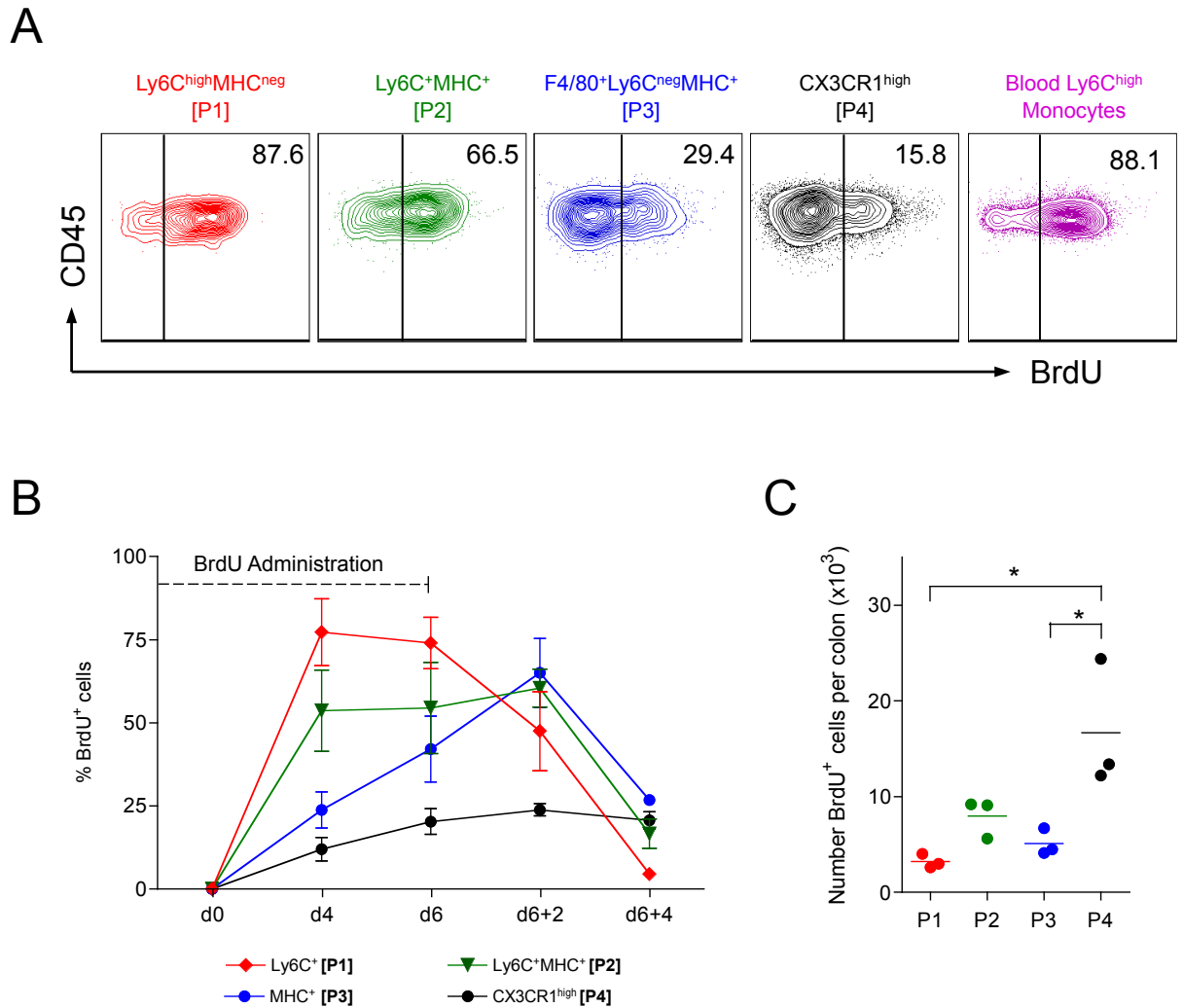


Figure 4.20: Long Term BrdU Incorporation by Colonic Macrophage Subsets

CX3CR1^{+/gfp} mice received 1mg BrdU by i.p. injection, followed by 0.8mg/ml BrdU in their drinking water for six days and the incorporation of BrdU by CX3CR1⁺ populations (P1-P4) in the colon was examined by flow cytometry. **A.** Representative BrdU staining by colonic m ϕ subsets and Ly6C^{high} blood monocytes at d4 of BrdU administration. **B.** The mean frequency of BrdU⁺ cells within P1, P2, P3 and P4 at the indicated time points. **C.** Absolute number of BrdU⁺ cells within P1 to P4 after 4 days of continuous BrdU administration. Results shown are the means \pm 1SD for 3 mice/group and are representative of a single experiment. (* $p < 0.05$ one-way ANOVA followed by Bonferoni's multi-comparison post-test)

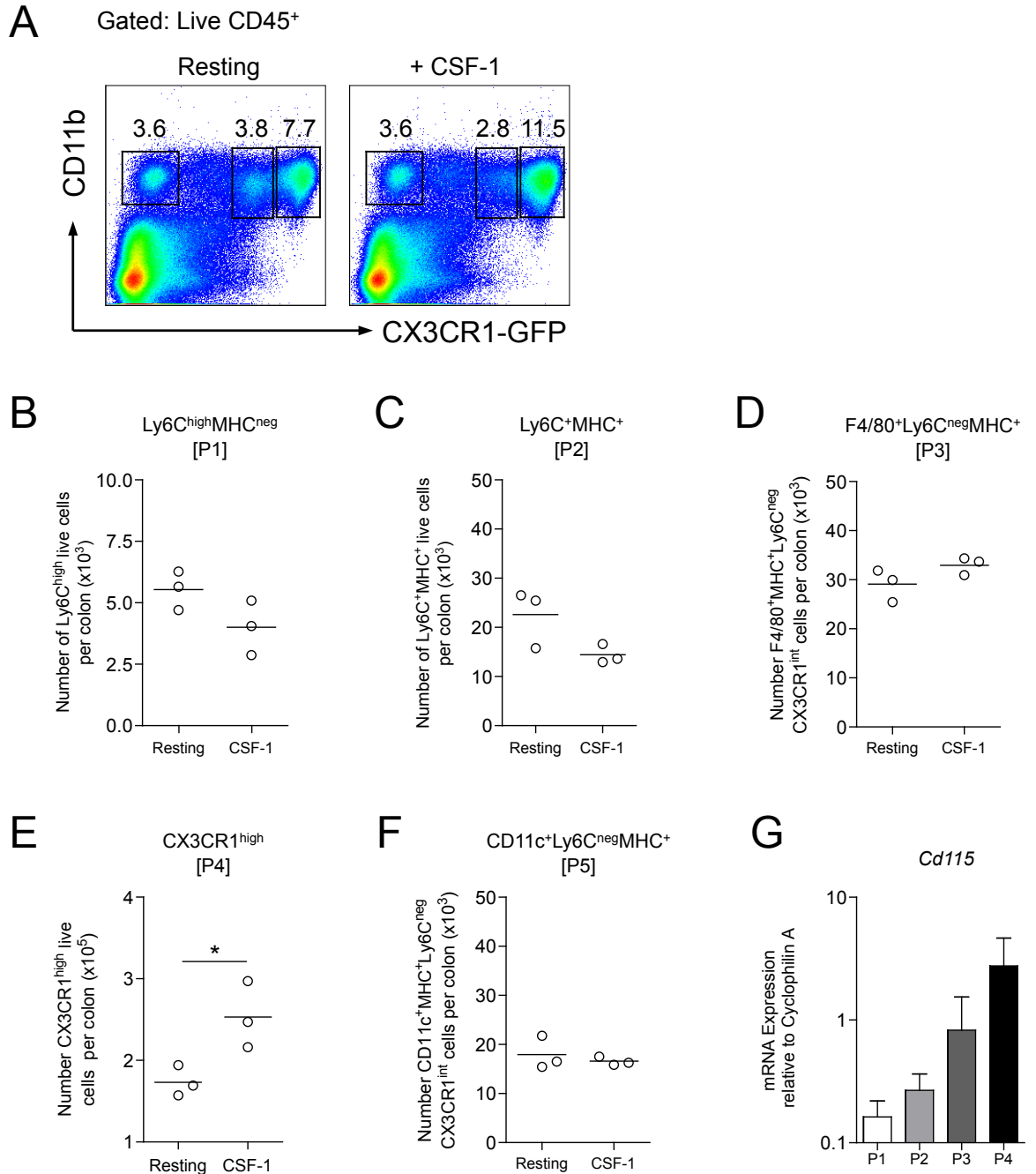


Figure 4.21: Effects of CSF-1 Administration on Colonic Macrophage Subsets

CX3CR1^{+gfp} mice received 20,000 units/day of recombinant human CSF-1 i.p. for 4 consecutive days and the numbers of colonic m ϕ determined by flow cytometry. **A**. Representative dot plots of CD11b and CX3CR1-GFP expression by live-gated CD45⁺ cells from the colon of resting (*left panel*) and CSF-1 treated (*right panel*) mice. **B-F**. The absolute numbers of P1-P5 after CSF-1 treatment compared with resting CX3CR1^{+gfp} mice (data from Figure 3.9). Results shown are the mean number of cells per colon \pm 1SD and are representative of a single experiment. (* p < 0.05, Student's t test) **G**. Levels of mRNA expression by P1-P4 for CD115 (CSF-1R) were analysed by qRT-PCR. Results shown are mean expression relative to Cyclophilin A using the $2^{-\Delta C(t)}$ method. The mean was obtained from two independent experiments using cells pooled from eleven/twelve mice. Primer sequences detailed in Table 2.4.

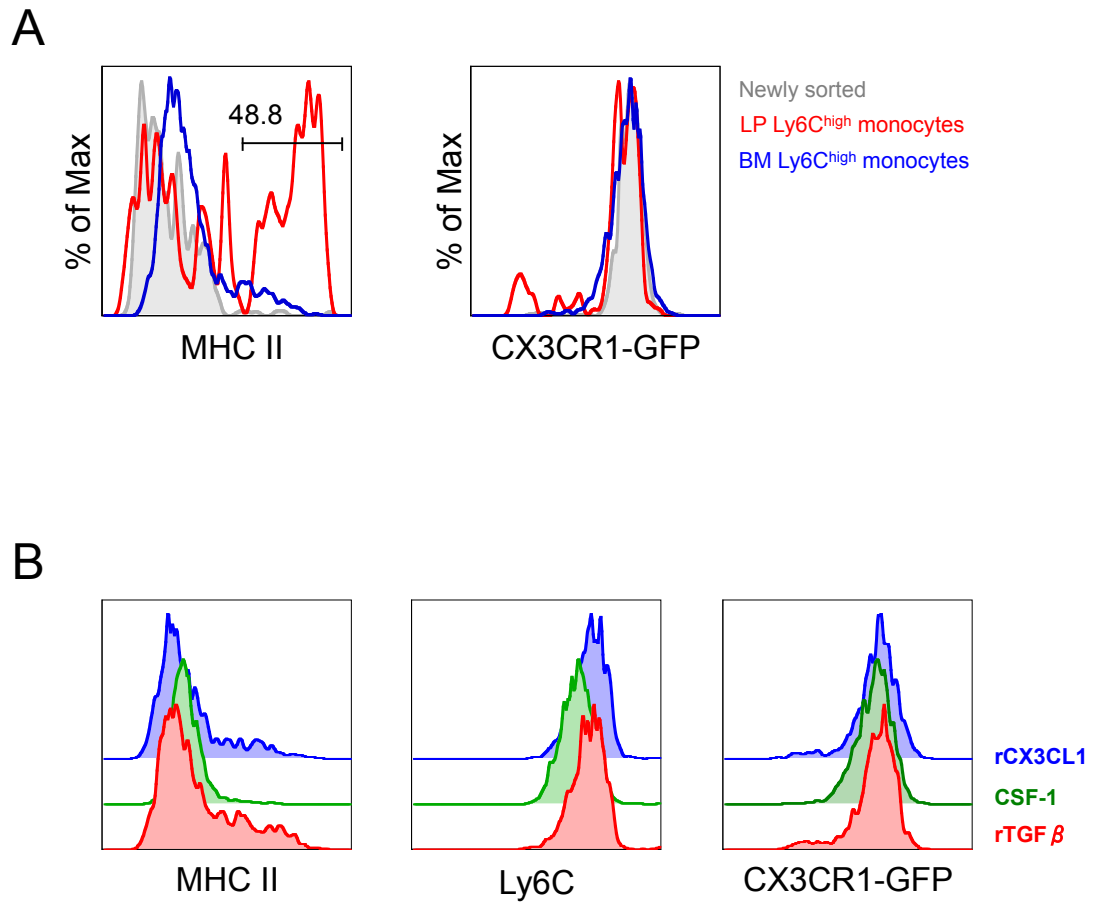


Figure 4.22: Effects of Culture of Colonic and BM Monocytes *In Vitro*

A. Colonic Ly6C^{high}MHCII^{neg}CX3CR1^{int} (P1) cells and Ly6C^{high} BM monocytes were FACS-purified from resting CX3CR1^{+/gfp} mice and cultured overnight in medium and the levels of class II MHC and CX3CR1-GFP were examined by flow cytometry after 24hrs. **B.** FACS-purified Ly6C^{high} BM monocytes were cultured overnight in 10ng/ml TGF β , 50ng/ml CX3CL1 (FKN) or 20% L929 fibroblast cell line supernatant (CSF-1) and the level of CX3CR1-GFP was assessed by flow cytometry. Representative of 2 individual experiments.

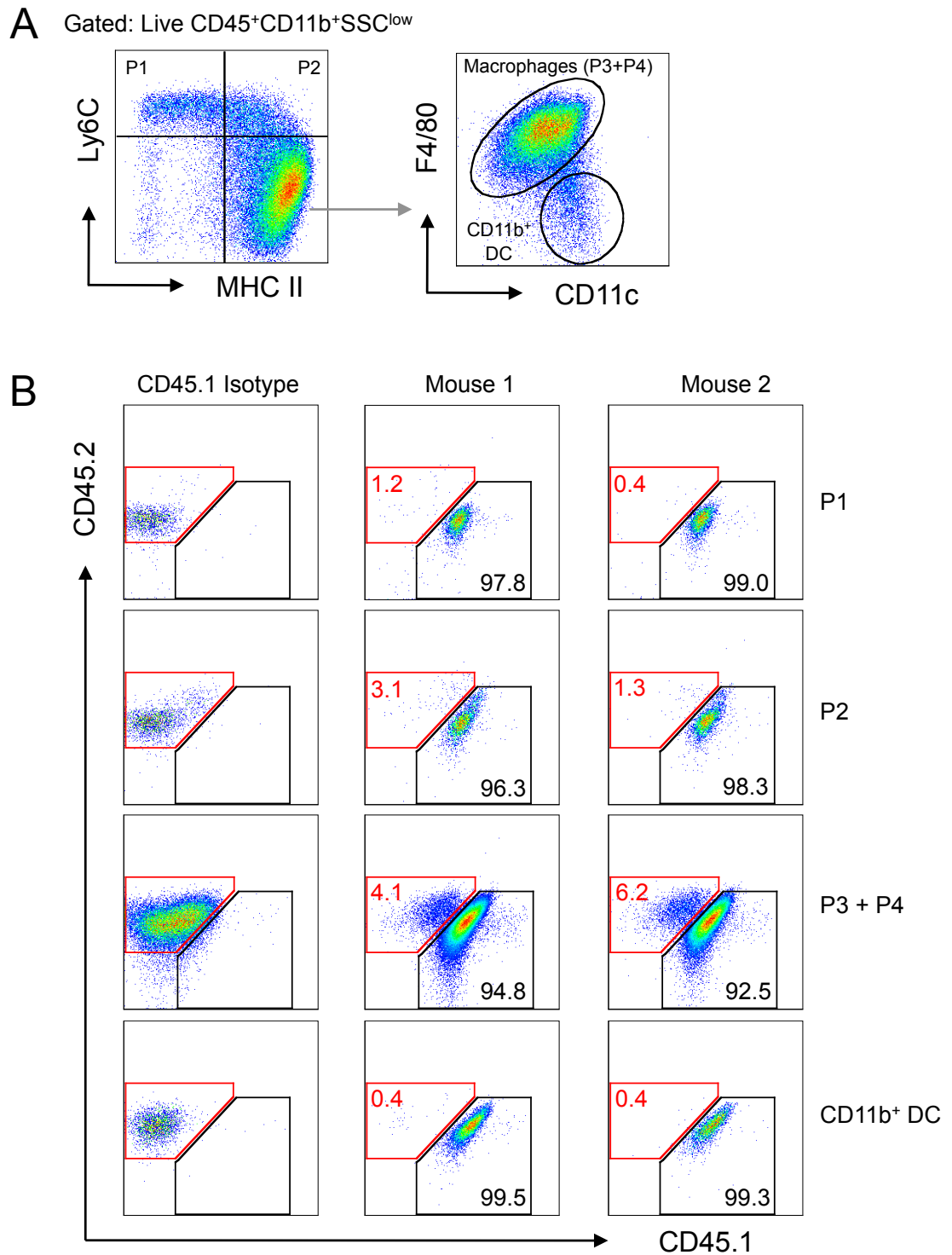


Figure 4.23: Radio-resistant Macrophages in the Colonic Mucosa

C57BL/6 mice (CD45.2) were irradiated and reconstituted with 1×10^7 total BM cells from CD45.1⁺/CD45.2⁺ C57BL/6 mice by intravenous infusion and 8 weeks later colonic LP myeloid cell subsets were examined for expression of CD45.1 and CD45.2. **A.** Representative dot plots showing the gating strategy adopted. **B.** Total live-gated cells were examined for the proportion of cells of host (CD45.2) and donor (CD45.1/CD45.2) origin within the P1, P2, P3+4 and CD11b⁺ DC populations. Plots show the staining from each mouse examined compared with staining with the isotype control for CD45.1. Representative of 1 individual experiment with 2 mice.

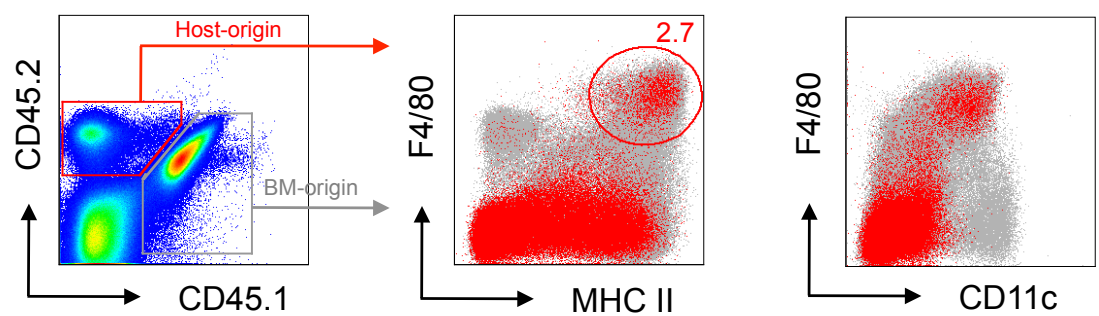


Figure 4.24: Radio-resistant Macrophages in the Colonic Mucosa are Phenotypically Indistinguishable from BM-derived Resident Colonic Macrophages

C57BL/6 mice (CD45.2) were irradiated and reconstituted with 1×10^7 total BM cells from CD45.1⁺/CD45.2⁺ C57BL/6 mice by intravenous infusion and 8 weeks later live-gated colonic LP cells were examined by flow cytometry. Host-derived (CD45.2; red) cells were analysed for expression of F4/80, class II MHC and CD11c, and overlaid on the donor-derived cells (CD45.1/CD45.2; grey). Representative of 1 individual experiment with 2 mice.

Chapter 5
Functional Analysis of Colonic
Macrophage Populations in Homeostasis
and Inflammation

5.1 Introduction

Like most tissue m ϕ , intestinal m ϕ are highly specialised to meet the requirements of their local environment. Previous studies have shown that intestinal m ϕ display selective functional inertia, whereby they are avidly phagocytic and express class II MHC, but phagocytosis or TLR stimulation does not lead to the production of pro-inflammatory mediators (171, 179). The extended and more rigorous phenotypic analysis I developed in the preceding chapters revealed unsuspected heterogeneity amongst the resident m ϕ population in healthy mouse colon. Some of the populations of cells I defined had the characteristics of blood monocytes and their immediate descendants. Furthermore, in contrast to current ideas of monocyte heterogeneity, I demonstrated that under physiological conditions, 'inflammatory' Ly6C^{high} monocytes can replenish the entire resident m ϕ population through an *in situ* differentiation process, involving the loss of Ly6C and the upregulation of class II MHC, CD11c, F4/80 and CX3CR1. As these results could suggest the presence of pro-inflammatory cells in the steady state colon, in this chapter I set out to investigate whether changes in functional capacity accompanied the differentiation process implied by phenotypic characterisation.

5.2 Baseline Cytokine Production by LP Myeloid Subsets

First, I examined the ability of the CX3CR1-defined subsets of MP to produce TNF α and IL10 as representative pro- and anti-inflammatory cytokines respectively. To do this, I established a method for intracellular cytokine staining that was sufficiently reproducible and sensitive for use with intestinal cells. This involved adapting standard protocols for the detection of intracellular cytokines in an attempt to prevent the colonic m ϕ from adhering to the culture plates, as I found this impaired cell retrieval and viability. I found the optimal method was to incubate colonic LP digests in non-adherent polystyrene (FACS) tubes in the absence of mitogens such as PMA or ionomycin. This allowed me to measure spontaneous cytokine levels.

Colonic LP cells from CX3CR1^{+gfp} mice were isolated and incubated together with brefeldin A (BFA) and monensin and the presence of intracellular TNF α and IL10 was assessed by flow cytometry. All F4/80⁺ CX3CR1⁺ populations

in P1 to P4 produced both TNF α and IL10 under baseline conditions, but there were marked differences in the pattern of cytokines produced by the different subsets. In particular, the proportion of cells producing IL10 alone increased progressively from the Ly6C^{high} monocyte stage (P1) to the CX3CR1^{high} m ϕ (P4) (Fig. 5.1). Conversely, the frequency of cells producing TNF α alone decreased significantly as the cells differentiated (Fig. 5.1). Surprisingly, cells producing both TNF α and IL10 were found in all populations, particularly after cells had left the Ly6C^{high}MHCII^{neg}CX3CR1^{int} (P1) stage. As a result, 72.4 \pm 2.9% of cytokine producing CX3CR1^{high} m ϕ were positive for IL10 either alone or together with TNF α , and only 27.6 \pm 3.0% produced TNF α alone. In contrast, 79.5 \pm 3.7% of the Ly6C^{high}MHCII^{neg}CX3CR1^{int} monocytes (P1) produced TNF α alone, or together with IL10, while only 20.6 \pm 3.7% produced IL10 alone (Fig. 5.1C).

To confirm the progressive switch towards IL10 production that occurred as colonic m ϕ differentiated from Ly6C^{high} monocytes, I next took advantage of IL10 reporter mice (VertX mice; (252)) to assess constitutive expression of IL10 without the need for any *in vitro* culture step. As CX3CR1 expression could not be examined in these mice, I had to use the alternative gating strategy detailed in Figure 4.4 to identify the individual m ϕ populations. This showed that Ly6C^{high} monocytes (P1) made little IL10, whereas the majority of F4/80⁺MHCII⁺ m ϕ produced IL10 constitutively (Fig. 5.2A and B). This production of IL10 was an unusual property of colonic m ϕ , as splenic, peritoneal and CSF-1 generated BM m ϕ all failed to produce IL10 constitutively (Fig. 5.2C). Similarly, CD11b⁺ CD11c⁺ F4/80^{neg} DC and eosinophils from the colon failed to produce IL10 (Fig. 5.2A and B).

To extend these findings, qRT-PCR was used to analyse mRNA expression by freshly isolated FACS-purified subsets from resting CX3CR1^{gfp/+} mice. This confirmed that IL10 mRNA levels increased progressively from Ly6C^{high} monocytes (P1) through P2 and P3 to CX3CR1^{high} m ϕ (Fig. 5.3A). Also consistent with the ICS data, the levels of mRNA for TNF α remained constant across the CX3CR1⁺ populations (Fig. 5.3B). In contrast, the level of mRNA for IL6 and iNOS was decreased in CX3CR1^{high} m ϕ compared with Ly6C^{high} colonic monocytes (Fig. 5.3C and D), supporting the idea of a switch from pro- to anti-inflammatory cytokine production.

Thus, the phenotypic maturation process of Ly6C^{high} monocytes to CX3CR1^{high} m ϕ in the steady state colon is associated with a transition from the predominant production of pro-inflammatory TNF α , IL6 and iNOS, to the constitutive production of IL10.

5.3 TLR Responsiveness of Intestinal CX3CR1⁺ Subsets

It is generally accepted that intestinal m ϕ are unresponsive to classical m ϕ stimuli such as TLR ligands (171). In contrast, blood monocytes are known to respond fully to stimulation by producing a wealth of pro-inflammatory mediators (171). Therefore if Ly6C^{high} monocyte differentiation occurs in the intestine, one would expect that as differentiation proceeds, the responsiveness to exogenous stimuli would alter. Thus I next set out to examine the responsiveness of the CX3CR1-defined populations to TLR stimulation.

For intestinal LP populations to respond to TLR stimulation they must possess the corresponding receptors. I therefore first examined the expression of TLR2, TLR4 and CD14 by P1-P4 using flow cytometry. As shown in Figure 5.4, TLR2 was uniformly expressed by all CX3CR1⁺ subsets (P1-P4), as was CD14. In contrast, TLR4 expression increased progressively from P1 to CX3CR1^{high} m ϕ in P4 (Fig. 5.4C). Expression of these pattern recognition receptors (PRR) was not a property of all CD11b⁺ cells in the colonic LP, as SiglecF⁺CX3CR1^{neg} eosinophils were negative for TLR2, TLR4 and CD14 (Fig. 5.4A-C). Similarly, the CD11b⁺ CD11c^{high}SSC^{low} DC population in the CX3CR1^{neg} fraction failed to express TLR4, although appeared to be heterogeneous for TLR2 and CD14 expression (Fig. 5.4A-C). I also attempted to examine the expression of intracellular TLR3 and TLR9 using commercially available monoclonal antibodies, but was unable to detect expression on any cell type tested including BM-derived and peritoneal m ϕ (not shown). Thus to examine the full range of TLR expression, the CX3CR1⁺ populations in P1 to P4 were FACS-purified and mRNA levels for TLR1-9 were analysed by qRT-PCR. This revealed that intestinal CX3CR1⁺ populations expressed most TLR at a similar level to, or greater than BMM used as a control population (Fig. 5.5). An exception to this was TLR2, which appeared to decrease between P1 and P4 (Fig. 5.5). The Ly6C⁺MHCII⁺CX3CR1^{int} cells within P2 also appeared to express lower levels of TLR1 and TLR3 than other populations, although the significance of this is unclear.

Thus having established that most cells in P1 to P4 express TLR, I next assessed TNF α and IL10 production by the CX3CR1⁺ subsets after stimulation with LPS or BLP, agonists for TLR4 and TLR2 respectively. Consistent with their close relationship to blood monocytes, Ly6C^{high}MHCII^{neg}CX3CR1^{int} (P1) and Ly6C⁺MHCII⁺CX3CR1^{int} (P2) cells amongst whole digests from the resting colon showed a robust response to LPS compared with their unstimulated counterparts (Fig. 5.6). This response was dominated by TNF α production and although a substantial proportion of stimulated P1 or P2 cells produced both IL10 and TNF α , virtually none produced IL10 alone (Fig. 5.6A-C). In contrast, the Ly6C^{neg}MHCII⁺CX3CR1^{int} (P3) cells showed little response to LPS stimulation above baseline, with no significant increase in the frequency of cells producing either cytokine compared with resting conditions. LPS stimulated CX3CR1^{high} m ϕ also showed a small but significant increase in the number of cells producing TNF α alone compared with baseline and there was a significant increase in the proportion of cells producing both IL10 and TNF α (Fig. 5.6A-C). LPS stimulation caused a significant reduction in the frequency of cells producing IL10 alone in all populations.

Stimulation with BLP did not induce such powerful changes in cytokine production, but it did show the same pattern of progressive reduction in responsiveness to exogenous stimulation as Ly6C^{high} monocytes differentiated into CX3CR1^{high} m ϕ (Fig. 5.7). In addition, whereas the Ly6C^{high}MHCII^{neg}CX3CR1^{int} cells in P1 again responded to BLP with a TNF α dominated response, the lesser response of CX3CR1^{high} m ϕ involved both TNF α and IL10 (Fig. 5.7A-C).

These results demonstrate that under normal physiological conditions, maturation of Ly6C^{high} monocytes into CX3CR1^{high} m ϕ is associated with a progressive loss of reactivity to exogenous stimuli such as TLR ligation.

5.4 Phagocytic Activity of CX3CR1⁺ LP Myeloid Cells

A crucial function of tissue m ϕ is their ability to maintain tissue homeostasis by scavenging apoptotic or senescent cells as well as clearance of microbial material or malignant cells. Phagocytosis is likely to be a particularly important function of intestinal m ϕ due to the close proximity of the microbiota, whose chance entry across the epithelial layer needs to be controlled. In addition, there

is extremely high turnover of epithelial cells in the gut. Therefore I next set out to examine the phagocytic ability of individual colonic LP CX3CR1⁺ cells.

To this end, whole colonic isolates were incubated with pHrodo *E. coli* bioparticles and their uptake assessed by flow cytometry. pHrodo *E. coli* bioparticles become highly fluorescent when in the acidic environment of the phagosome following internalisation, thereby allowing clear identification of actively phagocytic cells. As shown in Figure 5.8, Ly6C^{high}MHCII^{neg}CX3CR1^{int} cells (P1) and Ly6C⁺MHCII⁺CX3CR1^{int} cells (P2) were poor at phagocytosing the bioparticles, as there was little difference in fluorescence between cells incubated at 37°C and cells incubated at 4°C as a control. Although cells in P3 showed signs of some phagocytosis, CX3CR1^{high} mφ (P4) showed very high levels of phagocytosis as evidenced by the large shift in pHrodo fluorescence over control samples at 4°C (Fig. 5.8A and B). In contrast, CX3CR1^{int} CD11b⁺ DC (P5) and CD103⁺ DC from the colon appeared to lack any significant phagocytic activity (Fig. 5.8C).

These results demonstrate that as Ly6C^{high} monocytes mature into CX3CR1^{high} mφ, their phagocytic ability increases significantly (Fig. 5.8D).

5.5 Costimulatory Molecule Expression

It has been reported that human intestinal mφ express only low levels of costimulatory molecules (171) and therefore I next assessed the expression of the costimulatory molecules CD40, CD80 and CD86 by each of the CX3CR1-defined subsets in freshly isolated colonic isolates. This revealed that as Ly6C^{high} monocytes mature into CX3CR1^{high} mφ, the level of CD40 and CD80 expression is relatively constant, so that CX3CR1^{high} mφ expressed low levels of both these costimulatory molecules (Fig. 5.9A and B). In contrast, the level of CD86 increased progressively between P1 and P4, with the latter uniformly expressing CD86 (Fig. 5.9C). The significance of the differential expression of the individual costimulatory molecules is unclear.

5.6 Are Intestinal Macrophages 'Alternatively Activated'?

As described in Chapter 1, tissue mφ are highly specialised to perform specific functions dependent on their environment, probably dictated by local

cytokines/chemokines and cellular interactions. As I have shown, intestinal m ϕ are phenotypically and functionally distinct from other tissue m ϕ such as those found in the peritoneal cavity or spleen, in that they produce IL10 and do not respond in a 'classical' manner to pro-inflammatory stimuli despite the expression of class II MHC. To explore this further, I tested the hypothesis that they might represent a population of 'alternatively' activated (M2) m ϕ . M2 m ϕ are characterised by high IL10 production, the expression of CD206 (mannose receptor), the enzyme arginase-1 and vascular endothelial growth factor (VEGF), and are generally found in environments dominated by the T_H2 cytokines IL4 and IL13 (72). Therefore I assessed the expression of these markers in the CX3CR1⁺ subsets of colonic m ϕ . The expression of CD206 protein increased progressively as P1 monocytes differentiated into CX3CR1^{high} m ϕ (P4) and this was confirmed at the mRNA level in FACS-purified subsets using qRT-PCR (Fig. 5.10A and B). However, the levels of mRNA for arginase-1 and VEGF actually appeared to decrease between P1 and P4 (Fig. 5.10C and D). Thus none of the cells at any stage of the differentiation continuum meet the criteria of M2 m ϕ .

More recently the terms 'regulatory' or 'M2-like' have been applied to m ϕ found under conditions which favour immune suppression such as tumours, in the placenta or after Fc γ R cross-linking (62). In addition to the M2 markers IL10 and CD206, these regulatory m ϕ express the scavenger receptor CD163 and receptors for TGF β and IL10 (83). qRT-PCR analysis of sorted colonic m ϕ subsets revealed that the mRNA levels for CD163 and TGF β R2 expression increased progressively as Ly6C^{high} monocytes differentiate into CX3CR1^{high} m ϕ (Fig. 5.10E and F).

Collectively these data suggest that steady state intestinal m ϕ most closely resemble regulatory/M2-like m ϕ of the currently defined functional subsets.

5.7 Cytokine Production During Inflammation

As shown in Chapter 3, intestinal inflammation is associated with dramatic changes in the composition of the colonic LP myeloid cell compartment. There is a massive infiltration of the mucosa by Ly6C^{high}MHCII^{neg}CX3CR1^{int} (P1) and Ly6C⁺MHCII⁺CX3CR1^{int} cells (P2), the cells which I found in this chapter to produce high levels of TNF α and to be highly responsive to TLR stimulation under

resting conditions. In the next experiments, I examined the functions of the subsets I found in inflamed colon.

First I assessed the baseline cytokine production of the P1-P4 subsets in whole colonic digests obtained from CX3CR1^{+gfp} mice on day 4 of DSS-induced colitis. This revealed that a significantly greater proportion of the newly arrived Ly6C^{high} monocytes (P1) and their CX3CR1^{int} derivatives (P2 and P3) from colitic mice produced TNF α alone compared with the same populations in resting mice (Fig. 5.11). Similarly, there was a significant increase in the frequency of TNF α ⁺IL-10⁺ cells within P2 and P3 from colitic mice compared with the same populations in naïve mice. In contrast, the presence of inflammation did not lead to an increase in TNF α production by CX3CR1^{high} cells. Indeed inflammation caused a significant increase in the proportion of cells making IL10 alone within this population compared with resting conditions.

I next examined cells obtained from colitic animals for the production of TNF α and IL10 following TLR stimulation. This demonstrated that although LPS stimulation resulted in an increase in TNF α producing cells in most colitic populations when compared with unstimulated cells, the frequency of cells producing TNF α alone was highest amongst the Ly6C^{high} monocytes in P1 and decreased progressively as the cells matured into CX3CR1^{high} m ϕ (Fig. 5.12). LPS stimulation of colitic populations resulted in a significant increase in the abundance of TNF α ⁺IL-10⁺ cells within each population. However, whereas single producers of TNF α dominated the LPS-induced response by Ly6C^{high} monocytes, cells producing both TNF α and IL-10 dominated as cells progressed towards the CX3CR1^{high} compartment (Fig. 5.12). Again, stimulation with the TLR2 agonist BLP led to similar changes in the pattern of cytokine production, but consistent with the results I obtained from resting mice, the effects of BLP were less than those of LPS (Fig. 5.13).

Taken together these data demonstrate that during inflammation, CX3CR1^{int} cells (P1, P2 and P3) show increased pro-inflammatory cytokine production and P1 and P2 show robustly enhanced responses to TLR ligation. In contrast, the cytokine signature of CX3CR1^{high} m ϕ was unaltered by the presence of inflammation and the majority of cytokine producing cells in this subset

remained IL10⁺, although TLR stimulation caused some increase in the frequency of CX3CR1^{high} m ϕ producing TNF α and IL10.

5.8 Summary

In this chapter I investigated whether the functional properties of CX3CR1-defined LP populations were altered as Ly6C^{high} monocytes differentiated *in situ* into CX3CR1^{high} m ϕ . I was able to demonstrate that in steady state colon, there was a progressive switch in the baseline cytokine profile from the production of pro-inflammatory TNF α and IL6 by Ly6C^{high} colonic monocytes to high levels of constitutive IL10 production by CX3CR1^{high} m ϕ . In parallel, there was progressive hyporesponsiveness to TLR stimulation as cells moved from P1 to P4, together with the acquisition of regulatory m ϕ and phagocytic activity. During acute inflammation, the ability to produce increased amounts of TNF α was restricted to P1 and P2, the cells at the earliest stage of development and whose numbers increased the most in the local infiltrate. In contrast, the CX3CR1^{high} cells that remained did not acquire pro-inflammatory activity and retained their predilection to produce IL10. Thus intestinal m ϕ adapt to their environment under steady state conditions by losing the ability to respond in a classical pro-inflammatory manner, together with acquiring receptors that would assist in the uptake of microbes and becoming avidly phagocytic. Inflammation seems to involve the enhanced recruitment of pro-inflammatory monocytes rather than changes in the resident cells. I next investigated directly the contribution of pro-inflammatory Ly6C^{high} monocytes to intestinal pathology.

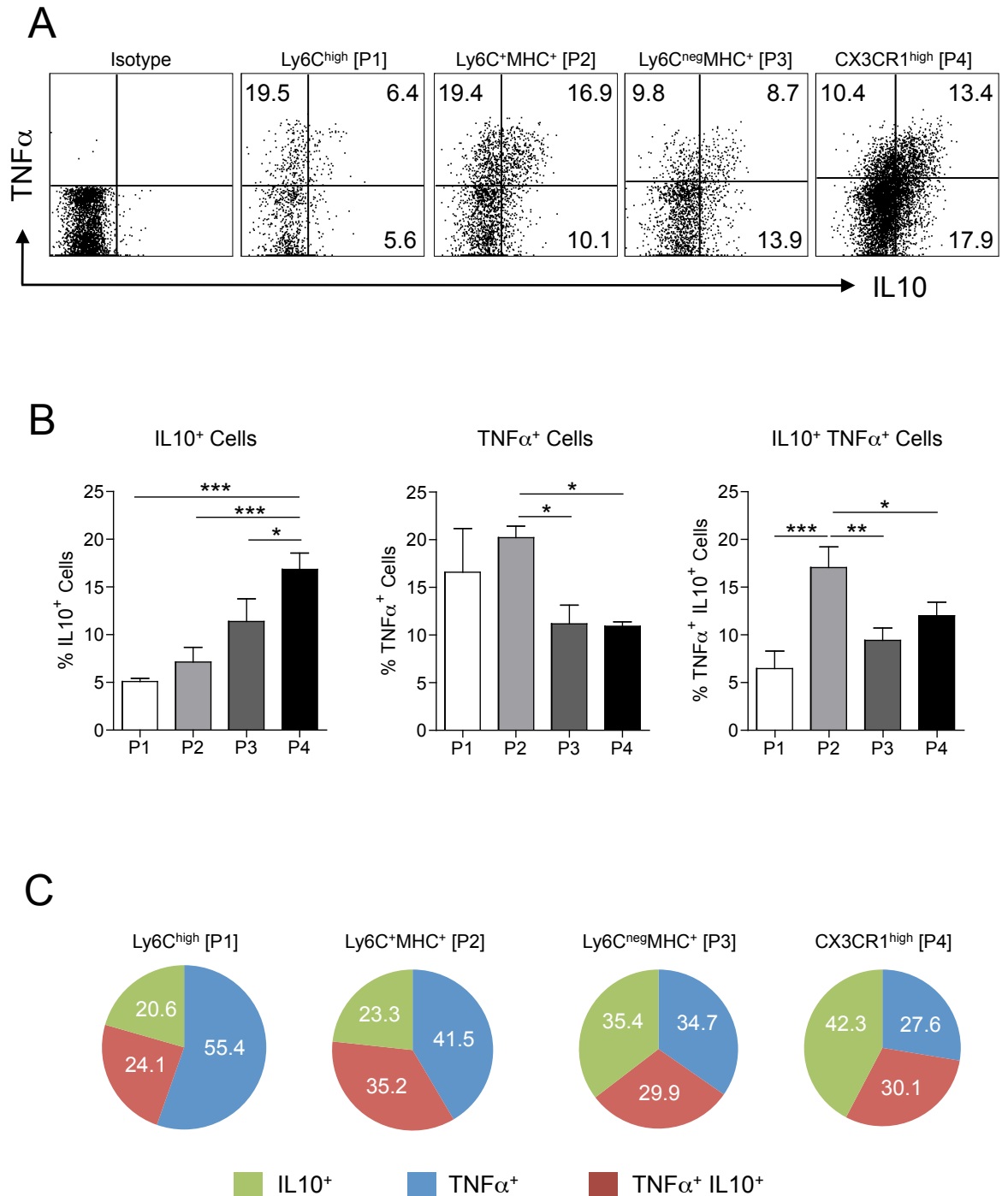


Figure 5.1: Cytokine Production by Colonic Macrophage Subsets in Steady State Colon

Whole digests of colonic LP cells were isolated from resting CX3CR1^{+gfp} mice and incubated with BFA and monensin in medium alone and analysed for the presence of intracellular TNF α and IL10 by flow cytometry after 4.5hrs. **A.** Representative TNF α and IL10 staining by each subset of m ϕ together with the isotype control. **B.** The mean percentage + 1SD of IL10⁺, TNF α ⁺ and IL10⁺TNF α ⁺ cells within P1, P2, P3 and P4. **C.** The frequency of IL10⁺, TNF α ⁺ and IL10⁺TNF α ⁺ cells within P1, P2, P3 and P4 as a proportion of the total cytokine producing cells. Results shown are the means + 1SD for 3-4 mice/group and are representative of 2 individual experiments. (* p<0.05, ** p<0.01, *** p<0.001. One-way ANOVA followed by Bonferroni's post-test)

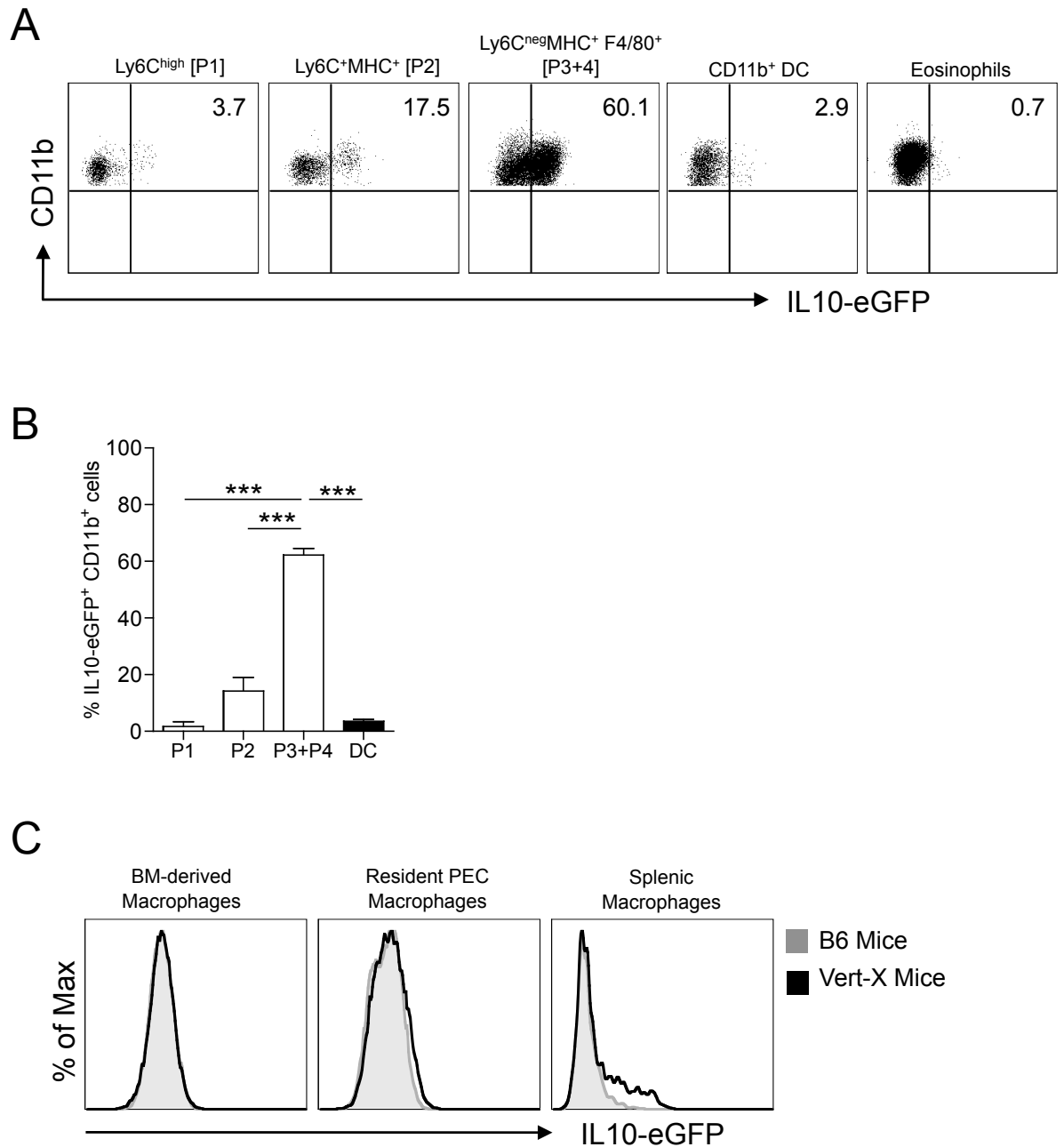


Figure 5.2: Constitutive Production of IL10 by Intestinal Myeloid Subsets

Colonic LP cells were isolated from resting VertX (IL10-eGFP) mice and individual populations were identified on the basis of CD11b, Ly6C, MHC II, F4/80 and CD11c as shown in Figure 4.4. **A**. Representative IL10-eGFP expression by Ly6C^{high}MHCII^{neg} monocytes (P1), Ly6C⁺MHCII⁺ cells (P2), Ly6C^{neg}MHCII⁺F4/80⁺ (P3+P4), Ly6C^{neg}MHCII⁺CD11c⁺F4/80^{neg} DC and eosinophils. **B**. The mean proportion of GFP⁺ cells within each LP population + 1SD. Results are representative of three individual experiments with 3-4 individual mice. **C**. Representative IL10-eGFP expression (*black line*) by CSF-1 generated BM macrophages (d7), resident peritoneal exudate cell (PEC; F4/80⁺MHCII^{neg}) macrophages and splenic (F4/80⁺CD11b^{low}MHCII^{int}) macrophages compared with the background fluorescence of same populations from WT mice. (* p<0.05, ** p<0.01, *** p<0.001. One-way ANOVA followed by Bonferroni's post-test)

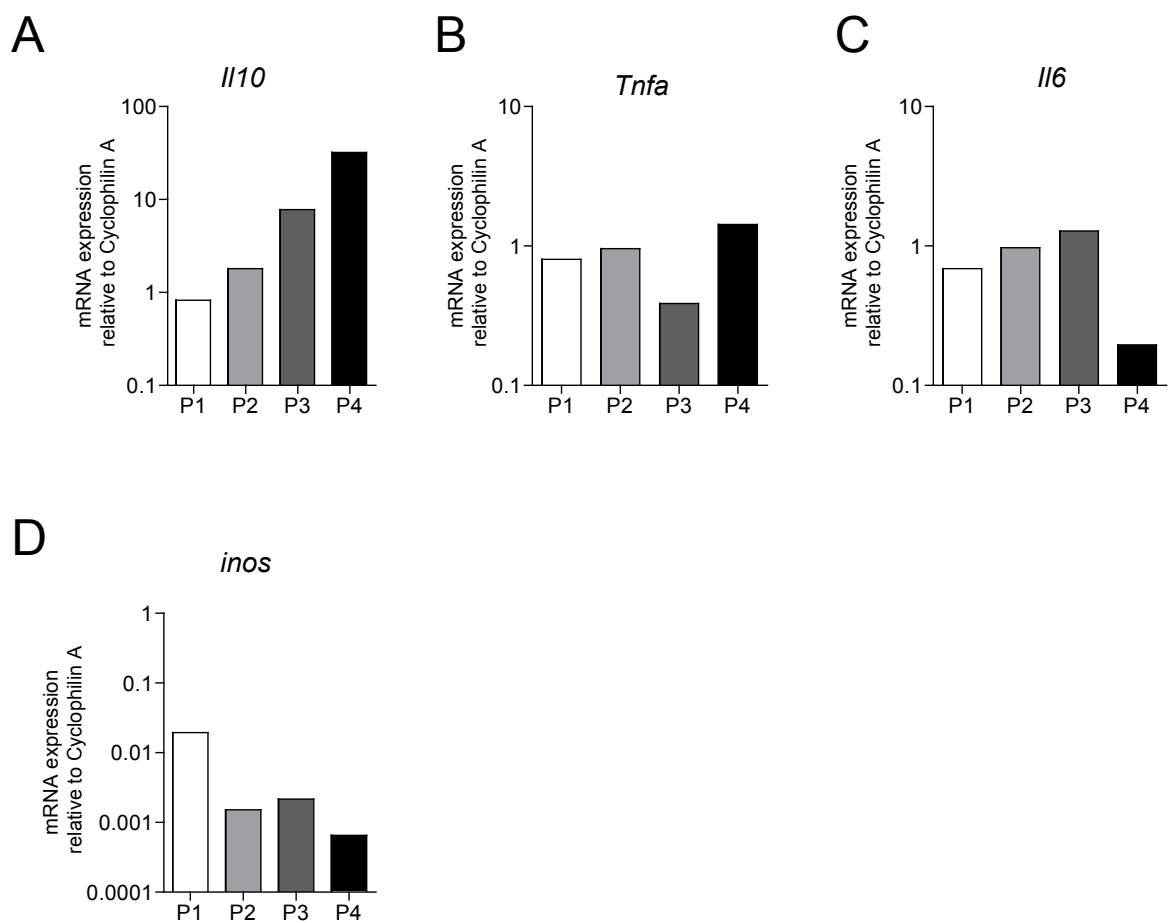


Figure 5.3: Quantitative Analysis of Cytokine mRNA expression by CX3CR1 Defined Subsets of Colonic Macrophages

P1-P4 subsets from the colonic LP were purified by FACS and mRNA isolated. Levels of mRNA for IL10 (A), TNF α (B), IL6 (C) and iNOS (D) were analysed by qRT-PCR. Results shown are mean expression relative to Cyclophilin A (CPA) using the $2^{-\Delta C(t)}$ method. The mean was obtained from two independent experiments using cells pooled from eleven/twelve mice. Primer sequences are detailed in Table 2.4.

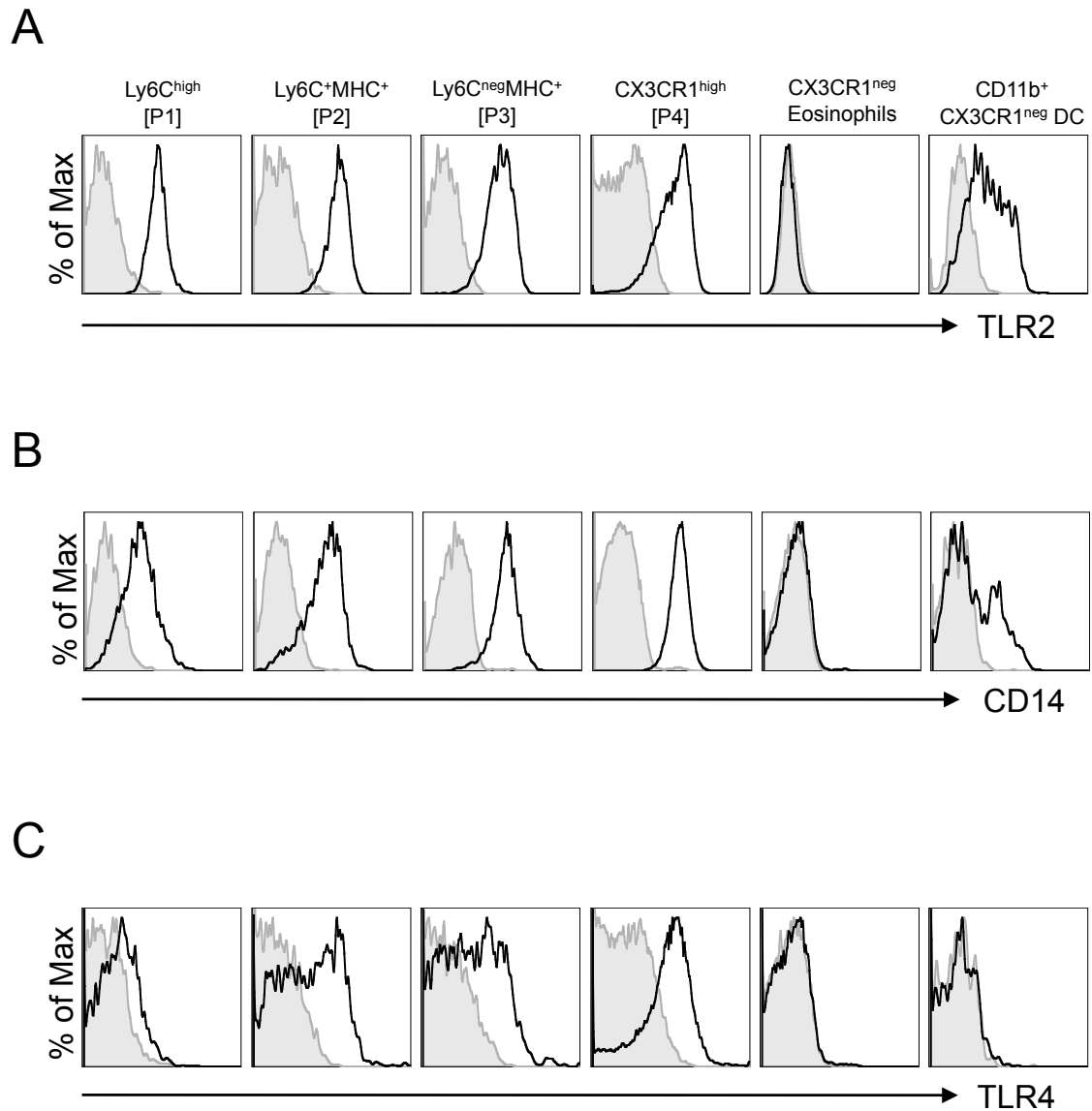


Figure 5.4: TLR expression by CX3CR1 Defined Subsets of Colonic Macrophages

Colonic LP cells were isolated from resting CX3CR1^{+gfp} mice and live-gated CD45⁺ CD11b⁺ CX3CR1⁺ subsets (P1-P4), CX3CR1^{neg}SSC^{high} intestinal eosinophils and CX3CR1^{neg}CD11b⁺ SSC^{low}CD11c⁺ DC were examined for the expression of TLR2 (**A**), CD14 (**B**) and TLR4 (**C**) by flow cytometry. Shaded histograms represent staining with the appropriate isotype controls. Results representative of 3 individual experiments.

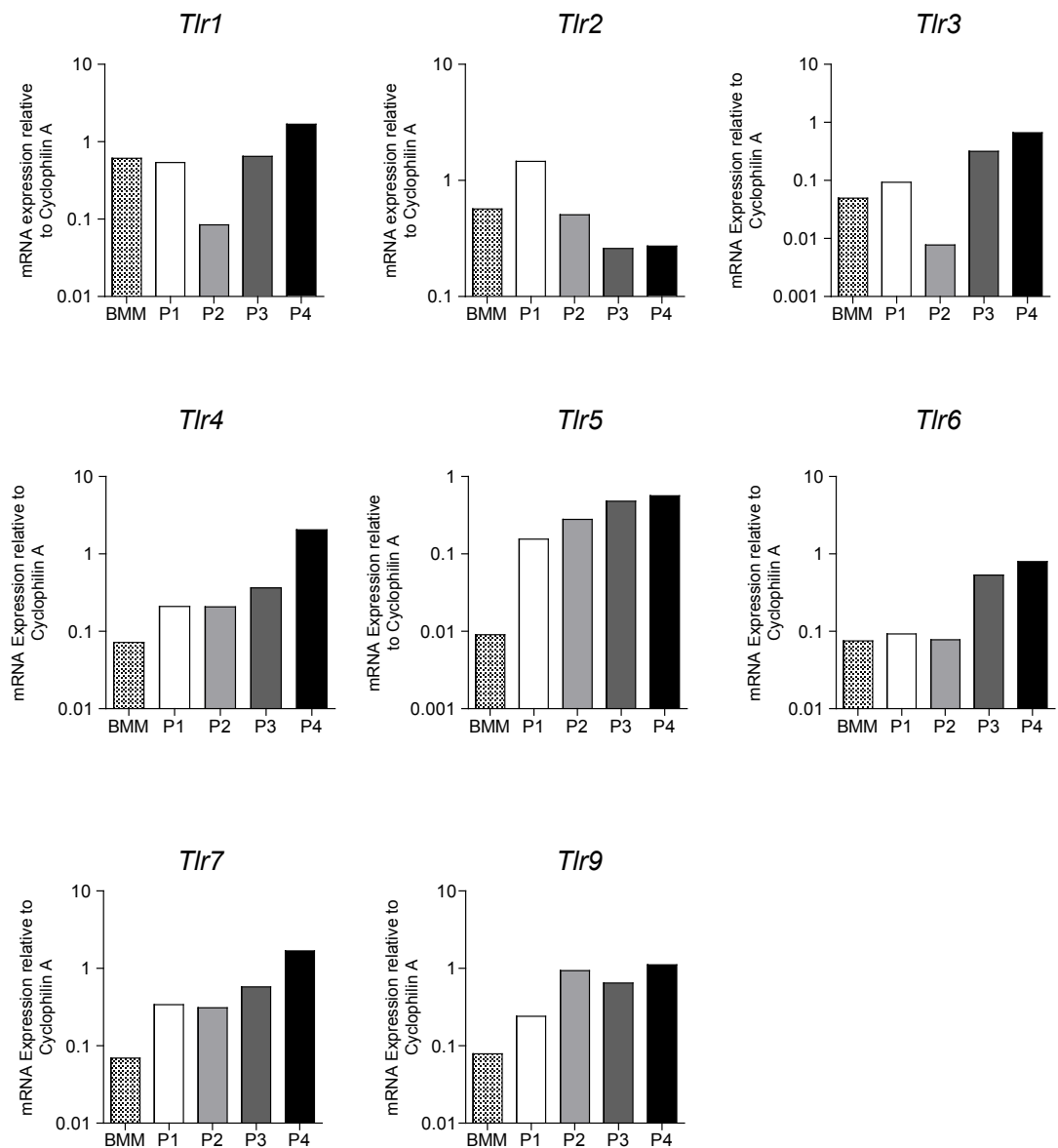


Figure 5.5: TLR expression by Purified CX3CR1 Defined Subsets of Colonic Macrophages

Colonic LP cells were isolated from resting CX3CR1^{+gfp} mice and live-gated CD45⁺ CD11b⁺ CX3CR1⁺ subsets (P1-P4) were FACS-sorted and mRNA isolated. Results show the expression of TLR1-9 mRNA by each CX3CR1⁺ population compared with M-CSF generated BM-derived macrophages (BMM) as analysed by qRT-PCR analysis. Results shown are mean expression relative to Cyclophilin A (CPA) using the $2^{-\Delta C(t)}$ method. The mean was obtained from two independent experiments using cells pooled from eleven/twelve mice. Primer sequences are detailed in Table 2.4.

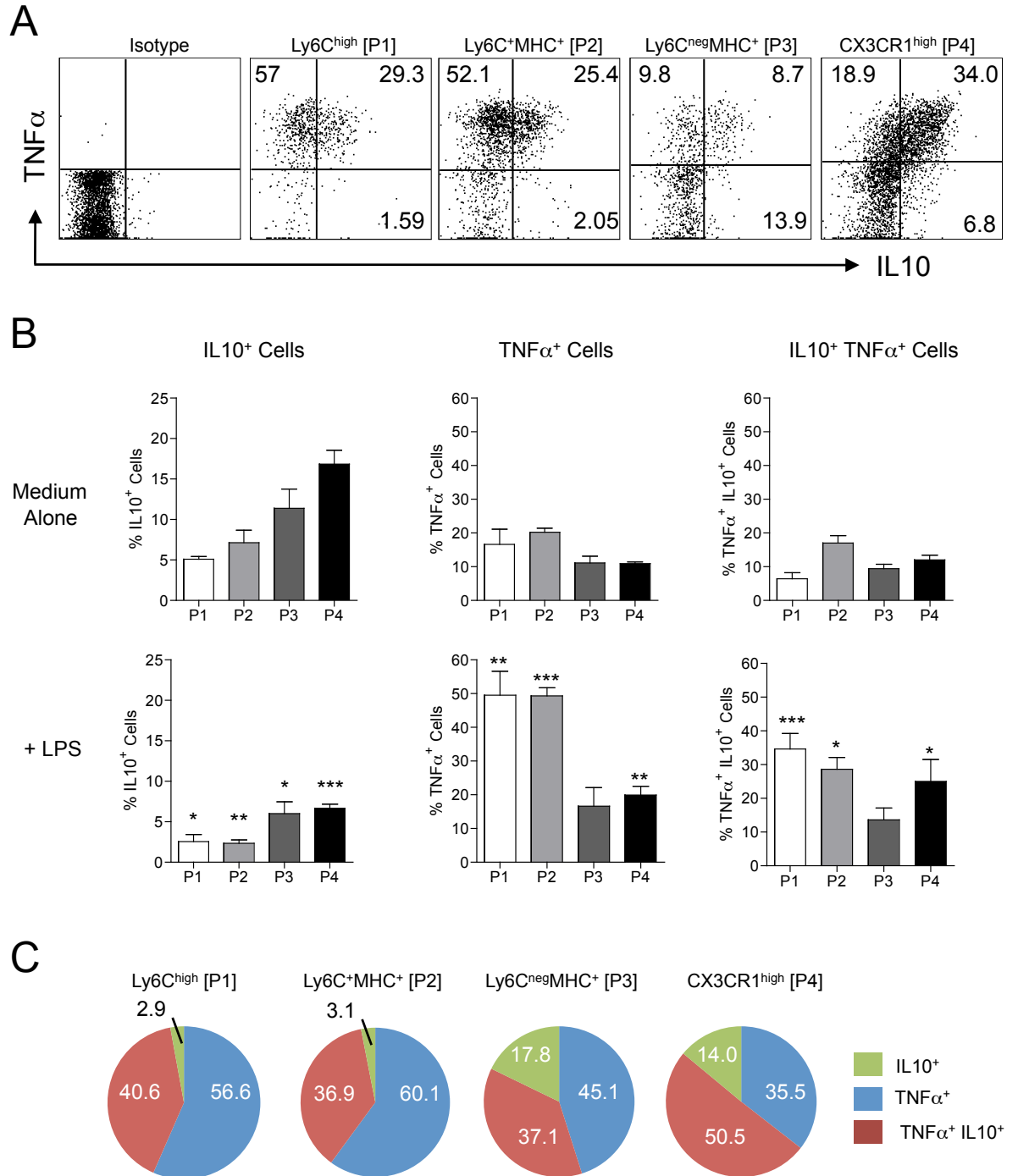


Figure 5.6: Cytokine Production by Colonic Macrophage Subsets in Response to TLR4 Stimulation

Whole digests of colonic LP cells were isolated from resting CX3CR1^{+/gfp} mice and incubated with BFA and monensin together with 1 μ g/ml LPS and analysed for the presence of intracellular TNF α and IL10 by flow cytometry after 4.5hrs. **A**. Representative TNF α and IL10 staining by each subset of m ϕ together with the isotype control. **B**. The mean percentage + 1 SD of IL10⁺, TNF α ⁺ and IL10⁺TNF α ⁺ cells within P1-P4 after culture in medium alone (from Figure 5.1) or together with LPS. **C**. The frequency of IL10⁺, TNF α ⁺ and IL10⁺TNF α ⁺ cells within P1-P4 as a proportion of the total cytokine producing cells. Data are representative of 2 individual experiments with 3 or 4 mice. (* p<0.05, ** p<0.01, *** p<0.001 vs. responses in medium alone using a one-way ANOVA followed by Bonferroni's post-test)

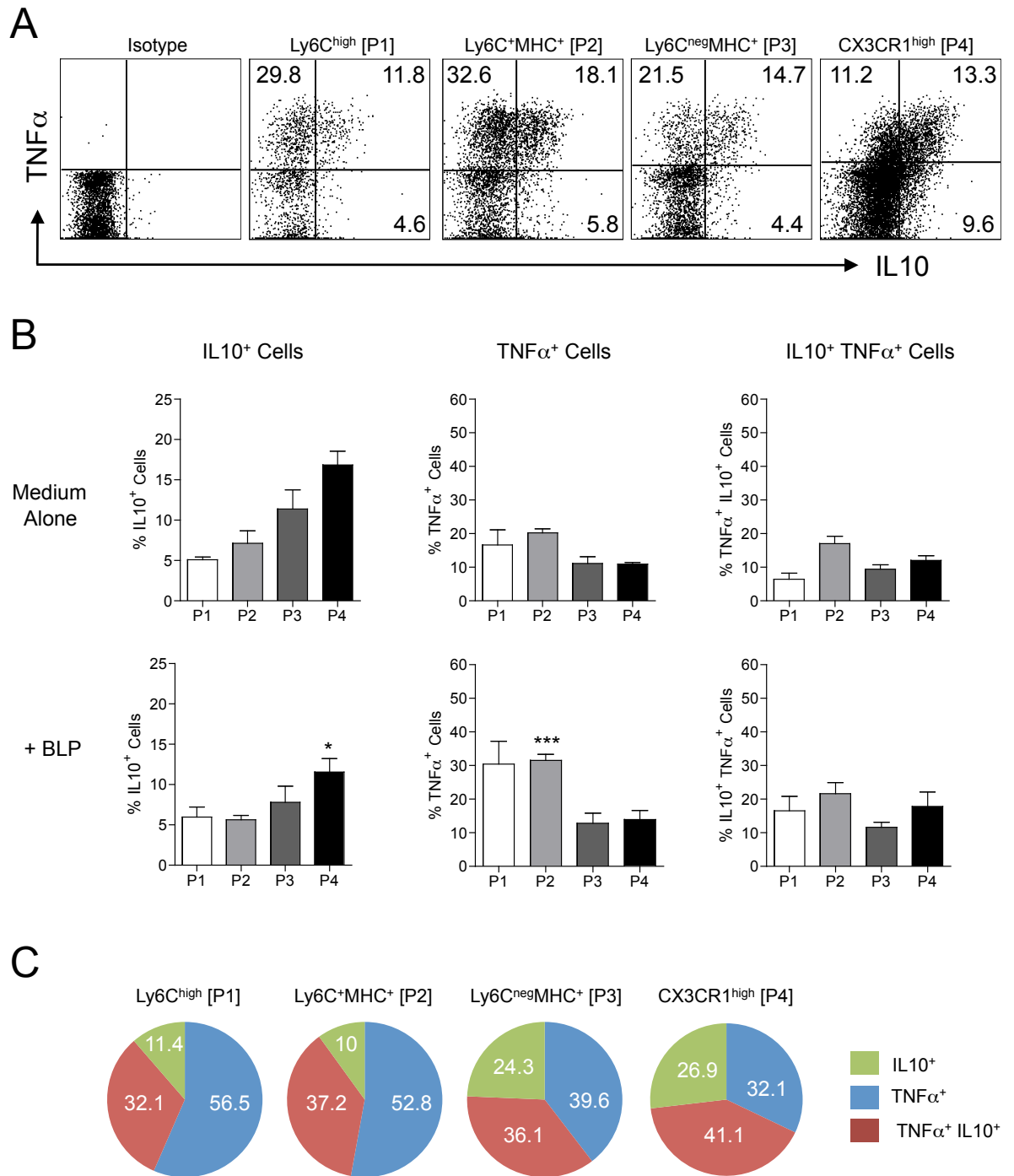


Figure 5.7: Cytokine Production by Colonic Macrophage Subsets in Response to TLR2 Stimulation

Whole digests of colonic LP cells were isolated from resting CX3CR1^{+/gfp} mice and incubated with BFA and monensin together with 1 μ g/ml BLP and analysed for the presence of intracellular TNF α and IL10 by flow cytometry after 4.5hrs. **A.** Representative TNF α and IL10 staining by each subset of m ϕ together with the isotype control. **B.** The mean percentage + 1 SD of IL10⁺, TNF α ⁺ and IL10⁺TNF α ⁺ cells within P1-P4 after culture in medium alone (from Figure 5.1) or together with BLP. **C.** The frequency of IL10⁺, TNF α ⁺ and IL10⁺TNF α ⁺ cells within P1-P4 as a proportion of the total cytokine producing cells. Data are representative of 2 individual experiments with 3 or 4 mice. (* p<0.05, ** p<0.01, *** p<0.001 vs. responses in medium alone using a one-way ANOVA followed by Bonferroni's post-test)

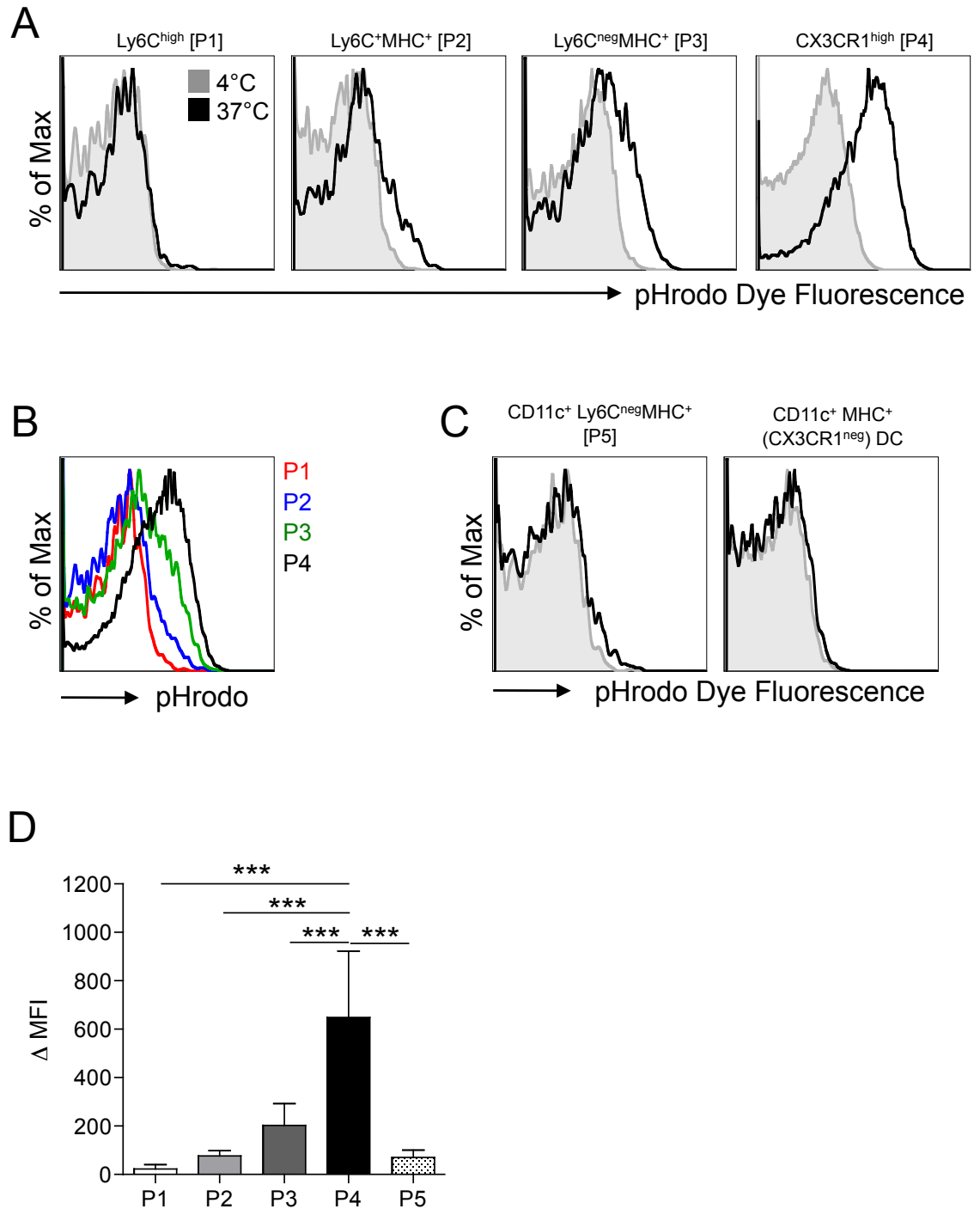


Figure 5.8: Phagocytic Activity of CX3CR1 Defined Subsets of Colonic Macrophages

Whole digests of colonic LP cells were isolated from resting CX3CR1^{+gfp} mice and incubated with pHrodo *E. coli* bioparticles for 15 mins at 37°C (*black line*) or at 4°C as a control (*shaded histogram*). **A**. Representative pHrodo dye fluorescence of CX3CR1 defined P1 to P4 subsets. **B**. pHrodo dye fluorescence of P1 to P4 shown as a composite histogram. **C**. Representative pHrodo dye fluorescence of CD11b⁺F4/80^{neg}CD11c⁺CX3CR1^{int} DC (P5) and CD103⁺ DC. **D**. Δ MFI (MFI at 37°C-MFI at 4°C control) + 1 SD for P1-P4. Data are representative of 2 individual experiments with 4-5 mice. (*p<0.05, **p<0.01, ***p<0.001. One-way ANOVA followed by Bonferroni's post-test)

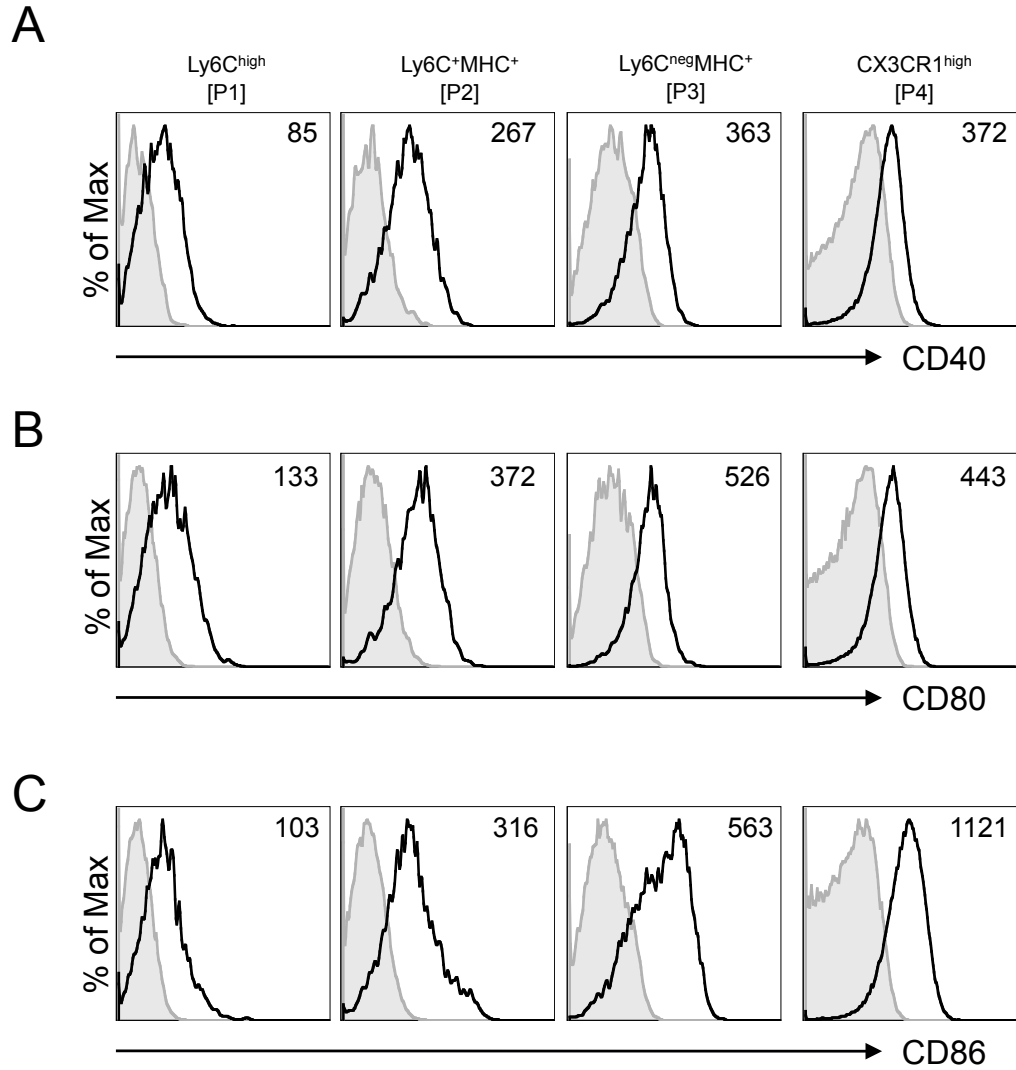


Figure 5.9: Expression of Costimulatory Molecules by CX3CR1 Defined Subsets of Colonic Macrophages

Colonic LP cells were isolated from resting CX3CR1^{+/-gfp} mice and live-gated CD45⁺CD11b⁺ CX3CR1⁺ subsets (P1-P4) were examined for the expression of CD40 (**A**), CD80 (**B**) and CD86 (**C**) by flow cytometry. Shaded histograms represent staining with the appropriate isotype controls. Numbers represent Δ MFI (MFI-MFI of isotype). Results representative of 3 individual experiments.

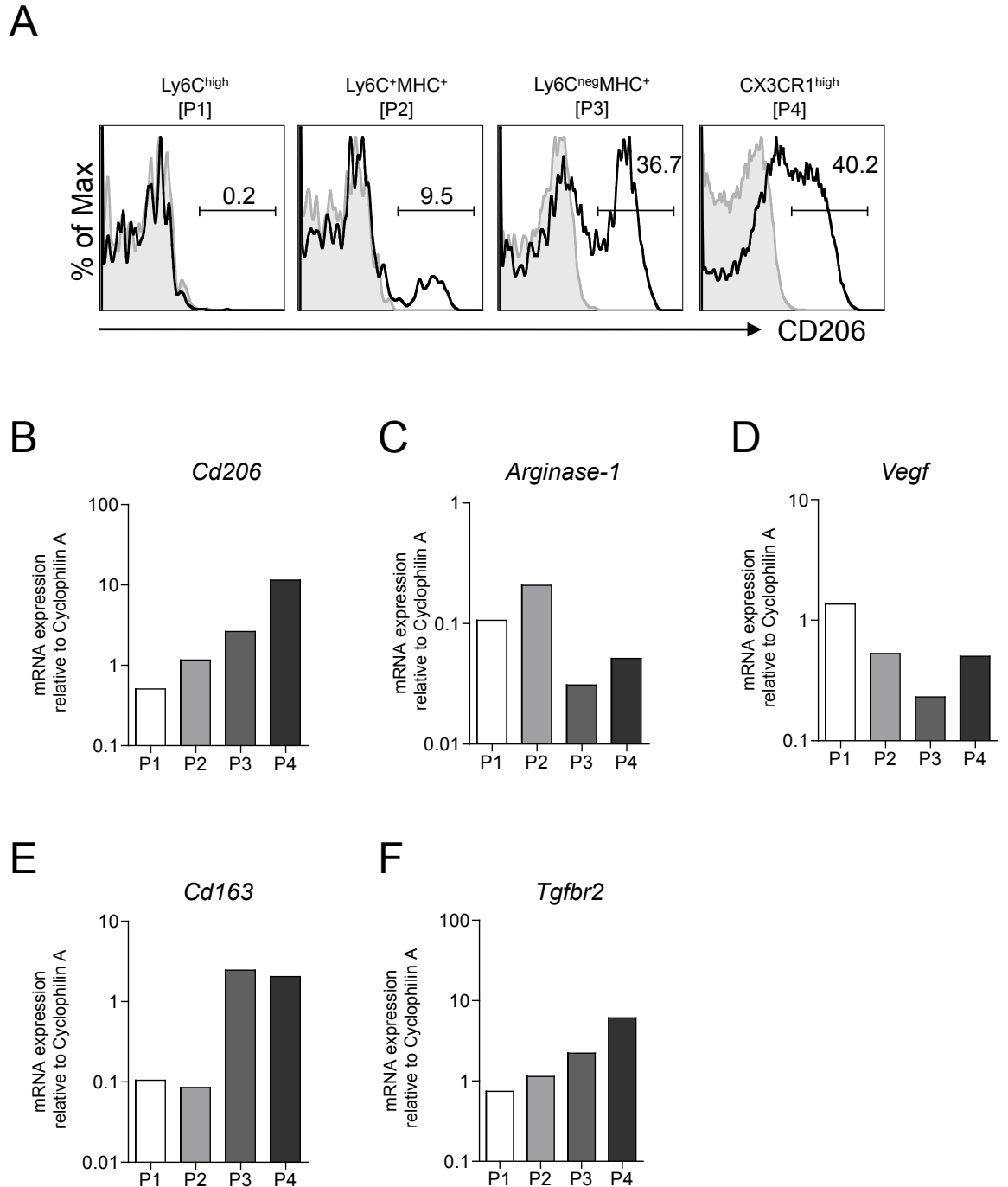


Figure 5.10: Expression of Alternatively Activated Macrophage Markers by CX3CR1 Defined Subsets of Colonic Macrophages

A. Colonic LP cells were isolated from resting CX3CR1^{+gfp} mice and live-gated CD45⁺CD11b⁺ CX3CR1^{int} and CX3CR1^{high} cells were examined for the expression of CD206 (mannose receptor) by flow cytometry. Populations 1 to 4 were FACS-purified and the level of mRNA for CD206 (**B**), arginase-1 (**C**), VEGF (**D**), CD163 (**E**) and TGFβ2 (**F**) was assessed by qRT-PCR analysis. Results shown are mean expression relative to cyclophilin A (CPA) using the $2^{-\Delta C(t)}$ method. The mean was obtained from two independent experiments using cells pooled from eleven/twelve mice. Primer sequences are detailed in Table 2.4

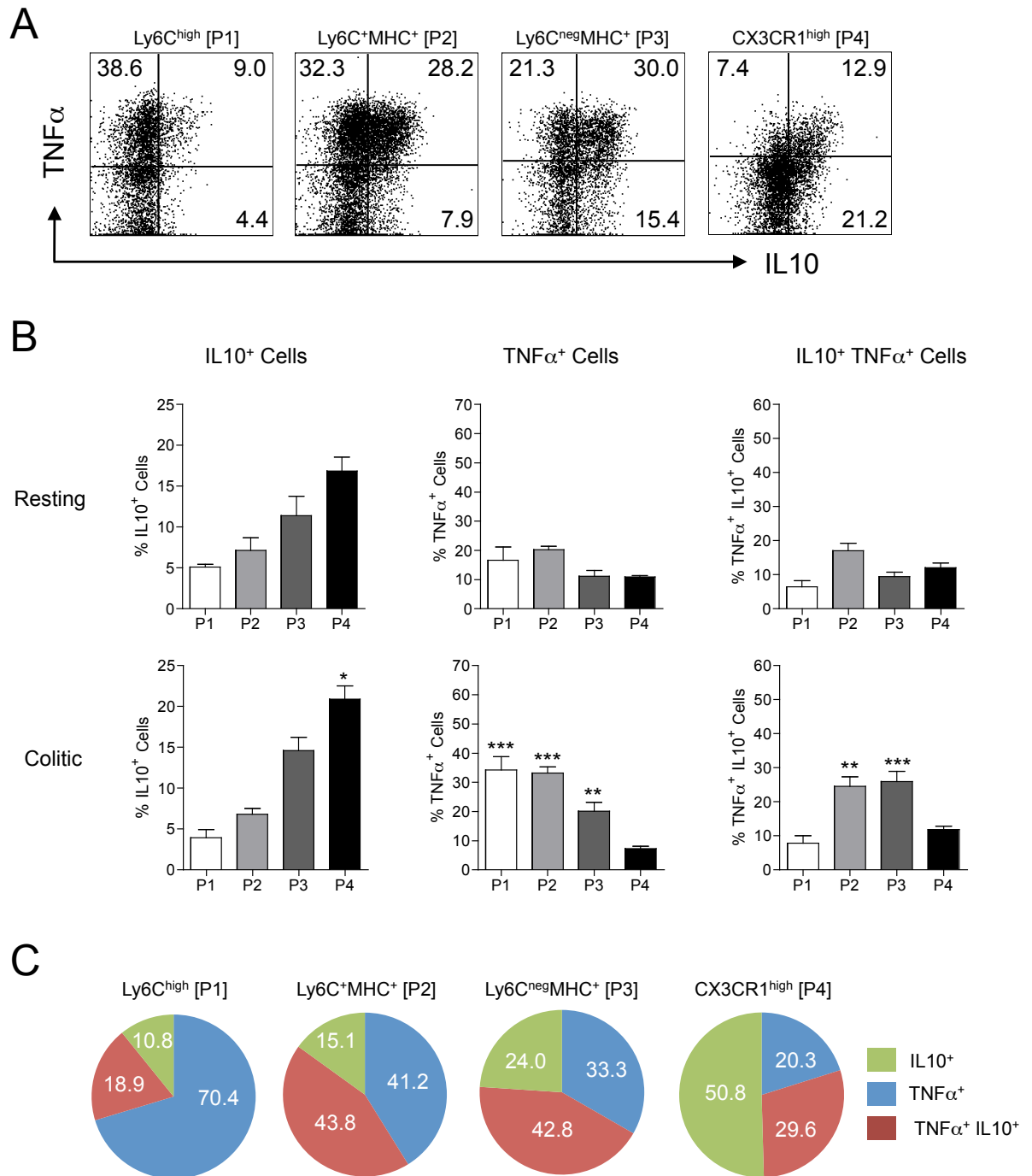


Figure 5.11: Cytokine Production by Colonic Macrophage Subsets During Inflammation

Whole digests of colonic LP cells were isolated from d4 colitic CX3CR1^{+/gfp} mice and incubated with BFA and monensin in medium alone and analysed for the presence of intracellular TNF α and IL10 by flow cytometry after 4.5hrs. **A**. Representative TNF α and IL10 staining by each subset of m ϕ together with the isotype control. **B**. The mean percentage + 1 SD of IL10⁺, TNF α ⁺ and IL10⁺TNF α ⁺ cells within P1-P4 from resting mice (*upper panel*; from Figure 5.1) or from colitic mice (*lower panel*). **C**. The frequency of IL10⁺, TNF α ⁺ and IL10⁺TNF α ⁺ cells within P1-P4 as a proportion of the total cytokine producing cells. Data are representative of 2 individual experiments with 3 or 4 mice. (* p<0.05, ** p<0.01, *** p<0.001 vs. responses by same populations from resting mice using a one-way ANOVA followed by Bonferroni's post-test)

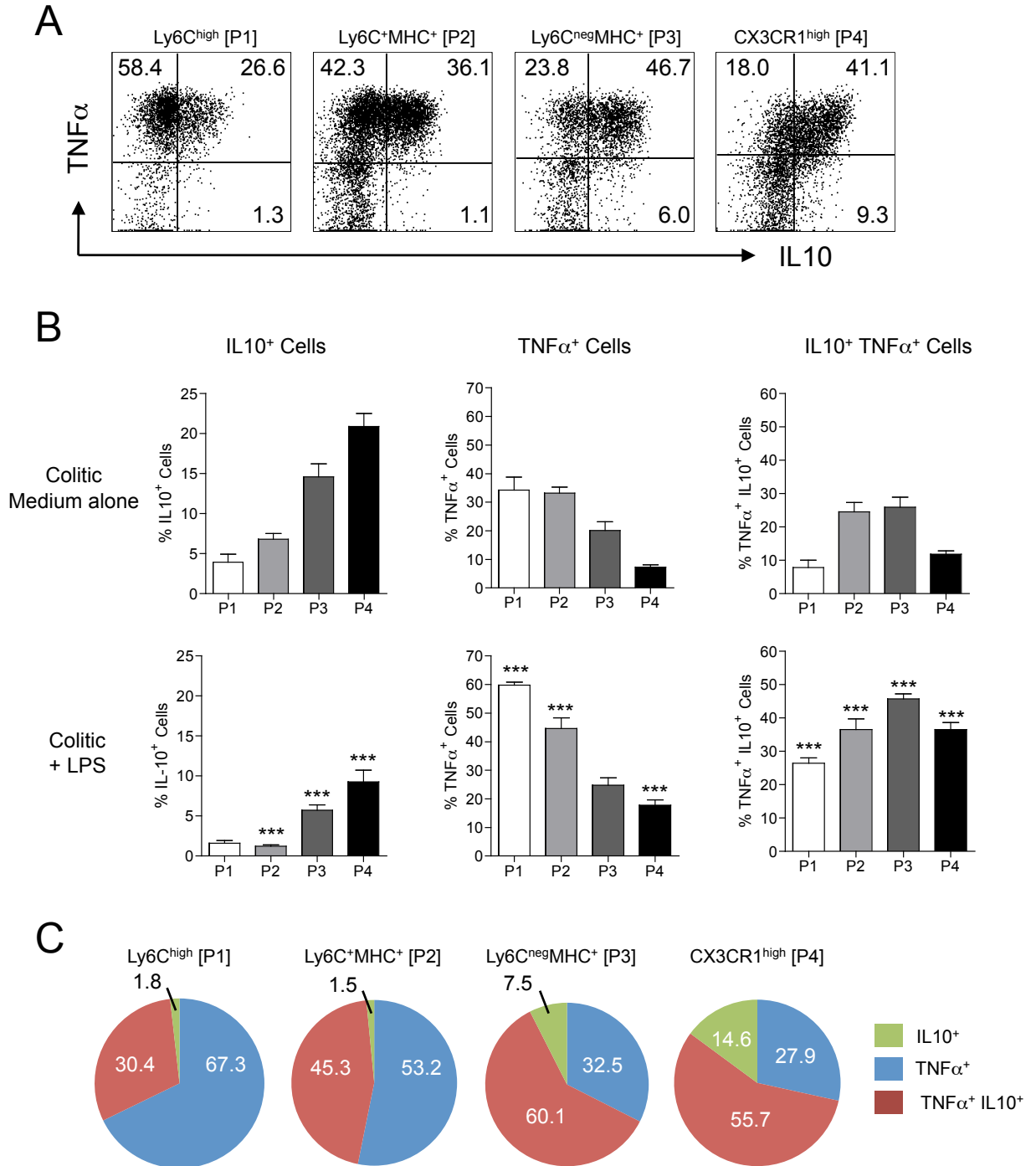


Figure 5.12: Cytokine Production by Colonic Macrophage Subsets in Response to TLR4 Stimulation During Inflammation

Whole digests of colonic LP cells were isolated from d4 colitic CX3CR1^{+/gfp} mice and incubated with BFA and monensin together with 1 μ g/ml LPS and analysed for the presence of intracellular TNF α and IL10 by flow cytometry after 4.5hrs. **A**. Representative TNF α and IL10 staining by each subset of m ϕ together with the isotype control. **B**. The mean percentage + 1 SD of IL10⁺, TNF α ⁺ and IL10⁺TNF α ⁺ cells within P1-P4 after culture in medium alone (*upper panel*; from Figure 5.11) or together with LPS (*lower panel*). **C**. The frequency of IL10⁺, TNF α ⁺ and IL10⁺TNF α ⁺ cells within P1-P4 as a proportion of the total cytokine producing cells. Data are representative of 2 individual experiments with 3 or 4 mice. (* p<0.05, ** p<0.01, *** p<0.001 vs. responses in medium alone using a one-way ANOVA followed by Bonferroni's post-test)

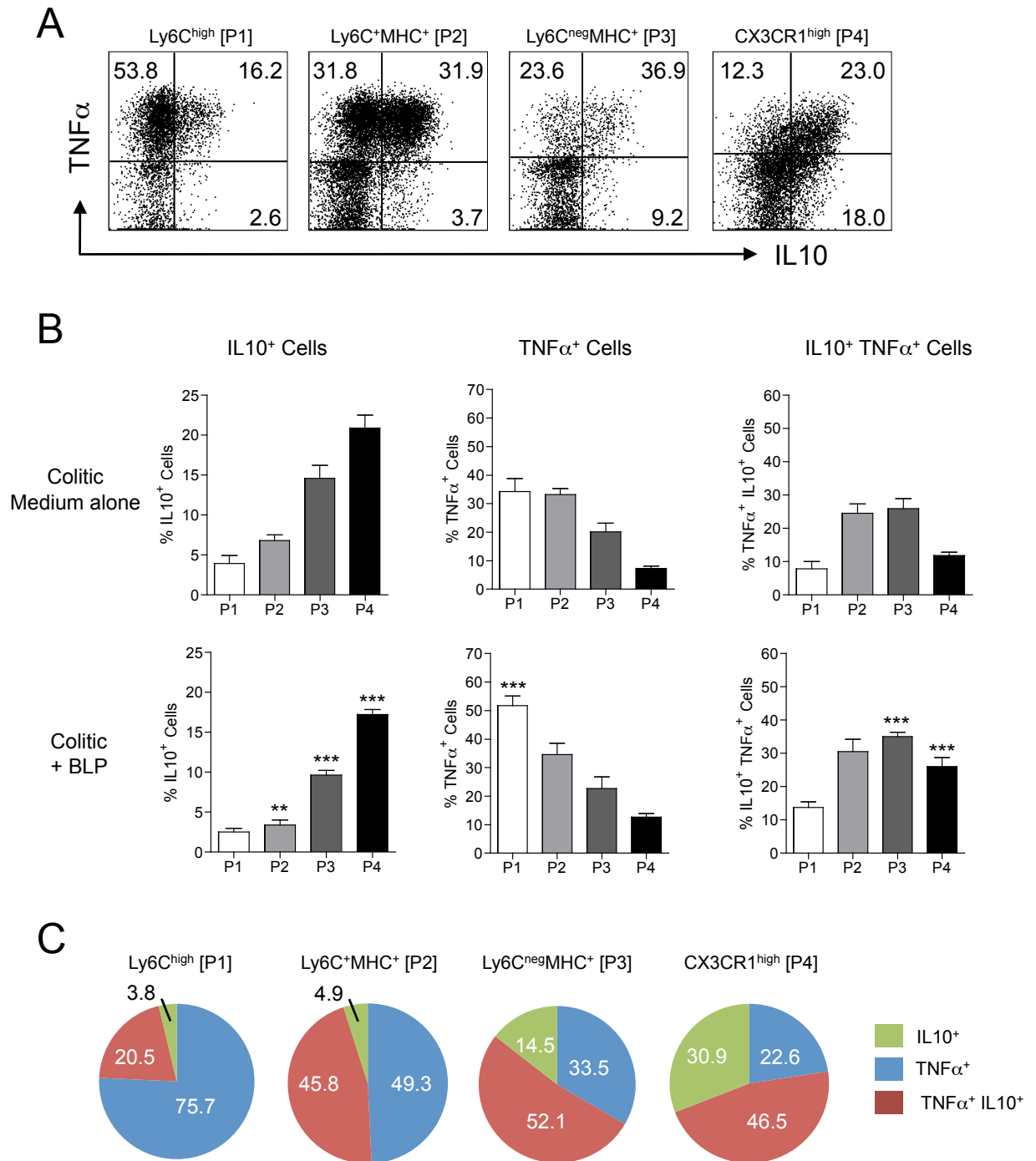


Figure 5.13: Cytokine Production by Colonic Macrophage Subsets in Response to TLR2 Stimulation During Inflammation

Whole digests of colonic LP cells were isolated from d4 colitic CX3CR1^{+/gfp} mice and incubated with BFA and monensin together with 1 μ g/ml BLP and analysed for the presence of intracellular TNF α and IL10 by flow cytometry after 4.5hrs. **A**. Representative TNF α and IL10 staining by each subset of m ϕ together with the isotype control. **B**. The mean percentage + 1 SD of IL10⁺, TNF α^+ and IL10⁺TNF α^+ cells within P1-P4 after culture in medium alone (*upper panel*; from Figure 5.11) or together with BLP (*lower panel*). **C**. The frequency of IL10⁺, TNF α^+ and IL10⁺TNF α^+ cells within P1-P4 as a proportion of the total cytokine producing cells. Data are representative of 2 individual experiments with 3 or 4 mice. (* p<0.05, ** p<0.01, *** p<0.001 vs. responses in medium alone using a one-way ANOVA followed by Bonferroni's post-test)

Chapter 6
The Contribution of Ly6C^{high} Monocytes to
Colonic Inflammation

6.1 Introduction

In the previous chapters, I demonstrated that under physiological conditions Ly6C^{high} monocytes are recruited continuously to the intestinal mucosa. Here they appear to differentiate into long-lived CX3CR1^{high} m ϕ that are avidly phagocytic and adept at producing IL10, but do not respond in a pro-inflammatory manner to TLR stimulation. My results in Chapter 3 demonstrated that in DSS colitis there was an accumulation of the P1 and P2 subsets of pro-inflammatory CX3CR1^{int} cells and a parallel loss of CX3CR1^{high} m ϕ . As these results suggest that the normal local differentiation process might be arrested in inflammation, the experiments in this chapter were designed to gain further insight into how the differentiation and recruitment of Ly6C^{high} monocytes are regulated during inflammation. First I determined the fate of Ly6C^{high} monocytes that had been transferred into mice with DSS colitis and then I explored the role of the CCR2 chemokine receptor that is expressed on these monocytes in m ϕ recruitment and pathology in colitis. Finally, I assessed the fate of recruited cells during the resolution of colitis to examine whether Ly6C^{high} monocytes recruited during inflammation could differentiate into CX3CR1^{high} m ϕ once the inflammatory stimulus had been removed.

6.2 Monocyte Differentiation During Inflammation

First, I adoptively transferred purified Ly6C^{high} BM monocytes from CX3CR1^{+gfp} CD45.1⁺/CD45.2⁺ mice into CD45.1⁺ B6 mice on d3 of DSS colitis (Fig. 6.1A) and assessed the phenotype of donor cells in the LP after 24hrs and 96hrs. To ensure that recipient mice survived until this later time point, mice were taken off DSS on d5 and were returned to normal drinking water for the remainder of the study. Consistent with the adoptive transfer studies in steady state mice, donor cells could be found in the LP within 24hrs after transfer (Fig. 6.1B) and over 75% had acquired class II MHC at this time, therefore moving into the population I had defined as P2 (Ly6C⁺MHCII⁺CX3CR1^{int}) (Fig. 6.1C). Very few donor cells could be detected 96hrs after transfer, but the majority of these had lost Ly6C expression and acquired class II MHC (Fig. 6.1C). However, in contrast to my studies on steady state colon, donor cells in inflamed mucosa did not upregulate CX3CR1 and move into P4 (CX3CR1^{high}). Indeed 95% of donor cells remained in P3 (Ly6C^{neg}MHCII⁺CX3CR1^{int}) (Fig. 6.1). As in my studies of steady state mice, it is unlikely that the donor cells found in the inflamed colonic LP at 96hrs are blood

contaminants, because donor cells in the bloodstream all lacked class II MHC expression (Fig. 6.2).

These results support the idea that disruption of tissue homeostasis in inflammation causes a blockade in the normal differentiation pattern of Ly6C^{high} monocytes in the colon, which goes some way to explaining the accumulation of CX3CR1^{int} cells under these conditions.

6.3 The Role of Ly6C^{high} Monocytes during Inflammation

These experiments indicate that Ly6C^{high} monocytes can give rise to both 'resident' and pro-inflammatory m ϕ in the intestine, with their fate depending on the context into which they are recruited. During inflammation Ly6C^{high} monocytes and their immediate descendants accumulate in the gut, retain their responsiveness to TLR stimulation and produce pro-inflammatory cytokines such as TNF α . To examine whether this recruitment of Ly6C^{high} monocytes contributes to the pathology of DSS colitis, I took advantage of CCR2-deficient mice which lack these cells in their bloodstream.

WT and CCR2-deficient mice received 2% DSS for 6 days, during which time their bodyweight and total clinical score were measured. This revealed a striking difference in the disease progression between CCR2 KO mice and their WT counterparts. As expected, WT mice lost weight progressively from day 4 and this was accompanied by increasing disease severity (Fig. 6.3A and B). In contrast, CCR2-deficient mice failed to lose weight even after 6 days of DSS administration. Consistently, CCR2 KO mice also had significantly lower clinical scores over the course of the study (Fig. 6.3B) and the extent of colon shortening was significantly less in CCR2-deficient mice (Fig. 6.3C). Furthermore, histological analysis of H&E stained sections of colitic WT and KO colon demonstrated that the disrupted architecture, epithelial damage and massive inflammatory leucocyte infiltration seen in WT mice was virtually absent in CCR2 KO mice (Fig. 6.3D). This was not due to differences in DSS consumption, as water intake was similar in the two groups (Fig. 6.3E).

Thus the absence of CCR2 protects mice from DSS-induced colitis. However many cell types have however been reported to express CCR2, including

monocytes, eosinophils and neutrophils as well as other non-myeloid cells such as T cells. Therefore I thought it important to assess which CCR2⁺ cells might explain the phenotype of CCR2 KO mice, concentrating on innate immune cells, which are the main drivers of DSS-induced colitis. Therefore I examined the intestinal myeloid cell compartment of WT and CCR2-deficient mice four days after feeding DSS using the alternative gating strategies I described in Chapter 4 for analysing non-CX3CR1-GFP mice.

As before, DSS administration led to a significant increase in CD11b⁺ cells in the LP of WT mice (Fig. 6.4), which involved Ly6G⁺ neutrophils, SiglecF⁺ eosinophils and monocytes/m ϕ . CCR2 KO mice showed significantly less recruitment of total CD11b⁺ cells than WT mice with colitis, as well as significantly lower numbers of neutrophils and eosinophils (Fig. 6.5 and 6.6). However these cells made up higher proportions of the infiltrate in CCR2 KO mice than in WT mice (Fig. 6.5 and 6.6). Indeed the numbers of eosinophils and neutrophils in the inflamed CCR2 KO colon were higher than those I found in an independent experiment on resting CCR2 KO mice. This recruitment of eosinophils and neutrophils to the CCR2 KO colon was consistent with the fact that I could not detect CCR2 expression by these cell types in blood (Fig. 6.5 and 6.6).

In stark contrast, the expansion of CD11b⁺SiglecF^{neg}Ly6G^{neg}Ly6C^{high}MHCII^{neg} monocytes (P1), which was marked in WT mice, was almost absent in CCR2-deficient mice, with a 24-fold reduction compared with WT mice (Fig. 6.7A-C). CCR2 KO mice also had significantly lower proportions and absolute numbers of Ly6C⁺MHCII⁺ cells (P2) compared with their WT counterparts (Fig. 6.7D and E). It must be noted that there were small but significant increases in cells in P1 and P2 in inflamed CCR2 KO colon compared with the numbers of these populations found in an independent experiment on resting CCR2 KO mice. During colitis, the LP of WT mice also contained significantly more F4/80⁺MHCII⁺ m ϕ than CCR2 KO (Fig. 6.8A and B), although both WT and CCR2 KO mice had greater numbers of F4/80⁺MHCII⁺ m ϕ during colitis compared with steady state numbers. In contrast, there was little difference in the numbers of CD11b⁺ DC during DSS colitis in the 'inflamed' CCR2 KO colon compared with resting intestine. Although resting CCR2 KO colon contained significantly fewer CD11b⁺ DC than WT colon, this difference was not seen during DSS colitis (Fig. 6.8C).

Thus the reduced susceptibility of CCR2-deficient mice to chemically induced colitis correlated with a selective lack of accumulation of Ly6C^{high} monocytes and their immediate progeny in the mucosa, supporting the idea that Ly6C^{high} monocytes are the mediators of inflammation.

Competitive co-transfer experiments that I carried out at the beginning of my project established that CCR2 is needed for entry of monocytes into the gut in addition to its known role of mediating monocyte exit from the BM (22). These were performed to complete a publication by my predecessor Andrew Platt, and were carried out before I had established the refined gating and sorting strategies used elsewhere in my project. In this study, whole unpurified BM cells from WT (CD45.1⁺) or CCR2 KO (CD45.2⁺) donor mice were fluorescently labelled and co-transferred into CD45.2⁺ WT recipients at a 1:1 ratio on day 5 of colitis (Fig. 6.9A and B). Donor derived F4/80⁺ cells were evident in the colon after 24hrs and could be distinguished within the total F4/80⁺ fraction on the basis of Far-Red fluorescence (Fig. 6.9C). Of the Far-Red⁺ cells present in the colon, the vast majority (>85%) were of WT origin (CD45.1⁺) and only a small number of CCR2 KO derived cells could be seen (CD45.1^{neg}) (Fig. 6.9D and E). In contrast, analysis of the donor cells present in the spleen of the same recipients showed that there was an approximately equal abundance of WT and CCR2 KO-derived donor cells (Fig. 6.9D and E).

Taken together these results demonstrate that recruitment of Ly6C^{high} monocytes into the colonic mucosa is a CCR2-dependent process. In contrast, accumulation of Ly6C^{high} monocytes in the spleen appears to be relatively unaffected by CCR2-deficiency.

6.4 Pathogenic Role of Ly6C^{high} Monocytes in Inflamed Colon

The previous experiments indicated that the CCR2-dependent recruitment of Ly6C^{high} monocytes was critical for the development of colitis and to explore this further, I examined whether adoptive transfer of WT Ly6C^{high} monocytes into CCR2 KO mice could restore their susceptibility to DSS colitis. To this end, CCR2 KO mice receiving DSS received purified Ly6C^{high} BM monocytes from WT (CD45.1⁺) mice on d1 and d3 of DSS colitis. As before, untransferred CCR2 KO mice were less susceptible to colitis, showing reduced bodyweight loss and clinical

disease scores compared with WT animals (Fig. 6.10). This was not affected by transfer of WT monocytes, even though I could find donor cells that had been recruited to the intestine (Fig. 6.10A and B). As in previous experiments, by day 6 of colitis, the majority of donor cells present in the colonic LP of recipient CCR2 KO mice now expressed class II MHC (Fig. 6.10C). However, a greater proportion of donor cells remained Ly6C⁺ when transferred into colitic CCR2 KO mice compared with what I had seen in resting KO mice, suggesting that the differentiation process might be altered in CCR2 KO mice receiving DSS. As the donor monocytes used in this experiment were obtained from WT mice, I could not examine CX3CR1 expression by donor derived cells.

These experiments suggest that adoptive transfer of WT Ly6C^{high} monocytes into CCR2 KO mice does not recapitulate the disease progression seen in WT mice and so could indicate that Ly6C^{high} monocytes alone are insufficient for establishing disease. Alternatively, it could be that the experimental setup was not optimal and transfer of more monocytes on different days might have given a different result. However I did not have time to repeat this experiment.

6.5 Monocytes and Macrophages in the Resolution of Colonic Inflammation

Thus far, my studies of acute DSS colitis have shown a critical role for the recruitment and accumulation of pro-inflammatory Ly6C^{high} monocytes. However my earlier studies had shown that these monocytes can also repopulate the resident m ϕ populations of the steady state mucosa. Therefore the question arose as to whether the monocytes that accumulate during active inflammation might differentiate further once colitis resolves.

To assess this, I adopted a colitis regime in which CX3CR1^{+gfp} mice received 2% DSS in their water for 4 days and were then returned to normal drinking water for the remainder of the study. As shown in Figure 6.11A, withdrawal of DSS resulted in all mice returning to their initial bodyweight within around 1 week, although there was considerable variability in the recovery rates of individual mice. Recovery of bodyweight was accompanied by the restoration of normal intestinal architecture (Fig. 6.11B)

As in my previous experiments, the acute phase of colitis was associated with a reversal in the normal ratio of CX3CR1^{high} and CX3CR1^{int} cells due to expansion of the latter population and a decrease in the absolute numbers of the CX3CR1^{high} mφ (Fig. 6C-E). This continued even after DSS withdrawal, with the proportion of CX3CR1^{int} cells remaining high until at least 3 days after stopping DSS and the frequency of CX3CR1^{high} cells continuing to fall to almost zero at this time. Thereafter, the proportions of CX3CR1^{high} cells began to increase gradually and this was paralleled by a decrease in the proportion of CX3CR1^{int} cells (Fig. 6.11C and D). However, even by 14 days after withdrawing DSS, the proportions and numbers of CX3CR1^{high} cells had not recovered to normal. This pattern suggested that these CX3CR1^{int} cells recruited during active colitis may be converting into CX3CR1^{high} 'resident' mφ during recovery, as is the case under steady state conditions.

To test this possibility, I employed BrdU labelling as a means of tracking newly recruited cells. Mice received 2% DSS and BrdU in their drinking water for 4 consecutive days and were then returned to normal drinking water for the following 14 days. The efficiency with which newly recruited monocytes enter the CX3CR1^{int} compartment was confirmed by the large accumulation of BrdU⁺ cells seen in this compartment during DSS and BrdU administration. There was also accumulation of BrdU⁺ cells in the CX3CR1^{high} compartment, although this was less than for the CX3CR1^{int} compartment (~10%) (Fig. 6.11F). Removal of DSS and BrdU at d4 resulted in the rapid loss of BrdU⁺ cells within both the CX3CR1^{int} and CX3CR1^{high} fractions, with no BrdU⁺ cells identifiable 14 days after cessation of DSS (Fig. 6.11F). This suggests that the vast majority of monocytes recruited to the inflamed colon do not subsequently differentiate into long-lived CX3CR1^{high} mφ, even during the repair phase that occurs after the removal of the inflammatory agent.

I also tried to examine the fate of newly recruited Ly6C^{high} monocytes during the resolution of DSS colitis using an adoptive transfer system. Purified Ly6C^{high} BM monocytes were transferred into d3 colitic mice and DSS administration was stopped 24hrs later. I then attempted to find the donor cells in the colon after a further 3 days, but was unsuccessful (data not shown). However this was before I had fully optimised the monocyte transfer system and when identification of donor cells was difficult as outlined in section 4.1. Given more time this experiment would have been repeated using the optimised transfer system.

6.6 Summary

In this chapter I set out to examine the fate of Ly6C^{high} monocytes recruited to the inflamed mucosa during DSS colitis. Altogether the results confirmed my previous findings that newly recruited Ly6C^{high} monocytes do not differentiate into CX3CR1^{high} m ϕ under inflammatory conditions. Rather they remain within the CX3CR1^{int} compartment, confirming that the context of the milieu into which Ly6C^{high} monocytes arrive determines their differentiation outcome.

I also showed that the development of intestinal pathology was dependent on the CCR2 chemokine receptor. This effect was due to the deficient recruitment of Ly6C^{high} monocytes to the inflamed mucosa, leading to the lack of accumulation of pro-inflammatory m ϕ , rather than an effect on other inflammatory cells. Studies of resolving inflammation showed that the population of resident CX3CR1^{high} m ϕ returned gradually towards normal, as the numbers of pro-inflammatory decreased and the intestine repaired. However, the recovery of the resident m ϕ population did not seem to reflect differentiation of the recently recruited inflammatory monocytes and m ϕ , which appeared to be short lived.

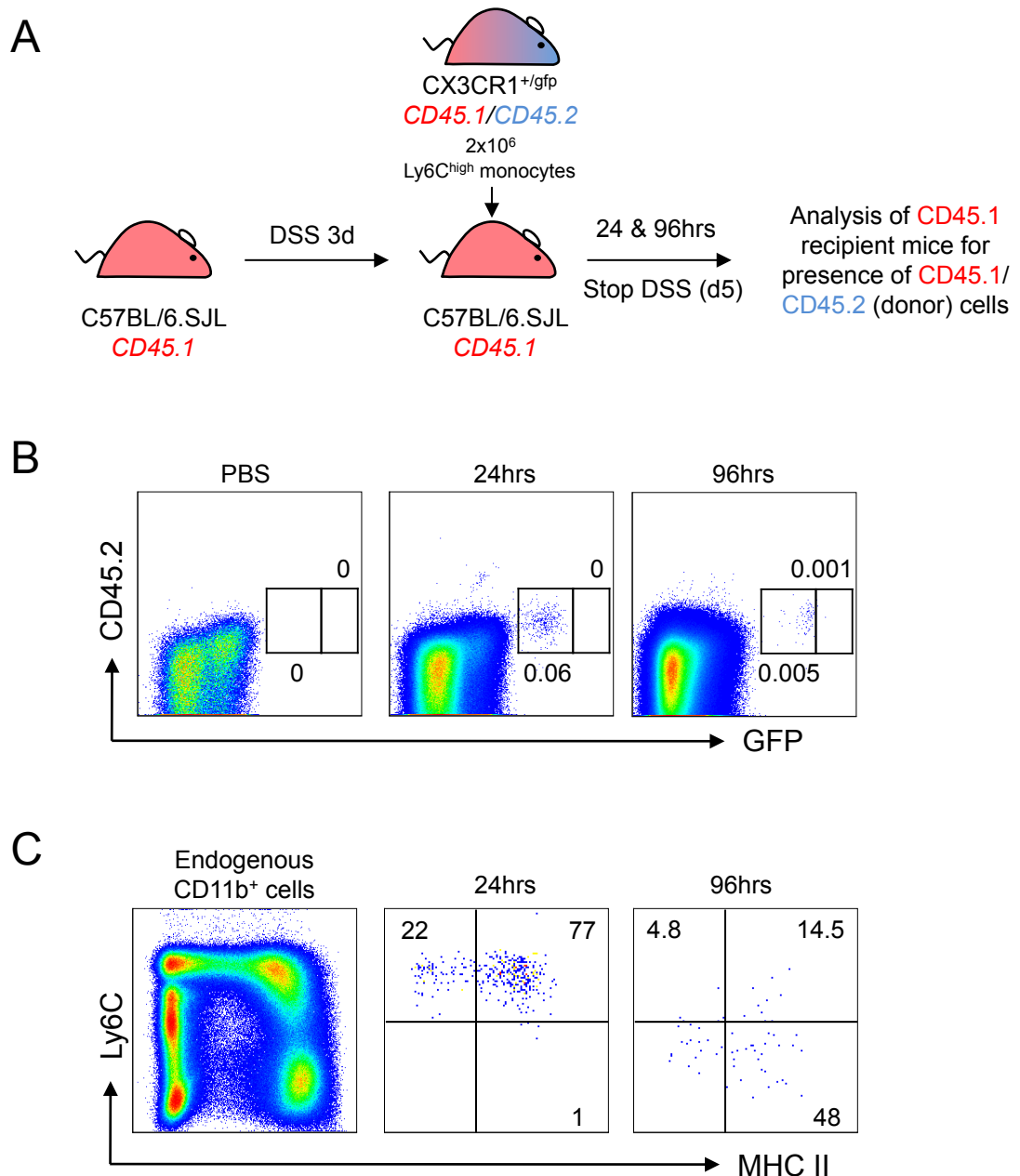


Figure 6.1: Fate of Adoptively Transferred Ly6C^{high} Monocytes in the Inflamed Mucosa

A. 2x10⁶ purified Ly6C^{high} BM monocytes from CD45.1⁺/CD45.2⁺ CX3CR1^{+/gfp} mice were adoptively transferred into CD45.1⁺ WT mice on d3 of DSS colitis and the presence of donor cells within the colonic LP was analysed 24hrs and 96hrs later. **B.** Representative dot plots of CD45.2 and CX3CR1-GFP expression on live-gated CD11b⁺ LP cells in the colon of mice that had received PBS or monocytes 24hrs and 96hrs before. Gates for CX3CR1^{int} and CX3CR1^{high} populations were set using the CX3CR1-GFP expression of donor monocytes in the bloodstream. **C.** Expression of Ly6C and class II MHC by endogenous CD11b⁺ cells (*left panel*) or donor CD45.1⁺CD45.2⁺ cells (*middle and right panels*) at indicated time points. 1 individual experiment with 2 recipient mice at each time point.

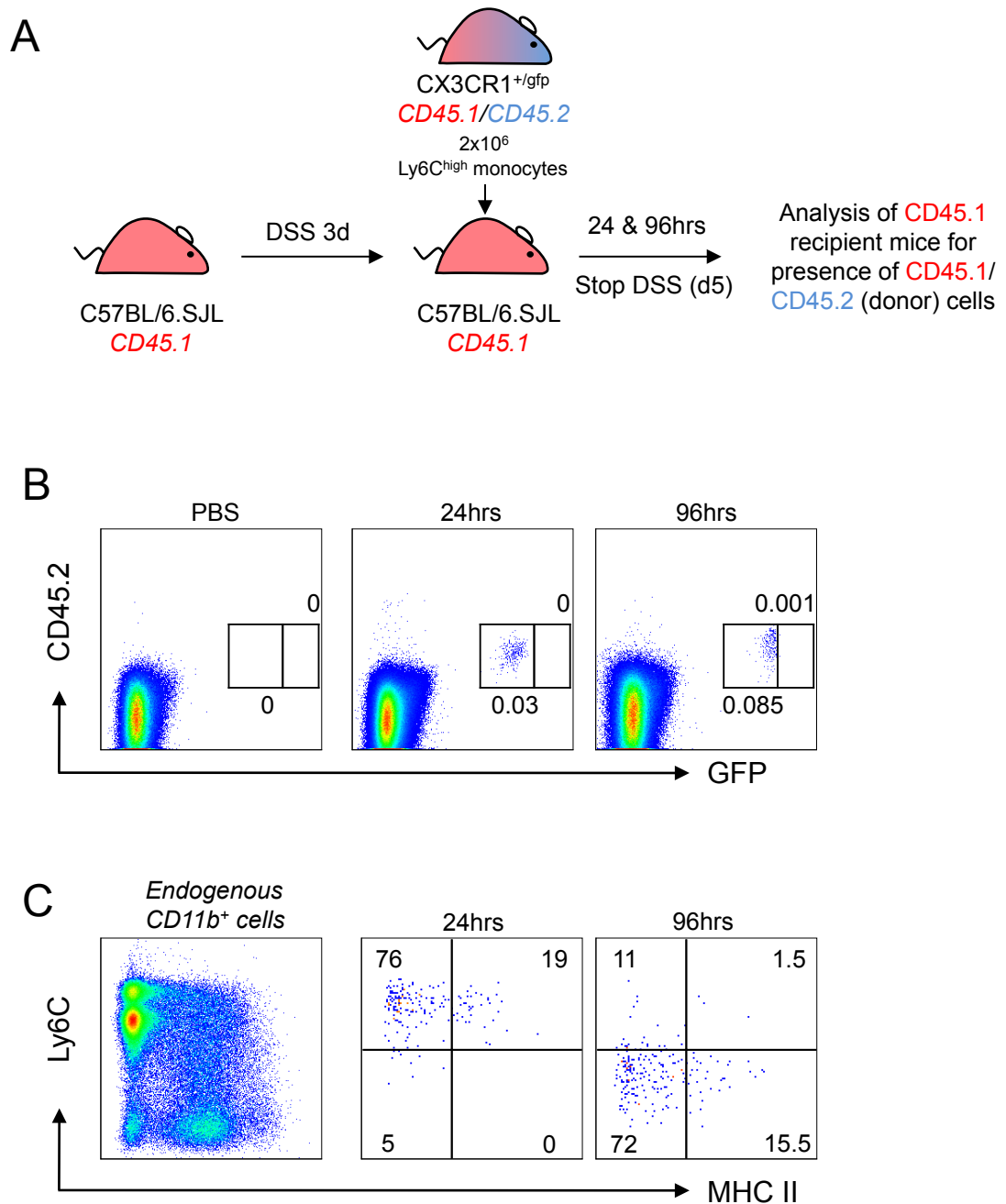


Figure 6.2: Fate of Adoptively Transferred Ly6C^{high} Monocytes in the Bloodstream of Colitic Mice

A. 2x10⁶ purified Ly6C^{high} BM monocytes from CD45.1⁺/CD45.2⁺ CX3CR1^{+/gfp} mice were adoptively transferred into CD45.1⁺ WT mice on d3 of DSS colitis and the presence of donor cells within the colonic LP was analysed 24hrs and 96hrs later. **B.** Representative dot plots of CD45.2 and CX3CR1-GFP expression on live-gated CD11b⁺ LP cells in the colon of mice that had received PBS or monocytes 24hrs and 96hrs before. **C.** Expression of Ly6C and class II MHC by endogenous CD11b⁺ cells (*left panel*) or donor CD45.1⁺CD45.2⁺ cells (*middle and right panels*) at indicated time points. 1 individual experiment with 2 recipient mice at each time point.

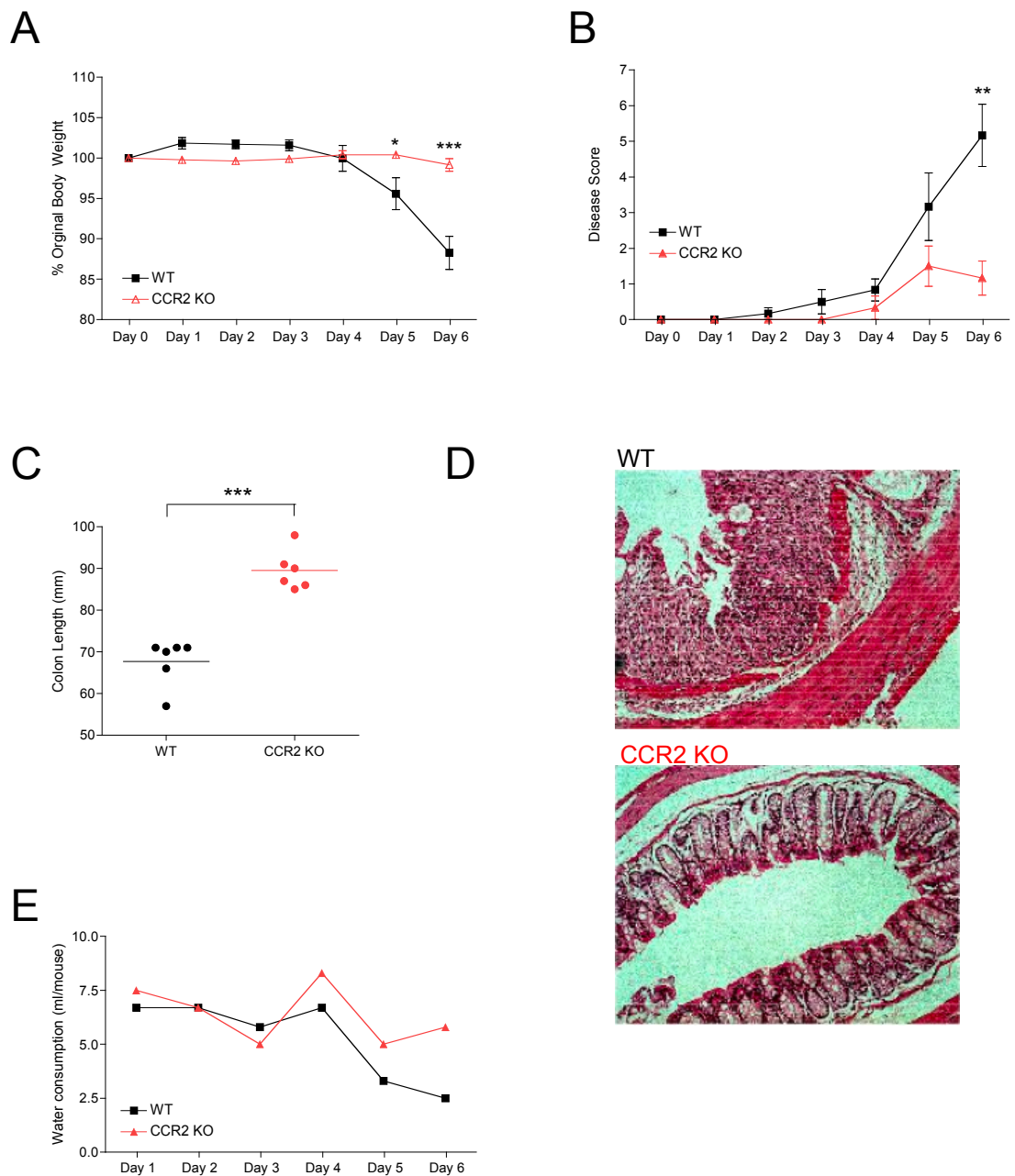


Figure 6.3: Progress of DSS Colitis in CCR2-deficient Mice

WT or CCR2 KO mice received 2% DSS in their drinking water for 6 days and their bodyweight (**A**) and clinical disease score (**B**) was recorded daily. Results are the means + 1 SD for 6 mice/group. **C**. On day 6 mice were culled and their colons measured. **D**. On day 7 sections of distal colon were fixed in 10% formalin, embedded in paraffin and stained with H&E for histological analysis (final magnification x100). **E**. Water consumption (ml/mouse) on each day of colitis. Results representative of at least 2 individual experiments. (* $p < 0.05$, ** $p < 0.01$, *** $p < 0.001$, Student's t test)

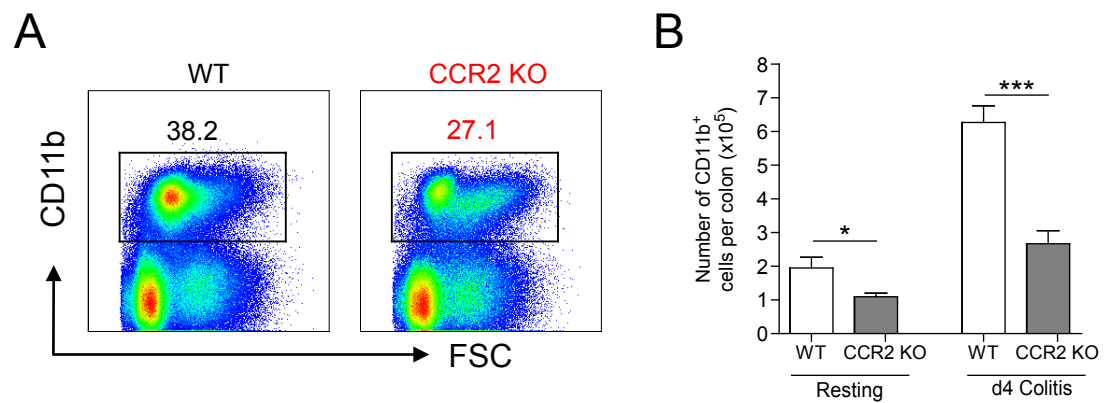


Figure 6.4: Enumeration of CD11b⁺ Myeloid Cells in Colon of CCR2 KO Mice with DSS Colitis

WT or CCR2 KO mice received 2% DSS in their drinking water for 4 days and the proportion of live-gated CD45⁺ CD11b⁺ cells was examined by flow cytometry. **A.** Representative dot plots of live-gated CD45⁺ CD11b⁺ cells obtained from d4 colitic WT or CCR2 KO mice. **B.** The mean absolute numbers of CD11b⁺ cells per colon of d4 colitic WT or CCR2 KO mice compared with the numbers in the resting colon from Figure 4.9. Results are the means + 1SD and are representative of 2 individual experiments with 3-4 mice/group. (*p<0.05, ***p<0.0001, Student's t test)

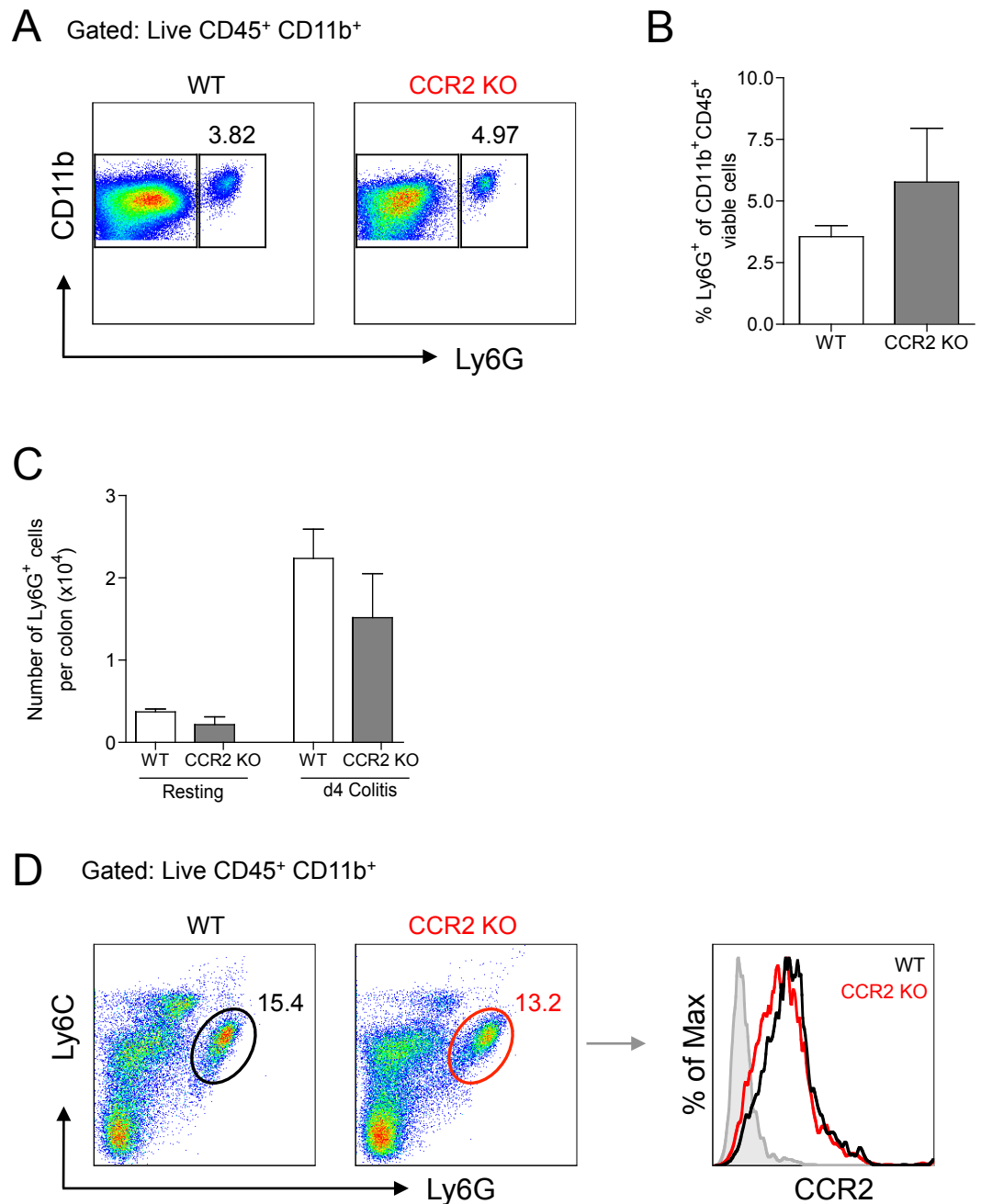


Figure 6.5: Presence of Neutrophils in the Mucosa of CCR2 KO Mice with DSS Colitis

WT or CCR2 KO mice received 2% DSS in their drinking water for 4 days and the presence of Ly6G⁺ neutrophils in the LP was examined by flow cytometry. **A.** Representative dot plots of Ly6G expression by live-gated CD45⁺ CD11b⁺ cells obtained from d4 colitic WT or CCR2 KO mice. **B.** The mean frequency of Ly6G⁺ neutrophils amongst the total CD11b⁺ cell compartment in WT and CCR2 KO mice. **C.** The absolute numbers of CD11b⁺ Ly6G⁺ neutrophils per colon of d4 colitic WT or CCR2 KO mice compared with those in resting colon from Figure 4.10. **D.** Expression of CCR2 on blood neutrophils (Ly6G⁺Ly6C^{int}) from resting WT (*black line*) or CCR2 KO (*red line*) mice compared with the isotype control (*shaded histogram*). Results are the means + 1SD and are representative of 2 individual experiments with 3-4 mice/group.

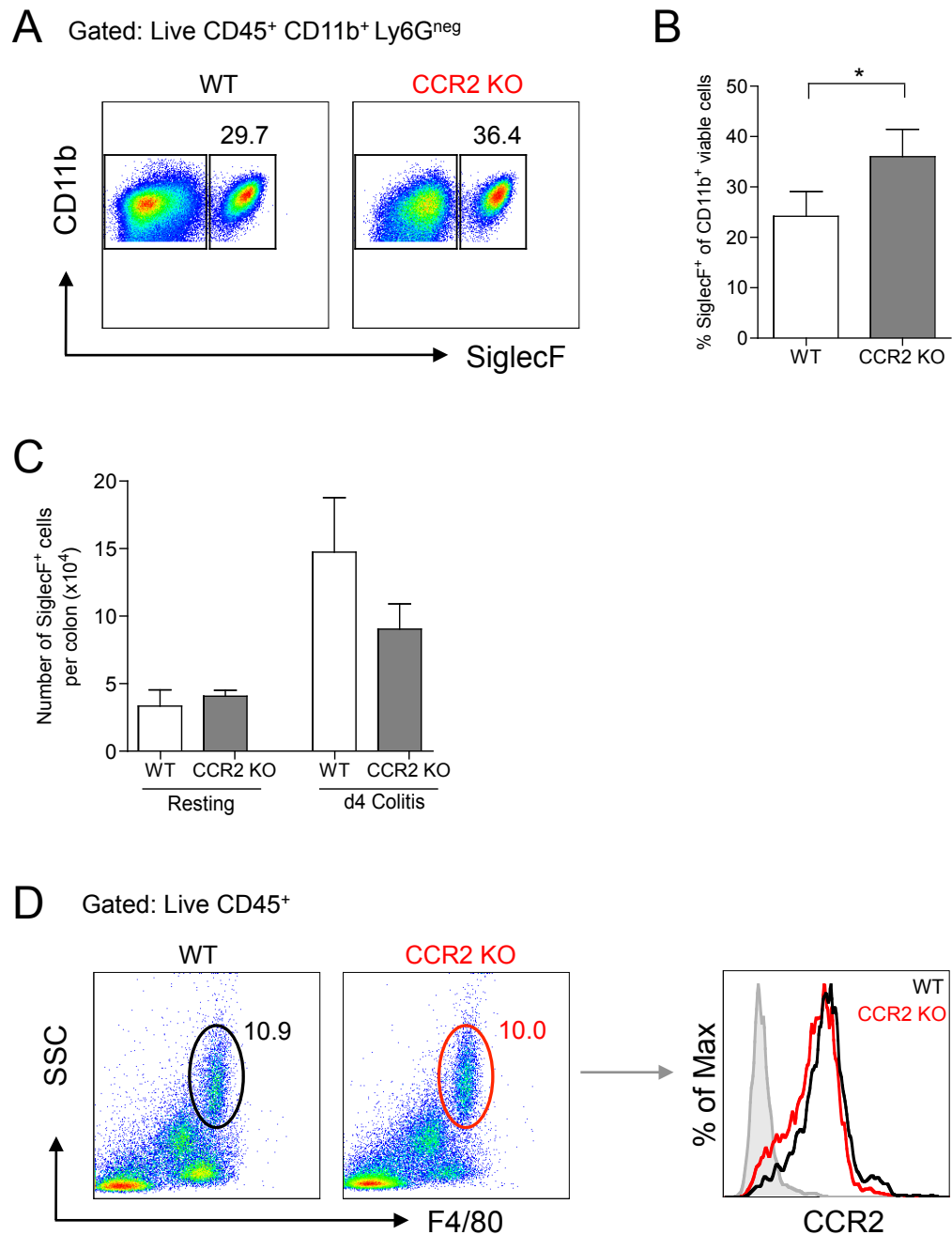


Figure 6.6: Presence of Eosinophils in the Mucosa of CCR2 KO Mice with DSS Colitis

WT or CCR2 KO mice received 2% DSS in their drinking water for 4 days and the presence of SiglecF⁺ eosinophils was examined by flow cytometry. **A**. Representative staining of SiglecF on live-gated CD45⁺ CD11b⁺ Ly6G^{neg} cells obtained from d4 colitic WT or CCR2 KO mice. **B**. The mean frequency of SiglecF⁺ eosinophils amongst the CD11b⁺ Ly6G^{neg} fraction in WT and CCR2 KO mice. **C**. The absolute numbers of eosinophils per colon of d4 colitic WT or CCR2 KO mice compared with those in resting colon from Figure 4.10. **D**. Expression of CCR2 on blood eosinophils (SSC^{high}F4/80⁺) from resting WT (*black line*) or CCR2 KO (*red line*) mice compared with the isotype control (*shaded histogram*). Results are the means + 1SD and are representative of 2 individual experiments with 3-4 mice/group. (*p<0.05, Student's t test)

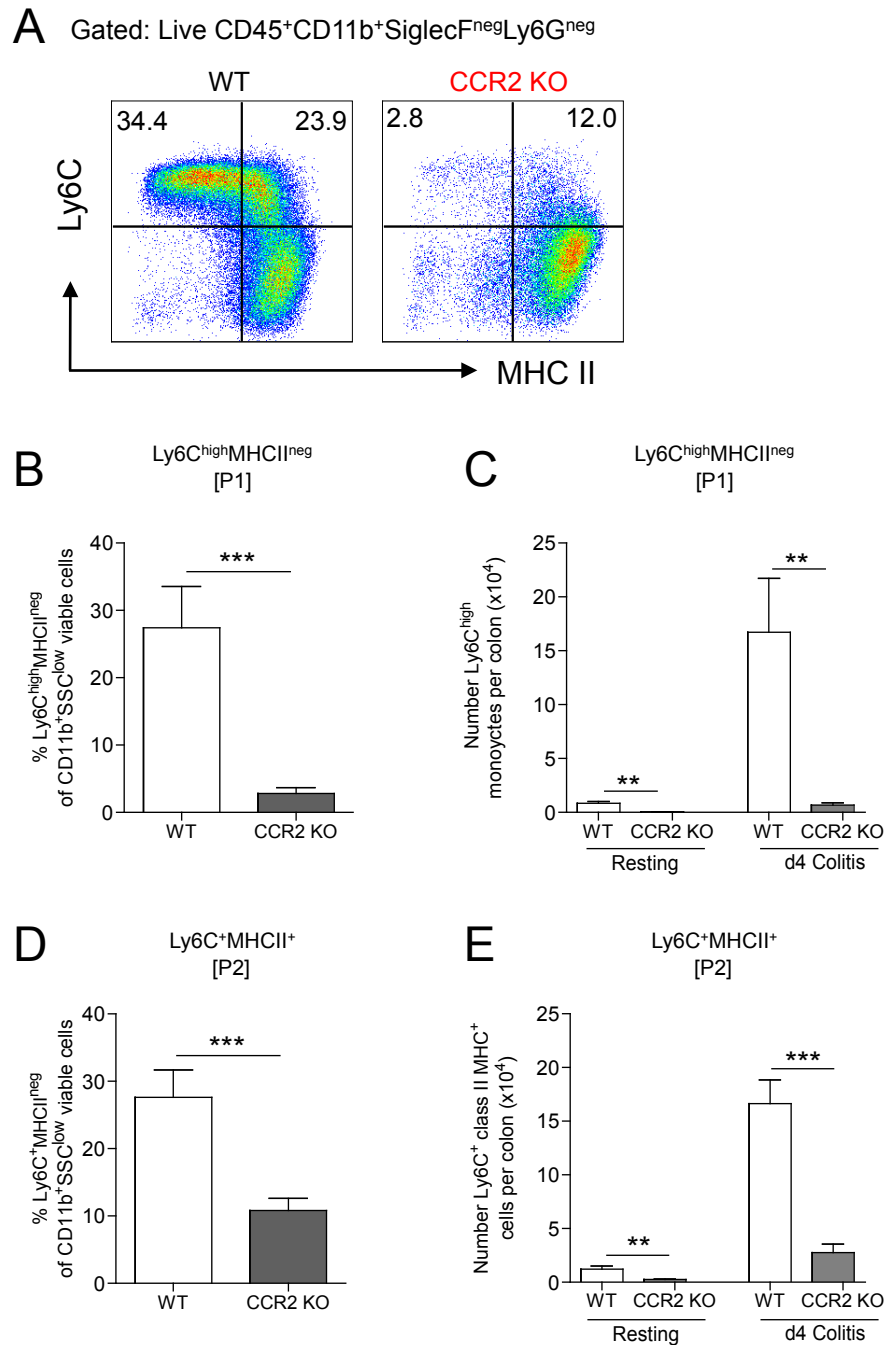


Figure 6.7: Monocyte/Macrophage Subsets in the Mucosa of CCR2 KO Mice with DSS Colitis

WT or CCR2 KO mice received 2% DSS in their drinking water for 4 days and the composition of the CD11b⁺ SiglecF^{neg} Ly6G^{neg} fraction was examined by flow cytometry. **A**. Representative dot plots of Ly6C and class II MHC expression by live-gated CD45⁺ CD11b⁺ SiglecF^{neg} Ly6G^{neg} cells and the proportions (**B**) and absolute numbers (**C**) of Ly6C^{high} MHCII^{neg} (P1) cells per colon of d4 colitic WT and CCR2 KO mice compared with those in resting colon from Figure 4.11. The proportions (**D**) and absolute numbers (**E**) of Ly6C⁺ MHCII⁺ (P2) cells per colon of d4 colitic WT and CCR2 KO mice compared with those in resting colon from Figure 4.11. The results are the means + 1SD and are representative of 2 individual experiments with 3-4 mice/group. (*p<0.05, **p<0.01, ***p<0.001, Student's t test)

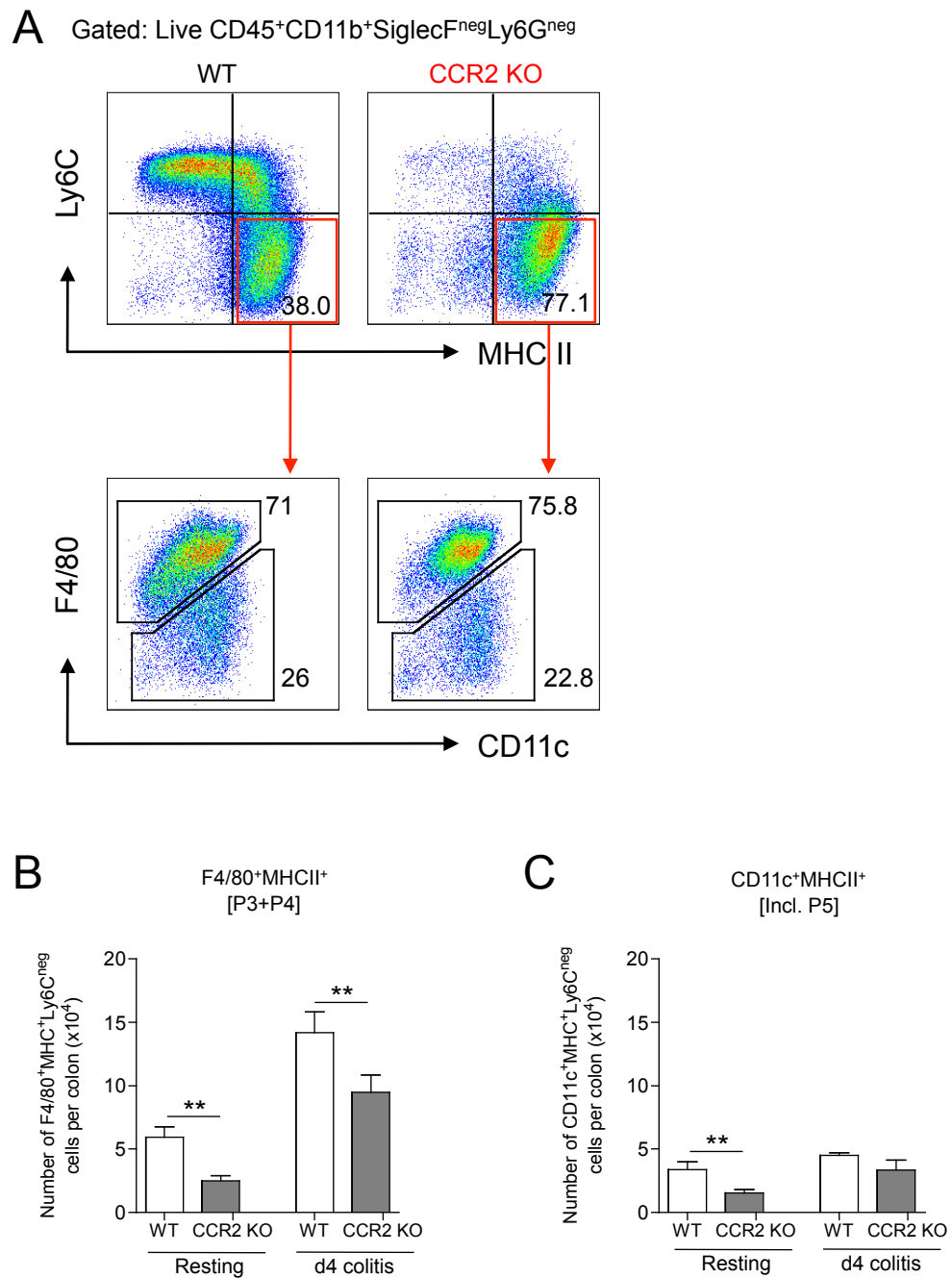


Figure 6.8: Class II MHC⁺ Resident Macrophages and DC in the Mucosa of CCR2 KO Mice with DSS Colitis

WT or CCR2 KO mice received 2% DSS in their drinking water for 4 days and the composition of the CD11b⁺ SiglecF^{neg} Ly6G^{neg} fraction was examined by flow cytometry. **A**. Representative dot plots of F4/80 and CD11c expression by live-gated CD45⁺ CD11b⁺ SiglecF^{neg} Ly6G^{neg} Ly6C^{neg} MHCII⁺ cells and the absolute numbers of **(B)** F4/80⁺ MHCII⁺ (P3+4) cells or **(C)** CD11c⁺ F4/80^{neg} MHCII⁺ (incl. P5) cells per colon of d4 colitic WT or CCR2 KO mice compared with those in resting colon from Figure 4.12. Resting data is the same data as shown in Figure 4.12). Results represent the means + 1SD for 3 (WT) or 4 (CCR2 KO) mice and are representative of 2 individual experiments. (**p<0.01, Student's t test)

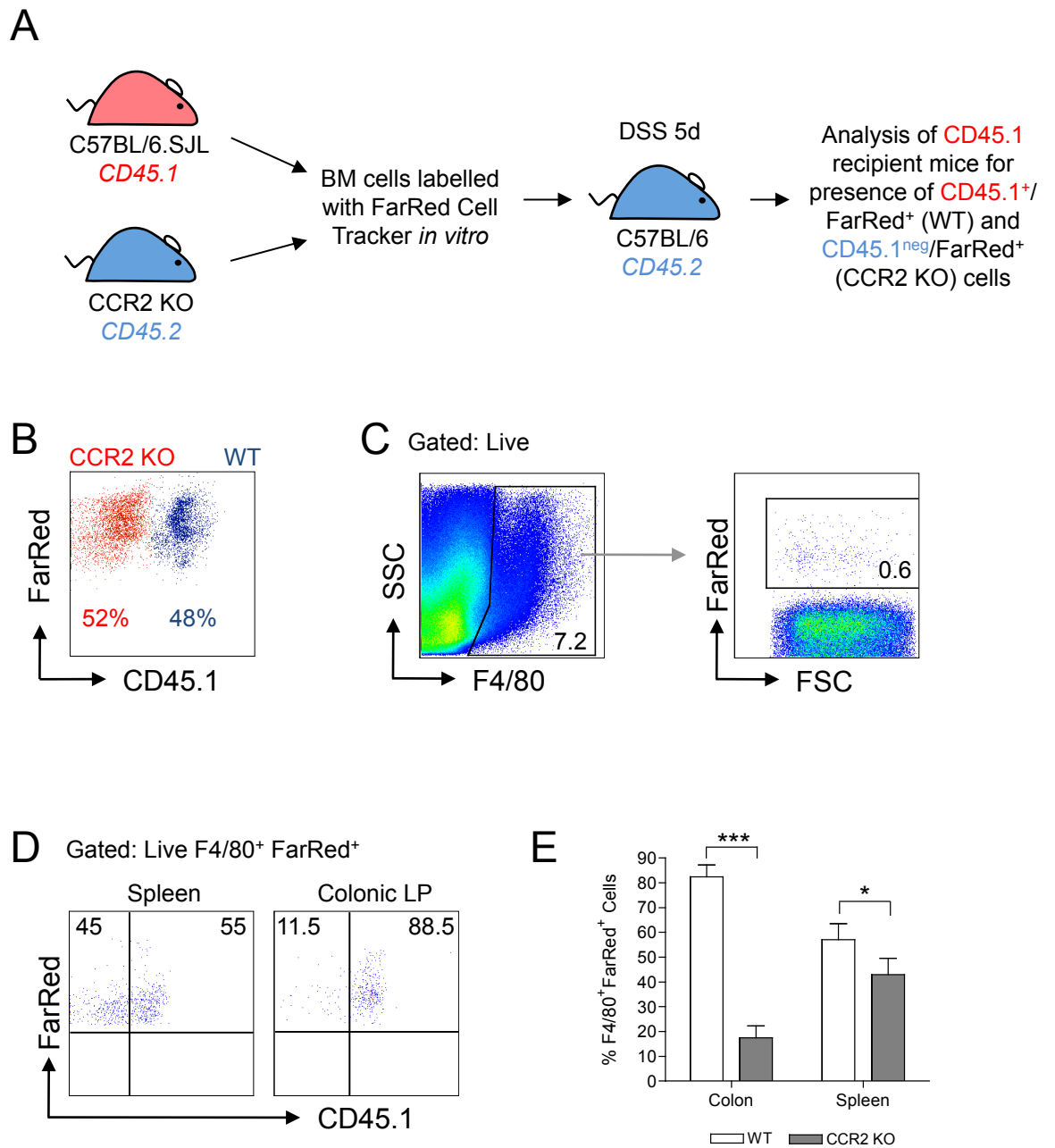


Figure 6.9: Competitive Adoptive Transfer of WT and CCR2KO BM Cells into Colitic Mice

A. Whole BM cells from CD45.1⁺ WT mice and CD45.2⁺ CCR2 KO mice were labelled with Cell Tracker Red (FarRed) and 12×10^6 cells were adoptively transferred into CD45.2⁺ WT mice at a 1:1 ratio on d5 of DSS colitis. The presence of donor cells within the colonic LP and the spleen was analysed 24hrs later. **B.** Representative dot plots of CD45.1 and FarRed fluorescence by BM cells prior to transfer, showing approximately equal proportions of WT (CD45.1⁺FarRed⁺) and CCR2 KO cells (CD45.1^{neg}FarRed⁺). **C.** Gating strategy used to identify donor cells whereby FarRed cells were selected from the total F4/80⁺ fraction of colonic LP cells. **D.** Representative dot plots showing the frequency of WT (CD45.1⁺FarRed⁺) and CCR2 KO cells (CD45.1^{neg}FarRed⁺) amongst live-gated F4/80⁺ FarRed⁺ cells in the spleen and colonic LP 24hrs after transfer. Results are the means + 1SD and are representative of 2 individual experiments with 4 recipient mice.

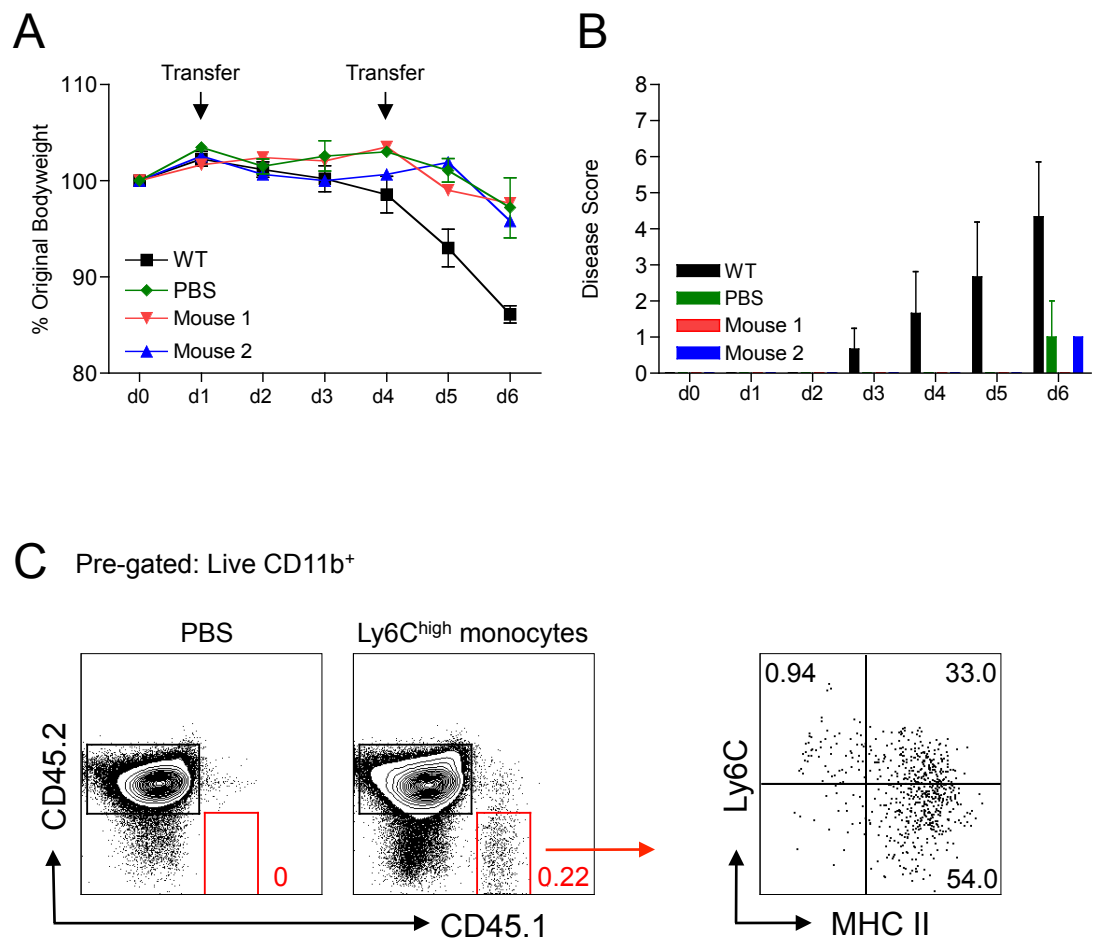


Figure 6.10: Effects of Adoptively Transferring WT Ly6C^{high} Monocytes on the Outcome of DSS Colitis in CCR2 KO Mice

CCR2 KO (CD45.2) mice received 2% DSS for 6 days and received $1-2 \times 10^6$ purified Ly6C^{high} BM monocytes from CD45.1 WT mice by intravenous infusion on d1 and d3 of colitis. Bodyweight (**A**) and clinical disease score (**B**) was measured daily and compared with untransferred WT mice receiving 2% DSS. Results are the means \pm 1 SD for 3 mice (WT and PBS) and 2 mice (Ly6C^{high} recipients) are representative of a single experiment. **C**. Representative CD45.1 and CD45.2 staining by live-gated CD11b⁺ LP cells from d6 'colitic' CCR2 KO mice that received PBS or BM monocytes and the expression of Ly6C and class II MHC on donor cells (CD45.1⁺CD45.2^{neg}).

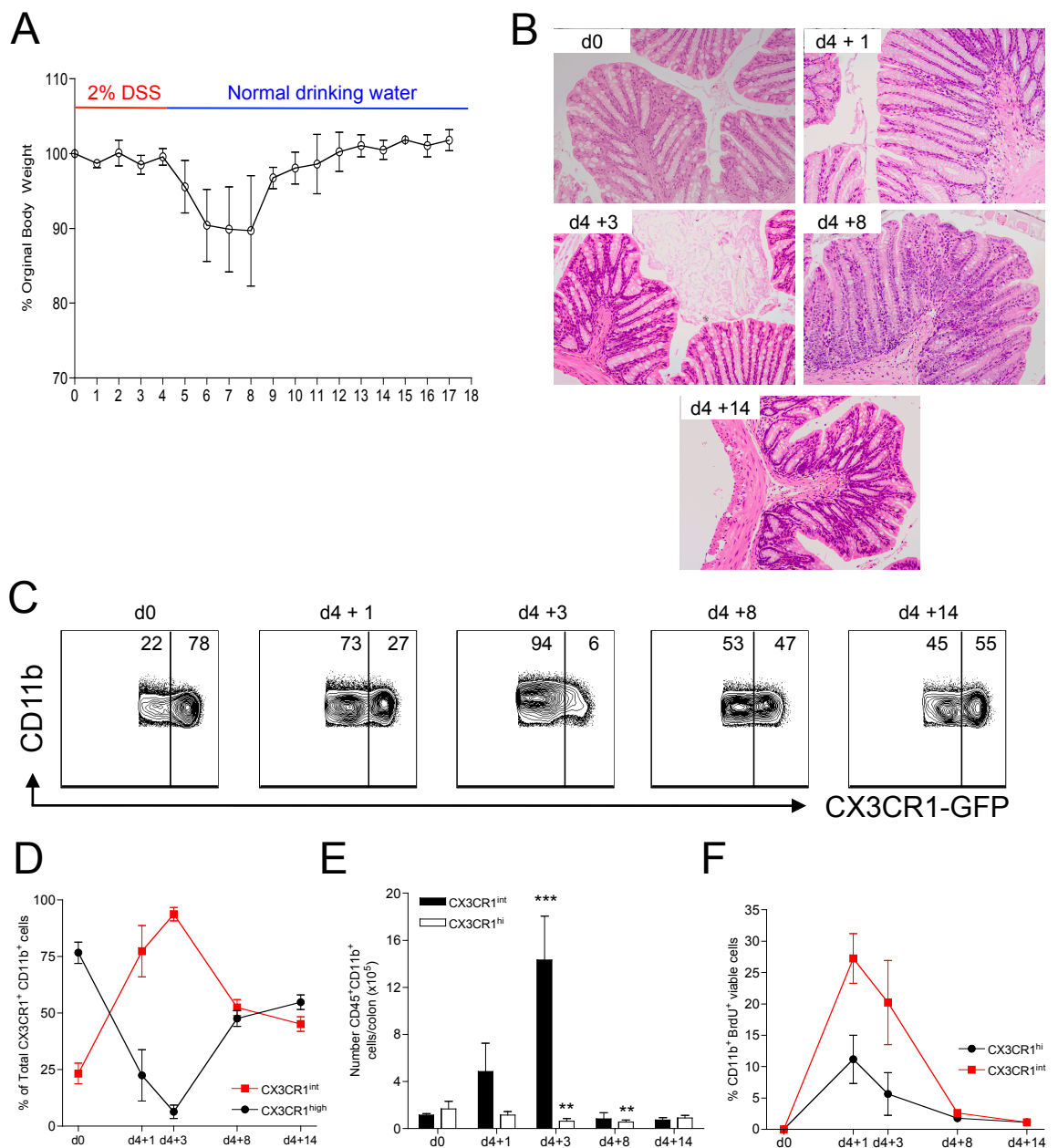


Figure 6.11: Myeloid Cells in Colon during Recovery from DSS Colitis

A. Bodyweights in CX3CR1^{+/gfp} mice receiving 2% DSS and BrdU in their drinking water for 4 days and were then returned to normal drinking water. **B.** Representative H&E sections of distal colon at each time point showing intense crypt lengthening and inflammation that does not resolve until 14 days after withdrawing DSS (final magnification x100). **C.** Representative contour plots showing the proportion of CX3CR1^{int} and CX3CR1^{high} cells amongst live-gated CD45⁺CD11b⁺CX3CR1-GFP LP cells from resting mice or mice culled at d1, d3, d8 and d14 after DSS withdrawal. **D.** The mean proportion \pm 1SD (**D**) and absolute numbers (**E**) of CX3CR1^{int} and CX3CR1^{high} cells within the total CD11b⁺CX3CR1-GFP⁺ fraction at each time point. **F.** The frequency of BrdU⁺ cells within live-gated CD45⁺ CD11b⁺ CX3CR1^{int} and CX3CR1^{high} populations at the indicated time points after DSS and BrdU withdrawal. Results are the means \pm 1SD and are representative of a single experiment with 4 mice at each time point.

Chapter 7
The Role of CD200R1 in the Regulation of
Intestinal Macrophage Activity

7.1 Introduction

As discussed in previous chapters, resident intestinal m ϕ are hyporesponsive to classical stimuli such as TLR ligands and in Chapter 5 I showed that this state of hyporesponsiveness was acquired *in situ* as Ly6C^{high} 'inflammatory' monocytes matured into CX3CR1^{high} m ϕ . Although a number of mechanisms have been proposed to maintain colonic m ϕ in this 'regulatory' state, the exact reason is unknown and it is likely that multiple mechanisms may be involved, including immunomodulatory cytokines such as IL10 and TGF β . In addition, intestinal m ϕ express a number of surface receptors that have been associated with inhibitory function, although their role(s) have not been studied in any detail.

One inhibitory receptor that has been shown to regulate m ϕ responsiveness at mucosal surfaces is CD200R1. Binding of its ligand, CD200, has been shown to cause inhibition of different m ϕ populations including microglia of the CNS and alveolar m ϕ , which share features with intestinal m ϕ (113, 119). Notably, loss of CD200R1-CD200 signalling increased susceptibility to inflammation in the lung (119). In addition, Snelgrove and co-workers suggested that m ϕ in the gut might express CD200R1, but the cells involved were not characterised precisely and the role of the CD200R1-CD200 regulatory axis in the intestinal compartment has never been formally tested. Therefore in this chapter, I set out to investigate the involvement of CD200R1 in the regulation of intestinal m ϕ behaviour using a combination of KO mice.

7.2 Expression of CD200R1 by Colonic Macrophages

I first assessed the expression of CD200R1 by individual myeloid cell populations in the colonic LP (Fig. 7.1). As the majority of work in this chapter was carried out before I had established the detailed gating strategies described in previous chapters and the mice did not express CX3CR1-GFP, the subsets described here were based on less complex patterns of surface molecules, with m ϕ routinely identified simply on the basis of F4/80 and class II MHC expression. Based on the work shown in my previous chapters and as illustrated in Figure 7.1, the vast majority of this population are equivalent to CX3CR1^{high} cells in P4 (Fig. 7.1A and B).

Initially I experienced technical problems using the recommended concentration of the anti-CD200R1 (OX-110) antibody (5 μ g/ml), which appeared to stain both WT and CD200R1 KO cells when compared with the isotype control. However, careful titration of the antibody showed that 0.5 μ g/ml was optimal for providing reproducible staining of WT cells that was not present in the CD200R1 KO (Fig. 7.1C). This showed that F4/80⁺MHCII⁺ intestinal m ϕ expressed CD200R1 at a level comparable to alveolar m ϕ (Fig. 7.1C-E). In contrast, F4/80^{low} MHCII^{neg} SSC^{high} intestinal eosinophils and Ly6C^{high}MHCII^{neg} monocytes (P1 cells) appeared to lack CD200R1 expression (Fig. 7.1D). Resident peritoneal m ϕ also lacked CD200R1 expression, whereas WT BMM expressed low but significant levels of the receptor when compared with CD200R1 KO BMM (Fig. 7.1E).

7.3 CD200 Expression in Steady State Colon

For CD200R1 to play a role in the gut, its ligand, CD200, should also be available. Therefore I next examined the expression of CD200 by both haematopoietic (CD45⁺) and non-haematopoietic (CD45^{neg}) cells, as previous reports have shown that CD200 can be expressed by a wide variety of cells. As shown in Figure 7.2, the CD45^{neg} population contained cells that expressed high levels of CD200. Of these CD200⁺ cells, approximately 40% expressed CD31 (PECAM-1), a marker of endothelial cells and ~25% of these CD200⁺CD31⁺ cells co-expressed LYVE-1, the lymphatic endothelial marker (Fig. 7.2A). Thus both vascular and lymphatic endothelium in the intestine express high levels of CD200. I was unable to identify the remaining CD200⁺ population of non-haematopoietic cells, and it was notable that intestinal epithelial cells did not express CD200 (Fig 7.2B).

I next explored the expression of CD200 by intestinal lymphocyte populations. This revealed that as in other tissues (119, 258), the majority of mucosal B cells (B220⁺) and a small proportion of CD4⁺ T lymphocytes expressed CD200 at low levels. In contrast, CD8⁺ T cells lacked CD200 expression (Fig. 7.2C and D).

7.4 Characterisation of Colonic Macrophages from CD200R1 KO Mice

Previous studies have shown that disruption of the CD200-CD200R1 axis results in the expansion and activation of tissue m ϕ populations, as well as increased susceptibility to inflammation (113). Thus, having established that intestinal m ϕ show selective expression of CD200R1 and that its ligand, CD200, is highly abundant in the mucosa, I next sought to determine the importance of this regulatory axis in controlling colonic m ϕ behaviour by examining colonic m ϕ from resting CD200R1-deficient mice.

Colonic LP cells were isolated from WT or CD200R1 KO mice and examined for the expression of F4/80 and class II MHC to identify m ϕ . Initial analysis showed that CD200R1 KO mice had fewer total viable leucocytes (live-gated CD45⁺) in colonic isolates than WT mice (Fig. 7.3A-C). In parallel, CD200R1 KO colon had a significantly higher frequency of F4/80⁺MHCII⁺ m ϕ and also had an additional population of F4/80⁺MHCII^{int} cells that was not evident in WT mice (Fig. 7.3D and E). This additional F4/80⁺MHCII^{int} population in CD200R1 KO colon did not express Ly6C, suggesting they did not represent recently arrived monocytes or 'inflammatory' m ϕ (Fig. 7.3G). However these proportional differences did not translate into a significant difference in absolute numbers, probably reflecting the difference in total leucocyte numbers between WT and CD200R1 KO mice (Fig. 7.3F). There were no differences in the proportions or numbers of the F4/80⁺MHCII^{neg} fraction, which contains SiglecF⁺ eosinophils and Ly6C^{high} monocytes (Fig. 7.3F).

Next, I assessed whether CD200R1 deficiency leads to m ϕ hyperactivation in the intestine by examining the levels of costimulatory molecule and TLR expression. This revealed that colonic m ϕ from both WT and CD200R1 KO mice failed to express CD40 and expressed CD86 at comparable levels (Fig. 7.4). Similarly there was no difference in the levels of TLR2 and TLR4 expression between WT and KO.

7.5 TLR Responsiveness of CD200R1 KO Macrophages

To examine further the role of CD200R1 in m ϕ function, I next compared the responses of CSF-1 generated BMM from WT and CD200R1 KO mice to

stimulation with LPS, IFN γ or a combination of these stimuli. As expected, stimulation of WT BMM with LPS and/or IFN γ led to upregulation of CD40 expression (Fig. 7.5A). Similarly CD86 expression was upregulated by either stimulus and even more when cells were treated with both LPS and IFN γ (Fig. 7.5B). Stimulation of WT BMM with IFN γ also resulted in class II MHC upregulation, but this effect was lost when BMM were incubated with both LPS and IFN γ (Fig. 7.5C). Importantly, there were no differences in the upregulation of costimulatory molecules or class II MHC between WT and CD200R1 KO BMM.

Next, I used intracellular cytokine staining to assess the production of TNF α by WT and CD200R1 KO colonic m ϕ after TLR stimulation. Due to technical issues, I was unable to assess the individual class II MHC-defined F4/80⁺ populations in this experiment and could only analyse total F4/80⁺MHCII⁺ cells. As expected, stimulation with either BLP or LPS resulted in little or no increase in TNF α production by F4/80⁺MHCII⁺ cells from WT mice compared with unstimulated cells. CD200R1 KO m ϕ also did not respond to TLR stimulation and there were no differences in TNF α production by either unstimulated or TLR-stimulated colonic m ϕ from WT and CD200R1 KO mice. Together these results indicate that CD200R1-deficiency does not result in intrinsic hyper-responsiveness of m ϕ in the gut (Fig. 7.6A and B).

7.6 Characterisation of Aged CD200R1 KO Mice

I then went on to examine whether the disruption of the CD200-CD200R1 regulatory axis predisposed mice to intestinal inflammation *in vivo*. First, I monitored for the development of spontaneous intestinal inflammation in cohorts of CD200R1 KO mice maintained under SPF conditions for up to 18 months. There were no signs of weight loss or clinical disease throughout this period (data not shown) and when culled at 16-18 months of age, CD200R1 KO mice had identical body weights and colon lengths to age-matched mice (Fig. 7.7A and B). Furthermore, there was no evidence of histological abnormalities such as inflammatory infiltrates or epithelial disruption in either WT or CD200R1 KO mice at this age (Fig. 7.7C).

To confirm the lack of spontaneous inflammation, I examined the composition of the colonic LP myeloid compartment in aged WT and CD200R1 KO

mice. As shown in Figure 7.7D, comparable numbers of living haematopoietic cells were retrieved from aged WT and KO mice and the numbers and proportions of the B- and T-lymphocytes in the colonic mucosa were also identical (Fig. 7.8). Despite the lack of overt inflammation, there were significantly more Ly6G⁺ neutrophils in the mucosa of aged CD200R1-deficient mice compared with their WT counterparts (Fig. 7.9). However there were equivalent proportions and absolute numbers of F4/80⁺MHCII^{neg} cells (eosinophils and monocytes) and F4/80⁺MHCII⁺ m ϕ in the two strains (Fig. 7.10A-E). Consistent with the results in young KO mice, aged CD200R1 KO mice had an expanded population of F4/80⁺MHCII^{int} cells within the LP compared with their WT counterparts (Fig. 7.10C-E).

In an attempt to examine whether the activation status of the F4/80⁺MHCII^{int} or F4/80⁺MHCII⁺ populations differed between WT and CD200R1 KO mice, I assessed their expression of CD40. As in young mice, there was no difference in the expression of CD40 by either F4/80⁺MHCII^{int} or F4/80⁺MHCII⁺ cells from WT and CD200R1 KO mice (Fig. 7.11A). Similarly, the expanded F4/80⁺MHCII^{int} population did not express Ly6C (Fig. 7.11B), suggesting that these cells did not represent recently arrived monocytes. Consistently, there were no differences in the FSC/SSC profiles of these cells from the two strains (Fig. 7.11C).

Finally to assess whether m ϕ derived from aged CD200R1 KO mice were hyper-responsive to stimulation, I examined TNF α production by BM-derived m ϕ after culture with LPS or BLP. As expected, both LPS and BLP stimulation caused a significant increase in the frequency of TNF α ⁺ m ϕ , but as in young mice, there was no significant difference between the responses mounted by m ϕ from CD200R1 KO m ϕ and WT mice (Fig. 7.12).

Taken together these data demonstrate that CD200R1-deficiency does not render animals susceptible to spontaneous intestinal disease as they age and this is reflected in the relatively normal composition of the intestinal myeloid (and lymphoid) compartment in CD200R1 KO mice.

7.7 Experimental Colitis in CD200R1 KO Mice

Although CD200R1-deficient mice did not develop spontaneous intestinal pathology even after 16-18 months, I postulated that there could be more subtle defects in m ϕ homeostasis that might be revealed in response to exogenous damage. Therefore I next examined the development of acute colitis in CD200R1 KO mice after feeding DSS.

As previously described, continuous administration of 2% DSS led to the development of colitis in WT mice within 5 to 6 days, as determined by significant weight loss and increasing clinical disease scores (Fig. 7.13A and B). There was no significant difference in the overall pattern of disease in CD200R1 KO mice, although these mice showed greater variability in weight loss, clinical disease score and colon shortening compared with the same parameters in WT mice (Fig. 7.13A-C). This increased variability was found in three individual experiments and was not due to differences in the intake of DSS, as water consumption was comparable in all experimental groups (Fig. 7.13D). Analysis of H&E sections of inflamed colon revealed identical histological damage in WT and CD200R1 KO mice (Fig. 7. 13E).

I next assessed if there were any differences in the composition of the intestinal myeloid cell compartment of WT and KO mice during colitis. Consistent with my results from previous chapters, DSS administration led to infiltration of the colon by CD11b⁺ myeloid cells and there were no differences in the numbers and proportions of these cells in WT and KO colon (Fig. 7.14A). The frequency of Ly6G⁺ neutrophils within the CD11b⁺ fraction of colon cells was also similar between colitic WT and CD200R1 KO mice (Fig. 7.14B). As I found in previous experiments, there was expansion in the numbers of F4/80⁺MHCII^{neg} cells in the inflamed colon, which included SiglecF⁺ eosinophils and Ly6C^{high} monocytes (equivalent to P1 in CX3CR1^{+gfp} mice). There were no significant differences in the abundance of these populations between colitic WT and CD200R1 KO mice and together these results demonstrate that lack of CD200R1 does not affect the susceptibility of mice to chemically induced colitis, or to alterations in the inflammatory myeloid cell recruitment.

7.8 Characterisation of CD200 KO Mice

Although it is generally accepted that CD200 is the only ligand of CD200R1, other CD200 receptors have been reported (108). Thus it remained possible that CD200-dependent regulation of intestinal m ϕ function could exist without the involvement of CD200R1. To investigate this, I next characterised intestinal myeloid cells and susceptibility to colitis in CD200 KO mice.

The proportions and absolute numbers of total viable intestinal leucocytes were identical in resting CD200 KO and WT colon, as were the numbers of F4/80⁺MHC^{neg} cells (Fig. 7.15A-C). However, the colon of CD200 KO mice contained significantly fewer F4/80⁺MHCII⁺ m ϕ than WT colon (Fig. 7.15D-F). As in CD200R1 KO mice, there was also an increased proportion of F4/80⁺MHC^{int} cells in resting CD200-deficient colon, whereas these cells were rare in WT colon (Fig. 7.15E). However this did not translate into significant differences in absolute numbers of F4/80⁺MHC^{int} cells, probably reflecting the decreased number of F4/80⁺MHCII⁺ m ϕ in CD200 KO colon. M ϕ isolated from CD200-deficient mice showed no difference in activation status compared with WT mice, as determined by CD40 expression (Fig. 7.15G). Interestingly however, the level of CD200R1 expression by CD200 KO F4/80⁺MHCII⁺ m ϕ was slightly increased compared with that in WT colonic m ϕ (Fig. 7.15G).

I also thought it important to examine whether there was any histological evidence of spontaneous intestinal inflammation in CD200 KO mice. However analysis of H&E stained sections revealed no inflammatory infiltrates, crypt elongation or epithelial disruption (Fig. 7.16). Consistent with this, there was no significant difference in the frequency of neutrophils in the LP of resting WT and CD200 KO mice, although there was a trend towards increased proportions and numbers of neutrophils in CD200 KO colon (Fig. 7.16B).

7.9 Experimental Colitis in CD200 KO Mice

Previous studies in CD200 KO mice have shown they are more susceptible to a number of forms of immunopathology (113, 116, 119) and therefore I examined whether lack of CD200 would influence the development of DSS colitis.

Consistent with my previous experiments, WT mice began to lose weight and developed clinical disease symptoms by d4 of DSS administration. Although CD200 KO mice showed slightly delayed disease onset, with statistically lower bodyweight loss at d4 and d5, their weight loss and disease score accelerated after this point so that by d6, there were no differences in weight loss or disease score between WT and CD200 KO mice (Fig. 7.17A and B). There were also no differences in colon shortening and both strains showed identical histological features of colitis (Fig. 7.17C and D).

Although insufficient CD200 KO mice were available for me to repeat these experiments or to assess the functional characteristics of CD200 KO colonic m ϕ , these studies suggest that spontaneous colitis or intestinal m ϕ hyperactivity is not a feature of CD200 deficiency. Furthermore, lack of CD200 does not render mice more susceptible to chemical colitis.

7.10 Effects of CD200-Fc Fusion Protein on Macrophage Responsiveness

In a final attempt to assess the importance of the CD200R1-CD200 axis in regulating m ϕ behaviour, I used a CD200-Fc fusion protein to ligate CD200R1 *in vitro*, as this has been shown previously to attenuate pro-inflammatory cytokine production (119, 125, 259). CSF-1 generated BMM were stimulated with LPS, IFN γ or with LPS + IFN γ *in vitro*, with or without pre-incubation with CD200-Fc fusion protein. Pre-treatment of BMM with CD200-Fc fusion protein had no effect on the frequency of TNF α -producing cells after stimulation with LPS (Fig. 7.18), or on the upregulation of CD40, CD86 and MHC class II after stimulation with LPS, IFN γ or LPS and IFN γ (Fig. 7.19).

7.11 Summary

The results in this chapter demonstrate that despite expression of CD200R1 by resident colonic m ϕ and the high abundance of CD200 in the intestine, deletion of CD200R1 had no consistent effect on the number, activation status and TLR-responsiveness of intestinal m ϕ . In addition, CD200R1 KO mice did not develop spontaneous intestinal inflammation, even when maintained under SPF conditions for up to 18 months. CD200R1 KO mice also had normal susceptibility to DSS-induced colitis. Together with the lack of abnormalities in

intrinsic m ϕ function, these results suggest that the absence of CD200R1 does not lead to m ϕ hyperactivity in the intestine. Similar results were seen in CD200 KO mice, which showed normal colonic m ϕ numbers and activation status, as well as no enhanced susceptibility to spontaneous or DSS induced colitis. Preliminary studies also indicated that deliberate ligation of CD200R1 on m ϕ *in vitro* did not alter their activation by innate stimuli. Thus, taken together, these studies suggest that it is unlikely the CD200R1-CD200 regulatory axis alone plays an essential role in controlling m ϕ behaviour in the steady state or inflamed colon.

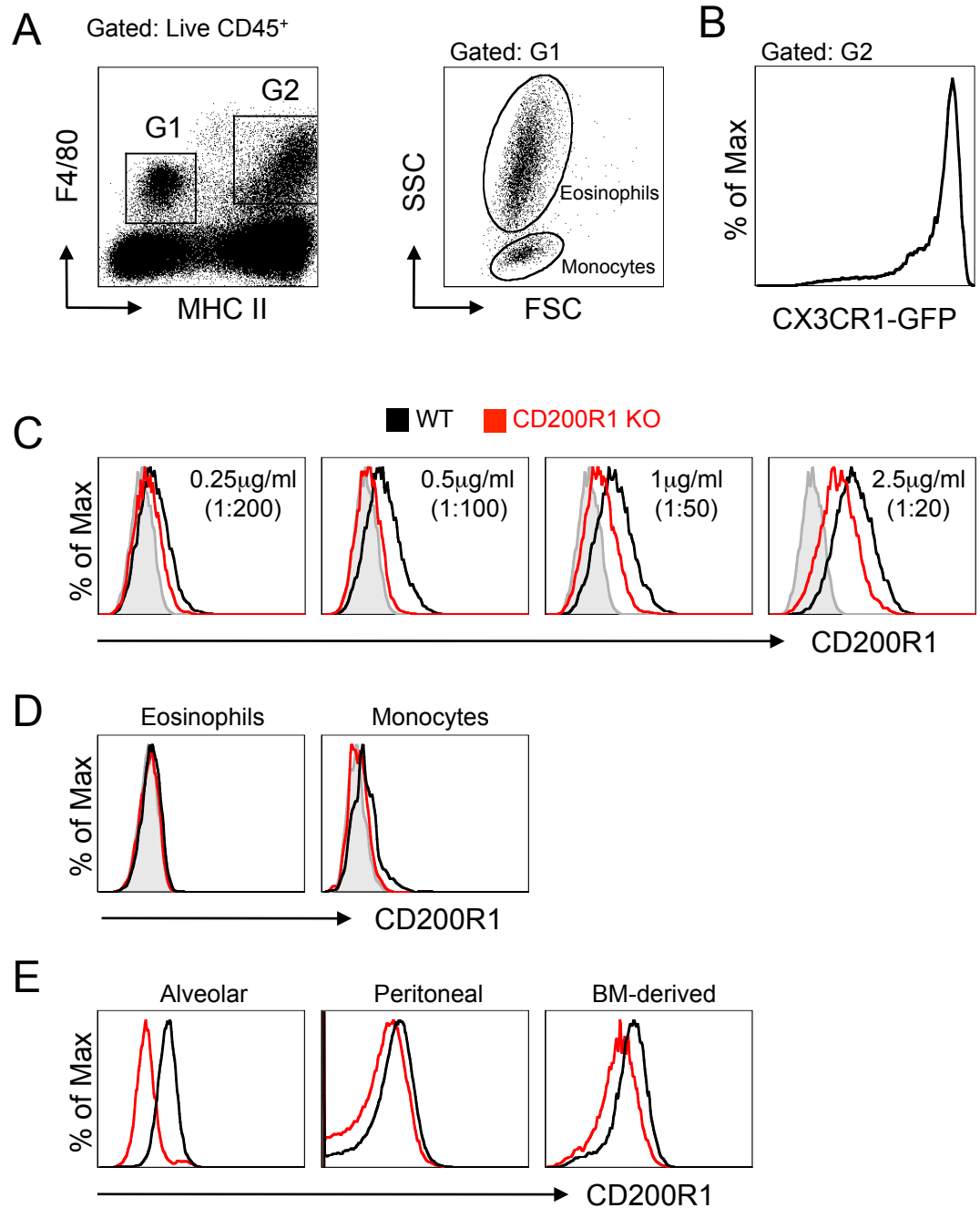


Figure 7.1: CD200R1 Expression by Myeloid Cells from Different Tissues

Colonic LP cells were isolated from resting WT mice and live-gated CD45⁺ cells were analysed for the expression of F4/80 and class II MHC. **A**. Representative dot plots showing the gating strategy used in this chapter, where m ϕ were identified as F4/80⁺MHCII⁺ and where eosinophils and monocytes could be distinguished in the F4/80^{low}MHCII^{neg} gate by their SSC profile. **B**. Expression of CX3CR1-GFP by live-gated CD45⁺F4/80⁺MHCII⁺ cells from resting CX3CR1^{+gfp} mice, showing that the vast majority are CX3CR1^{high}. **C**. Titration of anti-CD200R1 antibody using live-gated CD45⁺F4/80⁺MHCII⁺ colonic LP cells from WT (black) or CD200R1 (red) mice, showing the optimal concentration to be 0.5µg/ml. Expression of CD200R1 by intestinal eosinophils and monocytes (**D**) and by m ϕ from bronchoalveolar lavage (BAL), peritoneum or CSF-1 generated BMM (**E**) from resting WT (*black*) and CD200R1 KO (*red*) mice. Shaded histograms represent appropriate isotype control. Numbers represent the mean fluorescence intensity (MFI). Representative of 2 individual experiments.

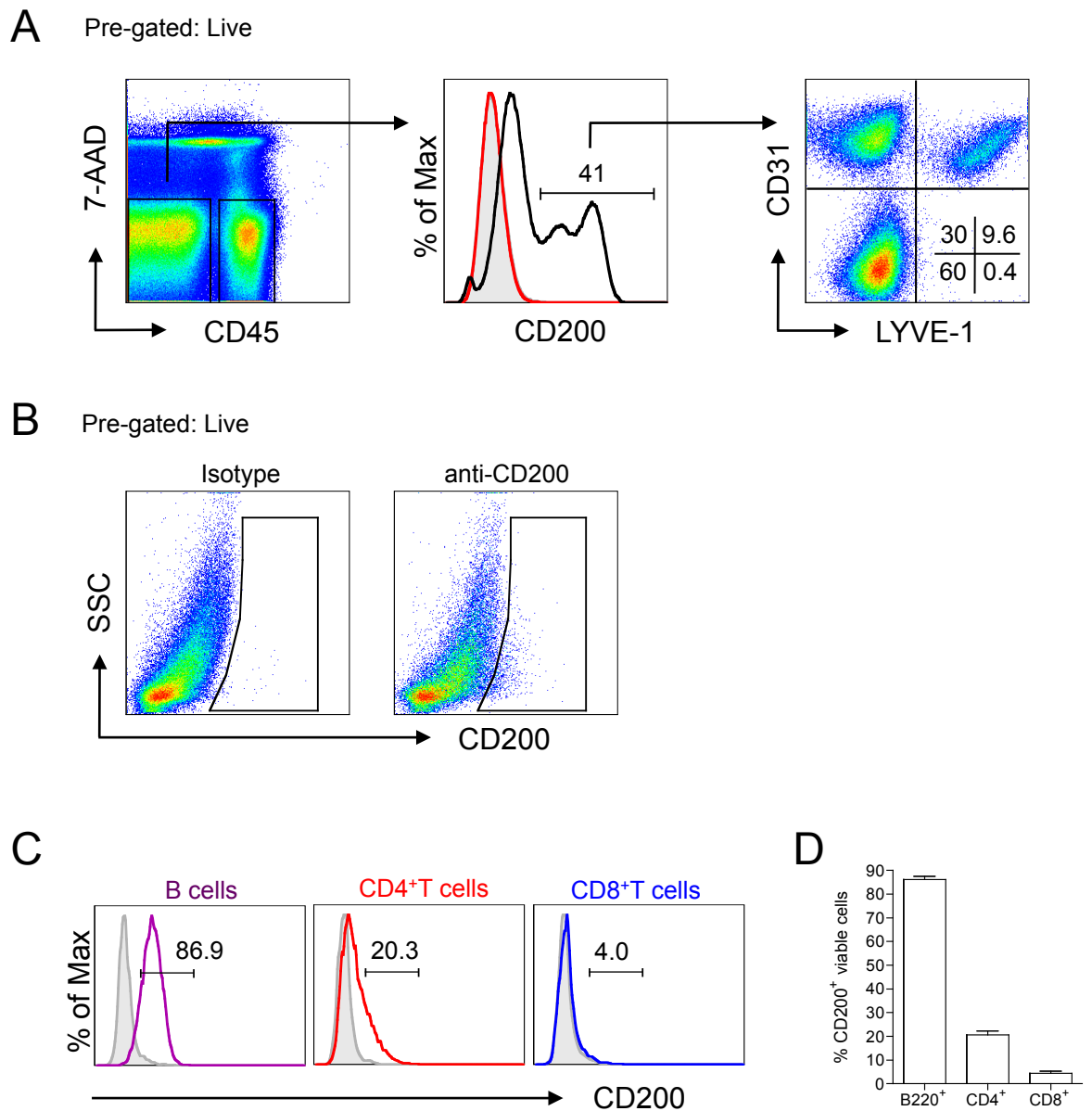


Figure 7.2: CD200 Expression in the Colon

A. Colonic LP cells were isolated from WT (*black line*) or CD200 KO (*red line*) mice and the expression of CD200 by live-gated CD45^{neg} cells (*middle panel*) was examined together with the expression of the endothelial markers CD31 (PECAM-1) and LYVE-1 on CD45^{neg} cells was examined by flow cytometry. Shaded histogram represents staining with the appropriate isotype control. **B.** Expression of CD200 on epithelial cells obtained from the first EDTA-wash step during colon isolation. **C.** Representative CD200 expression by live-gated CD45⁺ colonic B220⁺ (B cells), CD3⁺CD4⁺ (CD4⁺ T cells) and CD3⁺CD8⁺ cells (CD8⁺ T cells) from WT colon and the mean proportion + 1SD of CD200⁺ cells within each lymphocyte population. Shaded histograms represent appropriate isotype control. Representative of 2 individual experiments.

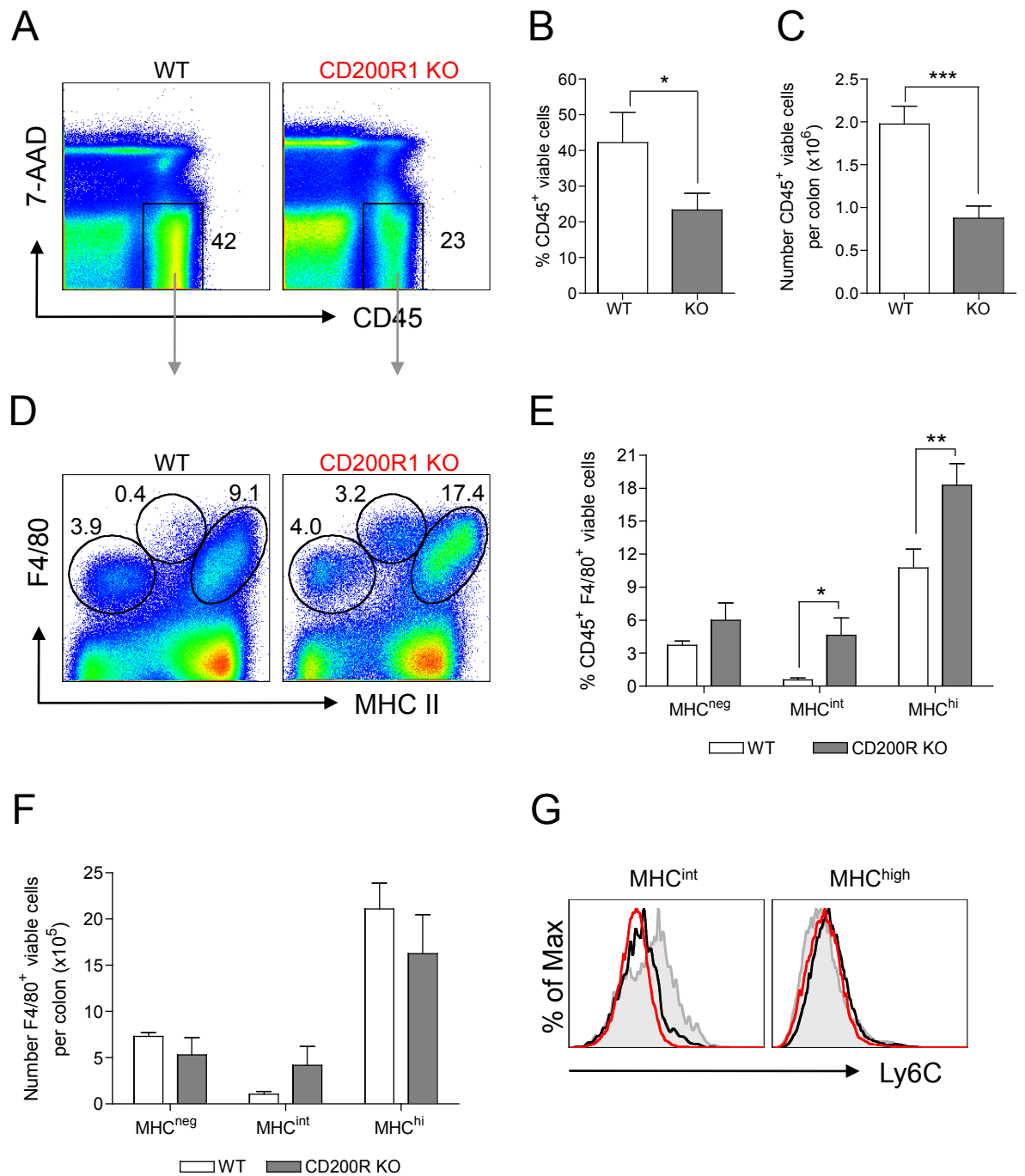


Figure 7.3: Characterisation of Colonic Macrophages in CD200R1 KO Mice

Colonic LP cells were isolated from resting WT and CD200R1 KO mice and analysed for the expression of CD45, F4/80, MHC II and Ly6C by flow cytometry. **A.** Representative dot plots of CD45 expression on single cells from WT and CD200R1 KO mice. The percentage (**B**) and absolute numbers (**C**) of live-gated CD45⁺ cells per colon. **D.** Representative dot plots of F4/80 and class II MHC expression by live-gated CD45⁺ cells from WT and CD200R1 KO mice. The percentage (**E**) and absolute numbers (**F**) of live F4/80⁺MHC II^{neg}, F4/80⁺MHC II^{int} and F4/80⁺MHC II^{high} (m ϕ) live cells per colon. Results are the mean percentages and absolute numbers + 1SD for 3-4mice/group and are representative of at least 3 individual experiments. **G.** Representative expression of Ly6C by F4/80⁺MHC II^{int} and F4/80⁺MHC II^{high} cells (* p<0.05, **p<0.01, ***p<0.001. Student's t test)

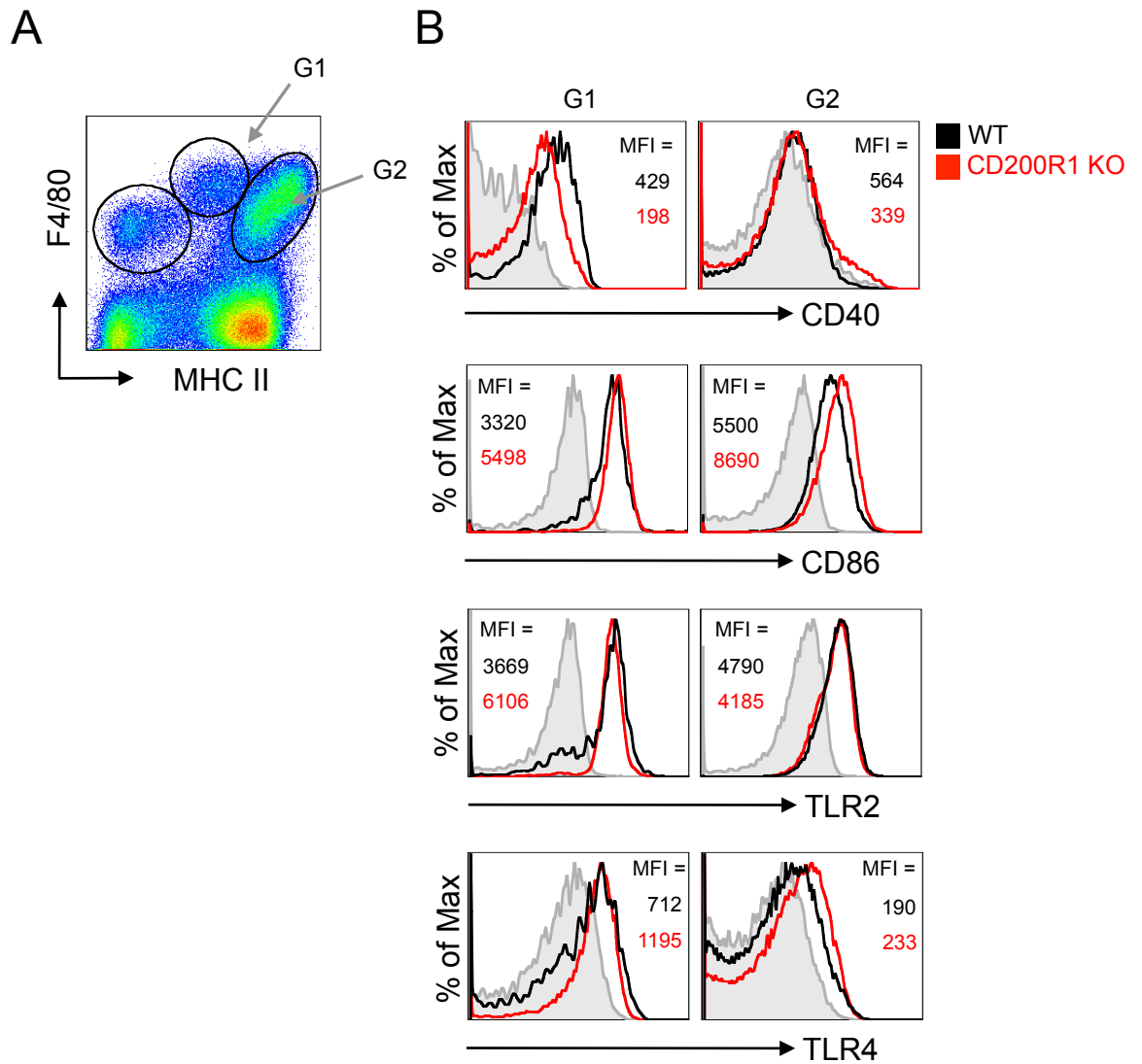


Figure 7.4: Activation Status of Colonic Macrophages from CD200R1 KO Mice

Colonic LP cells were isolated from resting WT and CD200R1 KO mice and live-gated CD45⁺ F4/80⁺MHCII⁺ cells analysed for the expression of CD40, CD86, TLR2 and TLR4 by flow cytometry. **A**. Representative dot plots of F4/80 and class II MHC expression on CD200R1 KO LP cells, showing G1 (F4/80⁺MHCII^{int}) and G2 (F4/80⁺MHCII^{high}) gates used in subsequent plots. **B**. Expression of CD40, CD86, TLR2 and TLR4 by cells in G1 and G2. Numbers represent the mean fluorescence intensity (MFI) for WT (*black*) and CD200R1 KO (*red*) cells. Representative of 2 individual experiments.

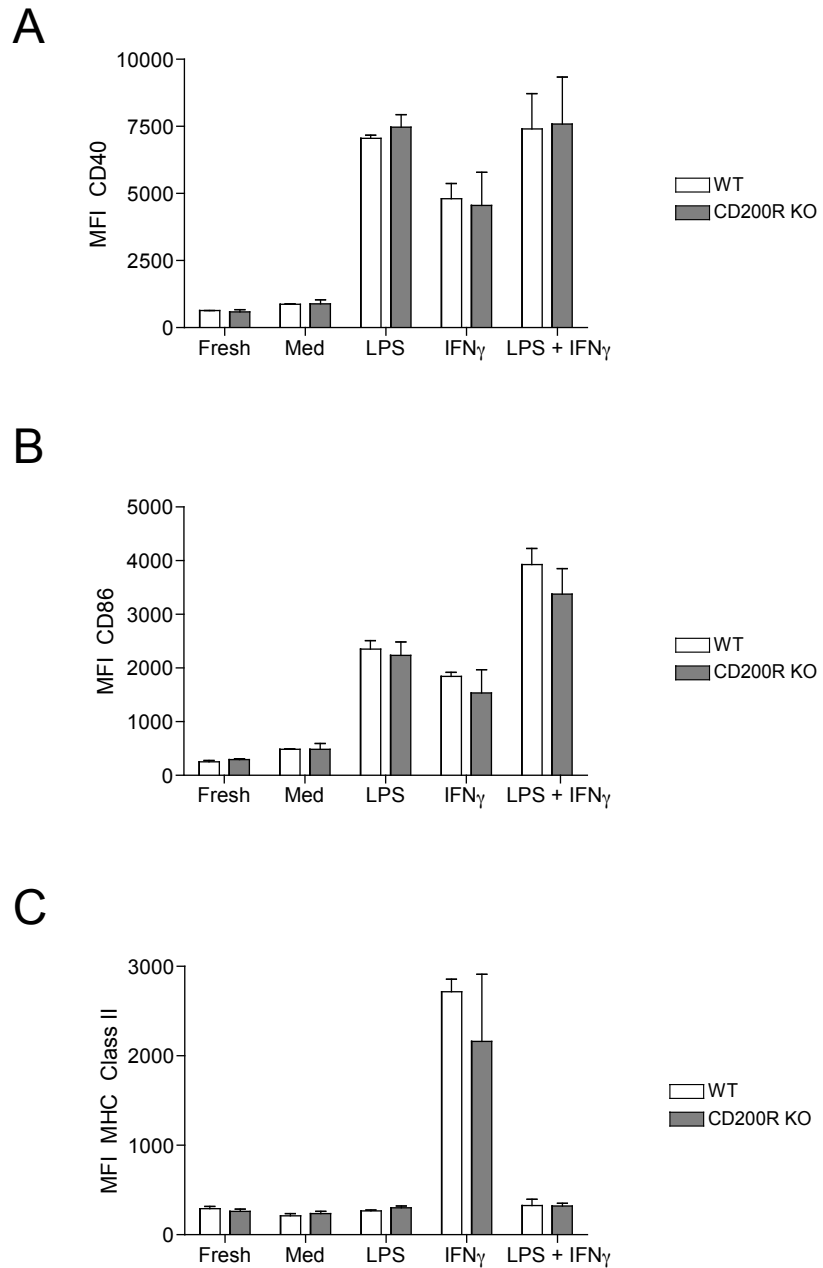


Figure 7.5: Responsiveness of CD200R1 KO Bone Marrow Derived Macrophages to Pro-inflammatory Stimuli

CSF-1 generated BM macrophages (BMM) from WT or CD200R1KO mice were harvested after 6 days of culture and incubated for 24hrs in medium alone (Med), 1 μ g/ml LPS, 100U IFN γ or LPS and IFN γ . Expression of CD40 (**A**), CD80 (**B**) and class II MHC (**C**) was determined by flow cytometry. Results shown are the mean fluorescence intensity (MFI) for WT (white bars) and CD200R1 KO (grey bars) cells + 1 SD for 3 mice/group and are representative of 2 individual experiments.

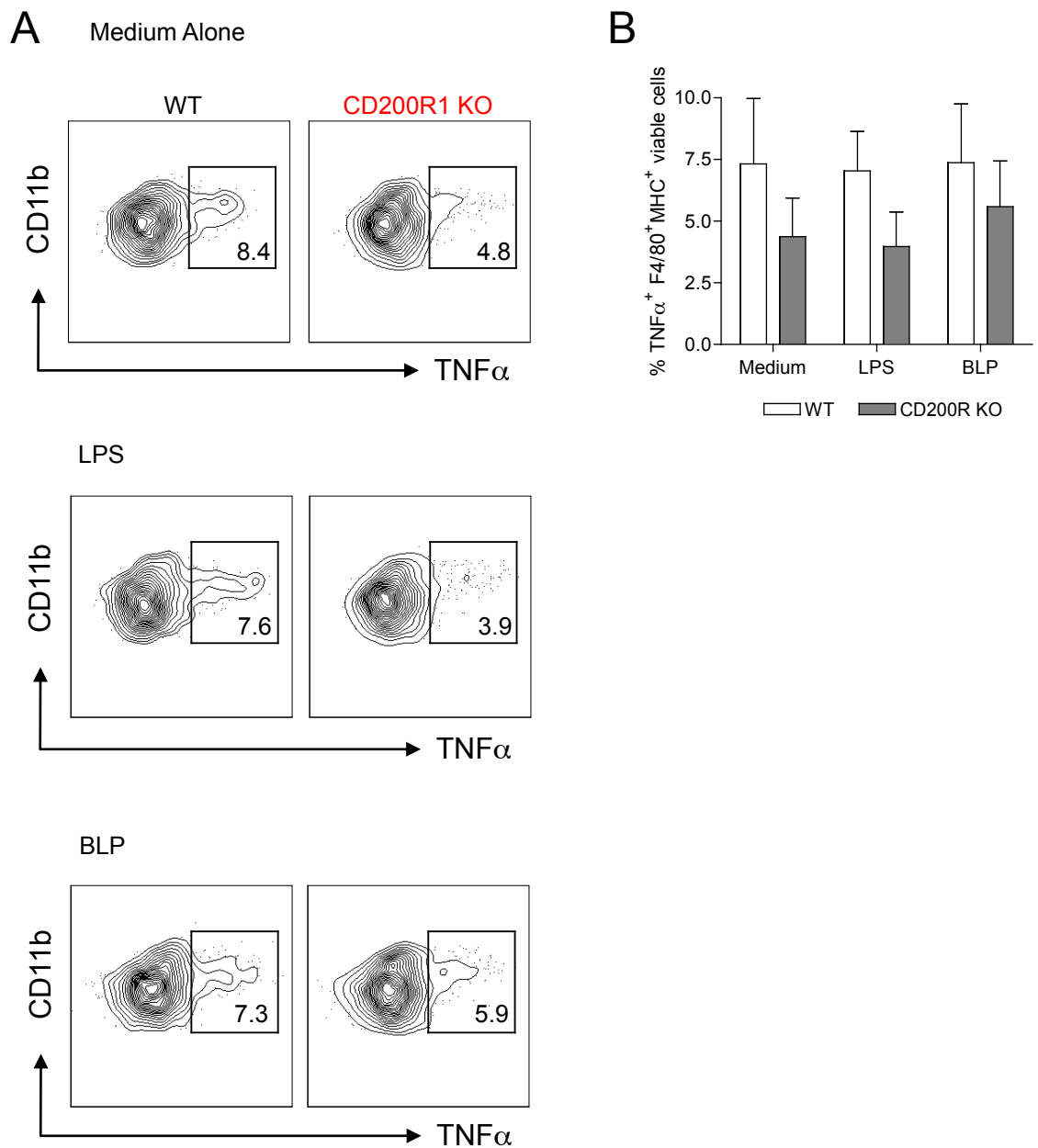


Figure 7.6: TNF α Production by Colonic Macrophages from CD200R1 KO Mice following TLR Stimulation

Colonic LP cells were isolated from resting WT or CD200R1 KO mice and incubated for 4.5hrs with BFA and monensin in either medium alone, or together with 1 μ g/ml LPS or 1 μ g/ml BLP and analysed for the presence of intracellular TNF α by flow cytometry. **A.** Representative CD11b and TNF α staining of colonic F4/80⁺MHCII⁺ cells from WT or CD200R1 KO mice. **B.** The mean frequency of TNF α ⁺ m ϕ from WT and CD200R1 KO mice + 1SD for 3-4 mice/group and results are representative of 2 individual experiments.

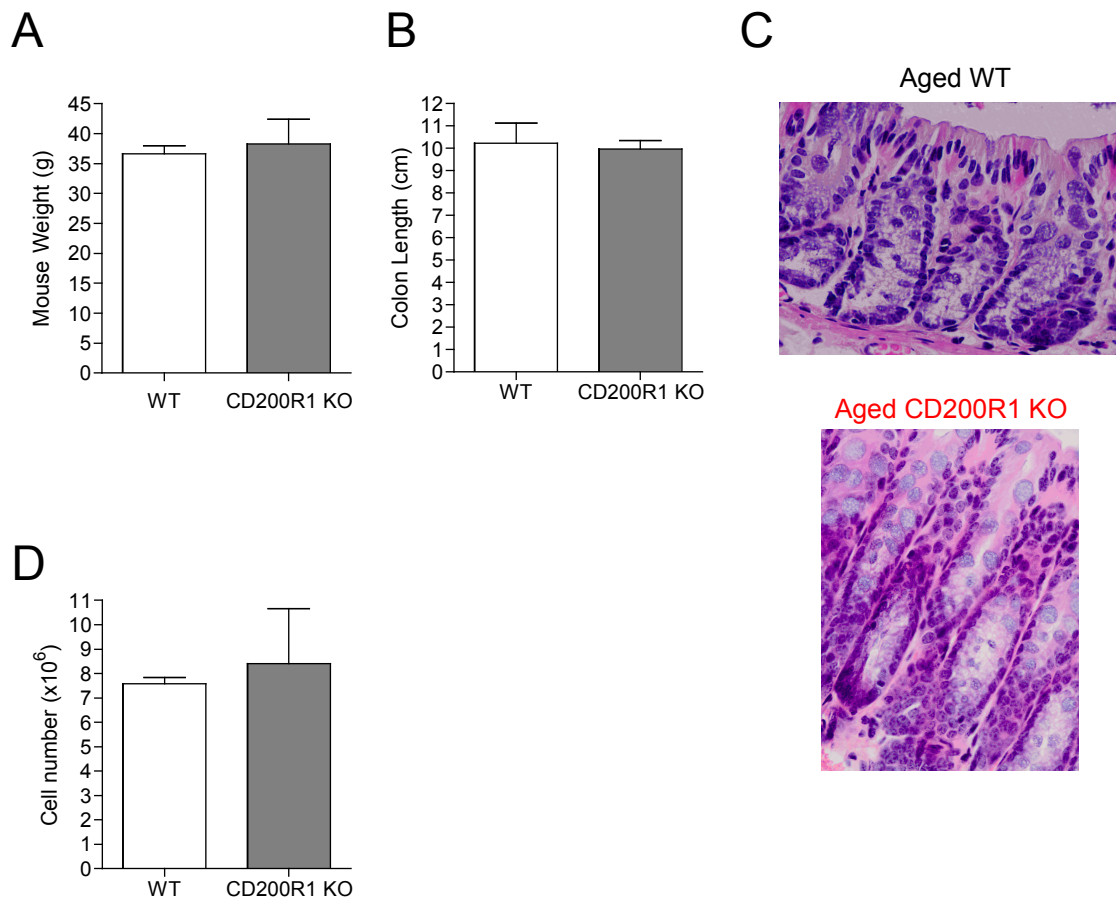


Figure 7.7: Absence of Spontaneous Intestinal Inflammation in Aged CD200R1 KO Mice

WT and CD200R1 KO mice were maintained under SPF conditions for 16-18months, after which time their bodyweights (**A**) and colon lengths (**B**) were assessed. **C**. Histological analysis of H&E stained sections of distal colon from aged WT and CD200R1 KO mice (final magnification x400). **D**. The number of colonic LP cells per colon from aged WT or CD200R1 KO mice. Results are the means + 1SD for 3-4 mice/group and are representative of 2 individual experiments.

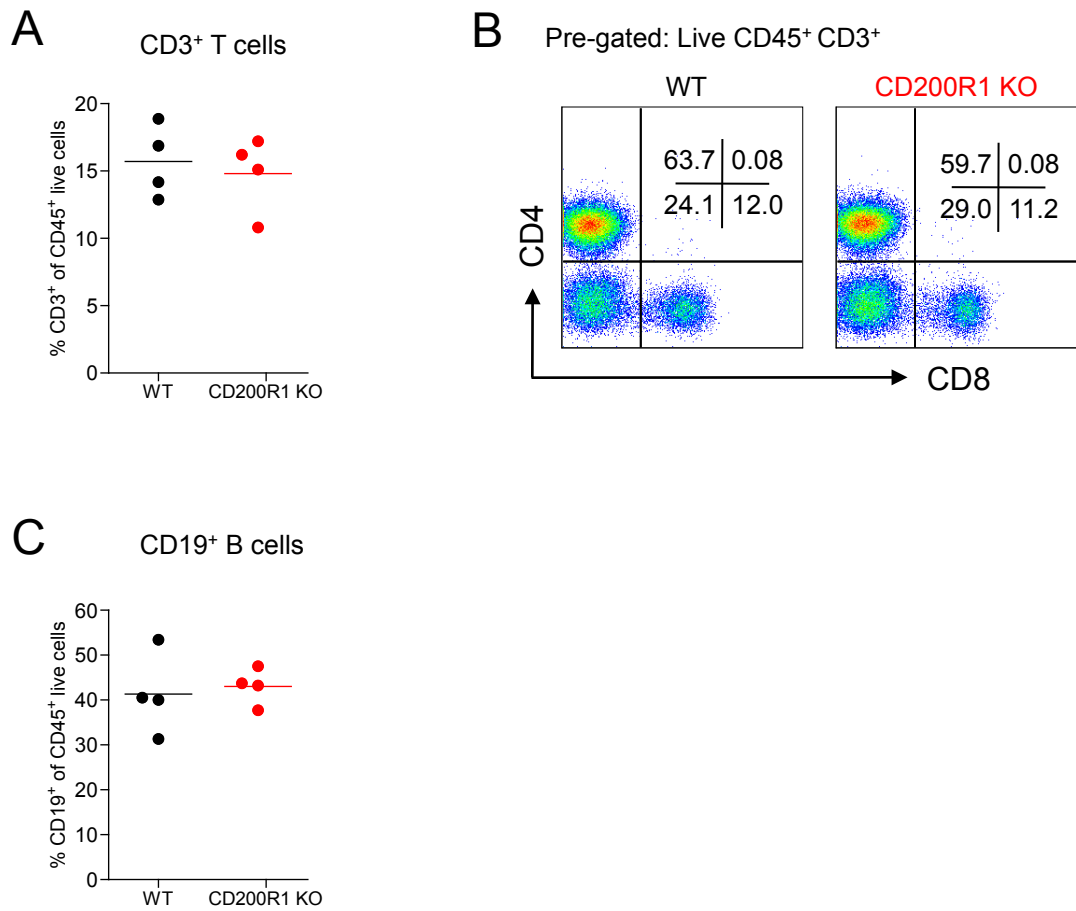


Figure 7.8: T- and B-lymphocytes in the Colonic Mucosa of Aged CD200R1 KO Mice

LP cells were isolated from the colon of resting 16 month old WT and CD200R1 KO mice and live-gated CD45⁺ cells were analysed for the expression of CD19 and CD3 by flow cytometry to detect B- and T-lymphocytes, respectively. **A.** Mean proportion of CD3⁺ T-cells amongst live-gated CD45⁺ cells. **B.** Representative dot plots of CD4 and CD8 expression showing the composition of the CD3⁺ compartment. **C.** The frequency of CD19⁺ B cells amongst live-gated CD45⁺ cells. Results are the means + 1SD and represent 1 experiment with 4mice/group.

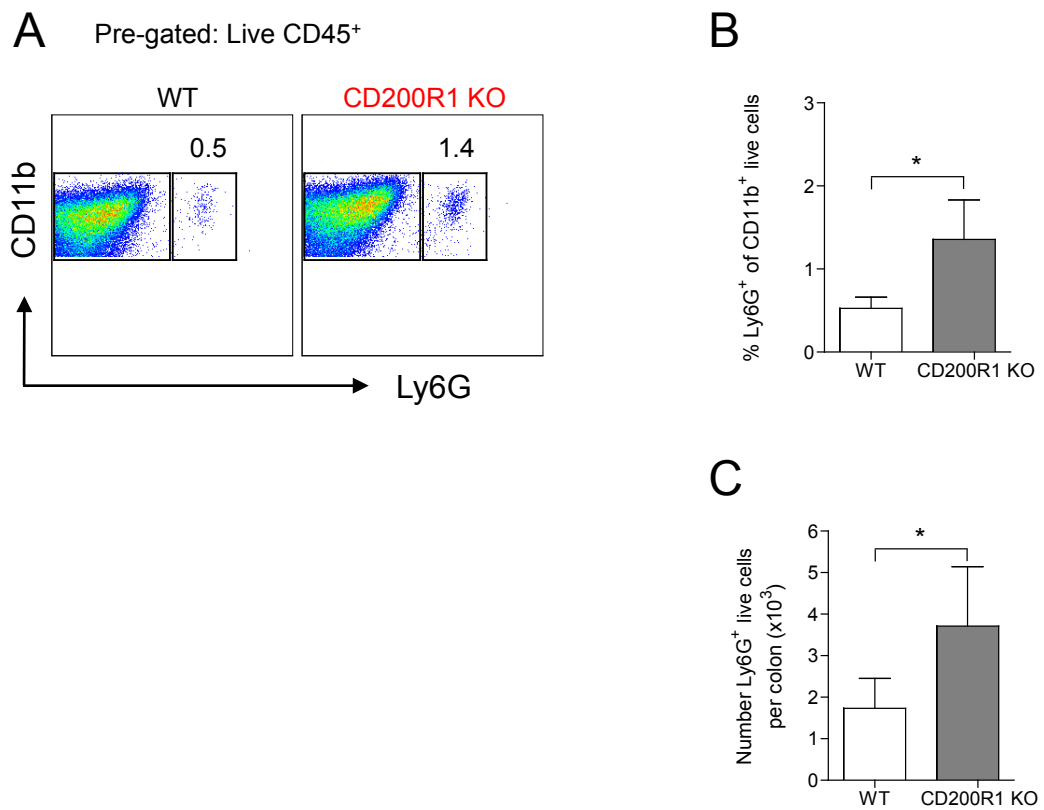


Figure 7.9: Presence of Neutrophils in the Colon of Aged CD200R1 KO Mice

LP cells were isolated from the colon of resting 16 month old WT and CD200R1 KO mice and analysed for the presence of Ly6G⁺ neutrophils by flow cytometry. **A**. Representative staining of Ly6G and CD11b amongst live-gated CD45⁺ cells. The proportion of Ly6G⁺ cells within the live CD11b⁺ fraction (**B**) and absolute numbers (**C**) of Ly6G⁺ cells per colon. Results are the means + 1SD and represent 1 experiment with 4 mice/group. (* p<0.05, Student's t test)

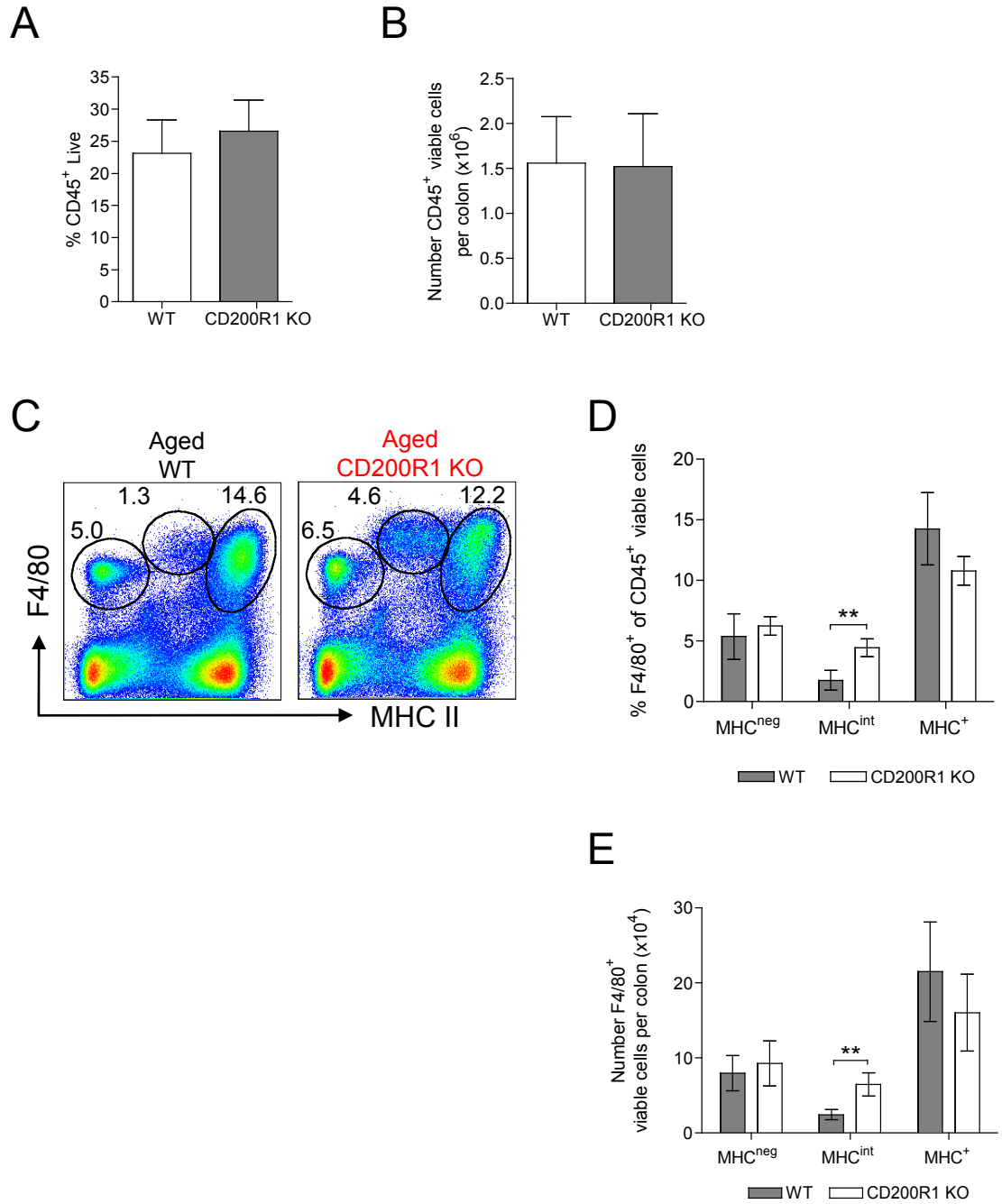


Figure 7.10: Characterisation of Colonic Macrophages from Aged CD200R1 KO Mice

Colonic LP cells were isolated from the colon of resting 16 month old WT and CD200R1 KO mice and live-gated cells analysed for the expression of CD45, F4/80 and MHC II by flow cytometry. The percentage **(A)** and absolute numbers **(B)** of live-gated CD45⁺ cells per colon. **C.** Representative dot plots of F4/80 and class II MHC expression by live-gated CD45⁺ cells from WT and CD200R1 KO mice. The percentages **(D)** and absolute numbers **(E)** of live F4/80⁺ MHC II^{neg}, F4/80⁺ MHC II^{int} and F4/80⁺ MHC II^{high} (mφ) cells per colon. Results are the mean percentages and absolute numbers + 1SD and represent 1 experiment with 4 mice/group. (* p<0.05, ** p<0.005, Student's t test)

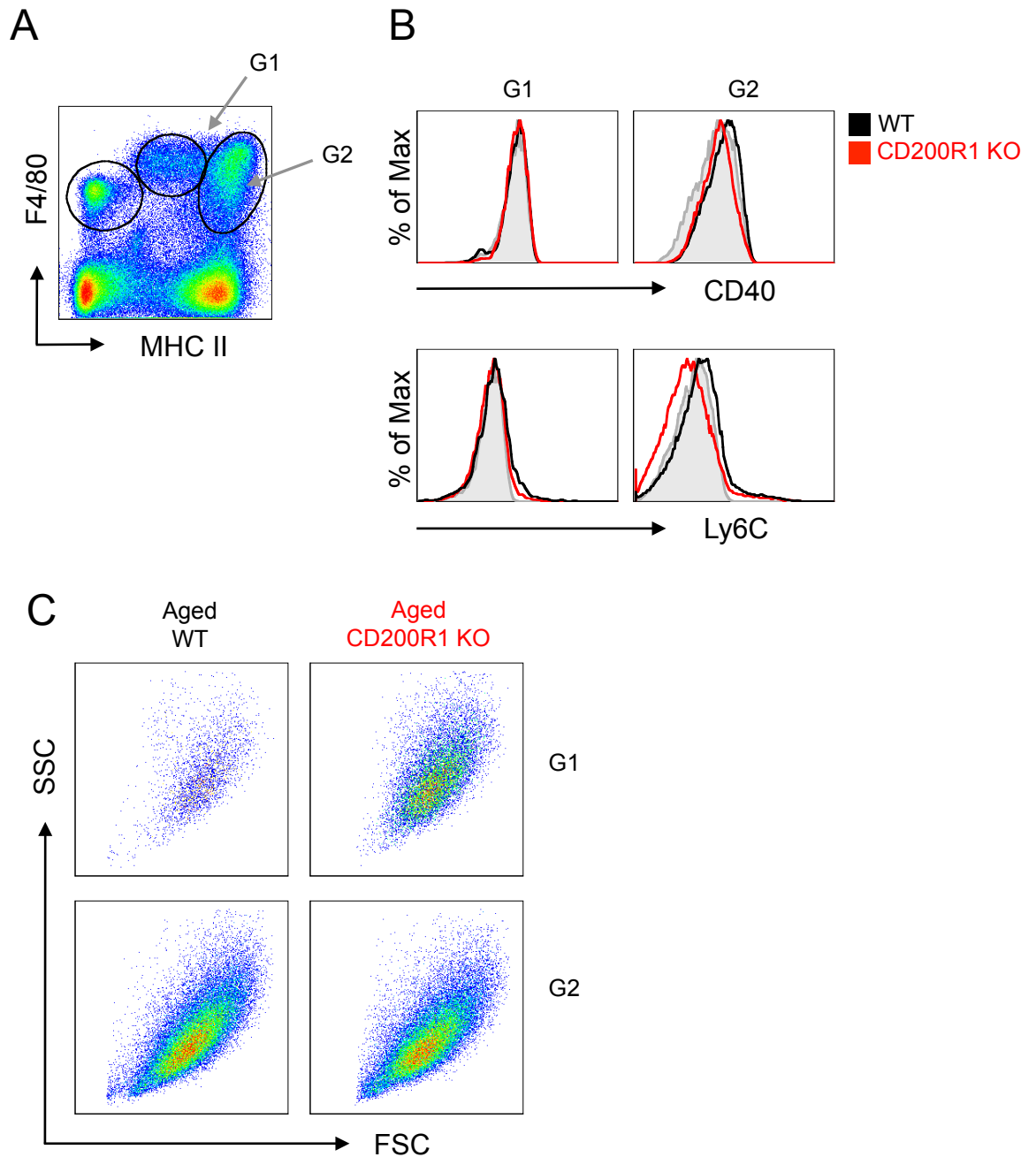


Figure 7.11: Characterisation of Colonic Macrophages from Aged CD200R1 KO Mice

A. Colonic LP cells were isolated from resting 16 month old WT and CD200R1 KO mice and live-gated CD45⁺ F4/80⁺ MHCII⁺ populations assessed for the expression of Ly6C and CD40 by flow cytometry. **B.** Expression of Ly6C and CD40 by F4/80⁺ MHCII^{int} cells (G1) and F4/80⁺ MHCII⁺ cells (G2) from WT (*black*) or CD200R1 KO (*red*) mice **C.** FSC and SSC profiles of F4/80⁺ MHCII^{int} cells (G1) and F4/80⁺ MHCII⁺ cells (G2) from aged WT or CD200R1 KO mice. Representative of 1 experiment.

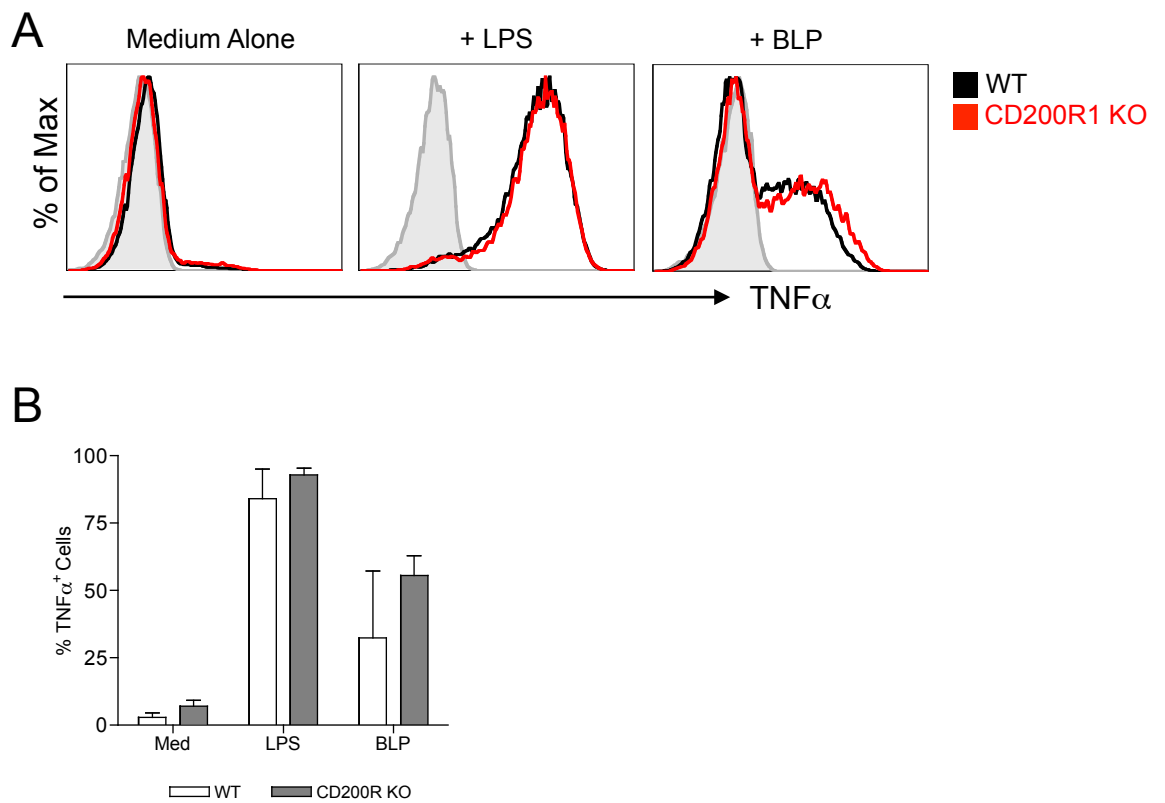


Figure 7.12: TLR Responsiveness of BM Macrophages from Aged CD200R1 KO Mice

CSF-1 generated BM macrophages (BMM) from 18 month aged WT or CD200R1KO mice were harvested after 6 days of culture and cultured with BFA and monensin for 4.5hrs in medium alone (Med), or together with 1 μ g/ml LPS or 1 μ g/ml BLP. Representative TNF α expression by WT or CD200R1 KO BMM (**A**) and the frequency of TNF α ⁺ cells after culture (**B**). Results shown are the mean frequency of TNF α ⁺ cells for WT (white bars) and CD200R1 KO mice (grey bars) + 1 SD and represent one experiment with 3 mice/group.

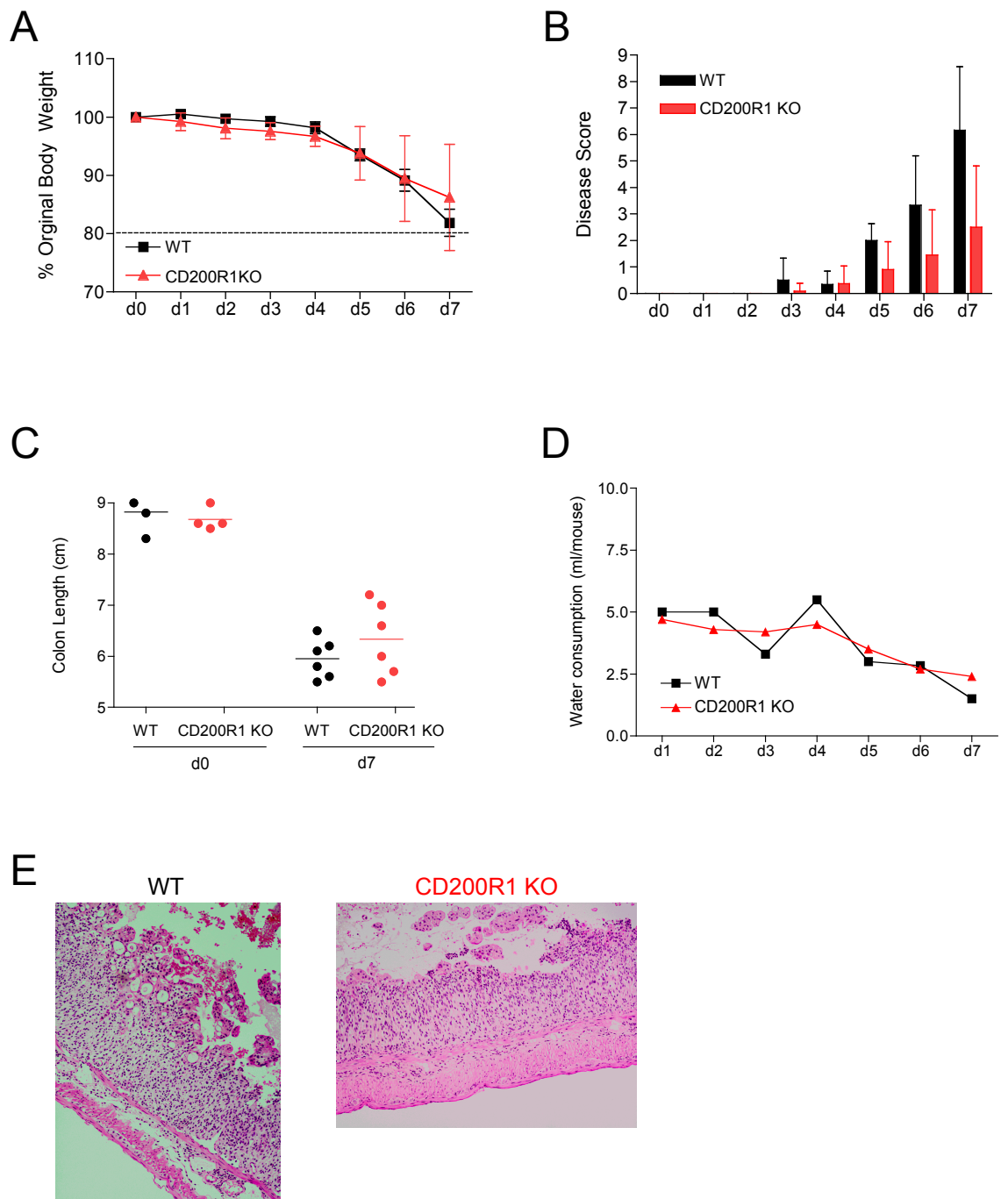


Figure 7.13: Progress of Experimental Colitis in CD200R1 KO Mice

WT or CD200R1 KO mice received 2% DSS in their drinking water for 7 days and their bodyweight (**A**) and clinical disease score (**B**) was recorded daily. Results are the means \pm 1 SD for 6 (WT) and 11 (CD200R1 KO) mice per group. On day 7 mice were culled and their colons measured and compared with resting mice (d0) (**C**). **D**. Water consumption (ml) per mouse on each day of colitis. On day 7 sections of distal colon were fixed in 10% formalin, embedded in paraffin and stained with H&E for histological analysis (final magnification x100). Identical degrees of architectural destruction and inflammation were seen. Results representative of 3 individual experiments.

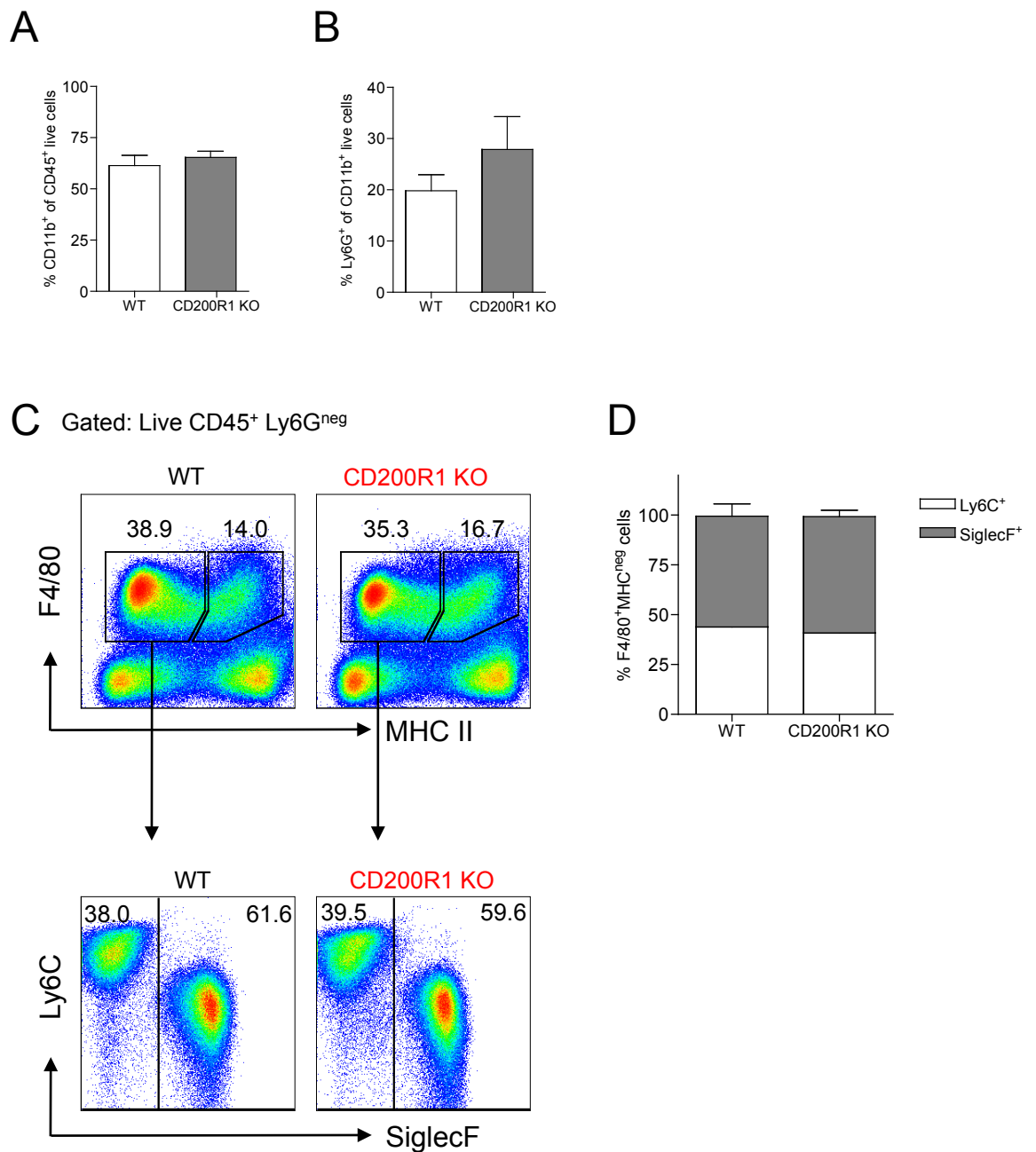


Figure 7.14: Characterisation of Myeloid Cells in Colon of CD200R1 KO Mice with DSS-induced Colitis

WT or CD200R1 KO mice received 2% DSS in their drinking water for 7 days. On day 7 mice were culled, their colons removed and LP cells isolated. Live-gated CD45⁺ LP cells were assessed for the expression of CD11b, Ly6G, F4/80, MHC II, Ly6C, and SiglecF by flow cytometry. **A.** The proportion of CD11b⁺ cells amongst the CD45⁺ live fraction. **B.** The proportion of Ly6G⁺ neutrophils amongst CD11b⁺ leucocytes. **C.** Representative dot plots of F4/80 and class II MHC expression by CD45⁺ Ly6G^{neg} cells (*upper panels*) and the composition of the F4/80⁺MHC^{neg} fraction (*lower panels*). **D.** The proportion of Ly6C^{high} monocytes and SiglecF⁺ eosinophils amongst F4/80⁺MHC^{neg} cells. Data are the means + 1SD for 3-4 mice/group and are representative of 2 individual experiments.

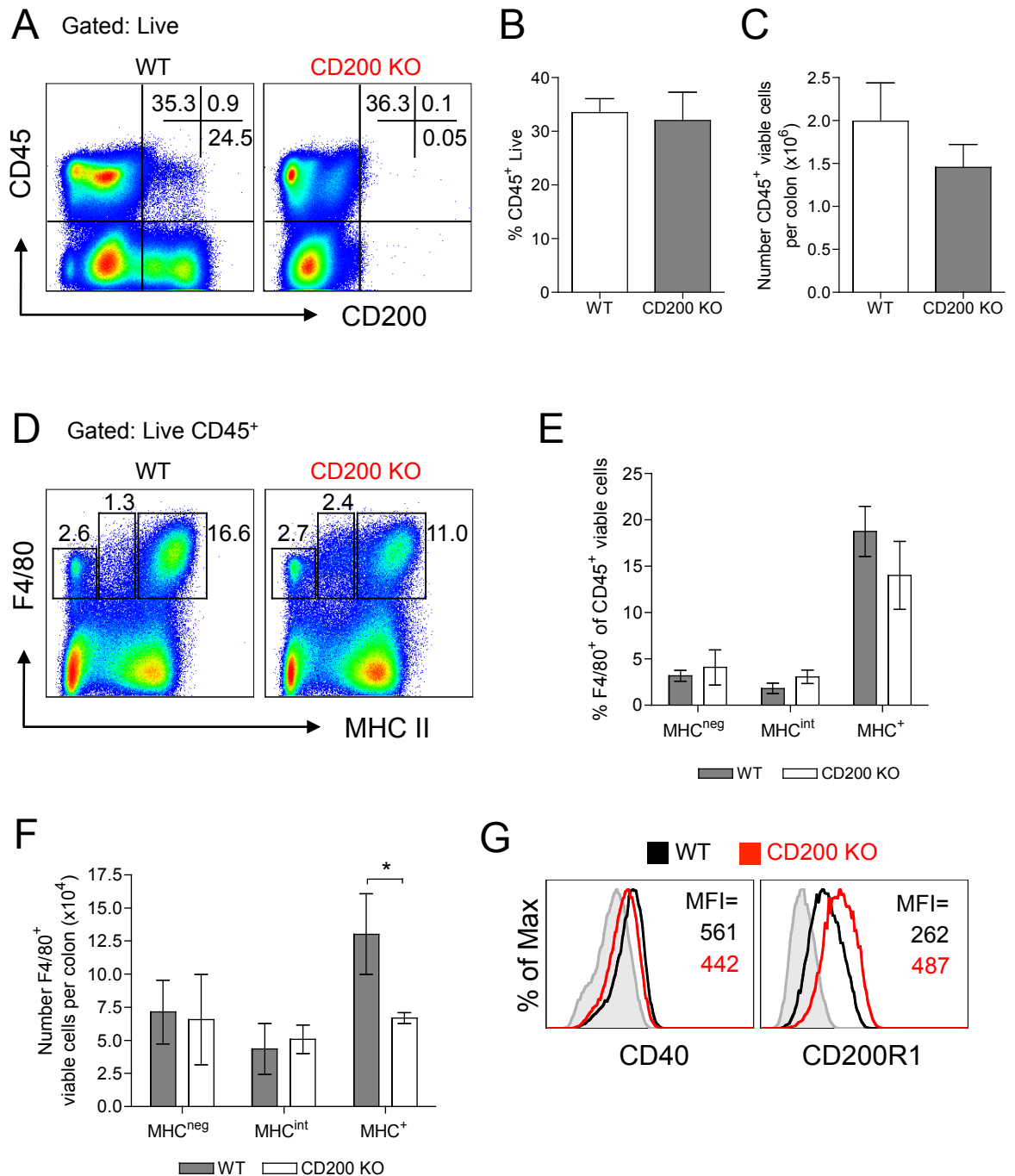


Figure 7.15: Characterisation of the Intestinal Myeloid Compartment of Resting CD200 KO Mice

Colonic LP cells were isolated from resting WT and CD200 KO mice and live-gated cells were analysed for the expression of CD45, CD200, F4/80 and MHC II by flow cytometry. **A**. Representative dot plots of CD45 and CD200 expression by live-gated cells. The percentages (**B**) and absolute numbers (**C**) of live-gated CD45⁺ cells per colon. **D**. Representative dot plots of F4/80 and class II MHC expression by live-gated CD45⁺ LP cells from WT and CD200 KO mice. The percentages (**E**) and absolute numbers (**F**) of F4/80⁺ MHCII^{neg}, F4/80⁺ MHCII^{int} and F4/80⁺ MHCII^{high} live cells per colon. **G**. Expression of CD40 and CD200R1 by F4/80⁺ MHCII^{high} mφ from WT (black) or CD200 KO mice (red). Results are the mean percentages and absolute numbers + 1SD and represent 1 experiment with 4 mice/group. (* p<0.05, ** p<0.005, Student's t test)

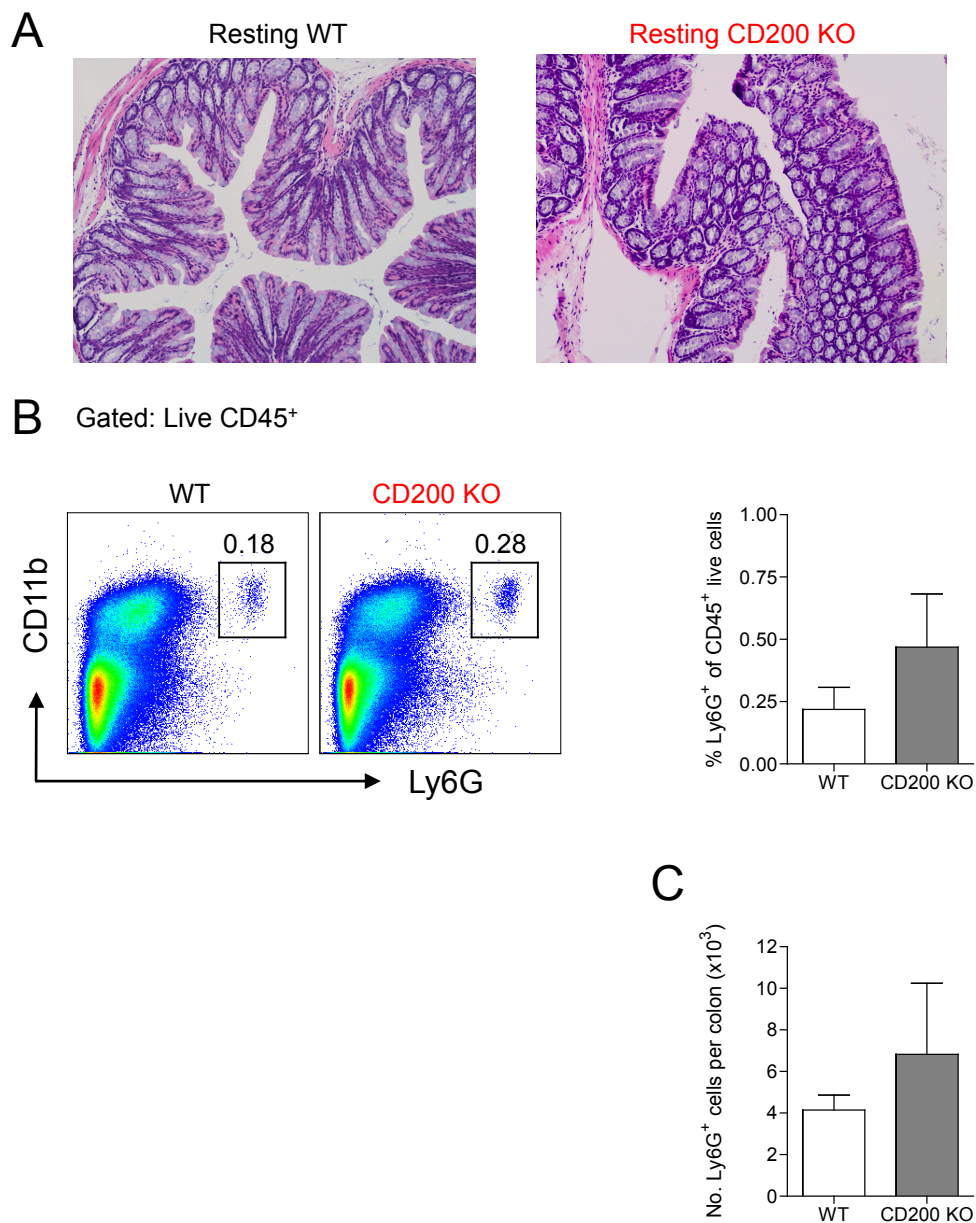


Figure 7.16: Absence of Spontaneous Intestinal Inflammation in CD200 KO Mice

A. Sections of distal colon from resting WT or CD200 KO mice were fixed in 10% formalin, embedded in paraffin and stained with H&E for histological analysis (final magnification x100). **B.** Colonic LP cells were isolated from resting WT and CD200 KO mice and live-gated CD45⁺ cells were analysed for the expression of Ly6G by flow cytometry. Representative expression of Ly6G and CD11b by live-gated CD45⁺ cells and the proportion of Ly6G⁺ neutrophils within the CD45⁺ live fraction. **C.** The absolute numbers of Ly6G⁺ neutrophils per colon of resting WT and CD200 KO mice. Results are the means + 1SD and represent a single experiment with 3-4 mice/group.

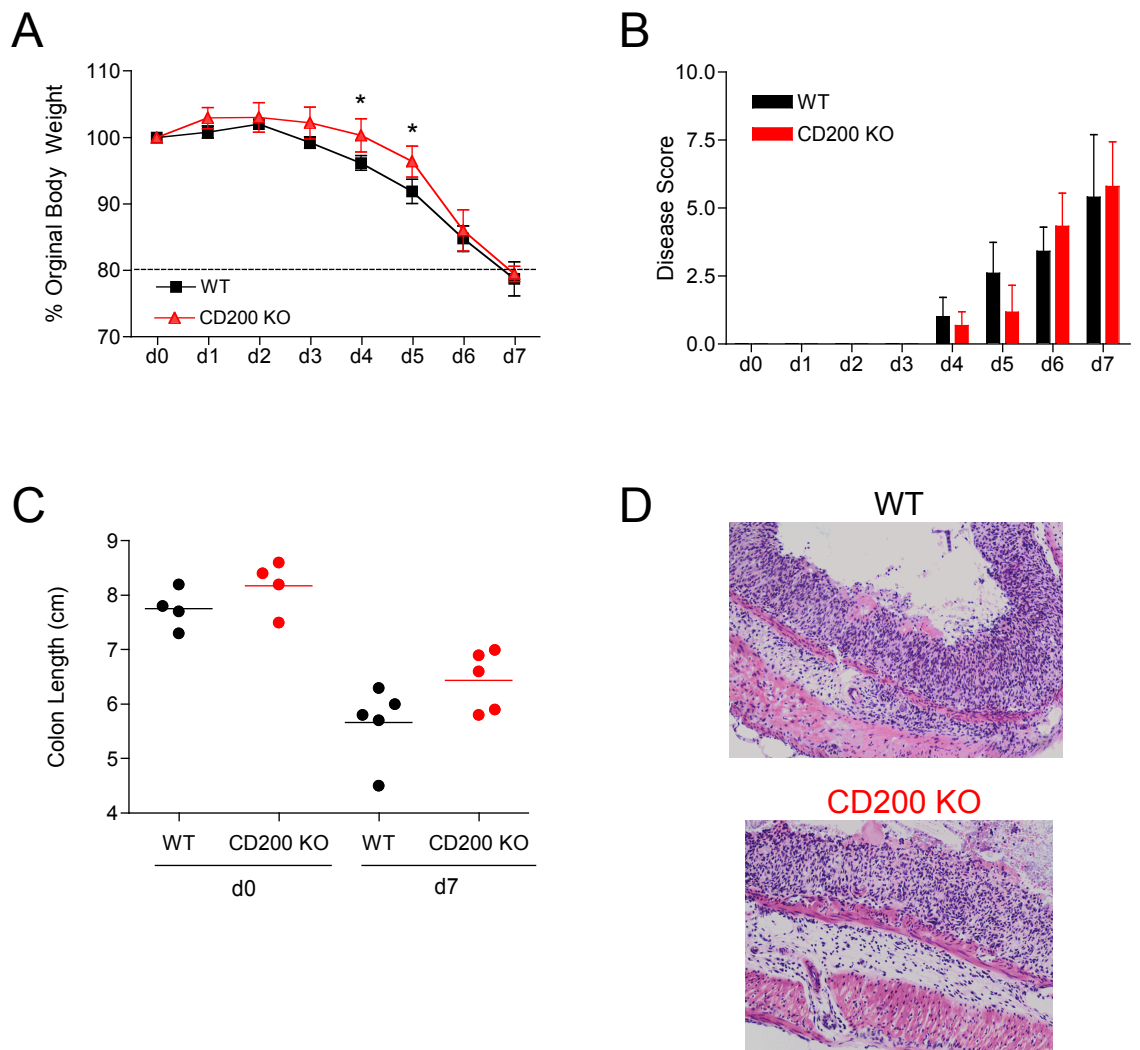


Figure 7.17: DSS Colitis in CD200 KO Mice

WT or CD200 KO mice received 2% DSS in their drinking water for 7 days and their bodyweight **(A)** and clinical disease score **(B)** was recorded daily. Results are representative of a single experiment and show the means \pm 1SD for 5 (WT) and 6 (CD200 KO) mice. On day 7 mice were culled and their colons measured and compared with resting mice (d0) **(C)**. **D.** Sections of distal colon from d7 colitic WT and CD200KO mice were fixed in 10% formalin, embedded in paraffin and stained with H&E for histological analysis showing identical patterns of colonic ulceration, loss of crypt architecture and inflammation (final magnification x100). (* $p < 0.05$, Student's t test)

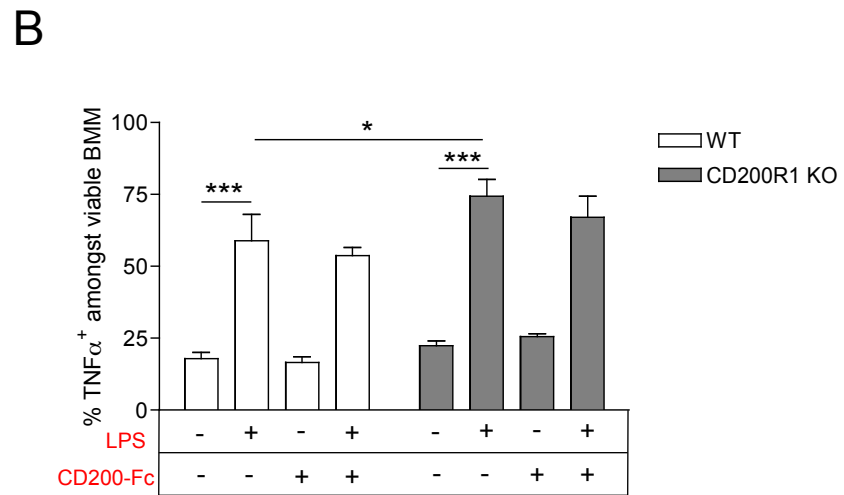
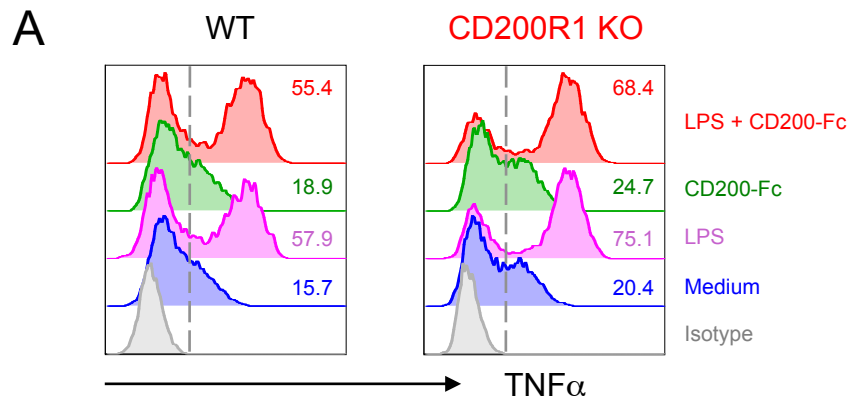


Figure 7.18: Effects of CD200-Fc Fusion Protein on Responsiveness of BMM to TLR Ligation

CSF-1 generated BM-derived macrophages (BMM) from WT or CD200R1 KO mice were harvested after 7 days of culture and incubated for 4.5 hrs in medium alone (Med), with 1 μ g/ml LPS, 100U IFN γ or with LPS + IFN γ together with BFA and monensin, after which the TNF α ⁺ cells was determined by flow cytometry. Cells were incubated or not with 2.5 μ g/ml CD200-Fc fusion protein from 1 hr before addition of TLR ligands. **A.** Representative histograms of TNF α expression by WT and CD200R1 KO BMM after culture under different conditions. **B.** Results are the mean proportions of TNF α ⁺ BMM for WT (*white bars*) and CD200R1 KO (*grey bars*) + 1 SD and represent a single experiment with 3 mice/group. (* p<0.05, *** p<0.001. One-way ANOVA followed by Bonferroni's post-test)

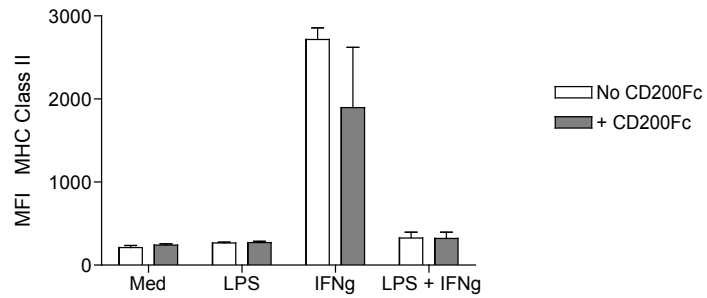
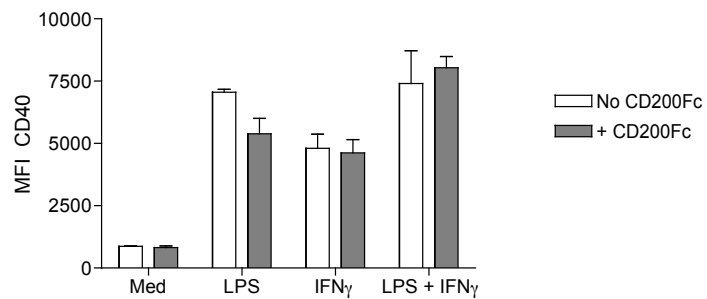
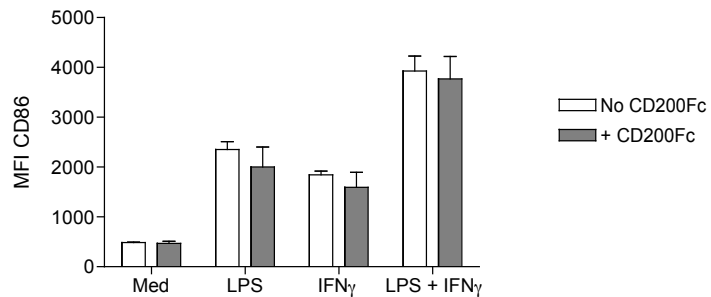
A**B****C**

Figure 7.19: Effects of CD200-Fc Fusion Protein on Responsiveness of BMM to TLR Ligation

CSF-1 generated BM-derived macrophages (BMM) from WT or CD200R1 KO mice were harvested after 7 days of culture and cultured for 4.5 hrs in medium alone (Med), with 1 μ g/ml LPS, 100U IFN γ or with LPS + IFN γ , together with BFA and monensin. Cells were incubated or not with 2.5 μ g/ml CD200-Fc fusion protein from 1 hr before addition of TLR ligands. Expression of MHC class II (**A**), CD40 (**B**) and CD86 (**C**) was determined by flow cytometry. Results are the mean fluorescence intensity (MFI) for WT (white bars) and CD200R1 KO (grey bars) + 1 SD and represent a single experiment with 3 mice/group.

Chapter 8

General Discussion

8.1 Introduction

The intestinal immune system has a constant task to perform in that it must respond robustly to pathogenic insult, but such responses mounted towards innocuous antigens such as dietary proteins or commensal microorganisms would be wasteful and dangerous. Indeed breakdown in the discrimination between harmless and harmful antigens results in the development of chronic inflammatory conditions such as IBD, where active immune responses are targeted against the commensal bacteria (130). M ϕ appear to play a central role in the pathogenesis of IBD, producing large quantities of pro-inflammatory cytokines and chemokines and thereby perpetuating inflammation. However intestinal m ϕ are also crucial for the maintenance of tissue homeostasis under resting conditions (260). How one population of cells can play such contrasting roles is unclear.

It is well established that resident intestinal m ϕ possess functional adaptations that are not seen in other peripheral tissue m ϕ , allowing them to exist in the microbe and antigen rich environment of the intestinal mucosa without provoking inflammation. Studies with m ϕ from human small intestinal biopsies have shown that intestinal m ϕ are extremely phagocytic and can kill bacteria very efficiently (171). However neither phagocytosis nor stimulation of gut m ϕ with bacterial products or pro-inflammatory cytokines results in 'classical' activation characterised by pro-inflammatory mediator release (171). Rather resident intestinal m ϕ appear to produce immunomodulatory cytokines such as IL10 and TGF β (178, 179). However, the composition of the intestinal m ϕ population changes markedly during IBD, with the accumulation of a phenotypically distinct population of pro-inflammatory CD14⁺ m ϕ in the inflamed mucosa (242). It is unclear whether these pro-inflammatory m ϕ represent newly recruited cells, or if resident m ϕ can alter their phenotype and function. As a result it is also unknown whether distinct precursor populations are involved in replenishing the different m ϕ populations. A better understanding of m ϕ subsets and their relationship to one another could allow them to be selectively targeted as a means of dampening inflammation during IBD.

My project set out to build on previous studies in the lab examining m ϕ of the mouse colon in steady state and experimental colitis, which had been carried out by a former PhD student, Andrew Platt. These studies concluded that the

mouse colon contained two independent subsets of m ϕ that were distinguishable on the basis of TLR2 (222). In the steady state, F4/80⁺TLR2^{neg} m ϕ were shown to dominate and they were unresponsive to TLR stimulation, as well as lacking expression of both class II MHC and CCR2. During experimental colitis, these F4/80⁺TLR2^{neg} m ϕ were outnumbered by newly recruited F4/80⁺TLR2⁺ m ϕ that expressed class II MHC and high levels of CCR2, and produced TNF α in response to TLR stimulation. However when I started my project there was growing concern that many of the standard techniques used to identify MP in the intestinal mucosa were not reliable. Not only were there major discrepancies in the ways in which different investigators isolated and defined mucosal m ϕ , but there was increased appreciation that markers such as F4/80, CD11b, class II MHC and in particular CD11c, could not discriminate between m ϕ and DC when used in isolation (261, 262). Therefore with the benefit of access to more powerful tools such as multi-parameter flow cytometry and CX3CR1-GFP reporter mice, the aims of this thesis were to carry out a comprehensive re-examination of the phenotype, function and origin of m ϕ in the mouse colon under different conditions.

8.2 Macrophages in Steady State Colon

8.2.1 The Phenotype of Macrophages in the Steady State Mucosa

Although much progress had been made in examining the phenotype and function of colonic m ϕ before I started my work, the studies in the lab had been restricted to 4-colour flow cytometry and had identified m ϕ solely on the basis of F4/80. Using the improved methodology available to me, I quickly identified several problems with the earlier findings. Firstly, there appeared to be a population of non-haematopoietic cells that expressed F4/80 and secondly, other leucocytes such as eosinophils also expressed F4/80, albeit at low levels. As a result, four colour flow cytometry was inadequate to identify and characterise m ϕ accurately. At this time, there were no published protocols for analysing mouse intestinal m ϕ using more detailed methods and therefore in Chapter 3, I first established multi-colour staining methods and gating strategies to assess the m ϕ populations of the colonic mucosa under physiological conditions.

As I was starting my work, findings in the Agace and Pabst labs suggested that mutually exclusive expression of CD103 and CX3CR1 could be used to identify mucosal DC and m ϕ respectively (189). This contested previous studies

which had classified CX3CR1⁺ MP in the intestine as DC because they expressed CD11c and class II MHC. The controversy surrounding classification of intestinal MP as m ϕ or DC may appear semantic, but it does have important functional implications. Although both m ϕ and DC are 'professional phagocytes' that can express class II MHC, their roles in immunity are quite distinct. DC in peripheral tissues survey the environment, take up antigen and migrate via afferent lymphatics to the draining LN. Here they interact with and cause the differentiation of naïve T cells into antigen-specific effector T cells that subsequently migrate back to the periphery to carry out effector functions. In contrast, it is generally accepted that m ϕ are sessile, tissue resident cells that play an important role in tissue remodelling and homeostasis. In addition, m ϕ scavenge foreign material in their local environment and eliminate it in highly degradative lysosomes. Although 'activated' m ϕ may upregulate class II MHC and present antigen to T cells, this is likely to involve previously primed T cells in the tissue and not in the LN. Thus accurate classification of MP is essential for understanding their function and contribution to homeostasis and protective immunity.

Using CX3CR1-GFP and CD11b expression, I found that there were three clear subsets of myeloid cells in the resting mucosa: CX3CR1^{neg}, CX3CR1^{int} and CX3CR1^{high}. As noted above, CX3CR1⁺ MP have been reported previously in the steady state intestinal mucosa (28, 169), but these studies did not always assess the level of CX3CR1 and some analysed the CX3CR1⁺ population as a single entity (195). In addition, many of these reports used cells that had been pre-enriched using density gradients or by gating on CD11c and class II MHC, on the assumption they were DC (28, 169, 195, 263). In contrast, my work showed that the level of CX3CR1 expression not only discriminated between different cell types, but also that some of the resulting populations were heterogeneous. The largest population was CX3CR1^{high} and these appeared to a homogeneous population of m ϕ . They uniformly expressed F4/80 and class II MHC and most expressed CD11c to some degree. They also displayed typical m ϕ morphology and had high phagocytic activity. Recent studies that have identified CX3CR1^{high} cells in the resting intestine have also concluded that these are sessile tissue m ϕ rather than DC, despite the presence of CD11c and class II MHC (189, 264). This is supported by the fact that they do not express CCR7 or migrate in afferent lymph to the MLN and are inefficient at priming naïve T cells *in vitro* (189). Furthermore, as I found, the numbers of CX3CR1^{high} m ϕ are independent of flt3L

(189), but instead are expanded by CSF-1 and reduced in CSF-1R KO mice (195). Very recent work which was reported while I was writing up provided further strong evidence to support my conclusions that CX3CR1^{high} MP are highly phagocytic tissue resident m ϕ (265).

As noted above, the expression of CD11c by the CX3CR1^{high} m ϕ has led to considerable confusion in identifying DC and m ϕ in the gut. However there is growing appreciation that many, if not all, tissue m ϕ can express CD11c. Indeed some groups have gone to extraordinary lengths to show that CD11c cannot discriminate between DC and m ϕ . Bradford *et al* created CD115-GFPxCD11c-DTR mice to demonstrate that the administration of DT results in complete ablation of CD115-GFP⁺ m ϕ in most tissues, including the colon (266). In my hands, the level of CD11c expression by CX3CR1^{high} m ϕ was extremely variable, being dependent on the clone of antibody and the particular fluorochrome conjugate. In some of my experiments, CD11c expression appeared to define two populations of CX3CR1^{high} cells, but more often, CD11c showed a continuous distribution. In addition, analysis of cytokine production and phagocytic activity did not suggest this population was heterogeneous. My findings contrast with those of Rivollier and colleagues, who suggest that CD11c defines two distinct populations of F4/80⁺ MP in mouse colon, of which only the CD11c⁺ population was replenished by Ly6C^{high} monocytes (265). However it is notable that their microarray analysis revealed that there were very few differences in gene expression between the CD11c-defined 'subsets'. Thus the exact importance of the level of CD11c expression by CX3CR1^{high} m ϕ is unclear, but it may be that CD11c expression is indicative of the maturation status of m ϕ , increasing as monocyte/m ϕ mature, in a similar fashion to that of F4/80 expression. Certainly in my hands, CD11c was expressed at higher levels by m ϕ in the colon than in other tissues. This was also the case for class II MHC which was expressed at very high levels on all CX3CR1^{high} colonic m ϕ , but not on m ϕ resident in the peritoneal cavity. Together with the fact that colonic m ϕ expressed much higher levels of CX3CR1 than any other myeloid cell I examined, these results suggest that local factors in the intestinal mucosa have unique effects on the differentiation of m ϕ during maturation from monocytes (see below).

The CX3CR1^{int} cells I identified in the resting colon have also not been studied in any depth previously, or were not characterised at all as a separate

subset (169, 189, 196). As a result, no consensus has been reached on the identity of these cells. By analysing the entire CD11b⁺ CX3CR1^{int} compartment without prior bias, I was able to show that in the resting state, this population was extremely heterogeneous, comprising at least four subsets which could be discriminated on the basis Ly6C, class II MHC, F4/80 and CD11c expression. Given that the Ly6C^{high}MHCII^{neg}, Ly6C⁺MHCII⁺ and Ly6C^{neg}MHCII⁺F4/80⁺CD11c^{neg} cells all expressed F4/80 to some degree and were not expanded by flt3L, they appeared to belong to the m ϕ lineage. I referred to them as P1, P2 and P3 respectively, and to the CX3CR1^{high} cells as P4. On the basis of the pattern of Ly6C and class II MHC staining, I proposed that P1, P2 and P3 represented cells at different stages of maturation, starting with P1 which was phenotypically indistinguishable from Ly6C^{high} monocytes in blood, via P2 to the F4/80⁺MHCII⁺ cells in P3 that were similar to the resident CX3CR1^{high} population, except for the level of CX3CR1. These findings are consistent with the study of Schulz *et al*, which reported that the CX3CR1^{int} compartment in normal small intestine contained monocyte-like cells and CD11b⁺ cells that expressed variable levels of class II MHC (189). However, this earlier work did not characterise these cells, or consider whether they were related to the CX3CR1^{high} m ϕ . A more recent study also described the presence of both CX3CR1^{int} and CX3CR1^{high} cells in resting colon, with the CX3CR1^{high} population outnumbering the CX3CR1^{int} cells (264). However this study did not detect heterogeneity within the CX3CR1^{int} population, and indeed they specifically reported that Ly6C⁺ cells were absent, which is in complete contrast to my results. The reason for this difference is unclear, as this study used a similar cell isolation technique and did not use a gating strategy that would have caused any populations to be omitted from analysis. Indeed the presence of Ly6C^{high}MHCII^{neg} monocytes in the resting colon was particularly unexpected given these cells are typically associated with acute inflammation (12, 22). Nevertheless the presence of Ly6C^{high} monocytes was consistent in all my studies and their presence in the resting small intestine and colon has been confirmed by recent unpublished studies of the Malissen group that I became aware of while writing up. Using Ly6C and CD64 expression, these studies identified a similar pattern of monocyte/m ϕ maturation that I found using Ly6C and class II MHC, which they have dubbed the 'monocyte waterfall'.

The remaining CX3CR1^{int} cells were Ly6C^{neg}MHCII⁺F4/80^{neg}CD11c⁺ and expanded markedly in response flt3L. The presence of flt3L-responsive cells within

the CX3CR1^{int} compartment has been reported previously, although the authors did not characterise the cells involved (189). The same study also showed that cells with a similar phenotype could be found migrating in lymph draining the intestine, albeit at very low frequencies (189). Similar findings have been made in lymph of mesenteric lymphadenectomised mice (Cerovic, V. personal communication). Thus it appears that the CX3CR1^{int} compartment may contain small numbers of true DC, and interestingly these are CD103^{neg}, suggesting that separating DC and m ϕ on the basis of CD103 and CX3CR1 may not be as accurate as currently proposed. Another study which suggested that the CX3CR1⁺ compartment might contain both m ϕ and DC relied on F4/80 and CD68 as m ϕ markers (169). However direct comparison of my results with this study is complicated, as the authors used density gradients to pre-enrich mononuclear LP cells, pre-gated on CD11c and class II MHC to identify 'DC' and analysed the CX3CR1 compartment as a single population. This approach would omit the cells that I found in P1 and P2, as these both lack CD11c and the former population does not express class II MHC.

An advantage of using CX3CR1 to define the colonic myeloid cell populations was that it allowed me to identify and exclude CD11b⁺ cells that were not related to m ϕ or DC. Substantial numbers of CX3CR1^{neg} granulocytic cells were present in the resting mucosa, the majority of which were eosinophils expressing SiglecF and possessing a unique ring-shaped nucleus and eosinophilic cytoplasm. Unusually, I found that colonic eosinophils did not express the CCL11 (eotaxin) receptor, CCR3, which characterises eosinophils in most other tissues such as the lung, small intestine and blood (253). Importantly, in my hands, colonic eosinophils expressed both F4/80 and CD11c, albeit at low levels, highlighting the inadequate nature of using these markers in isolation to discriminate between myeloid cells in the colon. Previous studies (253, 267) have identified eosinophils in the small intestinal lamina propria, and although in one case all CD11b^{int}CD11c^{int} cells were considered to be eosinophils (267), this is inconsistent with my observations which would suggest that many of such cells could be CX3CR1⁺ m ϕ or DC.

The apparent abundance of eosinophils in the steady state LP was surprising given their usual association with T_H2 cell driven inflammatory responses and their rarity when the normal mucosa is examined microscopically

(262). Thus their numbers may be overestimated by studies such as mine because they are released more easily by enzymatic digestion during isolation and can be identified readily by multi-parameter flow cytometry in whole colonic isolates that have not been enriched using density gradients that would normally remove granulocytes. Despite this proviso, there is increasing evidence that intestinal eosinophils probably form the single largest population of eosinophils in the body under steady state conditions (253). Why such large numbers of eosinophils are present in the steady state LP remains unclear, but interestingly their presence is not dependent upon the commensal microbiota, as intestinal eosinophil numbers are normal in germ-free mice (268). Several potential functions have been proposed for intestinal eosinophils. Firstly, they may form a specialised layer of innate defence at the mucosal barrier, protecting against helminth infection. Secondly, they have been shown to control colonic epithelial barrier function by regulating tight junction proteins such as occludin (269). They are also a rich source of cytokines such as TGF β (270), which has many effects in the intestine, including the regulation of m ϕ and Treg function (179, 191, 271). Finally, intestinal eosinophils may maintain IgA-producing plasma cells in the mucosa, as eosinophils have been shown to do with IgG-secreting plasma cells in the BM. This process is dependent on APRIL and IL6 (272), and although not reported here, I found colonic eosinophils to produce IL6 constitutively. Alternatively, IL6 together with TGF β has been shown to facilitate the differentiation of T_H17 cells (273) and thus eosinophil-derived IL6 could maintain IL17 levels in the intestinal mucosa. Therefore eosinophils may contribute to protective immunity by supporting IgA production and/or IL17 production, as well as acting as effector cells in their own right. Investigations of the role of eosinophils in the intestinal LP are currently being pursued by a number of groups and work on eosinophil-deficient mice (dblGATA mice; (274) should shed further light on their function.

As well as eosinophils, a very small population of Ly6G^{high}CD11b⁺Ly6C^{int} neutrophils could also be found in the CX3CR1^{neg}CD11b⁺ fraction of cells from healthy colon. The low number of neutrophils in the resting mucosa is consistent with the fact that neutrophils are only recruited into tissues during inflammation and it is unlikely these cells play a significant role in the steady state.

Thus it is clear that the MP compartment of the intestinal mucosa is extremely heterogeneous and that conventional markers such as F4/80, CD11b and CD11c cannot be used in isolation to identify individual MP populations. My findings demonstrate that CD11b and CX3CR1 expression together with F4/80, CD11c, Ly6C and class II MHC are powerful ways of identifying individual subsets of MP. Consistent with previous findings (189), CX3CR1^{high} cells represent a homogeneous population of tissue resident m ϕ , whereas the CX3CR1^{int} compartment contains cells that are indistinguishable from Ly6C^{high} blood monocytes, and cells that are phenotypically and morphologically similar to CX3CR1^{high} m ϕ . In addition, this population also includes a flt3L responsive DC population, which has not been characterised previously. Having identified these CX3CR1-defined populations of m ϕ , I went on to examine if they represented independent subsets of m ϕ , or if a relationship existed between them.

8.2.2 Ontogeny of Steady State Colonic Macrophages

As discussed in Chapter 1, a paradigm has arisen over the last decade that tissue resident and pro-inflammatory m ϕ are derived from Ly6C^{low} and Ly6C^{high} blood monocytes respectively. In Chapter 4, I set out to investigate whether CX3CR1^{high} and CX3CR1^{int} were derived from distinct monocyte subsets. My first approach involved transferring BM monocytes from CD45.2⁺ CX3CR1^{+/gfp} mice into unmanipulated resting CD45.1⁺/CD45.2⁺ CX3CR1^{+/gfp} mice. Although this did provide evidence that Ly6C^{high} monocytes could migrate to the steady state colon, it was extremely difficult to identify donor cells in the LP under these conditions, due to the small number of cells involved.

To overcome this problem, I decided to use recipients whose endogenous intestinal m ϕ had been reduced. The first system involved the depletion of endogenous MP using DT in the CD11c-DTR mouse. Although this mouse was generated to allow the selective ablation of DC, my studies confirmed the idea that most tissue m ϕ express CD11c to some degree (266). Indeed I found that DT administration resulted in almost complete depletion of the colonic F4/80⁺CD11c^{-/+} m ϕ , whereas CD11c^{high}CD11b⁺F4/80^{neg} DC were affected less profoundly. Similar findings have been reported very recently by the Kelsall group (265), showing extensive colonic m ϕ depletion in this model, including 'CD11c^{neg}' cells. In addition, as noted above, DT efficiently depleted CD115⁺ colonic m ϕ in CD115-

GFPxCD11c-DTR mice (266). However these results are in contrast to another previous study (196), which reported a selective effect on DC and preservation of colonic m ϕ in CD11c-DTR>WT BM chimeric mice that allow prolonged DT administration. This could account for the differences in the selectivity of cell ablation, although it should be noted that the Kelsall group also used CD11c-DTR>WT BM chimeric mice, and so other factors may be involved.

By utilising CD11c-DTR mice as recipients for adoptive transfer studies, I was able to demonstrate that Ly6C^{high} monocytes efficiently replenished the CX3CR1^{high} m ϕ compartment. This seemed to involve the progressive phenotypic maturation of Ly6C^{high} monocytes in the mucosa itself, via stages identical to those I identified as P1-P4 in resting colon. By suggesting that Ly6C^{high} monocytes are the precursors of tissue resident CX3CR1^{high} m ϕ , these results appear to contradict the current monocyte paradigm. However they are consistent with previous studies which demonstrated that Ly6C^{high} monocytes could repopulate CX3CR1^{high} MP cells in the colon of mice depleted chronically using the CD11c-DTR model (196). However in contrast to my observations, these authors reported that a small proportion of donor cells remained in the CX3CR1^{int} compartment, even two weeks following transfer. In my hands, all donor cells adopted the CX3CR1^{high} phenotype within 4 days and one explanation for this discrepancy could be that Varol and colleagues administered DT from one day before and throughout the two week period after BM monocyte transfer. This prolonged depletion may result in a degree of inflammation and an arrest in monocyte differentiation such as I found in DSS colitis. However it is believed that DT does not generate significant inflammation (251, 265). An alternative explanation could be that some of the CX3CR1^{int} progeny of Ly6C^{high} monocytes found by Varol *et al.* could be equivalent to the CD11c^{high}F4/80^{neg} DC I identified in P5. Although I was unable to detect DC arising from donor monocytes in my experiments, I did not examine this exhaustively. In addition, DC of this kind in the gut are thought to be derived from pre-DC (196), but it is possible that the long term depletion protocol used by Varol allowed accumulation of small numbers of monocyte-derived DC as has been demonstrated in other tissues (275).

Although these experiments in CD11c-DTR depleted mice were further evidence that CX3CR1^{high} m ϕ appeared to be derived from so-called 'inflammatory' Ly6C^{high} monocytes, I was concerned that the recruitment of monocytes following

DT-mediated depletion of resident CD11c⁺ MP may not reflect m ϕ maintenance during true 'steady state' conditions. As discussed above, DT administration results in extensive and rapid MP cell depletion thereby generating an empty niche that will be replenished rapidly, allowing recruitment of cells that are not necessarily recruited to the normal mucosa. Therefore, I next used CCR2-null mice as recipients for adoptive transfer experiments. Due to the indispensable role of CCR2 in Ly6C^{high} monocyte BM egress (22), these mice have a selective depletion of blood and tissue monocytes and their immediate progeny. In parallel, I found they lacked Ly6C^{high} monocytes in the colon, but had relative preservation of resident colonic m ϕ . Thus I predicted these mice might allow enhanced visualisation of monocyte recruitment in the absence of significant effects on tissue homeostasis. I found that adoptively transferred Ly6C^{high} monocytes entered the colonic mucosa of CCR2 KO mice and differentiated into CX3CR1^{high} m ϕ , exactly as happened when CD11c-DTR mice were used as recipients. In CCR2 KO mice, the maturation of donor monocytes from P1 to P2, then to P3 and finally to P4 (CX3CR1^{high} m ϕ) was even clearer. Again this was accompanied by the upregulation of class II MHC and F4/80, as well as increased levels of CD11c. However, the time taken for Ly6C^{high} monocytes to mature into CX3CR1^{high} m ϕ appeared to be longer in CCR2 KO mice than in the CD11c-DTR system, taking up to 7 days rather than 4 days. This may reflect the possibility that there is more physiological maturation of monocytes in the relatively replete mucosa of CCR2 KO mice, whereas it may be forcibly accelerated in the severely depleted mucosa of CD11c-DTR mice. Two further important features were revealed by these studies. Firstly, that the differentiation process of Ly6C^{high} monocytes was gut specific, as CX3CR1^{high}MHCII⁺ donor cells were not found in the bloodstream or lung parenchyma of recipient mice. As reported previously (29, 196), donor cells in the bloodstream lose Ly6C, but did not become CX3CR1^{high} or acquire class II MHC expression. Secondly, Ly6C^{low} monocytes failed to migrate to the intestinal mucosa, even in MP-depleted mice, which is consistent with previous studies examining Ly6C^{low} monocyte recruitment, although Ly6C^{low} monocytes were found to migrate to PP (196).

These experiments showed that adoptively transferred Ly6C^{high} monocytes entered the colonic LP and became CX3CR1^{high} m ϕ . However, this did not necessarily demonstrate that the endogenous cells in intact colon underwent the same differentiation process, even though this was suggested by the presence of

the different phenotypic subsets in P1-P4 and by the fact that the absence of Ly6C^{high} monocytes in CCR2 KO mice was associated with a significant reduction in mature gut m ϕ . Thus I next employed BrdU to investigate the population dynamics of endogenous colonic CX3CR1⁺ myeloid subsets. I found that 3hrs after pulsing with BrdU, around a quarter of all BM Ly6C^{high} monocytes were labelled, consistent with their generation from actively dividing pro-monocytes (11). In contrast, no Ly6C^{high} monocytes in the bloodstream were labelled at this time, consistent with their non-cycling status (12). More importantly, I found no BrdU incorporation by any of the CX3CR1-defined colonic myeloid subsets, implying that these cells were not in active cell division in the tissue. By 12hrs after the single pulse of BrdU, a greater frequency (~60%) of the BM Ly6C^{high} monocyte pool was now labelled and BrdU⁺ Ly6C^{high} monocytes were now in the circulation. Consistent with their appearance in the bloodstream, a small proportion of cells in P1 in the colon were also BrdU⁺, suggesting that by this time, precursors had incorporated BrdU in the BM, entered the blood and migrated to the steady state mucosa. Importantly at 12hrs, significant numbers of BrdU⁺ cells could not be detected in the other CX3CR1⁺ populations in the colon.

I next used a long-term BrdU administration protocol to examine the fate of monocytes in the colon over a longer period. Mice received BrdU for 6 days and then were returned to normal drinking water, with the hypothesis being that if cells in P1, P2 and P3 were successive, short-lived intermediaries in transition they would show stepwise accumulation of BrdU, but then lose it rapidly upon BrdU withdrawal. In contrast, the CX3CR1^{high} m ϕ population should accumulate BrdU-labelled cells more gradually and retain them longer. The results confirmed this idea, as BrdU⁺ cells rapidly accumulated in P1 during BrdU administration, but then disappeared very quickly from this compartment upon cessation of BrdU. BrdU⁺ cells also accumulated in P2 with slightly slower kinetics, although their numbers decayed just as quickly upon removing BrdU. P3 showed slower accumulation of BrdU⁺ cells and these persisted longer after BrdU withdrawal, before decaying rapidly thereafter. The proportion of BrdU⁺ CX3CR1^{high} m ϕ increased slowly and continued even after BrdU withdrawal. Rather surprisingly, the frequency of BrdU⁺ cells in CX3CR1^{high} population not only lagged behind that in other populations, but showed a slower increase which did not parallel exactly the disappearance of BrdU⁺ cells from the CX3CR1^{int} compartments. This could suggest that only a proportion of the CX3CR1^{int} cells differentiate into CX3CR1^{high}

m ϕ . Alternatively, this could be evidence that at least some of the CX3CR1^{high} m ϕ are not derived from Ly6C^{high} monocytes and that the gradual accumulation of BrdU⁺ cells within the CX3CR1^{high} compartment could represent *in situ* self-renewal. Such a mechanism has been shown to be responsible for the maintenance of other tissue m ϕ populations such as Langerhans cells in the skin, microglia in the CNS and alveolar m ϕ in the lung (56, 57, 60). These appear to be derived from non-haematopoietic stem cells in the yolk sac in foetal life which are then maintained by local turnover. The idea that there may be some monocyte independent m ϕ in the colon is consistent with the presence of colonic m ϕ in CCR2 KO mice and with the fact that 5-7% of colonic m ϕ were of host origin in CX3CR1^{+gfp} \rightarrow CX3CR1^{+gfp} BM chimeric mice. In addition, studies using intestinal grafts (189) provide little evidence for continuous replacement of the CX3CR1⁺ MP population in the steady state as would be expected if derived from circulating monocytes. However recent unpublished studies by the Malissen group using CCR2 KO x WT mixed BM chimeras have shown that when CCR2 KO precursors have to compete with CCR2-sufficient cells, the intestinal m ϕ pool is almost completely composed of WT-derived cells, paralleling exactly the loss of CCR2 KO circulating monocytes. Thus my results could be explained by the fact that in intact CCR2 KO mice, those monocytes remaining may use other chemokine receptors to enter the mucosa. Furthermore the fact that CX3CR1⁺ MP are not lost in small intestinal grafts (189) could simply indicate that these cells have a long lifespan once fully differentiated, which would be consistent with my BrdU and adoptive transfer studies. A dependence of resident colonic m ϕ on replenishment by Ly6C^{high} monocytes is also supported by recent studies using parabiosis of WT and CCL2 KO mice which have shown that CCL2 is crucial for the maintenance of the m ϕ pool in the resting intestine (276).

To the best of my knowledge, my results are the first demonstration that resident CX3CR1^{high} intestinal m ϕ in resting state are generated from Ly6C^{high} monocytes via a local differentiation process that involves a number of CX3CR1^{int} intermediary steps. As a result, it appears that CX3CR1^{int} and CX3CR1^{high} m ϕ in colon are directly related to each other, rather than being independent populations of 'inflammatory' and 'resident' m ϕ , as recently suggested (264). It is difficult to exclude completely the possibility that a few colonic m ϕ may be truly 'resident' and derived from mesenchymal precursors early in foetal life, and only lineage tracking strategies such as those used to study the origins and maintenance of microglia

and Langerhans cells, would provide insight into this possibility. However, my studies suggest that most if not all resident colonic m ϕ are derived from a continuous process of replenishment by circulating Ly6C^{high} monocytes.

8.2.3 Functional Attributes of CX3CR1^{high} Macrophages and their CX3CR1^{int} Precursors

I then went on to examine the functions of the subsets I had defined on the basis of CX3CR1 expression. Unlike m ϕ in other tissues, bulk populations of m ϕ from the intestine are known to be unresponsive to stimulation by classical stimuli such as TLR ligands (171). In contrast, the blood monocytes that I proposed to be the precursors of resident colonic m ϕ are fully responsive to stimulation (12, 22). Thus I was interested to see if and how the functions of the different subsets changed during the *in situ* differentiation process that I had uncovered. Analysis of the spontaneous production of TNF α and IL10 by intracellular cytokine staining revealed that all subsets contained cells that produced TNF α alone, IL10 alone and rather surprisingly, cells that produced both IL10 and TNF α . However there were marked differences in the pattern of cytokine production in the different CX3CR1-defined populations. Specifically, there was an incremental transition from predominant TNF α production by the Ly6C^{high}MHCII^{neg} cells in P1, to dominance of IL10 production amongst mature resident CX3CR1^{high} m ϕ . This was confirmed using both IL10-reporter (VertX) mice and qRT-PCR, while qRT-PCR analysis also showed that the levels of mRNA for IL6 and iNOS were downregulated in resident CX3CR1^{high} m ϕ compared with their Ly6C^{high} monocyte precursors. Thus the production of pro-inflammatory mediators appears to be extinguished as Ly6C^{high} monocytes mature, giving rise to anti-inflammatory, IL10 producing CX3CR1^{high} m ϕ . This switch to IL10 production did not appear to reflect differentiation into alternatively activated 'M2' m ϕ , because although CX3CR1^{high} m ϕ also acquired high levels of CD206 and CD163, they did not upregulate the M2 markers arginase-1 and VEGF. Instead they appeared to represent a population of regulatory m ϕ , which are characterised by high IL10 production and CD163 expression and have been identified in the placenta, the developing embryo and infiltrating tumours (83).

It is known that IL10 is exceptionally difficult to detect via intracellular cytokine staining and I only detected it when colonic LP isolates were maintained

in suspension and not when cultured in low adherence culture plates. Failure to detect IL10 using typical culture conditions could be due to the strong adherence of mature (CX3CR1^{high}) m ϕ to culture plates, which leads to poor cell retrieval and/or viability. However, by using the intracellular cytokine staining technique I was unable to quantify the amount of cytokine production and my attempts using sorted populations were hindered by poor cell viability following FACS purification, meaning that they could not be cultured long enough to obtain suitable supernatants.

A number of groups have recently focussed on the production of IL10 by intestinal m ϕ (139, 178, 183, 223), but in one of these cases m ϕ were identified on the basis of CD11b expression alone (223), which I showed to be present on many cell types in the mucosa. Similarly, although Denning *et al.* (178) showed that CD11b⁺F4/80⁺ CD11c^{neg} cells in the small intestine produced more IL10 than similar cells in the spleen, my results make it clear that this population probably included some eosinophils and it also excluded the large number of m ϕ that express CD11c. Therefore the authors of that study may have actually underestimated the ability of m ϕ to produce IL10. IL10 is a critically important mediator in the intestine, as IL10 KO mice develop severe spontaneous colitis (226) and m ϕ -specific KO of IL10R mediated signalling replicates this phenotype (227), but the role of m ϕ themselves as the source of IL10 has been unclear. The production of IL10 by colonic m ϕ appears to be partially dependent on the presence of the commensal microbiota, as gut m ϕ from mice reared in germ-free conditions produce significantly less IL10 (265, 277). Surprisingly however, the detection of the commensal microflora may occur in a MyD88-independent manner, as m ϕ isolated from MyD88-deficient mice produce equivalent levels of IL10 to those from WT mice (265). Recent studies have suggested that IL10 from intestinal m ϕ can drive the generation of FoxP3⁺ Treg from naïve precursors *in vitro* (178). However given that naïve T cells are rare in the LP (278) and resident intestinal m ϕ do not migrate to the draining LN (189), it seems unlikely they are involved in initial priming of Treg. In this respect, the work of Murai *et al.* (183) and Hadis *et al.* (139) suggests that IL10 derived from intestinal m ϕ is needed to maintain FoxP3 expression and Treg function in the intestinal LP. In the absence of IL10 from host myeloid cells, Treg cannot suppress T-cell mediated colitis and there is a defect in oral tolerance to protein antigens in CX3CR1^{gfp/gfp} mice that have defective IL10 production by small intestinal F4/80⁺CD11b⁺ m ϕ (139). In the

latter case, m ϕ -derived IL10 is essential for the secondary expansion of FoxP3⁺ Tregs in the small intestinal LP after they had been generated initially by CD103⁺DC in the MLN. Thus CD103⁺ DC and CX3CR1^{high} m ϕ may play complementary and successive roles in maintaining Treg-dependent intestinal homeostasis. The interaction of m ϕ and Tregs in the mucosa is likely to be bidirectional and affect the behaviour of m ϕ , as monocytes cultured with CD4⁺CD25⁺FoxP3⁺ Tregs have been shown to adopt an M2-like/regulatory phenotype (279, 280).

At first, my finding that Ly6C^{high} monocytes could give rise to mature IL10-producing m ϕ in the colon seemed somewhat surprising, given that they are usually associated with robust pro-inflammatory responses. However as noted above, disruption of Ly6C^{high} monocyte recruitment in CCL2-deficient mice is accompanied by a reduction in IL10-producing m ϕ in the colonic mucosa (276). Furthermore, Ly6C^{high} monocytes have been shown to give rise to IL10-producing m ϕ in other tissues, although in these cases the monocytes were recruited to inflamed or damaged tissues. For example, Ly6C^{high} monocytes give rise to anti-inflammatory macrophages that contribute to tissue repair during retinal inflammation (281) or following spinal cord (282) or skeletal muscle injury (283). Similar Ly6C^{high} monocyte-derived anti-inflammatory m ϕ have been described in the pregnant uterus, where they are involved in the remodelling of the growing tissue (50). Interestingly, I noted that CCR2 KO mice experienced breeding problems after their first litter, suggesting that CCR2-dependent accumulation of m ϕ in the uterus may be of major physiological importance. It would therefore be interesting to explore if this is directly related to the lack of tissue remodelling by local m ϕ . Ly6C^{high} monocytes have also been reported to give rise to IL10-producing, class II MHC⁺ m ϕ in tumours, where they go through very similar differentiation stages to those I observed in the colon (284). Thus there appears to be a growing appreciation that Ly6C^{high} monocytes can give rise to anti-inflammatory IL10-producing m ϕ in many tissues. However my observations are unique by showing that this happens continuously in the gut in the absence of overt inflammation or damage, and Ly6C^{high} monocytes are undetectable in other steady state tissues including the non-pregnant uterus (285) and the normal retina (281). These findings may reflect the 'physiological inflammation' that is produced in the gut by its enormous antigenic load and a constant flow of potentially

responsive cells into the mucosa would be a useful first line of defence against this material should it be needed.

A surprising feature of my functional analysis was that resident CX3CR1^{high} m ϕ produced TNF α constitutively and the levels of TNF α mRNA and protein did not change during maturation from monocytes. This was quite different to what I found with another pro-inflammatory mediator, IL6, where mRNA levels decreased progressively during maturation. Previous work on human and mouse intestinal m ϕ has usually suggested that resident m ϕ do not produce TNF α , although most of these studies used heterogeneous populations of cells (222). However, more recently, Takada and colleagues reported that steady state colonic m ϕ produced some TNF α together with IL10, although these cells were identified merely on the basis of CD11b and so could have included other cell types (276). In contrast, I found that highly defined CX3CR1^{high} m ϕ produce TNF α constitutively and the intracellular cytokine staining technique I developed showed directly that the vast majority of CX3CR1^{high} cells making TNF α also produced IL10. In contrast, most Ly6C^{high} colonic monocytes did not balance TNF α production with IL10, but this developed as maturation proceeded through the P1-P4 subsets. Why murine CX3CR1^{high} resident colonic m ϕ retain the ability to produce TNF α despite acquiring anti-inflammatory properties remains unclear. However, although classically considered as the archetypal pro-inflammatory cytokine, TNF α has been shown to have some anti-inflammatory effects. For example, TNF α can limit the duration and extent of inflammatory responses by regulating IL12 production by m ϕ *in vivo* (286). In addition, signalling through the TNF α R2 is essential for the ability of TGF β to induce a regulatory phenotype in peritoneal m ϕ (287). Thus low-level TNF α production alone, or in combination with mediators such as IL10 or TGF β , may act to regulate colonic m ϕ in an autocrine manner. TNF α is also known to induce the expression of metalloproteinases (288) and therefore it may enhance the tissue remodelling activity of gut m ϕ . Alternatively, TNF α has been shown to induce CX3CL1 expression by endothelial cells (289) and it is interesting to speculate that this may be needed to maintain the CX3CR1-dependent production of IL10 that appears to be critical for the homeostatic role of resident intestinal m ϕ . A further intriguing possibility is that the known ability of TNF α to increase epithelial cell permeability via effects on tight junction proteins such as occludin (290), might allow resident m ϕ to facilitate the extension of their protrusions into the

intestinal lumen. Therefore it would be interesting to examine the ability of TNF α KO intestinal m ϕ to form and extend transepithelial dendrites.

The constitutive production of TNF α and expression of class II MHC by resident colonic m ϕ indicate that they are not merely inert cells, but are probably responding actively to their environment. This is supported by their acquisition of phagocytic activity. My results extend previous findings that human intestinal m ϕ are avidly phagocytic and are able to engulf and eliminate bacteria without prior 'activation' (171, 173), by showing that this activity was acquired progressively as CX3CR1^{high} m ϕ matured from Ly6C^{high} monocytes and paralleled the acquisition of CD163, IL10 and class II MHC. It should be noted that the pHrodo *E. coli* bioparticle phagocytosis assay I used to measure phagocytic activity in Chapter 5 is based on the ability of cells not only to engulf the particles, but also to acidify the phagosome. This may explain the apparent lack of phagocytic activity I found in monocytes and DC, which are generally regarded as being phagocytic, but have less ability to acidify the phagosome than mature m ϕ (291). As the ability to acidify the phagosomal compartment is essential for the degradation of captured bacteria (292), my results show that as CX3CR1^{high} colonic m ϕ mature from monocytes, they acquire the ability to capture and destroy ingested bacteria.

Despite these features of activation, my studies confirmed previous findings that resident m ϕ in steady state colon are hyporesponsive to TLR stimulation (171, 222). The loss of responsiveness to TLR ligands developed progressively as CX3CR1^{high} m ϕ matured from Ly6C^{high} monocytes. Whereas Ly6C^{high} monocytes showed a robust TNF α -dominated response to stimulation with LPS or BLP, CX3CR1^{high} cells responded poorly to TLR stimulation, with any TNF α production accompanied by IL10. The mechanisms governing this hyporesponsiveness are unclear, however initial studies suggested that this was due to a lack of activating receptors such as TLR (171). Indeed the previous work in our lab had proposed that TLR expression could be used to discriminate between inflammatory and resident m ϕ in mouse colon. However, as discussed above, the interpretation of these results is complicated by my current observations which indicate that appropriately characterised resident CX3CR1^{high} m ϕ express all TLR at a similar level to or higher than CSF-1 generated BM m ϕ . This is consistent with recent work by Smythies *et al.* demonstrating that m ϕ isolated from the normal human small bowel express all TLR to some degree (179). However my results contrast

with recent findings from the Mueller group, which suggested that resident CX3CR1⁺ mφ in mouse colon lack surface TLR2 expression (264). The reason for this discrepancy is unclear, although this study used a different clone of antibody to detect surface TLR2 expression and my findings were confirmed using qRT-PCR. Thus my results would suggest that these cells do indeed express TLR2 protein. One difference between resident gut mφ in mouse and man is the expression of CD14. Whereas human intestinal mφ appear to lack this LPS co-receptor (170), I found that murine CX3CR1^{high} resident mφ, and indeed their CX3CR1^{int} precursors, uniformly expressed CD14, consistent with their expression of TLR4. The exact reason and importance of this difference is unclear. However the majority of blood monocytes in humans express CD14 and therefore it is possible that this molecule is equivalent to Ly6C in mice and is lost as monocytes mature into resident mφ in human gut, an idea consistent with findings on human intestinal mφ from our collaborators in Lund (Uronen-Hansson, H. and Agace, W. personal communication).

Together my studies show that under steady state conditions, the CX3CR1⁺ compartment in the colonic mucosa is phenotypically and functionally heterogeneous, but indicate that this represents a differentiation continuum in which 'inflammatory' Ly6C^{high} monocytes mature into resident mφ, rather than representing independent subsets. This phenotypic transition is accompanied by step-wise changes involving the acquisition of class II MHC, IL10 production, phagocytic activity and CD163 expression, as well as resistance to exogenous stimulation. The physiological implications of this will be discussed below.

8.3 Effects of Inflammation on Colonic Macrophages

It is well documented that inflammation in the intestine results in marked changes in the composition of the mφ compartment, with the appearance of mφ with heightened pro-inflammatory features and bactericidal capacity (239). In humans with IBD, there is an accumulation of CD14⁺ mφ that produce a range of pro-inflammatory mediators and are responsive to TLR stimulation (242). However it is not clear whether this reflects recruitment of new pro-inflammatory mφ, or if tissue resident cells alter their behaviour and become pro-inflammatory. Therefore having established strategies to characterise myeloid cells in the resting colon, I set out to explore the changes that occurred during inflammation. To do this I used

the DSS-induced model of acute colitis, which is well documented and leads to a reproducible form of inflammation with a well-defined pattern of disease. In the protocol I used, mice started to lose weight around 4 days after beginning DSS administration and this was accompanied by rectal bleeding and diarrhoea. In addition, DSS administration resulted in significant colon shortening and histological evidence of destruction of the epithelial monolayer and loss of normal intestinal architecture, with crypt elongation, ulceration and inflammatory cell infiltration.

My analyses showed a massive expansion of the CD11b⁺ myeloid compartment in colitic mice, made up predominantly of Ly6C^{high}MHCII^{neg} CX3CR1^{int} cells in P1 and Ly6C⁺MHCII⁺CX3CR1^{int} cells in P2, as well as accumulation of CX3CR1^{neg} eosinophils and neutrophils. There was also an increase in the number of F4/80⁺MHCII⁺Ly6C^{neg} cells in the P3 subset of CX3CR1^{int} cells, albeit to a lesser extent than in P1 and P2. Conversely the number of CX3CR1^{high} cells appeared to diminish as colitis progressed. In parallel with their increased numbers, more cells in P1, P2 and P3 produced TNF α spontaneously in inflammation compared with the same populations in resting mice. Significantly, the most dramatic expansion was associated with P1 and P2 cells producing TNF α alone. Interestingly however, the progressive acquisition of IL10 still occurred in those cells that did mature, so that the majority of TNF α ⁺ cells in P3 also produced IL10. In addition, the CX3CR1^{high} population remained biased to IL10 production and indeed a greater frequency of this population produced IL10 during inflammation than in resting colon. A characteristic feature of the analogous population of CD14⁺ pro-inflammatory m ϕ that accumulate in inflamed human intestine is their responsiveness to exogenous stimulation, unlike their counterparts in resting mucosa. Consistent with this, I found that it was mainly the cells in P1 or P2 that showed significant increases in pro-inflammatory cytokine production in whole colonic isolates from colitic mice stimulated with TLR2 or TLR4 agonists. As in steady state conditions, there was a progressive loss of sensitivity to TLR stimulation by the CX3CR1⁺ cells as they matured and those in P3 and P4 retained their balanced production of both TNF α and IL10 even after stimulation. Interestingly, the proportion of colitic P1 and P2 cells producing TNF α and/or IL10 after TLR stimulation was not significantly different to that found amongst these cells in resting mice, probably because around 90% of healthy P1

and P2 cells produced $\text{TNF}\alpha$ and/or IL10 under these conditions. Although it would be important to quantify the amounts of cytokine produced by FACS-purified populations during colitis, my results support the idea that the main effect of inflammation is the recruitment of more responsive cells, rather than an inherent change in the cells that have accumulated. One surprising finding was that the $\text{Ly6C}^{\text{high}}$ monocytes and their derivatives which accumulated during colitis did not express high levels of iNOS, in contrast to a number of studies which have shown that during inflammation, $\text{Ly6C}^{\text{high}}$ monocytes give rise to iNOS^+ myeloid cells which were often referred to as 'TipDC' due to their expression of CD11c (22, 293). In addition, recent work on T cell-dependent colitis by the Malissen group has shown upregulation of iNOS by colonic MP with the same phenotype of my P1/P2 cells. However this discrepancy could be explained by the fact that DSS colitis is not T cell dependent and so there may not be $\text{IFN}\gamma$ available to induce iNOS.

Together these results imply that the resident $\text{CX3CR1}^{\text{high}}$ $\text{m}\phi$ do not alter their behaviour during inflammation and that the presence of pro-inflammatory $\text{m}\phi$ in colitis appears to be due to enhanced accumulation of $\text{Ly6C}^{\text{high}}$ monocytes and their immediate $\text{CX3CR1}^{\text{int}}$ derivatives. During my project a number of studies documented the appearance of $\text{Ly6C}^{\text{high}}$ monocytes in the inflamed intestine, where they have been shown to give rise to E-cadherin-expressing inflammatory MP in T-cell dependent colitis (250). Although the authors interpreted these cells as being 'inflammatory' DC, this was solely on the basis of CD11c expression and it is probable that at least some of these cells were pro-inflammatory $\text{m}\phi$. As discussed above, Rivollier *et al.* (265) have recently shown that $\text{Ly6C}^{\text{high}}$ monocytes replenish the resident $\text{m}\phi$ population following DT-mediated depletion of endogenous MP. However in contrast to my results, they have suggested that $\text{Ly6C}^{\text{high}}$ monocytes recruited to the inflamed colon develop into $\text{CD11b}^+\text{F4/80}^{\text{low}}\text{CD11c}^+\text{CD103}^{\text{neg}}$ DC, rather than pro-inflammatory $\text{m}\phi$. In their study, the progeny of adoptively transferred $\text{Ly6C}^{\text{high}}$ monocytes in the inflamed colon were shown to have increased expression of $\text{TNF}\alpha$, IL6, iNOS, IL12 and IL23 compared with that of donor monocytes in resting recipients. Furthermore, these cells possessed potent APC function, being able to drive the differentiation of $\text{IFN}\gamma$ -producing T cells from naïve precursors. However it is unclear whether these cells represent *bona fide* DC because it is unknown if these cells migrate to

the draining LN. The unpublished observations of the Malissen group would support my findings that Ly6C^{high} monocytes recruited during intestinal inflammation give rise to pro-inflammatory m ϕ , on the basis that they express CD64, a marker which has recently been shown by this group to allow discrimination of cells of the m ϕ lineage and DC (294). Similarly, the findings of Weber *et al.* (264) also documented the expansion of the CX3CR1^{int} population during T-cell dependent colitis. However these authors did not find Ly6C^{high} monocytes in the CX3CR1⁺ cell fraction. Rather they suggest that Ly6C^{high} monocytes enter the inflamed mucosa as CX3CR1^{neg} cells, but this is inconsistent with the phenotype of Ly6C^{high} monocytes in the bloodstream, where they clearly express intermediate levels of CX3CR1. In addition to accumulation in several colitis models, Ly6C^{high} monocytes appear to be essential for protection against *T. gondii* and *C. rodentium* in the intestine (25, 295, 296).

My experiments did not investigate whether the inflammatory infiltrate in DSS colitis might involve cell division after Ly6C^{high} monocytes had arrived in the mucosa. Although this has been reported (196), it was only seen when the endogenous MP were repeatedly depleted using DT, which may create an environment which is not normally experienced by monocytes in MP-replete mice. It would be important to examine the possibility that proliferation is occurring within the CX3CR1^{int} compartment using BrdU incorporation and Ki-67 expression. Nevertheless, my results suggest that the main reason for accumulation of cells in P1 and P2 is accelerated recruitment and an arrest in the normal process by which monocytes mature into CX3CR1^{high} m ϕ . Although adoptively transferred monocytes acquired class II MHC and lost Ly6C expression in the colitic mucosa, they failed to transition into the CX3CR1^{high} compartment as they did in steady state recipients. This is consistent with the apparent loss of endogenous CX3CR1^{high} m ϕ as colitis progresses. The exact reasons underlying the breakdown in differentiation in inflammation remain to be elucidated. However, the milieu in the inflamed colon is radically different to that during resting conditions, with the accumulation of many inflammatory cytokines and chemokines (297). These may interfere with the factors that normally drive monocyte differentiation or may have direct effects on reprogramming monocytes. It is important to note that the remaining CX3CR1^{high} m ϕ continued to produce IL10 during inflammation, underlining how the fully differentiated m ϕ are unlikely to change in inflammation (Fig. 8.1). This may also reflect an attempt to re-establish homeostasis and

continued IL10 may influence the differentiation of newly arrived Ly6C^{high} monocytes. Consistent with this idea, myeloid cell-derived IL10 has been shown to limit differentiation of infiltrating Ly6C^{high} monocytes into TNF α /iNOS-producing MP during *T. brucei* infection in the liver (298).

My subsequent experiments indicated that the recruitment of monocytes to the inflamed colon was CCR2-dependent. Although it is recognised that CCR2 is essential for monocyte egress from the BM (22), the requirement for CCR2 in the entry of Ly6C^{high} monocytes into inflamed tissues is still a matter of debate. By performing competitive adoptive transfer experiments of WT and CCR2 KO BM cells into colitic mice, I was able to show that virtually all the recruited cells in the inflamed LP were of WT origin, which confirms directly that CCR2 is needed for this process. This is consistent with the increased levels of CCL2 found in the human and murine intestine during inflammation (222, 299). However, this contrasts with studies examining the recruitment of Ly6C^{high} monocytes to the inflamed bladder and *T. brucei* infected liver, which are unaffected by CCR2-deficiency (293, 300). Thus there may be tissue-specific differences in the role of CCR2 in monocyte recruitment during inflammation.

CCR2-dependent expansion of the CX3CR1^{int} compartment appears to be central to the pathogenesis of DSS colitis, as CCR2 KO mice were protected from this model of colitis and showed defective infiltration of Ly6C^{high} monocytes and Ly6C⁺MHCII⁺ cells in P1 and P2. The decreased pathology was not due to an effect on granulocytes, as although the numbers of eosinophils and neutrophils were lower in 'colitic' CCR2 KO mice than in their WT counterparts, these cells still showed marked recruitment. In addition, WT blood neutrophils and eosinophils showed a complete lack of CCR2 expression in my hands. Although these results need to be confirmed by comparing resting and colitic CCR2 KO mice in the same experiment, they indicate Ly6C^{high} monocytes and their CX3CR1^{int} descendants play the major role driving inflammation. Interestingly my finding of lower numbers of granulocytes in CCR2 KO mice compared with colitic WT mice could reflect a role for inflammatory monocytes in recruiting neutrophils and eosinophils. Indeed Ly6C^{high} monocytes recruited to the colon during acute DSS colitis have been shown to produce high levels of CCL11 (eotaxin-1) and CXCL2 (MIP-1 α) which are known chemoattractants for eosinophils and neutrophils, respectively (301). Clearly this mechanism is not absolutely essential, as there was still some

recruitment of neutrophils and eosinophils to the 'colitic' mucosa of CCR2 KO mice. It is also unlikely to play a role in the resting colon, as resting CCR2 KO mice had normal numbers of colonic eosinophils, despite the absence of Ly6C^{high} monocytes.

To try to examine the pathogenic role of Ly6C^{high} monocytes directly, I carried out a preliminary study in which I investigated if susceptibility to DSS could be restored in CCR2 KO mice by adoptive transfer with WT Ly6C^{high} monocytes. This had no effect, even though the CCR2 KO mice received over 3×10^6 WT monocytes and they could be detected in the recipient colon. However, it must be noted that this experiment was only done once with two recipient mice and it would be important to repeat with more recipients and if necessary, using more transferred cells. In addition, it might have been useful to use more sensitive parameters than bodyweight such as histological analysis.

The pro-inflammatory properties of Ly6C^{high} monocytes are not always harmful in the intestine and they play an essential role in protective immunity. As noted above, CCR2-dependent recruitment of Ly6C^{high} monocytes is important in defence against *T. gondii* (25, 295) and *C. rodentium* (296). Ly6C^{high} monocytes play a similar role in the clearance of *L. monocytogenes* from the spleen (22) and in protection against systemic West Nile virus infection (302). Presumably the damaging effects of these cells are prevented because the responses are terminated once infection has been resolved. Thus IBD may reflect unregulated expansion of pro-inflammatory monocytes and/or arrest in the process that normally drives these cells to mature into anti-inflammatory m ϕ .

The decreased number of CX3CR1^{high} cells during acute colitis probably reflects arrested monocyte differentiation rather than loss through the damaged surface, which is characteristic of DSS colitis, as CX3CR1^{high} m ϕ numbers also decrease in a more chronic colitis model which does not directly affect epithelial barrier function (Guilliams, M. and Malissen, B. personal communication). A further possible explanation for the loss of CX3CR1^{high} m ϕ could be that inflammation causes downregulation of CX3CR1 expression and so cells appear in the CX3CR1^{int} compartment. CX3CR1 is a chemokine receptor, molecules which usually downregulate on exposure to high levels of their ligand and increased levels of CX3CL1 have been found in IBD in mouse and man (219, 303). However

there is no evidence that CX3CR1 can downregulate in this way and experiments in the lab have found that exogenous CX3CL1 does not affect CX3CR1 expression by $m\phi$ *in vitro* (Bravo, A. personal communication). One way to examine if this conversion can occur in inflamed colon would be to transfer Ly6C^{high} BM monocytes into depleted CD11c-DTR mice and allow the monocytes time to differentiate into CX3CR1^{high} $m\phi$. Colitis could then be induced in these recipient mice and the donor compartment examined for evidence of loss of CX3CR1 expression.

An important function of $m\phi$ is to promote tissue repair during the resolution of inflammation. Recent studies have shown that $m\phi$ with repair functions can be derived from 'inflammatory' Ly6C^{high} monocytes (281, 282). To investigate whether this might apply to the intestine, I examined whether the Ly6C^{high} monocytes recruited during acute colitis could progress into the CX3CR1^{high} compartment once DSS was withdrawn. To do this, I adopted a colitis regime in which mice were fed 2% DSS for 4 days and then returned to normal drinking water for up to 18 days. Within 2 weeks after cessation of DSS, all mice recovered both in terms of bodyweight and intestinal pathology. There was also a partial restoration of the normal frequencies of CX3CR1^{high} and CX3CR1^{int} cells. To examine whether the reappearance of CX3CR1^{high} cells reflected differentiation of the recruited inflammatory monocytes, I used continuous BrdU labelling to track recruited cells. As I found in previous experiments, 4 days of continuous DSS and BrdU administration led to labelling of both CX3CR1^{int} and CX3CR1^{high} cells. When DSS and BrdU were removed there was a rapid decay of BrdU⁺ cells in both the CX3CR1^{int} and CX3CR1^{high} populations within 8 days and there was no preferential accumulation of BrdU⁺ cells in the CX3CR1^{high} compartment, as would be expected if CX3CR1^{int} cells recruited during inflammation were transitioning into CX3CR1^{high} cells during the recovery phase. Indeed the rapid loss of BrdU⁺ cells from the CX3CR1^{high} compartment during this period would appear to contradict my earlier BrdU findings in steady state mice that suggested CX3CR1^{high} cells were long lived. However as discussed above, CX3CR1^{high} $m\phi$ are lost as colitis progresses and therefore it is possible that the BrdU⁺ cells that accumulated in the CX3CR1^{high} compartment during the early phase of colitis were simply lost before I examined the colon when it began to repair.

To address further the fate of recruited monocytes in the resolution phase of colitis, I adoptively transferred Ly6C^{high} monocytes into mice on day 4 of colitis, before withdrawing DSS and examining the colon one week later. However as discussed in Chapter 6, this experiment used CX3CR1^{+gfp} mice both as donors and recipients, making the identification of donor cells impossible. Therefore the fate of the recruited monocytes during the resolution of acute colitis remains unclear and it would be interesting to conduct a more comprehensive analysis of the colonic CX3CR1⁺ compartment during this phase, to examine if and when recruited Ly6C^{high} monocytes start to repopulate the CX3CR1^{high} compartment. One way this may be done would be to adoptively transfer CD45 congenic Ly6C^{high} monocytes at different time points after the cessation of DSS and establish at what point the normal differentiation resumes.

8.4 Factors Influencing Colonic Macrophage Behaviour

8.4.1 The Role of Cytokines and Chemokines

The results here, together with previous work, show that resident intestinal m ϕ adapt to their environment by becoming anti-inflammatory and hyporesponsive to exogenous stimulation. My experiments indicate that this feature reflects *in situ* differentiation of Ly6C^{high} monocytes and is unique to the gut, as transferred monocytes did not acquire the same MHCII⁺CX3CR1^{high} phenotype elsewhere. In Chapter 4 I attempted to gain insight into what factors in the normal mucosa might be responsible for inducing these adaptations. First I FACS-sorted Ly6C^{high} MHCII^{neg} monocytes from the resting colon and BM and examined if their phenotype changed during culture *in vitro*. Unfortunately the low number of colonic monocytes I could obtain and their poor viability after culture hindered this approach. Despite these problems, colonic, but not BM Ly6C^{high} monocytes cultured overnight in medium alone started to acquire class II MHC expression, suggesting that factors in the mucosa had already begun to influence these early stages of the monocyte differentiation process. In contrast, the expression levels of CX3CR1 and Ly6C did not change on cultured colonic monocytes. However this is consistent with my adoptive transfer studies which showed that loss of Ly6C and upregulation of CX3CR1 occurred after class II MHC acquisition and took around 2-3 days.

To circumvent the problems with yield and viability, I next used sorted BM Ly6C^{high} monocytes to examine the effects of specific mediators present in the mucosa with known effects on m ϕ biology. These were TGF β , CSF-1 and CX3CL1. However none of these factors induced phenotypic changes in cultured monocytes and there was no evidence of acquisition of a mucosal m ϕ appearance. With the benefit of hindsight, these experiments were probably not carried out under optimal conditions. Firstly, the purified monocytes were only cultured for 24hrs, whereas my adoptive transfer experiments suggest that the differentiation of monocytes into the resident m ϕ phenotype probably takes 4-7 days *in vivo*. Secondly, it is unlikely that monocytes in the mucosa would be exposed to these factors in isolation, and so it would have been interesting to combine these factors. Furthermore, as discussed below, mediators in the mucosa other than those tested may play a role in influencing monocyte differentiation.

A number of possible factors have been implicated in defining the specific characteristics of gut m ϕ , although many reports have concentrated on what accounts for their TLR responsiveness. IL10 can prevent TLR function by inducing inhibitors of the NF- κ B pathway such as Bcl-3 and I κ BNS (229, 230). As discussed above, functional IL10R signalling by m ϕ is needed to maintain intestinal homeostasis and hence m ϕ from IL10 KO mice have a pro-inflammatory cytokine profile and respond vigorously to TLR stimulation (177), and these mice develop spontaneous colitis (226). Interest in IL-10-IL10R signalling in maintaining homeostasis in the gut has been fuelled further by GWAS showing that polymorphisms in the IL10R gene increase susceptibility of IBD and recently transplant of IL10R-sufficient BM has been shown to ameliorate Crohn's disease (228). Together these findings suggest that failure of haematopoietic cells to respond appropriately to IL10 is a major factor in IBD pathogenesis.

IL10 is produced by a variety of cells in the mucosa including Tregs and as discussed above, by m ϕ themselves. Therefore, whether IL10 acts in an autocrine manner to self-regulate m ϕ behaviour is unclear. It is also unknown if IL10 can influence *in situ* monocyte differentiation, but analysis of the colonic myeloid compartment of 'pre-colitic' IL10 KO mice could provide some insight, as could examination of monocyte differentiation after adoptive transfer of Ly6C^{high} monocytes into 'pre-colitic' IL10 KO mice. However one complication of these approaches is that the mucosa of IL10 KO mice may not be normal, even before

colitis appears, as these KO mice have increased intestinal epithelial permeability and heightened levels of TNF α in the mucosa by 2 weeks of age, long before the development of overt inflammation (304, 305). Better approaches would be to generate mice with selective defects in the production of, or responsiveness to IL10 in monocytes and m ϕ . Although this has been done using STAT3 KO and the LysM promoter (227), and these mice develop IBD, STAT3 is not specific to the IL10R signalling pathway and other myeloid cells, such as neutrophils, can express LysM. Therefore it would be useful to find a more specific promoter such as CD115, CD68 or CX3CR1. As well as examining the intestinal myeloid compartments in such animals, it would be interesting to investigate the fate of adoptively transferred monocytes from these mice in the normal steady state colon. Together these studies would provide some insight into whether IL10 directly affects the expression of CX3CR1 and class II MHC on maturing monocytes, as well as its specific role in m ϕ function in the intestine.

Another cytokine likely to be involved in modulating m ϕ behaviour and influencing monocyte maturation in the mucosa is TGF β . Indeed TGF β , along with IL8, has been shown to attract monocytes to the intestine (232). TGF β is abundant in the steady state intestine, being produced by a range of cells including stromal cells, epithelial cells, mast cells and regulatory T cells, as well as by m ϕ (179, 271). TGF β inactivates NF- κ B signalling in human small intestinal m ϕ via a failure of NF- κ B to translocate to the nucleus caused by repression of the Smad7 molecule, which normally inhibits TGF β signalling (179). The importance of this pathway is suggested by the finding that Smad7 is upregulated in human IBD leading to unrestrained NF- κ B activation (233). Furthermore, TGF β has been shown to condition m ϕ in the foetal intestine to acquire the anti-inflammatory cytokine profile and LPS resistance typical of adult gut m ϕ (271). In addition, intestinal tissue-conditioned medium causes human blood monocytes to adopt an intestinal m ϕ phenotype characterised by reduced CD14 expression and resistance to TLR stimulation and this is dependent on TGF β (179, 271). The expression of TGF β 2R increased incrementally as monocytes matured into resident colonic m ϕ , supporting the idea that these cells acquire responsiveness to TGF β and that this mediator may play an important role in determining their fate *in vivo*. However, it is not clear whether TGF β specifically influences the upregulation of CX3CR1 and class II MHC. Similar approaches to those described for

assessing the role of IL10 could be used to test this, such as conditional KO of TGF β R on m ϕ . This approach has been used to show that peritoneal m ϕ from CD68-TGF β RDN mice, which fail to respond to TGF β , produce less IL10 than WT m ϕ , and resolution of DSS colitis is impaired in these mice (306). However the nature of the baseline colonic LP m ϕ populations in these mice under normal conditions is unclear. In addition, it would be interesting to examine the effects of intestinal stromal cell-conditioned medium on the differentiation of BM or colonic Ly6C^{high} monocytes *in vitro*, as has been done with blood monocytes in human studies (179).

Although CSF-1 did not have an effect on BM monocytes cultured *in vitro*, this mediator is essential for m ϕ differentiation from monocytes and it is present in the steady state gut (307). The importance of CSF-1 is highlighted by the paucity of most tissue m ϕ in CSF-1-deficient mice (41) and by the fact that CSF-1R KO mice lack small intestinal CX3CR1⁺ m ϕ (195). As an alternative way of assessing the effects of CSF-1 on gut m ϕ , I administered recombinant CSF-1 *in vivo*. This caused a small, but significant increase in the number of CX3CR1^{high} colonic m ϕ and parallel reductions in P1 and P2, suggesting that CSF-1 may act locally to promote differentiation of recently recruited monocytes. However, CSF-1 may cause increased survival or even turnover of already differentiated CX3CR1^{high} m ϕ . Alternatively, it may accelerate the output and differentiation of monocytes before leaving the BM and these alternatives could be investigated using BrdU incorporation studies and Ki-67 staining. In addition to facilitating m ϕ differentiation, CSF-1 has also been shown to cause resident m ϕ in the pregnant uterus to produce chemokines such as CCL2 (MCP-1), enhancing the recruitment of further monocytes (50). However, the reduced numbers of cells in P1 and P2 I found after exogenous CSF-1 treatment, suggest that its effects were on enhanced differentiation of colonic monocytes, rather than accelerated recruitment. It is noteworthy to mention that the effects I saw with CSF-1 treatment were not dramatic and this may reflect the low dose I used. Although I chose the dose of 20,000 U/day of rCSF-1 based on an early study by Hume *et al.* (49), a very recent study used 1,000,000 U/day to cause doubling of m ϕ numbers in the spleen (308). Therefore it would be important to repeat this experiment using a higher dose of CSF-1 to assess its effects on the different colon m ϕ populations more precisely.

In view of the fact that the key feature of resident gut m ϕ is the acquisition of unusually high levels of CX3CR1, and that its ligand CX3CL1 is produced in the mucosa (203, 204), it seems logical to propose that this mediator might be involved in regulating local m ϕ maturation. Studies within our group, as well as those of others (169) (Bravo, A. personal communication), suggest that mice lacking CX3CR1 (CX3CR1^{gfp/gfp} mice) have no defect in the number of their colonic m ϕ . However, as discussed above, CX3CR1-deficiency is associated with reduced IL10 production by intestinal m ϕ , suggesting that the CX3CR1-CX3CL1 axis may be crucial for maintaining the status of colonic m ϕ . This contrasts with recent findings showing that CX3CR1^{gfp/gfp} mice have small reductions in the number of brain-resident microglia (309). Furthermore, we have been unable to find any effects of soluble or membrane-bound CX3CL1 on m ϕ function *in vitro*, although others have shown it may inhibit/enhance m ϕ function (203, 217). It is controversial whether disruption of the CX3CR1-CX3CL1 axis results in altered susceptibility to experimental colitis, with conflicting results being reported (169, 219, 310). Another, not exclusive possibility could be that the high levels of CX3CR1 on resident m ϕ may be involved in their positioning adjacent to the CX3CL1-expressing epithelial monolayer. This would be consistent with fluorescence microscopic analysis showing that CX3CR1⁺ MP tend to associate with the epithelium (189). In addition, although never directly shown to occur in the colon, CX3CR1 appears to be needed for the formation of transepithelial dendrites by CX3CR1⁺ m ϕ , allowing them to sense and sample the contents of the intestinal lumen (193, 203). Unfortunately it is currently impossible to discriminate CX3CR1^{int} from CX3CR1^{high} cells by immunohistochemistry and therefore it is not clear if these anatomical properties are features of *bona fide* CX3CR1^{high} m ϕ or other CX3CR1⁺ cells including the DC I identified in P5. Furthermore, it is unknown if CX3CR1^{high} and CX3CR1^{int} occupy different locations in the mucosa, as might be predicted.

In addition to the mediators discussed above, other factors such as TSLP, VIP and RA may play a role in influencing m ϕ , as they have been shown to induce tolerogenic properties in mucosal DC (234, 235, 311). Also PPAR γ ligands have been suggested to regulate intestinal m ϕ activity (312). In addition, mucosal blood vessels may imprint selective properties on extravasating monocytes, an idea supported by work suggesting that transendothelial migration of monocytes affects their subsequent differentiation (37).

8.4.2 Control of Macrophage Function by Inhibitory Receptors

As discussed in Chapter 1, the activation state of tissue m ϕ is likely to be influenced by signals received through both activating and inhibitory receptors. In Chapter 7 I set out to investigate whether the inhibitory receptor CD200R1 contributed to the maintenance of colonic m ϕ in their partially inert state, as CD200R1 has been implicated in the regulation of many other tissue m ϕ populations, although previous work had not examined CD200R1 expression on well characterised gut m ϕ (113, 116, 119). I found that CD200R1 was expressed by mature colonic m ϕ at levels similar to that of alveolar m ϕ , which have been shown to uniformly express this receptor (119). In contrast, peritoneal m ϕ lacked any expression of CD200R1 and CSF-1 generated BM m ϕ expressed only low levels of the receptor. Other intestinal leucocytes such as eosinophils appeared to lack CD200R1 expression, as did the Ly6C^{high}MHCII^{neg} colonic monocytes, suggesting this is a selective property of mature mucosal m ϕ . Unfortunately, because these experiments were carried out prior to the optimisation of the gating strategies used in the rest of this thesis, I was unable to assess how CD200R1 expression changed during the maturation from monocytes to CX3CR1^{high} m ϕ . However this could be assessed easily using the new gating strategy or by crossing the CD200R1 KO mice with CX3CR1^{+gfp} mice. It is also noteworthy to mention that I experienced difficulties when analysing CD200R1 expression initially, as I found identical staining by WT and CD200R1 KO cells using the only commercially available antibody. This required careful titration of the antibody using CD200R1 KO cells as the control to obtain conditions which allowed specific staining. This is clearly a technical issue that needs to be considered in future work when CD200R1 expression is being assessed.

The ligand for CD200R1, CD200, was also abundant in the resting colonic mucosa, being expressed at high levels on vascular and lymphatic endothelial cells and at low levels on mucosal B cells. This pattern is consistent with CD200 expression seen in other tissues, such as the lung (119, 313). Because KO of CD200 has been shown to lead to heightened m ϕ activity in multiple tissues including the MLN, spleen and CNS (113) and to increased immunopathology in the lung during influenza infection (119), I postulated that deletion of CD200R1 would lead to an alteration of m ϕ behaviour in the colon. However CD200R1 KO mice had normal numbers of mature F4/80⁺MHCII⁺ colonic m ϕ and these showed

no signs of enhanced activation as determined by costimulatory molecule expression. However CD200R1 KO mice did have an additional F4/80⁺MHCII^{int} population of cells which was not present to any great extent in WT mice. These F4/80⁺MHCII^{int} cells did not seem to represent recently recruited cells equivalent to the P1 and P2 cells I identified in CX3CR1^{+/gfp} mice, as they lacked Ly6C expression. Furthermore they did not appear to express higher levels of CD40 and CD80 costimulatory molecules or TLR, suggesting they were not simply 'activated' states of the F4/80⁺MHCII⁺ m ϕ population. However it must be noted that the numbers of the F4/80⁺MHCII^{int} population were variable between experiments and their significance is still unclear.

Although I was unable to examine the production of TNF α by these populations of F4/80⁺MHCII^{int} and F4/80⁺MHCII⁺ separately, analysis of the total m ϕ population showed that CD200R1 KO colonic m ϕ did not show increased production of TNF α in response to LPS stimulation. It is important to note that there were differences in the level of detection of intracellular cytokines in these experiments compared with the results in Chapter 5, which may reflect the fact that by the time the latter experiments were performed I had optimised the protocol for detecting intracellular cytokines. CSF-1 generated BMM from CD200R1 KO mice also did not show increased TNF α production in response to LPS stimulation alone or together with IFN γ . These findings of normal TNF α responsiveness seem to contradict previous studies on the ability of the CD200-CD200R1 axis to inhibit m ϕ activation (113, 119, 125). However others have suggested that TLR signalling may overcome the ability of CD200R1 to regulate m ϕ responses to IFN γ (126). Interestingly however, in some reports the regulatory effects of CD200R1 have only been seen when CD200R1 is co-ligated with a source of CD200 at the time of stimulation (119). Thus the role of CD200R1 *in vivo* may require contact between m ϕ and CD200-expressing cells at the same time as exposure to an activating stimulus.

My findings that CD200R1 does not play an essential role in controlling m ϕ activation in the steady state intestine were supported by the fact that CD200R1 KO mice did not develop any signs of spontaneous intestinal inflammation, systemic lymphoproliferative disease or autoimmunity, even when followed for up to 18 months of age. Similarly, CD200R1 KO mice showed identical susceptibility

to DSS-induced colitis to WT mice, with no differences in the composition of the colon m ϕ pool or inflammatory infiltrates in colitis.

Although CD200 is the only known ligand for CD200R1, CD200 has been shown to ligate other CD200R (110) and so I carried out similar analyses of intestinal m ϕ in CD200 KO mice. These mice had a significant decrease in the number of F4/80⁺MHCII⁺ m ϕ in the resting mucosa compared with WT mice, but this was not accompanied by an increase in the number F4/80⁺MHCII^{int} cells. Although this could suggest that there is a selective loss of the F4/80⁺MHCII⁺ m ϕ in the absence of CD200, I only had sufficient mice to carry out this experiment once and it would be important to repeat. If correct, it could suggest that CD200 may play a role in the survival of mature colonic m ϕ . However, as in CD200R1 KO mice, there was no evidence of spontaneous pathology or inflammatory infiltrates in the colon of the CD200 KO mice, which were brought from Bristol and kept under SPF conditions in our facility. These animals also showed no increase in susceptibility to DSS colitis. As CD200 KO mice have been reported to have increased susceptibility to autoimmunity in the eye, brain and joint (113, 114, 314), my results may indicate a differential role for CD200-CD200R1 regulation in different forms of immunopathology. Significantly, the disorders in which neutralisation or deletion of CD200 leads to increased inflammation are associated with T cell driven m ϕ activation. In contrast, DSS-induced colitis is driven predominantly by innate leucocytes, as evidenced by normal disease progression in NK-depleted SCID mice (315). Therefore it would be interesting to assess the progress of other, T cell dependent forms of intestinal pathology in CD200 or CD200R1 KO mice.

Previous studies have identified the role of CD200R1 in the regulation of myeloid cell activity by manipulating the CD200-CD200R1 axis *in vitro* using agonistic CD200-Fc fusion proteins or with antagonistic anti-CD200R1 antibodies (119, 120, 314). Thus I used this approach to examine the TLR responsiveness of CSF-1 generated BMM from WT and CD200R1 KO mice. Although this experiment indicated that BMM from CD200R1 KO mice had a marginally higher TNF α response to LPS stimulation, inclusion of a CD200-Fc fusion protein had no effect on the TNF α response by BMM from WT mice, again suggesting that signals delivered through CD200R1 had little effect on m ϕ responses to LPS and

supporting my observations of normal function by colonic m ϕ from CD200R1 KO mice.

Thus, in contrast to alveolar m ϕ in the lung which have been shown to be regulated via the CD200R1-CD200 axis (119), CD200R1 appears to play no essential role in the control of colonic m ϕ activity. This raises the possibility that distinct regulatory mechanisms regulate m ϕ at different mucosal surfaces. However, one cannot exclude the possibility that CD200R1 might be important in combination with other regulatory factors and it is probably not surprising that redundant mechanisms are involved.

8.5 Concluding Remarks

Taken together, my results reveal unsuspected heterogeneity in the MPS of the colonic mucosa. By using CX3CR1 to define mucosal myeloid cell subsets, I have been able to show that 'inflammatory' Ly6C^{high} monocytes are constantly recruited to the steady state LP, where they subsequently undergo an *in situ* differentiation process to replenish the majority CX3CR1^{high} m ϕ population. This phenotypically identifiable maturation process is accompanied by an alteration in functional capacity, so that resident CX3CR1^{high} m ϕ are relatively desensitised to exogenous stimuli, but remain avidly phagocytic and produce IL10 constitutively. These features, combined with their close association with the epithelium *in vivo*, probably allow resident m ϕ to act as non-inflammatory waste disposal units for cellular debris and any bacteria that breach the epithelial monolayer. CX3CR1^{high} resident m ϕ are probably the cells that have been shown to extend dendrites into the intestinal lumen, although the exact significance of luminal sampling by m ϕ is unclear, as the vast majority of these cells do not migrate to the MLN (189). However evidence is emerging that CX3CR1⁺ m ϕ may be able to transfer captured antigen to mucosal CD103⁺ DC, which then transport it to the MLN. In addition, it has recently been proposed that *bona fide* CD103⁺ DC can also extend protrusions into the intestinal lumen and directly sample the contents, suggesting that this may be a property of all intestinal MP and not only CX3CR1⁺ m ϕ . As well as tissue resident scavengers, there is also growing appreciation that through their production of IL10, intestinal m ϕ contribute to the maintenance of peripheral tolerance through the secondary expansion and maintenance of Treg in the mucosa. In addition, they contribute to epithelial integrity and ablation of resident

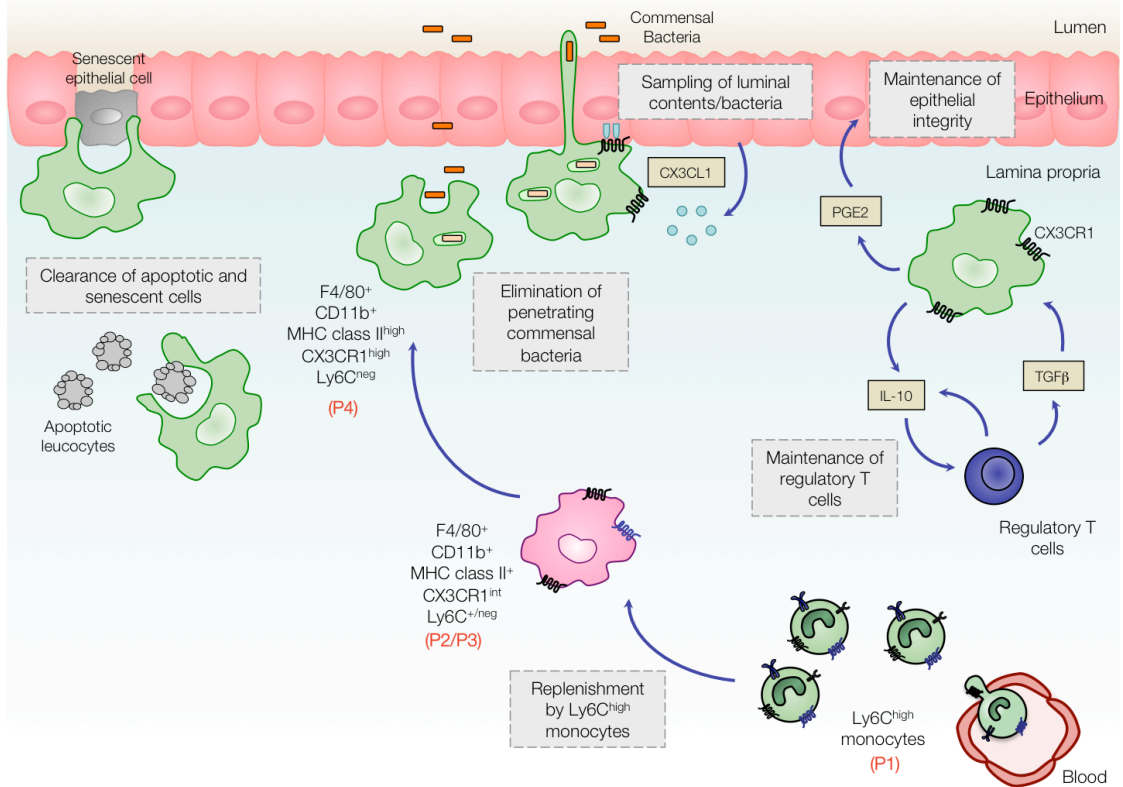
m ϕ results in increased susceptibility to chemically-induced colitis, showing these cells are playing a crucial regulatory role under normal circumstances.

My findings also show that pro-inflammatory m ϕ arise from the same Ly6C^{high} monocyte precursor and accumulation of these cells during experimental colitis is in part due to the breakdown in the local differentiation process. The CCR2-dependent accumulation of Ly6C^{high} monocytes and their derivatives in acute inflammation is important for pathology, but may also be essential for protective immunity to bacterial and parasitic infections in the intestine (25, 295, 296), due to their enhanced ability to produce pro-inflammatory cytokines such as TNF α . Importantly my studies demonstrate for the first time that so-called 'inflammatory' Ly6C^{high} monocytes give rise to both resident and pro-inflammatory monocytes, a concept that contradicts the current theory of monocyte heterogeneity. Furthermore these results show that 'resident' and 'pro-inflammatory' m ϕ in the colon are not independent cell types, but rather represent different differentiation outcomes of the same monocyte precursor and highlight the plastic nature of cells of the MPS. Reassuringly, an analogous monocyte differentiation process appears to be present in the normal human ileum and its breakdown may result in the accumulation of CD14⁺ pro-inflammatory m ϕ during IBD (Bain *et al.*, manuscript submitted). That Ly6C^{high} and CD14⁺ monocytes replenish steady state m ϕ populations in mice and humans, respectively, is contrary to their classification as 'inflammatory' monocytes, and thus I would agree with the recent proposal that these cells should be referred to as 'classical' monocytes, in contrast to Ly6C^{low} murine or CD14⁺CD16^{high} human monocytes which should be termed 'non-classical' (316).

These findings are important, as the selective blockade of inflammatory monocyte infiltration has been an attractive potential strategy for the treatment of human IBD. However given that these monocytes also replenish the resident m ϕ population, the depletion or selective targeting of these monocytes may cause collateral reductions in 'resident' m ϕ populations and therefore a loss of the essential immunoregulatory functions these cells perform. In light of these findings, future studies should focus on identifying the local factors that drive monocyte differentiation in the steady state mucosa and assess why this process is arrested in inflammation, rather than attempting to block monocyte recruitment. Identification of such factors could lead to therapies that aim to manipulate the

intestinal cytokine/chemokine milieu in order to favour differentiation into anti-inflammatory 'resident' $m\phi$ during active inflammation in IBD.

A Homeostasis



B Inflammation

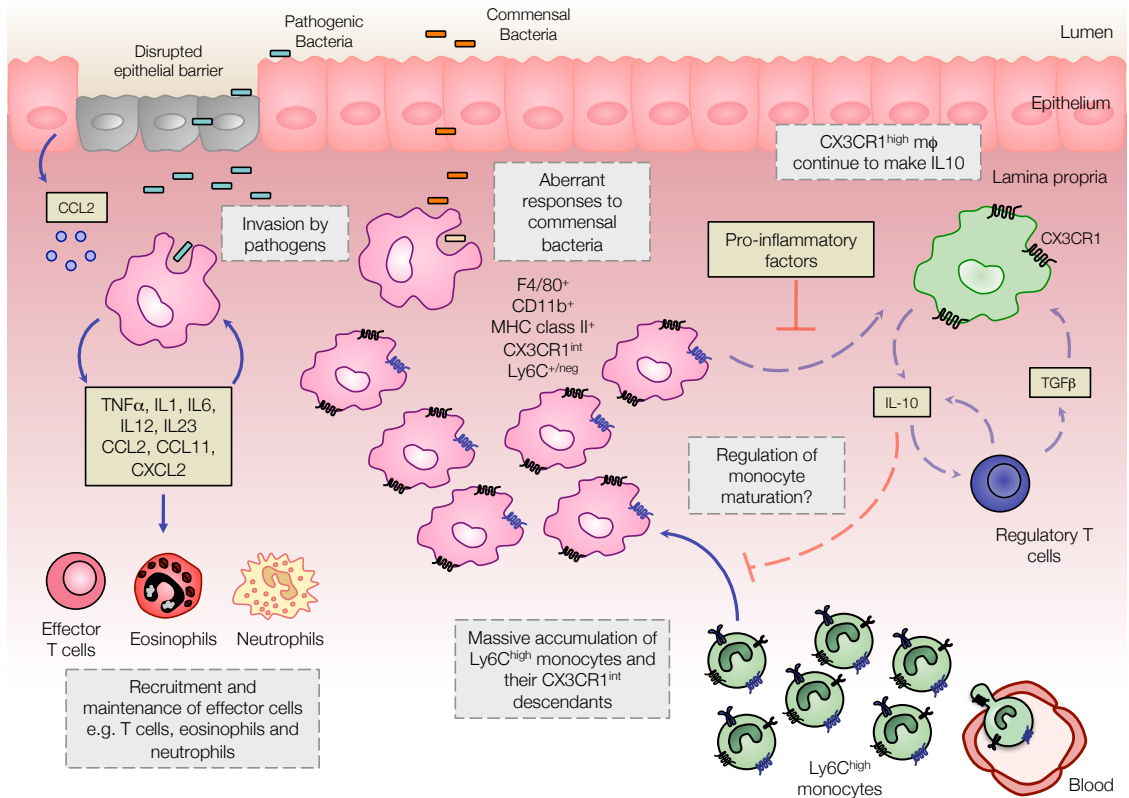


Figure 8.1: The Phenotype, Function and Origin of Intestinal Macrophages in the Normal and Inflamed Intestine

A. Resident $m\phi$ in the intestinal LP are crucial for maintaining local homeostasis by capturing and eliminating any bacteria that breach the epithelial barrier without provoking an inflammatory response. It is likely that they also clear apoptotic and senescent cells, as well as other cellular debris. In resting mucosa, the majority of $m\phi$ (identified in my work as P4) express unusually high levels of CX3CR1, the receptor for the chemokine CX3CL1 (fractalkine) expressed by enterocytes and goblet cells. $M\phi$ may also extend cellular processes through the epithelial layer to sense and perhaps sample the luminal contents, a process dependent on CX3CR1. $M\phi$ also produce immunoregulatory cytokines such as IL10, which may act in an autocrine manner to control $m\phi$ activation, as well as facilitating terminal differentiation and maintenance of FoxP3⁺ Treg within the mucosa. In turn, Treg produce TGF β and IL10, which together with other local factors, are likely to maintain resident $m\phi$ in their state of partial inertia. The results in this thesis indicate that resident intestinal $m\phi$ are continuously replenished by CX3CR1^{int}CCR2⁺Ly6C^{high} 'inflammatory' monocytes (P1), through a process of local differentiation that involves CX3CR1^{int} intermediaries (P2 and P3).

B. During intestinal inflammation induced by pathogen invasion or damage, there is intense recruitment and accumulation of CX3CR1^{int}CCR2⁺Ly6C^{high} monocytes due an arrest in the normal differentiation process. This gives rise to pro-inflammatory $m\phi$ distinguished from their resident counterparts by their lower levels of CX3CR1. They are potent producers of pro-inflammatory cytokines and appear to perpetuate the inflammatory response through the recruitment and maintenance of other effector cells, such as T cells, eosinophils and neutrophils. Some CX3CR1^{high} $m\phi$ remain in the inflamed mucosa and they continue to make IL10, perhaps in an attempt to restore homeostasis by influencing the differentiation of recently recruited monocytes.

References

1. Hopkinson-Woolley, J., D. Hughes, S. Gordon, and P. Martin. 1994. Macrophage recruitment during limb development and wound healing in the embryonic and foetal mouse. *J Cell Sci* 107 (Pt 5):1159-1167.
2. Takemura, R., and Z. Werb. 1984. Secretory products of macrophages and their physiological functions. *Am J Physiol* 246:C1-9.
3. Austyn, J. M., and S. Gordon. 1981. F4/80, a monoclonal antibody directed specifically against the mouse macrophage. *European journal of immunology* 11:805-815.
4. Gordon, S., J. Hamann, H. H. Lin, and M. Stacey. 2011. F4/80 and the related adhesion-GPCRs. *European journal of immunology* 41:2472-2476.
5. Sasmono, R. T., D. Oceandy, J. W. Pollard, W. Tong, P. Pavli, B. J. Wainwright, M. C. Ostrowski, S. R. Himes, and D. A. Hume. 2003. A macrophage colony-stimulating factor receptor-green fluorescent protein transgene is expressed throughout the mononuclear phagocyte system of the mouse. *Blood* 101:1155-1163.
6. Hamann, J., N. Koning, W. Pouwels, L. H. Ulfman, M. van Eijk, M. Stacey, H. H. Lin, S. Gordon, and M. J. Kwakkenbos. 2007. EMR1, the human homolog of F4/80, is an eosinophil-specific receptor. *European journal of immunology* 37:2797-2802.
7. McGarry, M. P., and C. C. Stewart. 1991. Murine eosinophil granulocytes bind the murine macrophage-monocyte specific monoclonal antibody F4/80. *Journal of leukocyte biology* 50:471-478.
8. van Furth, R., Z. A. Cohn, J. G. Hirsch, J. H. Humphrey, W. G. Spector, and H. L. Langevoort. 1972. The mononuclear phagocyte system: a new classification of macrophages, monocytes, and their precursor cells. *Bull World Health Organ* 46:845-852.
9. Hume, D. A. 2008. Differentiation and heterogeneity in the mononuclear phagocyte system. *Mucosal Immunol* 1:432-441.
10. Fogg, D. K., C. Sibon, C. Miled, S. Jung, P. Aucouturier, D. R. Littman, A. Cumano, and F. Geissmann. 2006. A clonogenic bone marrow progenitor specific for macrophages and dendritic cells. *Science (New York, N.Y)* 311:83-87.
11. Takahashi, K., M. Naito, and M. Takeya. 1996. Development and heterogeneity of macrophages and their related cells through their differentiation pathways. *Pathol Int* 46:473-485.
12. Geissmann, F., S. Jung, and D. R. Littman. 2003. Blood monocytes consist of two principal subsets with distinct migratory properties. *Immunity* 19:71-82.
13. Klemsz, M. J., S. R. McKercher, A. Celada, C. Van Beveren, and R. A. Maki. 1990. The macrophage and B cell-specific transcription factor PU.1 is related to the ets oncogene. *Cell* 61:113-124.
14. Scott, E. W., M. C. Simon, J. Anastasi, and H. Singh. 1994. Requirement of transcription factor PU.1 in the development of multiple hematopoietic lineages. *Science (New York, N.Y)* 265:1573-1577.
15. Zhang, D. E., C. J. Hetherington, S. Meyers, K. L. Rhoades, C. J. Larson, H. M. Chen, S. W. Hiebert, and D. G. Tenen. 1996. CCAAT enhancer-binding protein (C/EBP) and AML1 (CBF alpha2) synergistically activate the macrophage colony-stimulating factor receptor promoter. *Mol Cell Biol* 16:1231-1240.

16. Tsai, F. Y., G. Keller, F. C. Kuo, M. Weiss, J. Chen, M. Rosenblatt, F. W. Alt, and S. H. Orkin. 1994. An early haematopoietic defect in mice lacking the transcription factor GATA-2. *Nature* 371:221-226.
17. Shivdasani, R. A., E. L. Mayer, and S. H. Orkin. 1995. Absence of blood formation in mice lacking the T-cell leukaemia oncogene tal-1/SCL. *Nature* 373:432-434.
18. Mucenski, M. L., K. McLain, A. B. Kier, S. H. Swerdlow, C. M. Schreiner, T. A. Miller, D. W. Pietryga, W. J. Scott, Jr., and S. S. Potter. 1991. A functional c-myc gene is required for normal murine fetal hepatic hematopoiesis. *Cell* 65:677-689.
19. Valledor, A. F., F. E. Borrás, M. Cullell-Young, and A. Celada. 1998. Transcription factors that regulate monocyte/macrophage differentiation. *Journal of leukocyte biology* 63:405-417.
20. Huang, G., P. Zhang, H. Hirai, S. Elf, X. Yan, Z. Chen, S. Koschmieder, Y. Okuno, T. Dayaram, J. D. Gowney, R. A. Shivdasani, D. G. Gilliland, N. A. Speck, S. D. Nimer, and D. G. Tenen. 2008. PU.1 is a major downstream target of AML1 (RUNX1) in adult mouse hematopoiesis. *Nat Genet* 40:51-60.
21. Celada, A., F. E. Borrás, C. Soler, J. Lloberas, M. Klemsz, C. van Beveren, S. McKercher, and R. A. Maki. 1996. The transcription factor PU.1 is involved in macrophage proliferation. *The Journal of experimental medicine* 184:61-69.
22. Serbina, N. V., and E. G. Pamer. 2006. Monocyte emigration from bone marrow during bacterial infection requires signals mediated by chemokine receptor CCR2. *Nature immunology* 7:311-317.
23. van Furth, R., and Z. A. Cohn. 1968. The origin and kinetics of mononuclear phagocytes. *The Journal of experimental medicine* 128:415-435.
24. Yasaka, T., N. M. Mantich, L. A. Boxer, and R. L. Baehner. 1981. Functions of human monocyte and lymphocyte subsets obtained by countercurrent centrifugal elutriation: differing functional capacities of human monocyte subsets. *J Immunol* 127:1515-1518.
25. Dunay, I. R., R. A. Damatta, B. Fux, R. Presti, S. Greco, M. Colonna, and L. D. Sibley. 2008. Gr1(+) inflammatory monocytes are required for mucosal resistance to the pathogen *Toxoplasma gondii*. *Immunity* 29:306-317.
26. Getts, D. R., R. L. Terry, M. T. Getts, M. Muller, S. Rana, B. Shrestha, J. Radford, N. Van Rooijen, I. L. Campbell, and N. J. King. 2008. Ly6c+ "inflammatory monocytes" are microglial precursors recruited in a pathogenic manner in West Nile virus encephalitis. *The Journal of experimental medicine* 205:2319-2337.
27. Auffray, C., D. Fogg, M. Garfa, G. Elain, O. Join-Lambert, S. Kayal, S. Sarnacki, A. Cumano, G. Lauvau, and F. Geissmann. 2007. Monitoring of blood vessels and tissues by a population of monocytes with patrolling behavior. *Science (New York, N.Y)* 317:666-670.
28. Varol, C., L. Landsman, D. K. Fogg, L. Greenshtein, B. Gildor, R. Margalit, V. Kalchenko, F. Geissmann, and S. Jung. 2007. Monocytes give rise to mucosal, but not splenic, conventional dendritic cells. *The Journal of experimental medicine* 204:171-180.
29. Sunderkotter, C., T. Nikolic, M. J. Dillon, N. Van Rooijen, M. Stehling, D. A. Drevets, and P. J. Leenen. 2004. Subpopulations of mouse blood monocytes differ in maturation stage and inflammatory response. *J Immunol* 172:4410-4417.
30. Qu, C., E. W. Edwards, F. Tacke, V. Angeli, J. Llodra, G. Sanchez-Schmitz, A. Garin, N. S. Haque, W. Peters, N. van Rooijen, C. Sanchez-Torres, J. Bromberg, I. F. Charo, S. Jung, S. A. Lira, and G. J. Randolph. 2004. Role of CCR8 and other chemokine pathways in the migration of monocyte-derived dendritic cells to lymph nodes. *The Journal of experimental medicine* 200:1231-1241.

31. Mildner, A., H. Schmidt, M. Nitsche, D. Merkler, U. K. Hanisch, M. Mack, M. Heikenwalder, W. Bruck, J. Priller, and M. Prinz. 2007. Microglia in the adult brain arise from Ly-6ChiCCR2+ monocytes only under defined host conditions. *Nat Neurosci* 10:1544-1553.
32. Ingersoll, M. A., R. Spanbroek, C. Lottaz, E. L. Gautier, M. Frankenberger, R. Hoffmann, R. Lang, M. Haniffa, M. Collin, F. Tacke, A. J. Habenicht, L. Ziegler-Heitbrock, and G. J. Randolph. 2010. Comparison of gene expression profiles between human and mouse monocyte subsets. *Blood* 115:e10-19.
33. Ziegler-Heitbrock, H. W., B. Passlick, and D. Flieger. 1988. The monoclonal antimonocyte antibody My4 stains B lymphocytes and two distinct monocyte subsets in human peripheral blood. *Hybridoma* 7:521-527.
34. Weber, C., K. U. Belge, P. von Hundelshausen, G. Draude, B. Steppich, M. Mack, M. Frankenberger, K. S. Weber, and H. W. Ziegler-Heitbrock. 2000. Differential chemokine receptor expression and function in human monocyte subpopulations. *Journal of leukocyte biology* 67:699-704.
35. Skrzeczynska-Moncznik, J., M. Bzowska, S. Loseke, E. Grage-Griebenow, M. Zembala, and J. Pryjma. 2008. Peripheral blood CD14high CD16+ monocytes are main producers of IL-10. *Scand J Immunol* 67:152-159.
36. Grage-Griebenow, E., R. Zawatzky, H. Kahlert, L. Brade, H. Flad, and M. Ernst. 2001. Identification of a novel dendritic cell-like subset of CD64(+) / CD16(+) blood monocytes. *European journal of immunology* 31:48-56.
37. Randolph, G. J., S. Beaulieu, S. Lebecque, R. M. Steinman, and W. A. Muller. 1998. Differentiation of monocytes into dendritic cells in a model of transendothelial trafficking. *Science (New York, N.Y)* 282:480-483.
38. Onai, N., A. Obata-Onai, M. A. Schmid, T. Ohteki, D. Jarrossay, and M. G. Manz. 2007. Identification of clonogenic common Flt3+M-CSFR+ plasmacytoid and conventional dendritic cell progenitors in mouse bone marrow. *Nature immunology* 8:1207-1216.
39. Naik, S. H., P. Sathe, H. Y. Park, D. Metcalf, A. I. Proietto, A. Dakic, S. Carotta, M. O'Keeffe, M. Bahlo, A. Papenfuss, J. Y. Kwak, L. Wu, and K. Shortman. 2007. Development of plasmacytoid and conventional dendritic cell subtypes from single precursor cells derived in vitro and in vivo. *Nature immunology* 8:1217-1226.
40. Auffray, C., D. K. Fogg, E. Narni-Mancinelli, B. Senechal, C. Trouillet, N. Saederup, J. Leemput, K. Bigot, L. Campisi, M. Abitbol, T. Molina, I. Charo, D. A. Hume, A. Cumano, G. Lauvau, and F. Geissmann. 2009. CX3CR1+ CD115+ CD135+ common macrophage/DC precursors and the role of CX3CR1 in their response to inflammation. *The Journal of experimental medicine* 206:595-606.
41. Wiktor-Jedrzejczak, W., E. Urbanowska, S. L. Aukerman, J. W. Pollard, E. R. Stanley, P. Ralph, A. A. Ansari, K. W. Sell, and M. Szperl. 1991. Correction by CSF-1 of defects in the osteopetrotic op/op mouse suggests local, developmental, and humoral requirements for this growth factor. *Exp Hematol* 19:1049-1054.
42. Hamilton, J. A. 1993. Colony stimulating factors, cytokines and monocyte-macrophages--some controversies. *Immunol Today* 14:18-24.
43. Felix, R., M. G. Cecchini, W. Hofstetter, P. R. Elford, A. Stutzer, and H. Fleisch. 1990. Impairment of macrophage colony-stimulating factor production and lack of resident bone marrow macrophages in the osteopetrotic op/op mouse. *J Bone Miner Res* 5:781-789.
44. Dai, X. M., G. R. Ryan, A. J. Hapel, M. G. Dominguez, R. G. Russell, S. Kapp, V. Sylvestre, and E. R. Stanley. 2002. Targeted disruption of the mouse colony-stimulating factor 1 receptor gene results in osteopetrosis, mononuclear phagocyte deficiency, increased primitive progenitor cell frequencies, and reproductive defects. *Blood* 99:111-120.

45. Lin, H., E. Lee, K. Hestir, C. Leo, M. Huang, E. Bosch, R. Halenbeck, G. Wu, A. Zhou, D. Behrens, D. Hollenbaugh, T. Linnemann, M. Qin, J. Wong, K. Chu, S. K. Doberstein, and L. T. Williams. 2008. Discovery of a cytokine and its receptor by functional screening of the extracellular proteome. *Science (New York, N.Y)* 320:807-811.
46. Cecchini, M. G., M. G. Dominguez, S. Mocci, A. Wetterwald, R. Felix, H. Fleisch, O. Chisholm, W. Hofstetter, J. W. Pollard, and E. R. Stanley. 1994. Role of colony stimulating factor-1 in the establishment and regulation of tissue macrophages during postnatal development of the mouse. *Development* 120:1357-1372.
47. Moore, K. J., T. Naito, C. Martin, and V. R. Kelley. 1996. Enhanced response of macrophages to CSF-1 in autoimmune mice: a gene transfer strategy. *J Immunol* 157:433-440.
48. Lin, E. Y., A. V. Nguyen, R. G. Russell, and J. W. Pollard. 2001. Colony-stimulating factor 1 promotes progression of mammary tumors to malignancy. *The Journal of experimental medicine* 193:727-740.
49. Hume, D. A., P. Pavli, R. E. Donahue, and I. J. Fidler. 1988. The effect of human recombinant macrophage colony-stimulating factor (CSF-1) on the murine mononuclear phagocyte system in vivo. *J Immunol* 141:3405-3409.
50. Tagliani, E., C. Shi, P. Nancy, C. S. Tay, E. G. Pamer, and A. Erlebacher. 2011. Coordinate regulation of tissue macrophage and dendritic cell population dynamics by CSF-1. *The Journal of experimental medicine*.
51. Lenda, D. M., E. Kikawada, E. R. Stanley, and V. R. Kelley. 2003. Reduced macrophage recruitment, proliferation, and activation in colony-stimulating factor-1-deficient mice results in decreased tubular apoptosis during renal inflammation. *J Immunol* 170:3254-3262.
52. Witmer-Pack, M. D., D. A. Hughes, G. Schuler, L. Lawson, A. McWilliam, K. Inaba, R. M. Steinman, and S. Gordon. 1993. Identification of macrophages and dendritic cells in the osteopetrotic (op/op) mouse. *J Cell Sci* 104 (Pt 4):1021-1029.
53. Niida, S., M. Kaku, H. Amano, H. Yoshida, H. Kataoka, S. Nishikawa, K. Tanne, N. Maeda, and H. Kodama. 1999. Vascular endothelial growth factor can substitute for macrophage colony-stimulating factor in the support of osteoclastic bone resorption. *The Journal of experimental medicine* 190:293-298.
54. Lean, J. M., K. Fuller, and T. J. Chambers. 2001. FLT3 ligand can substitute for macrophage colony-stimulating factor in support of osteoclast differentiation and function. *Blood* 98:2707-2713.
55. Ginhoux, F., M. Greter, M. Leboeuf, S. Nandi, P. See, S. Gokhan, M. F. Mehler, S. J. Conway, L. G. Ng, E. R. Stanley, I. M. Samokhvalov, and M. Merad. 2010. Fate mapping analysis reveals that adult microglia derive from primitive macrophages. *Science (New York, N.Y)* 330:841-845.
56. Tarling, J. D., H. S. Lin, and S. Hsu. 1987. Self-renewal of pulmonary alveolar macrophages: evidence from radiation chimera studies. *Journal of leukocyte biology* 42:443-446.
57. Merad, M., M. G. Manz, H. Karsunky, A. Wagers, W. Peters, I. Charo, I. L. Weissman, J. G. Cyster, and E. G. Engleman. 2002. Langerhans cells renew in the skin throughout life under steady-state conditions. *Nature immunology* 3:1135-1141.
58. Alliot, F., E. Lecain, B. Grima, and B. Pessac. 1991. Microglial progenitors with a high proliferative potential in the embryonic and adult mouse brain. *Proc Natl Acad Sci U S A* 88:1541-1545.

59. Ajami, B., J. L. Bennett, C. Krieger, W. Tetzlaff, and F. M. Rossi. 2007. Local self-renewal can sustain CNS microglia maintenance and function throughout adult life. *Nat Neurosci* 10:1538-1543.
60. Chorro, L., A. Sarde, M. Li, K. J. Woollard, P. Chambon, B. Malissen, A. Kissenpfennig, J. B. Barbaroux, R. Groves, and F. Geissmann. 2009. Langerhans cell (LC) proliferation mediates neonatal development, homeostasis, and inflammation-associated expansion of the epidermal LC network. *The Journal of experimental medicine* 206:3089-3100.
61. Ajami, B., J. L. Bennett, C. Krieger, K. M. McNagny, and F. M. Rossi. 2011. Infiltrating monocytes trigger EAE progression, but do not contribute to the resident microglia pool. *Nat Neurosci* 14:1142-1149.
62. Mosser, D. M., and J. P. Edwards. 2008. Exploring the full spectrum of macrophage activation. *Nature reviews* 8:958-969.
63. Krausgruber, T., K. Blazek, T. Smallie, S. Alzabin, H. Lockstone, N. Sahgal, T. Hussell, M. Feldmann, and I. A. Udalova. 2011. IRF5 promotes inflammatory macrophage polarization and TH1-TH17 responses. *Nature immunology* 12:231-238.
64. Meraz, M. A., J. M. White, K. C. Sheehan, E. A. Bach, S. J. Rodig, A. S. Dighe, D. H. Kaplan, J. K. Riley, A. C. Greenlund, D. Campbell, K. Carver-Moore, R. N. DuBois, R. Clark, M. Aguet, and R. D. Schreiber. 1996. Targeted disruption of the Stat1 gene in mice reveals unexpected physiologic specificity in the JAK-STAT signaling pathway. *Cell* 84:431-442.
65. Adams, L. B., M. C. Dinauer, D. E. Morgenstern, and J. L. Krahenbuhl. 1997. Comparison of the roles of reactive oxygen and nitrogen intermediates in the host response to Mycobacterium tuberculosis using transgenic mice. *Tuber Lung Dis* 78:237-246.
66. Shiloh, M. U., J. D. MacMicking, S. Nicholson, J. E. Brause, S. Potter, M. Marino, F. Fang, M. Dinauer, and C. Nathan. 1999. Phenotype of mice and macrophages deficient in both phagocyte oxidase and inducible nitric oxide synthase. *Immunity* 10:29-38.
67. Woollard, K. J., and F. Geissmann. 2010. Monocytes in atherosclerosis: subsets and functions. *Nat Rev Cardiol* 7:77-86.
68. Murphy, C. A., C. L. Langrish, Y. Chen, W. Blumenschein, T. McClanahan, R. A. Kastelein, J. D. Sedgwick, and D. J. Cua. 2003. Divergent pro- and antiinflammatory roles for IL-23 and IL-12 in joint autoimmune inflammation. *The Journal of experimental medicine* 198:1951-1957.
69. Abraham, C., and R. Medzhitov. 2011. Interactions between the host innate immune system and microbes in inflammatory bowel disease. *Gastroenterology* 140:1729-1737.
70. Satoh, T., O. Takeuchi, A. Vandenbon, K. Yasuda, Y. Tanaka, Y. Kumagai, T. Miyake, K. Matsushita, T. Okazaki, T. Saitoh, K. Honma, T. Matsuyama, K. Yui, T. Tsujimura, D. M. Standley, K. Nakanishi, K. Nakai, and S. Akira. 2010. The Jmjd3-Irf4 axis regulates M2 macrophage polarization and host responses against helminth infection. *Nature immunology* 11:936-944.
71. Ohmori, Y., and T. A. Hamilton. 1997. IL-4-induced STAT6 suppresses IFN-gamma-stimulated STAT1-dependent transcription in mouse macrophages. *J Immunol* 159:5474-5482.
72. Gordon, S. 2003. Alternative activation of macrophages. *Nature reviews* 3:23-35.
73. Loke, P., M. G. Nair, J. Parkinson, D. Guiliano, M. Blaxter, and J. E. Allen. 2002. IL-4 dependent alternatively-activated macrophages have a distinctive in vivo gene expression phenotype. *BMC Immunol* 3:7.

74. Bleau, G., F. Massicotte, Y. Merlen, and C. Boisvert. 1999. Mammalian chitinase-like proteins. *EXS* 87:211-221.
75. Lin, E. Y., J. F. Li, L. Gnatovskiy, Y. Deng, L. Zhu, D. A. Grzesik, H. Qian, X. N. Xue, and J. W. Pollard. 2006. Macrophages regulate the angiogenic switch in a mouse model of breast cancer. *Cancer Res* 66:11238-11246.
76. Roberts, A. B., M. B. Sporn, R. K. Assoian, J. M. Smith, N. S. Roche, L. M. Wakefield, U. I. Heine, L. A. Liotta, V. Falanga, J. H. Kehrl, and et al. 1986. Transforming growth factor type beta: rapid induction of fibrosis and angiogenesis in vivo and stimulation of collagen formation in vitro. *Proc Natl Acad Sci U S A* 83:4167-4171.
77. Shimokado, K., E. W. Raines, D. K. Madtes, T. B. Barrett, E. P. Benditt, and R. Ross. 1985. A significant part of macrophage-derived growth factor consists of at least two forms of PDGF. *Cell* 43:277-286.
78. Watanabe, K., P. J. Jose, and S. M. Rankin. 2002. Eotaxin-2 generation is differentially regulated by lipopolysaccharide and IL-4 in monocytes and macrophages. *J Immunol* 168:1911-1918.
79. Bonecchi, R., S. Sozzani, J. T. Stine, W. Luini, G. D'Amico, P. Allavena, D. Chantry, and A. Mantovani. 1998. Divergent effects of interleukin-4 and interferon-gamma on macrophage-derived chemokine production: an amplification circuit of polarized T helper 2 responses. *Blood* 92:2668-2671.
80. Katakura, T., M. Miyazaki, M. Kobayashi, D. N. Herndon, and F. Suzuki. 2004. CCL17 and IL-10 as effectors that enable alternatively activated macrophages to inhibit the generation of classically activated macrophages. *J Immunol* 172:1407-1413.
81. Jenkins, S. J., D. Ruckerl, P. C. Cook, L. H. Jones, F. D. Finkelman, N. van Rooijen, A. S. MacDonald, and J. E. Allen. 2011. Local macrophage proliferation, rather than recruitment from the blood, is a signature of TH2 inflammation. *Science (New York, N.Y)* 332:1284-1288.
82. Pluddemann, A., S. Mukhopadhyay, and S. Gordon. 2011. Innate immunity to intracellular pathogens: macrophage receptors and responses to microbial entry. *Immunol Rev* 240:11-24.
83. Biswas, S. K., and A. Mantovani. 2010. Macrophage plasticity and interaction with lymphocyte subsets: cancer as a paradigm. *Nature immunology* 11:889-896.
84. Liu, Y., J. M. Cousin, J. Hughes, J. Van Damme, J. R. Seckl, C. Haslett, I. Dransfield, J. Savill, and A. G. Rossi. 1999. Glucocorticoids promote nonphlogistic phagocytosis of apoptotic leukocytes. *J Immunol* 162:3639-3646.
85. Martinez, F. O., A. Sica, A. Mantovani, and M. Locati. 2008. Macrophage activation and polarization. *Front Biosci* 13:453-461.
86. Fadok, V. A., D. L. Bratton, A. Konowal, P. W. Freed, J. Y. Westcott, and P. M. Henson. 1998. Macrophages that have ingested apoptotic cells in vitro inhibit proinflammatory cytokine production through autocrine/paracrine mechanisms involving TGF-beta, PGE2, and PAF. *J Clin Invest* 101:890-898.
87. Sutterwala, F. S., G. J. Noel, P. Salgame, and D. M. Mosser. 1998. Reversal of proinflammatory responses by ligating the macrophage Fc gamma receptor type I. *The Journal of experimental medicine* 188:217-222.
88. Roca, H., Z. S. Varsos, S. Sud, M. J. Craig, C. Ying, and K. J. Pienta. 2009. CCL2 and interleukin-6 promote survival of human CD11b+ peripheral blood mononuclear cells and induce M2-type macrophage polarization. *J Biol Chem* 284:34342-34354.
89. Gustafsson, C., J. Mjosberg, A. Matussek, R. Geffers, L. Matthiesen, G. Berg, S. Sharma, J. Buer, and J. Ernerudh. 2008. Gene expression profiling of human

decidual macrophages: evidence for immunosuppressive phenotype. *PLoS One* 3:e2078.

90. Pucci, F., M. A. Venneri, D. Biziato, A. Nonis, D. Moi, A. Sica, C. Di Serio, L. Naldini, and M. De Palma. 2009. A distinguishing gene signature shared by tumor-infiltrating Tie2-expressing monocytes, blood "resident" monocytes, and embryonic macrophages suggests common functions and developmental relationships. *Blood* 114:901-914.
91. Curiel, T. J., G. Coukos, L. Zou, X. Alvarez, P. Cheng, P. Mottram, M. Evdemon-Hogan, J. R. Conejo-Garcia, L. Zhang, M. Burow, Y. Zhu, S. Wei, I. Kryczek, B. Daniel, A. Gordon, L. Myers, A. Lackner, M. L. Disis, K. L. Knutson, L. Chen, and W. Zou. 2004. Specific recruitment of regulatory T cells in ovarian carcinoma fosters immune privilege and predicts reduced survival. *Nat Med* 10:942-949.
92. Smith, H. O., P. S. Anderson, D. Y. Kuo, G. L. Goldberg, C. L. DeVictoria, C. A. Boocock, J. G. Jones, C. D. Runowicz, E. R. Stanley, and J. W. Pollard. 1995. The role of colony-stimulating factor 1 and its receptor in the etiopathogenesis of endometrial adenocarcinoma. *Clin Cancer Res* 1:313-325.
93. O'Neill, L. A., and A. G. Bowie. 2007. The family of five: TIR-domain-containing adaptors in Toll-like receptor signalling. *Nature reviews* 7:353-364.
94. Burns, K., S. Janssens, B. Brissoni, N. Olivos, R. Beyaert, and J. Tschopp. 2003. Inhibition of interleukin 1 receptor/Toll-like receptor signaling through the alternatively spliced, short form of MyD88 is due to its failure to recruit IRAK-4. *The Journal of experimental medicine* 197:263-268.
95. Kobayashi, K., L. D. Hernandez, J. E. Galan, C. A. Janeway, Jr., R. Medzhitov, and R. A. Flavell. 2002. IRAK-M is a negative regulator of Toll-like receptor signaling. *Cell* 110:191-202.
96. Zhang, G., and S. Ghosh. 2002. Negative regulation of toll-like receptor-mediated signaling by Tollip. *J Biol Chem* 277:7059-7065.
97. Boone, D. L., E. E. Turer, E. G. Lee, R. C. Ahmad, M. T. Wheeler, C. Tsui, P. Hurley, M. Chien, S. Chai, O. Hitotsumatsu, E. McNally, C. Pickart, and A. Ma. 2004. The ubiquitin-modifying enzyme A20 is required for termination of Toll-like receptor responses. *Nature immunology* 5:1052-1060.
98. Lee, E. G., D. L. Boone, S. Chai, S. L. Libby, M. Chien, J. P. Lodolce, and A. Ma. 2000. Failure to regulate TNF-induced NF-kappaB and cell death responses in A20-deficient mice. *Science (New York, N.Y)* 289:2350-2354.
99. Garlanda, C., F. Riva, N. Polentarutti, C. Buracchi, M. Sironi, M. De Bortoli, M. Muzio, R. Bergottini, E. Scanziani, A. Vecchi, E. Hirsch, and A. Mantovani. 2004. Intestinal inflammation in mice deficient in Tir8, an inhibitory member of the IL-1 receptor family. *Proc Natl Acad Sci U S A* 101:3522-3526.
100. Alam, M. M., and L. A. O'Neill. 2011. MicroRNAs and the resolution phase of inflammation in macrophages. *European journal of immunology* 41:2482-2485.
101. Taganov, K. D., M. P. Boldin, K. J. Chang, and D. Baltimore. 2006. NF-kappaB-dependent induction of microRNA miR-146, an inhibitor targeted to signaling proteins of innate immune responses. *Proc Natl Acad Sci U S A* 103:12481-12486.
102. Boldin, M. P., K. D. Taganov, D. S. Rao, L. Yang, J. L. Zhao, M. Kalwani, Y. Garcia-Flores, M. Luong, A. Devrekanli, J. Xu, G. Sun, J. Tay, P. S. Linsley, and D. Baltimore. 2011. miR-146a is a significant brake on autoimmunity, myeloproliferation, and cancer in mice. *The Journal of experimental medicine* 208:1189-1201.
103. Ravetch, J. V., and L. L. Lanier. 2000. Immune inhibitory receptors. *Science (New York, N.Y)* 290:84-89.

104. Kharitonov, A., Z. Chen, I. Sures, H. Wang, J. Schilling, and A. Ullrich. 1997. A family of proteins that inhibit signalling through tyrosine kinase receptors. *Nature* 386:181-186.
105. Bouchon, A., J. Dietrich, and M. Colonna. 2000. Cutting edge: inflammatory responses can be triggered by TREM-1, a novel receptor expressed on neutrophils and monocytes. *J Immunol* 164:4991-4995.
106. Turnbull, I. R., S. Gilfillan, M. Cella, T. Aoshi, M. Miller, L. Piccio, M. Hernandez, and M. Colonna. 2006. Cutting edge: TREM-2 attenuates macrophage activation. *J Immunol* 177:3520-3524.
107. Akkaya, M., and A. N. Barclay. 2010. Heterogeneity in the CD200R paired receptor family. *Immunogenetics* 62:15-22.
108. Wright, G. J., H. Cherwinski, M. Foster-Cuevas, G. Brooke, M. J. Puklavec, M. Bigler, Y. Song, M. Jenmalm, D. Gorman, T. McClanahan, M. R. Liu, M. H. Brown, J. D. Sedgwick, J. H. Phillips, and A. N. Barclay. 2003. Characterization of the CD200 receptor family in mice and humans and their interactions with CD200. *J Immunol* 171:3034-3046.
109. Webb, M., and A. N. Barclay. 1984. Localisation of the MRC OX-2 glycoprotein on the surfaces of neurones. *J Neurochem* 43:1061-1067.
110. Gorczynski, R., Z. Chen, Y. Kai, L. Lee, S. Wong, and P. A. Marsden. 2004. CD200 is a ligand for all members of the CD200R family of immunoregulatory molecules. *J Immunol* 172:7744-7749.
111. Hatherley, D., H. M. Cherwinski, M. Moshref, and A. N. Barclay. 2005. Recombinant CD200 protein does not bind activating proteins closely related to CD200 receptor. *J Immunol* 175:2469-2474.
112. Borriello, F., J. Lederer, S. Scott, and A. H. Sharpe. 1997. MRC OX-2 defines a novel T cell costimulatory pathway. *J Immunol* 158:4548-4554.
113. Hoek, R. M., S. R. Ruuls, C. A. Murphy, G. J. Wright, R. Goddard, S. M. Zurawski, B. Blom, M. E. Homola, W. J. Streit, M. H. Brown, A. N. Barclay, and J. D. Sedgwick. 2000. Down-regulation of the macrophage lineage through interaction with OX2 (CD200). *Science (New York, N.Y)* 290:1768-1771.
114. Wright, G. J., M. J. Puklavec, A. C. Willis, R. M. Hoek, J. D. Sedgwick, M. H. Brown, and A. N. Barclay. 2000. Lymphoid/neuronal cell surface OX2 glycoprotein recognizes a novel receptor on macrophages implicated in the control of their function. *Immunity* 13:233-242.
115. Cherwinski, H. M., C. A. Murphy, B. L. Joyce, M. E. Bigler, Y. S. Song, S. M. Zurawski, M. M. Moshrefi, D. M. Gorman, K. L. Miller, S. Zhang, J. D. Sedgwick, and J. H. Phillips. 2005. The CD200 receptor is a novel and potent regulator of murine and human mast cell function. *J Immunol* 174:1348-1356.
116. Dick, A. D., D. Carter, M. Robertson, C. Broderick, E. Hughes, J. V. Forrester, and J. Liversidge. 2003. Control of myeloid activity during retinal inflammation. *Journal of leukocyte biology* 74:161-166.
117. Taylor, N., K. McConachie, C. Calder, R. Dawson, A. Dick, J. D. Sedgwick, and J. Liversidge. 2005. Enhanced tolerance to autoimmune uveitis in CD200-deficient mice correlates with a pronounced Th2 switch in response to antigen challenge. *J Immunol* 174:143-154.
118. Rosenblum, M. D., E. B. Olsz, K. B. Yancey, J. E. Woodliff, Z. Lazarova, K. A. Gerber, and R. L. Truitt. 2004. Expression of CD200 on epithelial cells of the murine hair follicle: a role in tissue-specific immune tolerance? *J Invest Dermatol* 123:880-887.
119. Snelgrove, R. J., J. Goulding, A. M. Didierlaurent, D. Lyonga, S. Vekaria, L. Edwards, E. Gwyer, J. D. Sedgwick, A. N. Barclay, and T. Hussell. 2008. A critical

- function for CD200 in lung immune homeostasis and the severity of influenza infection. *Nature immunology* 9:1074-1083.
120. Gorczynski, R. M., Z. Chen, L. Lee, K. Yu, and J. Hu. 2002. Anti-CD200R ameliorates collagen-induced arthritis in mice. *Clin Immunol* 104:256-264.
 121. Zhang, S., H. Cherwinski, J. D. Sedgwick, and J. H. Phillips. 2004. Molecular mechanisms of CD200 inhibition of mast cell activation. *J Immunol* 173:6786-6793.
 122. Shinohara, H., A. Inoue, N. Toyama-Sorimachi, Y. Nagai, T. Yasuda, H. Suzuki, R. Horai, Y. Iwakura, T. Yamamoto, H. Karasuyama, K. Miyake, and Y. Yamanashi. 2005. Dok-1 and Dok-2 are negative regulators of lipopolysaccharide-induced signaling. *The Journal of experimental medicine* 201:333-339.
 123. Fallarino, F., C. Asselin-Paturel, C. Vacca, R. Bianchi, S. Gizzi, M. C. Fioretti, G. Trinchieri, U. Grohmann, and P. Puccetti. 2004. Murine plasmacytoid dendritic cells initiate the immunosuppressive pathway of tryptophan catabolism in response to CD200 receptor engagement. *J Immunol* 173:3748-3754.
 124. Rosenblum, M. D., E. Olasz, J. E. Woodliff, B. D. Johnson, M. C. Konkol, K. A. Gerber, R. J. Orentas, G. Sandford, and R. L. Truitt. 2004. CD200 is a novel p53-target gene involved in apoptosis-associated immune tolerance. *Blood* 103:2691-2698.
 125. Boudakov, I., J. Liu, N. Fan, P. Gulay, K. Wong, and R. M. Gorczynski. 2007. Mice lacking CD200R1 show absence of suppression of lipopolysaccharide-induced tumor necrosis factor-alpha and mixed leukocyte culture responses by CD200. *Transplantation* 84:251-257.
 126. Jenmalm, M. C., H. Cherwinski, E. P. Bowman, J. H. Phillips, and J. D. Sedgwick. 2006. Regulation of myeloid cell function through the CD200 receptor. *J Immunol* 176:191-199.
 127. Foster-Cuevas, M., G. J. Wright, M. J. Puklavec, M. H. Brown, and A. N. Barclay. 2004. Human herpesvirus 8 K14 protein mimics CD200 in down-regulating macrophage activation through CD200 receptor. *J Virol* 78:7667-7676.
 128. Mowat, A. M. 2003. Anatomical basis of tolerance and immunity to intestinal antigens. *Nature reviews* 3:331-341.
 129. Macpherson, A. J., E. Slack, M. B. Geuking, and K. D. McCoy. 2009. The mucosal firewalls against commensal intestinal microbes. *Semin Immunopathol* 31:145-149.
 130. Xavier, R. J., and D. K. Podolsky. 2007. Unravelling the pathogenesis of inflammatory bowel disease. *Nature* 448:427-434.
 131. Rakoff-Nahoum, S., J. Paglino, F. Eslami-Varzaneh, S. Edberg, and R. Medzhitov. 2004. Recognition of commensal microflora by toll-like receptors is required for intestinal homeostasis. *Cell* 118:229-241.
 132. Vaishnava, S., C. L. Behrendt, A. S. Ismail, L. Eckmann, and L. V. Hooper. 2008. Paneth cells directly sense gut commensals and maintain homeostasis at the intestinal host-microbial interface. *Proc Natl Acad Sci U S A* 105:20858-20863.
 133. Mashimo, H., D. C. Wu, D. K. Podolsky, and M. C. Fishman. 1996. Impaired defense of intestinal mucosa in mice lacking intestinal trefoil factor. *Science (New York, N.Y)* 274:262-265.
 134. Salzman, N. H., M. A. Underwood, and C. L. Bevins. 2007. Paneth cells, defensins, and the commensal microbiota: a hypothesis on intimate interplay at the intestinal mucosa. *Semin Immunol* 19:70-83.
 135. Tytgat, K. M., J. W. van der Wal, A. W. Einerhand, H. A. Buller, and J. Dekker. 1996. Quantitative analysis of MUC2 synthesis in ulcerative colitis. *Biochem Biophys Res Commun* 224:397-405.

136. Van der Sluis, M., B. A. De Koning, A. C. De Bruijn, A. Velcich, J. P. Meijerink, J. B. Van Goudoever, H. A. Buller, J. Dekker, I. Van Seuning, I. B. Renes, and A. W. Einerhand. 2006. Muc2-deficient mice spontaneously develop colitis, indicating that MUC2 is critical for colonic protection. *Gastroenterology* 131:117-129.
137. Harrison, O. J., and K. J. Maloy. 2011. Innate immune activation in intestinal homeostasis. *J Innate Immun* 3:585-593.
138. Annacker, O., J. L. Coombes, V. Malmstrom, H. H. Uhlig, T. Bourne, B. Johansson-Lindbom, W. W. Agace, C. M. Parker, and F. Powrie. 2005. Essential role for CD103 in the T cell-mediated regulation of experimental colitis. *The Journal of experimental medicine* 202:1051-1061.
139. Hadis, U., B. Wahl, O. Schulz, M. Hardtke-Wolenski, A. Schippers, N. Wagner, W. Muller, T. Sparwasser, R. Forster, and O. Pabst. 2011. Intestinal tolerance requires gut homing and expansion of FoxP3+ regulatory T cells in the lamina propria. *Immunity* 34:237-246.
140. Carman, P. S., P. B. Ernst, K. L. Rosenthal, D. A. Clark, A. D. Befus, and J. Bienenstock. 1986. Intraepithelial leukocytes contain a unique subpopulation of NK-like cytotoxic cells active in the defense of gut epithelium to enteric murine coronavirus. *J Immunol* 136:1548-1553.
141. Buzoni-Gatel, D., A. C. Lepage, I. H. Dimier-Poisson, D. T. Bout, and L. H. Kasper. 1997. Adoptive transfer of gut intraepithelial lymphocytes protects against murine infection with *Toxoplasma gondii*. *J Immunol* 158:5883-5889.
142. Yang, H., P. A. Antony, B. E. Wildhaber, and D. H. Teitelbaum. 2004. Intestinal intraepithelial lymphocyte gamma delta-T cell-derived keratinocyte growth factor modulates epithelial growth in the mouse. *J Immunol* 172:4151-4158.
143. Maloy, K. J., and F. Powrie. 2011. Intestinal homeostasis and its breakdown in inflammatory bowel disease. *Nature* 474:298-306.
144. Hooper, L. V., and A. J. Macpherson. 2010. Immune adaptations that maintain homeostasis with the intestinal microbiota. *Nature reviews* 10:159-169.
145. Fiocchi, C. 2008. What is "physiological" intestinal inflammation and how does it differ from "pathological" inflammation? *Inflamm Bowel Dis* 14 Suppl 2:S77-78.
146. Maslowski, K. M., A. T. Vieira, A. Ng, J. Kranich, F. Sierro, D. Yu, H. C. Schilter, M. S. Rolph, F. Mackay, D. Artis, R. J. Xavier, M. M. Teixeira, and C. R. Mackay. 2009. Regulation of inflammatory responses by gut microbiota and chemoattractant receptor GPR43. *Nature* 461:1282-1286.
147. Ivanov, II, K. Atarashi, N. Manel, E. L. Brodie, T. Shima, U. Karaoz, D. Wei, K. C. Goldfarb, C. A. Santee, S. V. Lynch, T. Tanoue, A. Imaoka, K. Itoh, K. Takeda, Y. Umesaki, K. Honda, and D. R. Littman. 2009. Induction of intestinal Th17 cells by segmented filamentous bacteria. *Cell* 139:485-498.
148. Hooper, L. V., M. H. Wong, A. Thelin, L. Hansson, P. G. Falk, and J. I. Gordon. 2001. Molecular analysis of commensal host-microbial relationships in the intestine. *Science (New York, N.Y)* 291:881-884.
149. Araki, A., T. Kanai, T. Ishikura, S. Makita, K. Uraushihara, R. Iiyama, T. Totsuka, K. Takeda, S. Akira, and M. Watanabe. 2005. MyD88-deficient mice develop severe intestinal inflammation in dextran sodium sulfate colitis. *J Gastroenterol* 40:16-23.
150. Powrie, F., M. W. Leach, S. Mauze, L. B. Caddle, and R. L. Coffman. 1993. Phenotypically distinct subsets of CD4+ T cells induce or protect from chronic intestinal inflammation in C. B-17 scid mice. *Int Immunol* 5:1461-1471.
151. Lakatos, P. L. 2006. Recent trends in the epidemiology of inflammatory bowel diseases: up or down? *World J Gastroenterol* 12:6102-6108.

152. Annunziato, F., L. Cosmi, V. Santarlasci, L. Maggi, F. Liotta, B. Mazzinghi, E. Parente, L. Fili, S. Ferri, F. Frosali, F. Giudici, P. Romagnani, P. Parronchi, F. Tonelli, E. Maggi, and S. Romagnani. 2007. Phenotypic and functional features of human Th17 cells. *The Journal of experimental medicine* 204:1849-1861.
153. Danese, S., and C. Fiocchi. 2011. Ulcerative colitis. *N Engl J Med* 365:1713-1725.
154. Whelan, R. A., S. Hartmann, and S. Rausch. 2011. Nematode modulation of inflammatory bowel disease. *Protoplasma*.
155. Sellon, R. K., S. Tonkonogy, M. Schultz, L. A. Dieleman, W. Grenther, E. Balish, D. M. Rennick, and R. B. Sartor. 1998. Resident enteric bacteria are necessary for development of spontaneous colitis and immune system activation in interleukin-10-deficient mice. *Infect Immun* 66:5224-5231.
156. Garrett, W. S., G. M. Lord, S. Punit, G. Lugo-Villarino, S. K. Mazmanian, S. Ito, J. N. Glickman, and L. H. Glimcher. 2007. Communicable ulcerative colitis induced by T-bet deficiency in the innate immune system. *Cell* 131:33-45.
157. Gionchetti, P., F. Rizzello, U. Helwig, A. Venturi, K. M. Lammers, P. Brigidi, B. Vitali, G. Poggioli, M. Miglioli, and M. Campieri. 2003. Prophylaxis of pouchitis onset with probiotic therapy: a double-blind, placebo-controlled trial. *Gastroenterology* 124:1202-1209.
158. Frank, D. N., A. L. St Amand, R. A. Feldman, E. C. Boedeker, N. Harpaz, and N. R. Pace. 2007. Molecular-phylogenetic characterization of microbial community imbalances in human inflammatory bowel diseases. *Proc Natl Acad Sci U S A* 104:13780-13785.
159. Greenstein, R. J. 2003. Is Crohn's disease caused by a mycobacterium? Comparisons with leprosy, tuberculosis, and Johne's disease. *Lancet Infect Dis* 3:507-514.
160. Saitoh, T., N. Fujita, M. H. Jang, S. Uematsu, B. G. Yang, T. Satoh, H. Omori, T. Noda, N. Yamamoto, M. Komatsu, K. Tanaka, T. Kawai, T. Tsujimura, O. Takeuchi, T. Yoshimori, and S. Akira. 2008. Loss of the autophagy protein Atg16L1 enhances endotoxin-induced IL-1beta production. *Nature* 456:264-268.
161. Kobayashi, K. S., M. Chamillard, Y. Ogura, O. Henegariu, N. Inohara, G. Nunez, and R. A. Flavell. 2005. Nod2-dependent regulation of innate and adaptive immunity in the intestinal tract. *Science (New York, N.Y)* 307:731-734.
162. Wehkamp, J., J. Harder, M. Weichenthal, M. Schwab, E. Schaffeler, M. Schlee, K. R. Herrlinger, A. Stallmach, F. Noack, P. Fritz, J. M. Schroder, C. L. Bevins, K. Fellermann, and E. F. Stange. 2004. NOD2 (CARD15) mutations in Crohn's disease are associated with diminished mucosal alpha-defensin expression. *Gut* 53:1658-1664.
163. Henry, S. C., X. G. Daniell, A. R. Burroughs, M. Indaram, D. N. Howell, J. Coers, M. N. Starnbach, J. P. Hunn, J. C. Howard, C. G. Feng, A. Sher, and G. A. Taylor. 2009. Balance of Irgm protein activities determines IFN-gamma-induced host defense. *Journal of leukocyte biology* 85:877-885.
164. MacMicking, J. D., G. A. Taylor, and J. D. McKinney. 2003. Immune control of tuberculosis by IFN-gamma-inducible LRG-47. *Science (New York, N.Y)* 302:654-659.
165. Targan, S. R., S. B. Hanauer, S. J. van Deventer, L. Mayer, D. H. Present, T. Braakman, K. L. DeWoody, T. F. Schaible, and P. J. Rutgeerts. 1997. A short-term study of chimeric monoclonal antibody cA2 to tumor necrosis factor alpha for Crohn's disease. Crohn's Disease cA2 Study Group. *N Engl J Med* 337:1029-1035.
166. Noguchi, D., D. Wakita, M. Tajima, S. Ashino, Y. Iwakura, Y. Zhang, K. Chamoto, H. Kitamura, and T. Nishimura. 2007. Blocking of IL-6 signaling pathway prevents

- CD4+ T cell-mediated colitis in a T(h)17-independent manner. *Int Immunol* 19:1431-1440.
167. Lee, S. H., P. M. Starkey, and S. Gordon. 1985. Quantitative analysis of total macrophage content in adult mouse tissues. Immunochemical studies with monoclonal antibody F4/80. *The Journal of experimental medicine* 161:475-489.
 168. Mowat, A. M., and C. C. Bain. 2011. Mucosal macrophages in intestinal homeostasis and inflammation. *J Innate Immun* 3:550-564.
 169. Niess, J. H., and G. Adler. 2010. Enteric flora expands gut lamina propria CX3CR1+ dendritic cells supporting inflammatory immune responses under normal and inflammatory conditions. *J Immunol* 184:2026-2037.
 170. Smith, P. D., L. E. Smythies, M. Mosteller-Barnum, D. A. Sibley, M. W. Russell, M. Merger, M. T. Sellers, J. M. Orenstein, T. Shimada, M. F. Graham, and H. Kubagawa. 2001. Intestinal macrophages lack CD14 and CD89 and consequently are down-regulated for LPS- and IgA-mediated activities. *J Immunol* 167:2651-2656.
 171. Smythies, L. E., M. Sellers, R. H. Clements, M. Mosteller-Barnum, G. Meng, W. H. Benjamin, J. M. Orenstein, and P. D. Smith. 2005. Human intestinal macrophages display profound inflammatory anergy despite avid phagocytic and bacteriocidal activity. *J Clin Invest* 115:66-75.
 172. Rogler, G., M. Hausmann, D. Vogl, E. Aschenbrenner, T. Andus, W. Falk, R. Andreesen, J. Scholmerich, and V. Gross. 1998. Isolation and phenotypic characterization of colonic macrophages. *Clin Exp Immunol* 112:205-215.
 173. Macpherson, A. J., and T. Uhr. 2004. Induction of protective IgA by intestinal dendritic cells carrying commensal bacteria. *Science (New York, N.Y)* 303:1662-1665.
 174. Hedl, M., J. Li, J. H. Cho, and C. Abraham. 2007. Chronic stimulation of Nod2 mediates tolerance to bacterial products. *Proc Natl Acad Sci U S A* 104:19440-19445.
 175. Mahida, Y. R., K. C. Wu, and D. P. Jewell. 1989. Respiratory burst activity of intestinal macrophages in normal and inflammatory bowel disease. *Gut* 30:1362-1370.
 176. Ikeda, I., T. Kasajima, S. Ishiyama, T. Shimojo, Y. Takeo, T. Nishikawa, S. Kameoka, M. Hiroe, and A. Mitsunaga. 1997. Distribution of inducible nitric oxide synthase in ulcerative colitis. *Am J Gastroenterol* 92:1339-1341.
 177. Kamada, N., T. Hisamatsu, S. Okamoto, T. Sato, K. Matsuoka, K. Arai, T. Nakai, A. Hasegawa, N. Inoue, N. Watanabe, K. S. Akagawa, and T. Hibi. 2005. Abnormally differentiated subsets of intestinal macrophage play a key role in Th1-dominant chronic colitis through excess production of IL-12 and IL-23 in response to bacteria. *J Immunol* 175:6900-6908.
 178. Denning, T. L., Y. C. Wang, S. R. Patel, I. R. Williams, and B. Pulendran. 2007. Lamina propria macrophages and dendritic cells differentially induce regulatory and interleukin 17-producing T cell responses. *Nature immunology* 8:1086-1094.
 179. Smythies, L. E., R. Shen, D. Bimczok, L. Novak, R. H. Clements, D. E. Eckhoff, P. Bouchard, M. D. George, W. K. Hu, S. Dandekar, and P. D. Smith. 2010. Inflammation anergy in human intestinal macrophages is due to Smad-induced I κ B α expression and NF- κ B inactivation. *J Biol Chem* 285:19593-19604.
 180. Pull, S. L., J. M. Doherty, J. C. Mills, J. I. Gordon, and T. S. Stappenbeck. 2005. Activated macrophages are an adaptive element of the colonic epithelial progenitor niche necessary for regenerative responses to injury. *Proc Natl Acad Sci U S A* 102:99-104.

181. Morteau, O., S. G. Morham, R. Sellon, L. A. Dieleman, R. Langenbach, O. Smithies, and R. B. Sartor. 2000. Impaired mucosal defense to acute colonic injury in mice lacking cyclooxygenase-1 or cyclooxygenase-2. *J Clin Invest* 105:469-478.
182. Qualls, J. E., A. M. Kaplan, N. van Rooijen, and D. A. Cohen. 2006. Suppression of experimental colitis by intestinal mononuclear phagocytes. *Journal of leukocyte biology* 80:802-815.
183. Murai, M., O. Turovskaya, G. Kim, R. Madan, C. L. Karp, H. Cheroutre, and M. Kronenberg. 2009. Interleukin 10 acts on regulatory T cells to maintain expression of the transcription factor Foxp3 and suppressive function in mice with colitis. *Nature immunology* 10:1178-1184.
184. Lin, H. H., D. E. Faunce, M. Stacey, A. Terajewicz, T. Nakamura, J. Zhang-Hoover, M. Kerley, M. L. Mucenski, S. Gordon, and J. Stein-Streilein. 2005. The macrophage F4/80 receptor is required for the induction of antigen-specific efferent regulatory T cells in peripheral tolerance. *The Journal of experimental medicine* 201:1615-1625.
185. Hume, D. A., W. Allan, P. G. Hogan, and W. F. Doe. 1987. Immunohistochemical characterisation of macrophages in human liver and gastrointestinal tract: expression of CD4, HLA-DR, OKM1, and the mature macrophage marker 25F9 in normal and diseased tissue. *Journal of leukocyte biology* 42:474-484.
186. Pavli, P., C. E. Woodhams, W. F. Doe, and D. A. Hume. 1990. Isolation and characterization of antigen-presenting dendritic cells from the mouse intestinal lamina propria. *Immunology* 70:40-47.
187. Wilders, M. M., T. Sminia, and E. M. Janse. 1983. Ontogeny of non-lymphoid and lymphoid cells in the rat gut with special reference to large mononuclear Ia-positive dendritic cells. *Immunology* 50:303-314.
188. Hume, D. A. 2008. Macrophages as APC and the dendritic cell myth. *J Immunol* 181:5829-5835.
189. Schulz, O., E. Jaensson, E. K. Persson, X. Liu, T. Worbs, W. W. Agace, and O. Pabst. 2009. Intestinal CD103+, but not CX3CR1+, antigen sampling cells migrate in lymph and serve classical dendritic cell functions. *The Journal of experimental medicine* 206:3101-3114.
190. Johansson-Lindbom, B., M. Svensson, O. Pabst, C. Palmqvist, G. Marquez, R. Forster, and W. W. Agace. 2005. Functional specialization of gut CD103+ dendritic cells in the regulation of tissue-selective T cell homing. *The Journal of experimental medicine* 202:1063-1073.
191. Coombes, J. L., K. R. Siddiqui, C. V. Arancibia-Carcamo, J. Hall, C. M. Sun, Y. Belkaid, and F. Powrie. 2007. A functionally specialized population of mucosal CD103+ DCs induces Foxp3+ regulatory T cells via a TGF-beta and retinoic acid-dependent mechanism. *The Journal of experimental medicine* 204:1757-1764.
192. Jaensson, E., H. Uronen-Hansson, O. Pabst, B. Eksteen, J. Tian, J. L. Coombes, P. L. Berg, T. Davidsson, F. Powrie, B. Johansson-Lindbom, and W. W. Agace. 2008. Small intestinal CD103+ dendritic cells display unique functional properties that are conserved between mice and humans. *The Journal of experimental medicine* 205:2139-2149.
193. Niess, J. H., S. Brand, X. Gu, L. Landsman, S. Jung, B. A. McCormick, J. M. Vyas, M. Boes, H. L. Ploegh, J. G. Fox, D. R. Littman, and H. C. Reinecker. 2005. CX3CR1-mediated dendritic cell access to the intestinal lumen and bacterial clearance. *Science (New York, N.Y)* 307:254-258.
194. Rescigno, M., M. Urbano, B. Valzasina, M. Francolini, G. Rotta, R. Bonasio, F. Granucci, J. P. Kraehenbuhl, and P. Ricciardi-Castagnoli. 2001. Dendritic cells express tight junction proteins and penetrate gut epithelial monolayers to sample bacteria. *Nature immunology* 2:361-367.

195. Bogunovic, M., F. Ginhoux, J. Helft, L. Shang, D. Hashimoto, M. Greter, K. Liu, C. Jakubzick, M. A. Ingersoll, M. Leboeuf, E. R. Stanley, M. Nussenzweig, S. A. Lira, G. J. Randolph, and M. Merad. 2009. Origin of the lamina propria dendritic cell network. *Immunity* 31:513-525.
196. Varol, C., A. Vallon-Eberhard, E. Elinav, T. Aychek, Y. Shapira, H. Luche, H. J. Fehling, W. D. Hardt, G. Shakhar, and S. Jung. 2009. Intestinal lamina propria dendritic cell subsets have different origin and functions. *Immunity* 31:502-512.
197. MacDonald, K. P., J. S. Palmer, S. Cronau, E. Seppanen, S. Olver, N. C. Raffelt, R. Kuns, A. R. Pettit, A. Clouston, B. Wainwright, D. Branstetter, J. Smith, R. J. Paxton, D. P. Cerretti, L. Bonham, G. R. Hill, and D. A. Hume. 2010. An antibody against the colony-stimulating factor 1 receptor depletes the resident subset of monocytes and tissue- and tumor-associated macrophages but does not inhibit inflammation. *Blood* 116:3955-3963.
198. Bonecchi, R., E. Galliera, E. M. Borroni, M. M. Corsi, M. Locati, and A. Mantovani. 2009. Chemokines and chemokine receptors: an overview. *Front Biosci* 14:540-551.
199. Bazan, J. F., K. B. Bacon, G. Hardiman, W. Wang, K. Soo, D. Rossi, D. R. Greaves, A. Zlotnik, and T. J. Schall. 1997. A new class of membrane-bound chemokine with a CX3C motif. *Nature* 385:640-644.
200. Garton, K. J., P. J. Gough, C. P. Blobel, G. Murphy, D. R. Greaves, P. J. Dempsey, and E. W. Raines. 2001. Tumor necrosis factor-alpha-converting enzyme (ADAM17) mediates the cleavage and shedding of fractalkine (CX3CL1). *J Biol Chem* 276:37993-38001.
201. Tsou, C. L., C. A. Haskell, and I. F. Charo. 2001. Tumor necrosis factor-alpha-converting enzyme mediates the inducible cleavage of fractalkine. *J Biol Chem* 276:44622-44626.
202. Muehlhoefer, A., L. J. Saubermann, X. Gu, K. Luedtke-Heckenkamp, R. Xavier, R. S. Blumberg, D. K. Podolsky, R. P. MacDermott, and H. C. Reinecker. 2000. Fractalkine is an epithelial and endothelial cell-derived chemoattractant for intraepithelial lymphocytes in the small intestinal mucosa. *J Immunol* 164:3368-3376.
203. Kim, K. W., A. Vallon-Eberhard, E. Zigmond, J. Farache, E. Shezen, G. Shakhar, A. Ludwig, S. A. Lira, and S. Jung. 2011. In vivo structure/function and expression analysis of the CX3C chemokine fractalkine. *Blood*.
204. Lucas, A. D., N. Chadwick, B. F. Warren, D. P. Jewell, S. Gordon, F. Powrie, and D. R. Greaves. 2001. The transmembrane form of the CX3CL1 chemokine fractalkine is expressed predominantly by epithelial cells in vivo. *Am J Pathol* 158:855-866.
205. Harrison, J. K., Y. Jiang, S. Chen, Y. Xia, D. Maciejewski, R. K. McNamara, W. J. Streit, M. N. Salafranca, S. Adhikari, D. A. Thompson, P. Botti, K. B. Bacon, and L. Feng. 1998. Role for neuronally derived fractalkine in mediating interactions between neurons and CX3CR1-expressing microglia. *Proc Natl Acad Sci U S A* 95:10896-10901.
206. Ludwig, A., T. Berkhout, K. Moores, P. Groot, and G. Chapman. 2002. Fractalkine is expressed by smooth muscle cells in response to IFN-gamma and TNF-alpha and is modulated by metalloproteinase activity. *J Immunol* 168:604-612.
207. Papadopoulos, E. J., C. Sasseti, H. Saeki, N. Yamada, T. Kawamura, D. J. Fitzhugh, M. A. Saraf, T. Schall, A. Blauvelt, S. D. Rosen, and S. T. Hwang. 1999. Fractalkine, a CX3C chemokine, is expressed by dendritic cells and is up-regulated upon dendritic cell maturation. *European journal of immunology* 29:2551-2559.

208. Greaves, D. R., T. Hakkinen, A. D. Lucas, K. Liddiard, E. Jones, C. M. Quinn, J. Senaratne, F. R. Green, K. Tyson, J. Boyle, C. Shanahan, P. L. Weissberg, S. Gordon, and S. Yla-Hertuala. 2001. Linked chromosome 16q13 chemokines, macrophage-derived chemokine, fractalkine, and thymus- and activation-regulated chemokine, are expressed in human atherosclerotic lesions. *Arterioscler Thromb Vasc Biol* 21:923-929.
209. Jung, S., J. Aliberti, P. Graemmel, M. J. Sunshine, G. W. Kreutzberg, A. Sher, and D. R. Littman. 2000. Analysis of fractalkine receptor CX(3)CR1 function by targeted deletion and green fluorescent protein reporter gene insertion. *Mol Cell Biol* 20:4106-4114.
210. Kobayashi, T., S. Okamoto, Y. Iwakami, A. Nakazawa, T. Hisamatsu, H. Chinen, N. Kamada, T. Imai, H. Goto, and T. Hibi. 2007. Exclusive increase of CX3CR1+CD28-CD4+ T cells in inflammatory bowel disease and their recruitment as intraepithelial lymphocytes. *Inflamm Bowel Dis* 13:837-846.
211. Imai, T., K. Hieshima, C. Haskell, M. Baba, M. Nagira, M. Nishimura, M. Kakizaki, S. Takagi, H. Nomiyama, T. J. Schall, and O. Yoshie. 1997. Identification and molecular characterization of fractalkine receptor CX3CR1, which mediates both leukocyte migration and adhesion. *Cell* 91:521-530.
212. Fong, A. M., L. A. Robinson, D. A. Steeber, T. F. Tedder, O. Yoshie, T. Imai, and D. D. Patel. 1998. Fractalkine and CX3CR1 mediate a novel mechanism of leukocyte capture, firm adhesion, and activation under physiologic flow. *The Journal of experimental medicine* 188:1413-1419.
213. Chieppa, M., M. Rescigno, A. Y. Huang, and R. N. Germain. 2006. Dynamic imaging of dendritic cell extension into the small bowel lumen in response to epithelial cell TLR engagement. *The Journal of experimental medicine* 203:2841-2852.
214. Landsman, L., L. Bar-On, A. Zerneck, K. W. Kim, R. Krauthgamer, E. Shagdarsuren, S. A. Lira, I. L. Weissman, C. Weber, and S. Jung. 2009. CX3CR1 is required for monocyte homeostasis and atherogenesis by promoting cell survival. *Blood* 113:963-972.
215. Boehme, S. A., F. M. Lio, D. Maciejewski-Lenoir, K. B. Bacon, and P. J. Conlon. 2000. The chemokine fractalkine inhibits Fas-mediated cell death of brain microglia. *J Immunol* 165:397-403.
216. Brand, S., T. Sakaguchi, X. Gu, S. P. Colgan, and H. C. Reinecker. 2002. Fractalkine-mediated signals regulate cell-survival and immune-modulatory responses in intestinal epithelial cells. *Gastroenterology* 122:166-177.
217. Mizutani, N., T. Sakurai, T. Shibata, K. Uchida, J. Fujita, R. Kawashima, Y. I. Kawamura, N. Toyama-Sorimachi, T. Imai, and T. Dohi. 2007. Dose-dependent differential regulation of cytokine secretion from macrophages by fractalkine. *J Immunol* 179:7478-7487.
218. Combadiere, C., S. Potteaux, J. L. Gao, B. Esposito, S. Casanova, E. J. Lee, P. Debre, A. Tedgui, P. M. Murphy, and Z. Mallat. 2003. Decreased atherosclerotic lesion formation in CX3CR1/apolipoprotein E double knockout mice. *Circulation* 107:1009-1016.
219. Kostadinova, F. I., T. Baba, Y. Ishida, T. Kondo, B. K. Popivanova, and N. Mukaida. 2010. Crucial involvement of the CX3CR1-CX3CL1 axis in dextran sulfate sodium-mediated acute colitis in mice. *Journal of leukocyte biology* 88:133-143.
220. Schenk, M., A. Bouchon, S. Birrer, M. Colonna, and C. Mueller. 2005. Macrophages expressing triggering receptor expressed on myeloid cells-1 are underrepresented in the human intestine. *J Immunol* 174:517-524.

221. Hausmann, M., S. Kiessling, S. Mestermann, G. Webb, T. Spottl, T. Andus, J. Scholmerich, H. Herfarth, K. Ray, W. Falk, and G. Rogler. 2002. Toll-like receptors 2 and 4 are up-regulated during intestinal inflammation. *Gastroenterology* 122:1987-2000.
222. Platt, A. M., C. C. Bain, Y. Bordon, D. P. Sester, and A. M. Mowat. 2010. An independent subset of TLR expressing CCR2-dependent macrophages promotes colonic inflammation. *J Immunol* 184:6843-6854.
223. Hirotani, T., P. Y. Lee, H. Kuwata, M. Yamamoto, M. Matsumoto, I. Kawase, S. Akira, and K. Takeda. 2005. The nuclear I κ B protein I κ BNS selectively inhibits lipopolysaccharide-induced IL-6 production in macrophages of the colonic lamina propria. *J Immunol* 174:3650-3657.
224. Monteleone, I., A. M. Platt, E. Jaensson, W. W. Agace, and A. M. Mowat. 2008. IL-10-dependent partial refractoriness to Toll-like receptor stimulation modulates gut mucosal dendritic cell function. *European journal of immunology* 38:1533-1547.
225. Spencer, S. D., F. Di Marco, J. Hooley, S. Pitts-Meek, M. Bauer, A. M. Ryan, B. Sordat, V. C. Gibbs, and M. Aguet. 1998. The orphan receptor CRF2-4 is an essential subunit of the interleukin 10 receptor. *The Journal of experimental medicine* 187:571-578.
226. Kuhn, R., J. Lohler, D. Rennick, K. Rajewsky, and W. Muller. 1993. Interleukin-10-deficient mice develop chronic enterocolitis. *Cell* 75:263-274.
227. Takeda, K., B. E. Clausen, T. Kaisho, T. Tsujimura, N. Terada, I. Forster, and S. Akira. 1999. Enhanced Th1 activity and development of chronic enterocolitis in mice devoid of Stat3 in macrophages and neutrophils. *Immunity* 10:39-49.
228. Glocker, E. O., D. Kotlarz, K. Boztug, E. M. Gertz, A. A. Schaffer, F. Noyan, M. Perro, J. Diestelhorst, A. Allroth, D. Murugan, N. Hatscher, D. Pfeifer, K. W. Sykora, M. Sauer, H. Kreipe, M. Lacher, R. Nustede, C. Woellner, U. Baumann, U. Salzer, S. Koletzko, N. Shah, A. W. Segal, A. Sauerbrey, S. Buderus, S. B. Snapper, B. Grimbacher, and C. Klein. 2009. Inflammatory bowel disease and mutations affecting the interleukin-10 receptor. *N Engl J Med* 361:2033-2045.
229. Kuwata, H., M. Matsumoto, K. Atarashi, H. Morishita, T. Hirotani, R. Koga, and K. Takeda. 2006. I κ BNS inhibits induction of a subset of Toll-like receptor-dependent genes and limits inflammation. *Immunity* 24:41-51.
230. Kuwata, H., Y. Watanabe, H. Miyoshi, M. Yamamoto, T. Kaisho, K. Takeda, and S. Akira. 2003. IL-10-inducible Bcl-3 negatively regulates LPS-induced TNF-alpha production in macrophages. *Blood* 102:4123-4129.
231. Tsunawaki, S., M. Sporn, A. Ding, and C. Nathan. 1988. Deactivation of macrophages by transforming growth factor-beta. *Nature* 334:260-262.
232. Smythies, L. E., A. Maheshwari, R. Clements, D. Eckhoff, L. Novak, H. L. Vu, L. M. Mosteller-Barnum, M. Sellers, and P. D. Smith. 2006. Mucosal IL-8 and TGF-beta recruit blood monocytes: evidence for cross-talk between the lamina propria stroma and myeloid cells. *Journal of leukocyte biology* 80:492-499.
233. Monteleone, G., M. Boirivant, F. Pallone, and T. T. MacDonald. 2008. TGF-beta1 and Smad7 in the regulation of IBD. *Mucosal Immunol* 1 Suppl 1:S50-53.
234. Delgado, M., A. Chorny, D. Ganea, and E. Gonzalez-Rey. 2006. Vasoactive intestinal polypeptide induces regulatory dendritic cells that prevent acute graft versus host disease and leukemia relapse after bone marrow transplantation. *Ann N Y Acad Sci* 1070:226-232.
235. Iwata, M., A. Hirakiyama, Y. Eshima, H. Kagechika, C. Kato, and S. Y. Song. 2004. Retinoic acid imprints gut-homing specificity on T cells. *Immunity* 21:527-538.

236. Contractor, N., J. Louten, L. Kim, C. A. Biron, and B. L. Kelsall. 2007. Cutting edge: Peyer's patch plasmacytoid dendritic cells (pDCs) produce low levels of type I interferons: possible role for IL-10, TGFbeta, and prostaglandin E2 in conditioning a unique mucosal pDC phenotype. *J Immunol* 179:2690-2694.
237. Jiang, C., A. T. Ting, and B. Seed. 1998. PPAR-gamma agonists inhibit production of monocyte inflammatory cytokines. *Nature* 391:82-86.
238. Shah, Y. M., K. Morimura, and F. J. Gonzalez. 2007. Expression of peroxisome proliferator-activated receptor-gamma in macrophage suppresses experimentally induced colitis. *Am J Physiol Gastrointest Liver Physiol* 292:G657-666.
239. Rogler, G., T. Andus, E. Aschenbrenner, D. Vogl, W. Falk, J. Scholmerich, and V. Gross. 1997. Alterations of the phenotype of colonic macrophages in inflammatory bowel disease. *Eur J Gastroenterol Hepatol* 9:893-899.
240. Grimm, M. C., P. Pavli, E. Van de Pol, and W. F. Doe. 1995. Evidence for a CD14+ population of monocytes in inflammatory bowel disease mucosa--implications for pathogenesis. *Clin Exp Immunol* 100:291-297.
241. Rugtveit, J., E. M. Nilsen, A. Bakka, H. Carlsen, P. Brandtzaeg, and H. Scott. 1997. Cytokine profiles differ in newly recruited and resident subsets of mucosal macrophages from inflammatory bowel disease. *Gastroenterology* 112:1493-1505.
242. Kamada, N., T. Hisamatsu, S. Okamoto, H. Chinen, T. Kobayashi, T. Sato, A. Sakuraba, M. T. Kitazume, A. Sugita, K. Koganei, K. S. Akagawa, and T. Hibi. 2008. Unique CD14 intestinal macrophages contribute to the pathogenesis of Crohn disease via IL-23/IFN-gamma axis. *J Clin Invest* 118:2269-2280.
243. Grimm, M. C., W. E. Pullman, G. M. Bennett, P. J. Sullivan, P. Pavli, and W. F. Doe. 1995. Direct evidence of monocyte recruitment to inflammatory bowel disease mucosa. *J Gastroenterol Hepatol* 10:387-395.
244. Schenk, M., A. Bouchon, F. Seibold, and C. Mueller. 2007. TREM-1--expressing intestinal macrophages crucially amplify chronic inflammation in experimental colitis and inflammatory bowel diseases. *J Clin Invest* 117:3097-3106.
245. Palmen, M. J., L. A. Dieleman, M. B. van der Ende, A. Uyterlinde, A. S. Pena, S. G. Meuwissen, and E. P. van Rees. 1995. Non-lymphoid and lymphoid cells in acute, chronic and relapsing experimental colitis. *Clin Exp Immunol* 99:226-232.
246. Kanai, T., M. Watanabe, A. Okazawa, T. Sato, M. Yamazaki, S. Okamoto, H. Ishii, T. Totsuka, R. Iiyama, R. Okamoto, M. Ikeda, M. Kurimoto, K. Takeda, S. Akira, and T. Hibi. 2001. Macrophage-derived IL-18-mediated intestinal inflammation in the murine model of Crohn's disease. *Gastroenterology* 121:875-888.
247. Grose, R. H., G. S. Howarth, C. J. Xian, and A. W. Hohmann. 2001. Expression of B7 costimulatory molecules by cells infiltrating the colon in experimental colitis induced by oral dextran sulfate sodium in the mouse. *J Gastroenterol Hepatol* 16:1228-1234.
248. Watanabe, N., K. Ikuta, K. Okazaki, H. Nakase, Y. Tabata, M. Matsuura, H. Tamaki, C. Kawanami, T. Honjo, and T. Chiba. 2003. Elimination of local macrophages in intestine prevents chronic colitis in interleukin-10-deficient mice. *Dig Dis Sci* 48:408-414.
249. Tokuyama, H., S. Ueha, M. Kurachi, K. Matsushima, F. Moriyasu, R. S. Blumberg, and K. Kakimi. 2005. The simultaneous blockade of chemokine receptors CCR2, CCR5 and CXCR3 by a non-peptide chemokine receptor antagonist protects mice from dextran sodium sulfate-mediated colitis. *Int Immunol* 17:1023-1034.
250. Siddiqui, K. R., S. Laffont, and F. Powrie. 2010. E-cadherin marks a subset of inflammatory dendritic cells that promote T cell-mediated colitis. *Immunity* 32:557-567.

251. Jung, S., D. Unutmaz, P. Wong, G. Sano, K. De los Santos, T. Sparwasser, S. Wu, S. Vuthoori, K. Ko, F. Zavala, E. G. Pamer, D. R. Littman, and R. A. Lang. 2002. In vivo depletion of CD11c+ dendritic cells abrogates priming of CD8+ T cells by exogenous cell-associated antigens. *Immunity* 17:211-220.
252. Madan, R., F. Demircik, S. Surianarayanan, J. L. Allen, S. Divanovic, A. Trompette, N. Yogev, Y. Gu, M. Khodoun, D. Hildeman, N. Boespflug, M. B. Fogolin, L. Grobe, M. Greweling, F. D. Finkelman, R. Cardin, M. Mohrs, W. Muller, A. Waisman, A. Roers, and C. L. Karp. 2009. Nonredundant roles for B cell-derived IL-10 in immune counter-regulation. *J Immunol* 183:2312-2320.
253. Carlens, J., B. Wahl, M. Ballmaier, S. Bulfone-Paus, R. Forster, and O. Pabst. 2009. Common gamma-chain-dependent signals confer selective survival of eosinophils in the murine small intestine. *J Immunol* 183:5600-5607.
254. Zhang, J. Q., B. Biedermann, L. Nitschke, and P. R. Crocker. 2004. The murine inhibitory receptor mSiglec-E is expressed broadly on cells of the innate immune system whereas mSiglec-F is restricted to eosinophils. *European journal of immunology* 34:1175-1184.
255. Klebl, F. H., J. E. Olsen, S. Jain, and W. F. Doe. 2001. Expression of macrophage-colony stimulating factor in normal and inflammatory bowel disease intestine. *J Pathol* 195:609-615.
256. Chorro, L., and F. Geissmann. 2010. Development and homeostasis of 'resident' myeloid cells: the case of the Langerhans cell. *Trends Immunol* 31:438-445.
257. Sato, N., S. K. Ahuja, M. Quinones, V. KostECKi, R. L. Reddick, P. C. Melby, W. A. Kuziel, and S. S. Ahuja. 2000. CC chemokine receptor (CCR)2 is required for langerhans cell migration and localization of T helper cell type 1 (Th1)-inducing dendritic cells. Absence of CCR2 shifts the Leishmania major-resistant phenotype to a susceptible state dominated by Th2 cytokines, b cell outgrowth, and sustained neutrophilic inflammation. *The Journal of experimental medicine* 192:205-218.
258. Barclay, A. N. 1981. Different reticular elements in rat lymphoid tissue identified by localization of Ia, Thy-1 and MRC OX 2 antigens. *Immunology* 44:727-736.
259. Gorczynski, R. M., M. S. Cattral, Z. Chen, J. Hu, J. Lei, W. P. Min, G. Yu, and J. Ni. 1999. An immunoadhesin incorporating the molecule OX-2 is a potent immunosuppressant that prolongs allo- and xenograft survival. *J Immunol* 163:1654-1660.
260. Platt, A. M., and A. M. Mowat. 2008. Mucosal macrophages and the regulation of immune responses in the intestine. *Immunology letters* 119:22-31.
261. Geissmann, F., S. Gordon, D. A. Hume, A. M. Mowat, and G. J. Randolph. 2010. Unravelling mononuclear phagocyte heterogeneity. *Nature reviews* 10:453-460.
262. Pabst, O., and G. Bernhardt. 2010. The puzzle of intestinal lamina propria dendritic cells and macrophages. *European journal of immunology* 40:2107-2111.
263. Vallon-Eberhard, A., L. Landsman, N. Yogev, B. Verrier, and S. Jung. 2006. Transepithelial pathogen uptake into the small intestinal lamina propria. *J Immunol* 176:2465-2469.
264. Weber, B., L. Saurer, M. Schenk, N. Dickgreber, and C. Mueller. 2011. CX3CR1 defines functionally distinct intestinal mononuclear phagocyte subsets which maintain their respective functions during homeostatic and inflammatory conditions. *European journal of immunology* 41:773-779.
265. Rivollier, A., J. He, A. Kole, V. Valatas, and B. L. Kelsall. 2012. Inflammation switches the differentiation program of Ly6Chi monocytes from antiinflammatory macrophages to inflammatory dendritic cells in the colon. *The Journal of experimental medicine* 209:139-155.

266. Bradford, B. M., D. P. Sester, D. A. Hume, and N. A. Mabbott. 2011. Defining the anatomical localisation of subsets of the murine mononuclear phagocyte system using integrin alpha X (Itgax, CD11c) and colony stimulating factor 1 receptor (Csf1r, CD115) expression fails to discriminate dendritic cells from macrophages. *Immunobiology* 216:1228-1237.
267. Uematsu, S., K. Fujimoto, M. H. Jang, B. G. Yang, Y. J. Jung, M. Nishiyama, S. Sato, T. Tsujimura, M. Yamamoto, Y. Yokota, H. Kiyono, M. Miyasaka, K. J. Ishii, and S. Akira. 2008. Regulation of humoral and cellular gut immunity by lamina propria dendritic cells expressing Toll-like receptor 5. *Nature immunology* 9:769-776.
268. Mishra, A., S. P. Hogan, J. J. Lee, P. S. Foster, and M. E. Rothenberg. 1999. Fundamental signals that regulate eosinophil homing to the gastrointestinal tract. *J Clin Invest* 103:1719-1727.
269. Furuta, G. T., E. E. Nieuwenhuis, J. Karhausen, G. Gleich, R. S. Blumberg, J. J. Lee, and S. J. Ackerman. 2005. Eosinophils alter colonic epithelial barrier function: role for major basic protein. *Am J Physiol Gastrointest Liver Physiol* 289:G890-897.
270. Rothenberg, M. E., and S. P. Hogan. 2006. The eosinophil. *Annu Rev Immunol* 24:147-174.
271. Maheshwari, A., D. R. Kelly, T. Nicola, N. Ambalavanan, S. K. Jain, J. Murphy-Ullrich, M. Athar, M. Shimamura, V. Bhandari, C. Aprahamian, R. A. Dimmitt, R. Serra, and R. K. Ohls. 2011. TGF-beta2 suppresses macrophage cytokine production and mucosal inflammatory responses in the developing intestine. *Gastroenterology* 140:242-253.
272. Chu, V. T., A. Frohlich, G. Steinhauser, T. Scheel, T. Roch, S. Fillatreau, J. J. Lee, M. Lohning, and C. Berek. 2011. Eosinophils are required for the maintenance of plasma cells in the bone marrow. *Nature immunology* 12:151-159.
273. Bettelli, E., Y. Carrier, W. Gao, T. Korn, T. B. Strom, M. Oukka, H. L. Weiner, and V. K. Kuchroo. 2006. Reciprocal developmental pathways for the generation of pathogenic effector TH17 and regulatory T cells. *Nature* 441:235-238.
274. Yu, C., A. B. Cantor, H. Yang, C. Browne, R. A. Wells, Y. Fujiwara, and S. H. Orkin. 2002. Targeted deletion of a high-affinity GATA-binding site in the GATA-1 promoter leads to selective loss of the eosinophil lineage in vivo. *The Journal of experimental medicine* 195:1387-1395.
275. Jakubzick, C., F. Tacke, F. Ginhoux, A. J. Wagers, N. van Rooijen, M. Mack, M. Merad, and G. J. Randolph. 2008. Blood monocyte subsets differentially give rise to CD103+ and CD103- pulmonary dendritic cell populations. *J Immunol* 180:3019-3027.
276. Takada, Y., T. Hisamatsu, N. Kamada, M. T. Kitazume, H. Honda, Y. Oshima, R. Saito, T. Takayama, T. Kobayashi, H. Chinen, Y. Mikami, T. Kanai, S. Okamoto, and T. Hibi. 2010. Monocyte chemoattractant protein-1 contributes to gut homeostasis and intestinal inflammation by composition of IL-10-producing regulatory macrophage subset. *J Immunol* 184:2671-2676.
277. Ueda, Y., H. Kayama, S. G. Jeon, T. Kusu, Y. Isaka, H. Rakugi, M. Yamamoto, and K. Takeda. 2010. Commensal microbiota induce LPS hyporesponsiveness in colonic macrophages via the production of IL-10. *Int Immunol* 22:953-962.
278. MacDonald, T. T., and S. L. Pender. 1998. Lamina propria T cells. *Chem Immunol* 71:103-117.
279. Tiemessen, M. M., A. L. Jagger, H. G. Evans, M. J. van Herwijnen, S. John, and L. S. Taams. 2007. CD4+CD25+Foxp3+ regulatory T cells induce alternative activation of human monocytes/macrophages. *Proc Natl Acad Sci U S A* 104:19446-19451.

280. Liu, G., H. Ma, L. Qiu, L. Li, Y. Cao, J. Ma, and Y. Zhao. 2010. Phenotypic and functional switch of macrophages induced by regulatory CD4+CD25+ T cells in mice. *Immunology and cell biology* 89:130-142.
281. London, A., E. Itskovich, I. Benhar, V. Kalchenko, M. Mack, S. Jung, and M. Schwartz. 2011. Neuroprotection and progenitor cell renewal in the injured adult murine retina requires healing monocyte-derived macrophages. *The Journal of experimental medicine* 208:23-39.
282. Shechter, R., A. London, C. Varol, C. Raposo, M. Cusimano, G. Yovel, A. Rolls, M. Mack, S. Pluchino, G. Martino, S. Jung, and M. Schwartz. 2009. Infiltrating blood-derived macrophages are vital cells playing an anti-inflammatory role in recovery from spinal cord injury in mice. *PLoS Med* 6:e1000113.
283. Arnold, L., A. Henry, F. Poron, Y. Baba-Amer, N. van Rooijen, A. Plonquet, R. K. Gherardi, and B. Chazaud. 2007. Inflammatory monocytes recruited after skeletal muscle injury switch into antiinflammatory macrophages to support myogenesis. *The Journal of experimental medicine* 204:1057-1069.
284. Movahedi, K., D. Laoui, C. Gysemans, M. Baeten, G. Stange, J. Van den Bossche, M. Mack, D. Pipeleers, P. In't Veld, P. De Baetselier, and J. A. Van Ginderachter. 2010. Different tumor microenvironments contain functionally distinct subsets of macrophages derived from Ly6C(high) monocytes. *Cancer Res* 70:5728-5739.
285. Collins, M. K., C. S. Tay, and A. Erlebacher. 2009. Dendritic cell entrapment within the pregnant uterus inhibits immune surveillance of the maternal/fetal interface in mice. *J Clin Invest* 119:2062-2073.
286. Hodge-Dufour, J., M. W. Marino, M. R. Horton, A. Jungbluth, M. D. Burdick, R. M. Strieter, P. W. Noble, C. A. Hunter, and E. Pure. 1998. Inhibition of interferon gamma induced interleukin 12 production: a potential mechanism for the anti-inflammatory activities of tumor necrosis factor. *Proc Natl Acad Sci U S A* 95:13806-13811.
287. Masli, S., and B. Turpie. 2009. Anti-inflammatory effects of tumour necrosis factor (TNF)-alpha are mediated via TNF-R2 (p75) in tolerogenic transforming growth factor-beta-treated antigen-presenting cells. *Immunology* 127:62-72.
288. O'Connor, C. M., and M. X. FitzGerald. 1994. Matrix metalloproteases and lung disease. *Thorax* 49:602-609.
289. Sung, M. J., D. H. Kim, M. Davaatseren, H. J. Hur, W. Kim, Y. J. Jung, S. K. Park, and D. Y. Kwon. 2010. Genistein suppression of TNF-alpha-induced fractalkine expression in endothelial cells. *Cell Physiol Biochem* 26:431-440.
290. Cui, W., L. X. Li, C. M. Sun, Y. Wen, Y. Zhou, Y. L. Dong, and P. Liu. 2010. Tumor necrosis factor alpha increases epithelial barrier permeability by disrupting tight junctions in Caco-2 cells. *Braz J Med Biol Res* 43:330-337.
291. Delamarre, L., M. Pack, H. Chang, I. Mellman, and E. S. Trombetta. 2005. Differential lysosomal proteolysis in antigen-presenting cells determines antigen fate. *Science (New York, N.Y)* 307:1630-1634.
292. Ip, W. K., A. Sokolovska, G. M. Charriere, L. Boyer, S. Dejardin, M. P. Cappillino, L. M. Yantosca, K. Takahashi, K. J. Moore, A. Lacy-Hulbert, and L. M. Stuart. 2010. Phagocytosis and phagosome acidification are required for pathogen processing and MyD88-dependent responses to Staphylococcus aureus. *J Immunol* 184:7071-7081.
293. Bosschaerts, T., M. Guilliams, B. Stijlemans, Y. Morias, D. Engel, F. Tacke, M. Herin, P. De Baetselier, and A. Beschin. 2010. Tip-DC development during parasitic infection is regulated by IL-10 and requires CCL2/CCR2, IFN-gamma and MyD88 signaling. *PLoS Pathog* 6:e1001045.

294. Langlet, C., S. Tamoutounour, S. Henri, H. Luche, L. Ardouin, C. Gregoire, B. Malissen, and M. Guilliams. 2012. CD64 Expression Distinguishes Monocyte-Derived and Conventional Dendritic Cells and Reveals Their Distinct Role during Intramuscular Immunization. *J Immunol*.
295. Dunay, I. R., A. Fuchs, and L. D. Sibley. 2010. Inflammatory monocytes but not neutrophils are necessary to control infection with *Toxoplasma gondii* in mice. *Infect Immun* 78:1564-1570.
296. Kim, Y. G., N. Kamada, M. H. Shaw, N. Warner, G. Y. Chen, L. Franchi, and G. Nunez. 2011. The Nod2 sensor promotes intestinal pathogen eradication via the chemokine CCL2-dependent recruitment of inflammatory monocytes. *Immunity* 34:769-780.
297. Bordon, Y., C. A. Hansell, D. P. Sester, M. Clarke, A. M. Mowat, and R. J. Nibbs. 2009. The atypical chemokine receptor D6 contributes to the development of experimental colitis. *J Immunol* 182:5032-5040.
298. Guilliams, M., K. Movahedi, T. Bosschaerts, T. VandenDriessche, M. K. Chuah, M. Herin, A. Acosta-Sanchez, L. Ma, M. Moser, J. A. Van Ginderachter, L. Brys, P. De Baetselier, and A. Beschin. 2009. IL-10 dampens TNF/inducible nitric oxide synthase-producing dendritic cell-mediated pathogenicity during parasitic infection. *J Immunol* 182:1107-1118.
299. Smith, P. D., L. E. Smythies, R. Shen, T. Greenwell-Wild, M. Gliozzi, and S. M. Wahl. 2010. Intestinal macrophages and response to microbial encroachment. *Mucosal Immunol*.
300. Engel, D. R., J. Maurer, A. P. Tittel, C. Weisheit, T. Cavlar, B. Schumak, A. Limmer, N. van Rooijen, C. Trautwein, F. Tacke, and C. Kurts. 2008. CCR2 mediates homeostatic and inflammatory release of Gr1(high) monocytes from the bone marrow, but is dispensable for bladder infiltration in bacterial urinary tract infection. *J Immunol* 181:5579-5586.
301. Waddell, A., R. Ahrens, K. Steinbrecher, B. Donovan, M. E. Rothenberg, A. Munitz, and S. P. Hogan. 2011. Colonic eosinophilic inflammation in experimental colitis is mediated by Ly6C(high) CCR2(+) inflammatory monocyte/macrophage-derived CCL11. *J Immunol* 186:5993-6003.
302. Lim, J. K., C. J. Obara, A. Rivollier, A. G. Pletnev, B. L. Kelsall, and P. M. Murphy. 2011. Chemokine receptor Ccr2 is critical for monocyte accumulation and survival in West Nile virus encephalitis. *J Immunol* 186:471-478.
303. Brand, S., K. Hofbauer, J. Dambacher, F. Schnitzler, T. Staudinger, S. Pfennig, J. Seiderer, C. Tillack, A. Konrad, B. Goke, T. Ochsenkuhn, and P. Lohse. 2006. Increased expression of the chemokine fractalkine in Crohn's disease and association of the fractalkine receptor T280M polymorphism with a fibrostenosing disease Phenotype. *Am J Gastroenterol* 101:99-106.
304. Madsen, K. L., D. Malfair, D. Gray, J. S. Doyle, L. D. Jewell, and R. N. Fedorak. 1999. Interleukin-10 gene-deficient mice develop a primary intestinal permeability defect in response to enteric microflora. *Inflamm Bowel Dis* 5:262-270.
305. Arrieta, M. C., K. Madsen, J. Doyle, and J. Meddings. 2009. Reducing small intestinal permeability attenuates colitis in the IL10 gene-deficient mouse. *Gut* 58:41-48.
306. Rani, R., A. G. Smulian, D. R. Greaves, S. P. Hogan, and D. R. Herbert. 2011. TGF-beta limits IL-33 production and promotes the resolution of colitis through regulation of macrophage function. *European journal of immunology* 41:2000-2009.
307. Ryan, G. R., X. M. Dai, M. G. Dominguez, W. Tong, F. Chuan, O. Chisholm, R. G. Russell, J. W. Pollard, and E. R. Stanley. 2001. Rescue of the colony-stimulating

- factor 1 (CSF-1)-nullizygous mouse (Csf1(op)/Csf1(op)) phenotype with a CSF-1 transgene and identification of sites of local CSF-1 synthesis. *Blood* 98:74-84.
308. Hashimoto, D., A. Chow, M. Greter, Y. Saenger, W. H. Kwan, M. Leboeuf, F. Ginhoux, J. C. Ochando, Y. Kunisaki, N. van Rooijen, C. Liu, T. Teshima, P. S. Heeger, E. R. Stanley, P. S. Frenette, and M. Merad. 2011. Pretransplant CSF-1 therapy expands recipient macrophages and ameliorates GVHD after allogeneic hematopoietic cell transplantation. *The Journal of experimental medicine*.
309. Paolicelli, R. C., G. Bolasco, F. Pagani, L. Maggi, M. Scianni, P. Panzanelli, M. Giustetto, T. A. Ferreira, E. Guiducci, L. Dumas, D. Ragozzino, and C. T. Gross. 2011. Synaptic pruning by microglia is necessary for normal brain development. *Science (New York, N.Y)* 333:1456-1458.
310. Medina-Contreras, O., D. Geem, O. Laur, I. R. Williams, S. A. Lira, A. Nusrat, C. A. Parkos, and T. L. Denning. 2011. CX3CR1 regulates intestinal macrophage homeostasis, bacterial translocation, and colitogenic Th17 responses in mice. *J Clin Invest*.
311. Zhang, F., G. Huang, B. Hu, Y. Song, and Y. Shi. 2011. A soluble thymic stromal lymphopoietin (TSLP) antagonist, TSLPR-immunoglobulin, reduces the severity of allergic disease by regulating pulmonary dendritic cells. *Clin Exp Immunol* 164:256-264.
312. Hontecillas, R., W. T. Horne, M. Climent, A. J. Guri, C. Evans, Y. Zhang, B. W. Sobral, and J. Bassaganya-Riera. 2011. Immunoregulatory mechanisms of macrophage PPAR-gamma in mice with experimental inflammatory bowel disease. *Mucosal Immunol* 4:304-313.
313. Ko, Y. C., H. F. Chien, Y. F. Jiang-Shieh, C. Y. Chang, M. H. Pai, J. P. Huang, H. M. Chen, and C. H. Wu. 2009. Endothelial CD200 is heterogeneously distributed, regulated and involved in immune cell-endothelium interactions. *J Anat* 214:183-195.
314. Copland, D. A., C. J. Calder, B. J. Raveney, L. B. Nicholson, J. Phillips, H. Cherwinski, M. Jenmalm, J. D. Sedgwick, and A. D. Dick. 2007. Monoclonal antibody-mediated CD200 receptor signaling suppresses macrophage activation and tissue damage in experimental autoimmune uveoretinitis. *Am J Pathol* 171:580-588.
315. Dieleman, L. A., B. U. Ridwan, G. S. Tennyson, K. W. Beagley, R. P. Bucy, and C. O. Elson. 1994. Dextran sulfate sodium-induced colitis occurs in severe combined immunodeficient mice. *Gastroenterology* 107:1643-1652.
316. Ziegler-Heitbrock, L., P. Ancuta, S. Crowe, M. Dalod, V. Grau, D. N. Hart, P. J. Leenen, Y. J. Liu, G. MacPherson, G. J. Randolph, J. Scherberich, J. Schmitz, K. Shortman, S. Sozzani, H. Strobl, M. Zembala, J. M. Austyn, and M. B. Lutz. 2010. Nomenclature of monocytes and dendritic cells in blood. *Blood* 116:e74-80.
317. Shaul, M. E., G. Bennet, K. J. Strissel, A. S. Greenberg, and M. S. Obin. 2010. M2-like remodelling phenotypes of CD11c+ adipose tissue macrophages during high fat diet-induced obesity in mice. *Diabetes*. 59:1171-1181.
318. Dewals, BG, R.G. Marillier, J. C. Hoving, M. Leeto, A. Schwegmann, and F Brombacher. 2010. IL-4Ralpha-independent expression of mannose receptor and Ym1 by macrophages depends on their IL-10 responsiveness. *PLoS Negl Trop Dis*. 4:e689.
319. Ito, A., T. Suganami, A. Yamauchi, M. Degawa-Yamauchi, M. Tanaka, R. Kouyama, Y. Kobayashi, N. Nitta, K. Yasuda, Y Hirata, W. A. Kuziel, M. Takeya, S. Kanegasaki, Y Kamei, and Y. Ogawa. 2008. Role of CC chemokine receptor 2 in bone marrow cells in the recruitment of macrophages into obese adipose tissue. *J Biol Chem*. 283:35715-35723.

320. Nhu, Q. M., N. Cuesta, and S. N. Vogel. 2006. Transcriptional regulation of lipopolysaccharide (LPS)-induced Toll-like receptor (TLR) expression in murine macrophages: role of interferon regulatory factors 1 (IRF-1) and 2 (IRF-2). *J Endotoxin Res.* 12:285-295.